

Frequency Domain Analysis of Sampled-Data Control Systems

Julio Hernán Braslavsky

*A thesis submitted in partial fulfilment of
the requirements for the degree of*

Doctor of Philosophy

THE DEPARTMENT OF
ELECTRICAL AND COMPUTER ENGINEERING



THE UNIVERSITY OF NEWCASTLE
NEW SOUTH WALES, 2308
AUSTRALIA

October 1995

Copyright ©1995 by Julio H. Braslavsky
Department of Electrical and Computer Engineering
The University of Newcastle
NSW 2308 Australia

Revised April 1, 1996.

ISBN 7259 0905 6

Frequency Domain Analysis of Sampled-data Control Systems
Braslavsky, Julio Hernán - The University of Newcastle.

Thesis - With index, references.

Subject headings: Control systems analysis, sampled-data systems, discrete-time systems, frequency response.

This thesis was typeset by the author on a DEC Station using \LaTeX 2.09 + NFSS and **Emacs**. Typeset chapters were translated into PostScript files using **dvips**. The typeface used for the main text is Concrete Roman, designed by Donald Knuth, and the mathematics font is Euler, designed by Hermann Zapf.

Printed in Australia by Lloyd Scott Document Production Services.

I hereby certify that the work embodied in this thesis is the result of original research and has not been submitted for a higher degree to any other University or Institution.

Julio H. Braslavsky

Acknowledgments

As somebody¹ once said: “These summer days go very slow, but — let me tell you, sweetheart — the years . . . fly by.”. And so went my years of postgrad student at the bushy campus of the University of Newcastle. Today, this period is almost at its end, and the time of looking back has come. I’m indebted to many people for making this an enriching and unforgettable experience. First of all, I’d like to thank my supervisor, Rick Middleton. To work with him has been a real pleasure to me, with heaps of fun and excitement. Rick has oriented and supported me with promptness and care, and has always been patient and encouraging in times of difficulties. Above all, he made me feel a mate, which I appreciate from my heart. My deep gratitude goes also to Jim Freudenberg. His dropping in Newcastle initiated the project that made this thesis possible. I learned many things from Jim, who has always been generous and patient in letting me grasp them. I was certainly lucky in having such a fine duo in the same team, of which I’m very proud to be part.

Thanks go also to Marcelo Laca, George Willis, and Brailey Sims. These guys endured with grace my visits to the Math Department, and deciphered the gibberish I brought into well-formulated questions. I truly enjoyed the sessions of “amplification of doubts” spent with Marcelo in some lazy afternoons. Many times, I walked back the hill with some precious answers too.

The postgrads and post-postgrads of the EF Building have been an invaluable support day in, day out, during all these years. Special thanks to Juan, Sing Kiong, Gjerrit, Huai Zhong, Yash, Guillermo, Dragana, Misko, Lin, Bhujanga, Kim, Peng, Teresa, Brett, Steve, Jovica, Yuming, Ross, Jing Qiong, and Jaehoon. Very special thanks go to Gjerrit, a hero that proofread the thing and — at least in compensation — enjoyed finding mistakes in my proofs². Without the magic powers of the wizard Huai Zhong — and, at the beginning of times, Michael Lund — working in front of the screen would have been a real pain. Thanks to them for this.

Finally, my dearest thanks to people in this unique Department: Graham, Carlos, Minyue, Stefan, Hernán, Peter, Andrew S., Fernando, Andrew A., Marcia, Dianne, Denise, Roslyn and Vilma. You made me love this place. I take you all in my heart³.

¹Frank — Richard Harris in the excellent movie *Wrestling Ernest Hemingway* (1993).

²I forgive him; he also introduced me to the enchanting art of boomeranging.

³Hopefully, some of them will also remember a fisherman that once put a handkerchief in his mouth.

Agradecimientos

Mi más cálido reconocimiento es para quienes estuvieron siempre conmigo — aún sin estar — y así hicieron esta experiencia posible, con apoyo constante y, sobre todo, con mucho mucho cariño. Para mi mamá y mi papá, María Elena y Julio, que incansablemente estimularon mis iniciativas, a pesar de que muchas de ellas significaran largos años de vivir a la distancia, lejos del pago familiar tan querido. A ellos que con su ejemplo me enseñaron que toda experiencia vale mucho más si es compartida.

Para Martha y Rafael, que fueron una conexión constante con la patria rosarina. Un afecto que no se puede medir en las toneladas de diarios, revistas y compactos, que se la pasaron en gruesos sobres marrones haciendo el transpolar para aterrizar en Newcastle.

Para los entrañables amigos y compañeros de estudio y de trabajo: Germán, Sergio, Monina, Juan Carlos, Roberto Riva⁴; de los que me llevé una parte en el corazón⁵ y a los que volveré. Para Roberto González y Ricardo Aimaretti, con quienes, allá lejos y hace tiempo, empezó toda esta historia.

Para Carmen, que a fuerza de cariño hizo de Newcastle nuestro lugar.

Y especialmente, para Marimar, mi compañera y amada. Para ella también, mi canción es otra.

⁴Bueh, este de trabajo mucho no... pero buena joda.

⁵Juan Carlos caso extremo: se vino entero.

*A María Elena y Julio Oscar.
A Encarnación.*

Contents

Abstract	1
1 Introduction	3
1.1 Recent Developments in Sampled-data Systems	4
1.2 Contributions of this Thesis	7
2 Preliminaries	11
2.1 Analog and Discrete Signals	11
2.1.1 Signal Spaces	11
2.1.2 Samplers and Holds	12
2.1.3 A Key Sampling Formula	15
2.2 Hybrid Systems	17
2.2.1 Basic Feedback Configuration	17
2.2.2 Non-pathological Sampling and Internal Stability	20
2.3 Summary	21
3 Generalized Sampled-data Hold Functions	23
3.1 Frequency Response of Generalized Sampled-data Holds	24
3.1.1 Norms and the Frequency Response of a GSHF	25
3.1.2 GSHF Frequency Responses from Boundary Values	27
3.1.3 Two Simple Classes of GSHFs	28
3.2 Distribution of Zeros of GSHFs	30
3.2.1 Zeros of PC and FDLTI GSHFs	31
3.2.2 GSHFs with all Zeros on the $j\omega$ -axis	32
3.2.3 Example: Zeros of a FDLTI GSHF	36
3.3 Integral Relations	38
3.3.1 Poisson Integral for GSHFs	40
3.3.2 Middleton Integral for GSHFs	42
3.3.3 Example: Tradeoffs in $H(j\omega)$	46
3.4 Summary	46
4 Frequency Response and Performance Limitations	49
4.1 Frequency Response of a Sampled-data System	50
4.2 Interpolation Constraints	55
4.3 Hybrid Disturbance Rejection Properties	61
4.4 Integral Relations	68
4.4.1 Notation	69
4.4.2 Poisson Sensitivity Integral	70

4.4.3	Poisson Complementary Sensitivity Integral	73
4.4.4	Poisson Harmonic Response Integral	75
4.4.5	Bode Sensitivity Integral	77
4.4.6	Middleton Complementary Sensitivity Integral	77
4.5	Summary	80
5	Sensitivity Operators on L_2	81
5.1	A Frequency-domain Lifting	82
5.2	L_2 -induced Norms and Frequency-gains	85
5.2.1	Sensitivity Operators	85
5.2.2	Numerical Implementation	93
5.3	Summary	99
6	Stability Robustness	101
6.1	Multiplicative Perturbation	102
6.2	Divisive Perturbation	110
6.3	Summary	113
7	An Application: Design Implications of Discrete Zero-placement	115
7.1	Discrete Zero-placement and ORHP Zeros of GSHFs	117
7.2	Gedanken Experiment No. 1: Analog Performance	120
7.3	Gedanken Experiment No. 2: Discrete Response	122
7.3.1	Formulation of Gedanken Experiment No. 2	122
7.3.2	Interpolation Constraints and an Integral Relation	124
7.3.3	Result of Gedanken Experiment No. 2	126
7.3.4	Example: Robustness of Zero-placement	129
7.4	Summary	132
8	Conclusions	133
A	Proofs of Some Results in the Chapters	137
A.1	Proofs for Chapter 2	137
A.2	Proofs for Chapter 3	139
A.3	Proofs for Chapter 4	141
A.3.1	Proof of Lemma 4.1.2	141
A.3.2	Proof of Theorem 4.4.11	144
A.4	Proofs for Chapter 5	147
A.5	Proofs for Chapter 6	148
B	Order and Type of an Entire Function	151
C	Discrete Sensitivity Integrals	153
	Bibliography	157
	Notation	165

Abstract

This thesis is aimed at analysis of sampled-data feedback systems. Our approach is in the frequency-domain, and stresses the study of sensitivity and complementary sensitivity operators. Frequency-domain methods have proven very successful in the analysis and design of linear time-invariant control systems, for which the importance and utility of sensitivity operators is well-recognized. The extension of these methods to sampled-data systems, however, is not straightforward, since they are inherently time-varying due to the intrinsic sample and hold operations.

In this thesis we present a systematic frequency-domain framework to describe sampled-data systems considering full-time information. Using this framework, we develop a theory of design limitations for sampled-data systems. This theory allows us to quantify the essential constraints in design imposed by inherent open-loop characteristics of the analog plant. Our results show that: (i) sampled-data systems inherit the difficulty imposed upon analog feedback design by the plant's non-minimum phase zeros, unstable poles, and time-delays, independently of the type of hold used; (ii) sampled-data systems are subject to additional design limitations imposed by potential non-minimum phase zeros of the hold device; and (iii) sampled-data systems, unlike analog systems, are subject to limits upon the ability of high compensator gain to achieve disturbance rejection. As an application, we quantitatively analyze the sensitivity and robustness characteristics of digital control schemes that rely on the use of generalized sampled-data hold functions, whose frequency-response properties we describe in detail.

In addition, we derive closed-form expressions to compute the L_2 -induced norms of the sampled-data sensitivity and complementary sensitivity operators. These expressions are important both in analysis and design, particularly when uncertainty in the model of the plant is considered. Our methods provide some interesting interpretations in terms of signal spaces, and admit straightforward implementation in a numerically reliable fashion.

1

Introduction

This thesis deals with frequency-domain properties and essential design limitations in linear sampled-data feedback control systems.

A sampled-data system combines both continuous and discrete-time dynamic subsystems. Because of this inherent mixture of time domains, we shall also refer to a sampled-data system as a *hybrid* system, understanding both terms as synonyms. A typical hybrid feedback control configuration is shown in Figure 1.1. Although the plant is usually a continuous-time, or *analog*, system, the controller is a discrete-time device in most practical applications. This is mainly due to the numerous advantages that digital equipments offer over their analog counterparts. With the great advances in computer technology, today digital controllers are more compact, reliable, flexible and often less expensive than analog ones.

There is a fundamental operational difference between digital and analog controllers: the digital system acts on *samples* of the measured plant output rather than on the continuous-time signal. A practical implication of this difference is that a digital controller requires special interfaces that link it to the analog world.

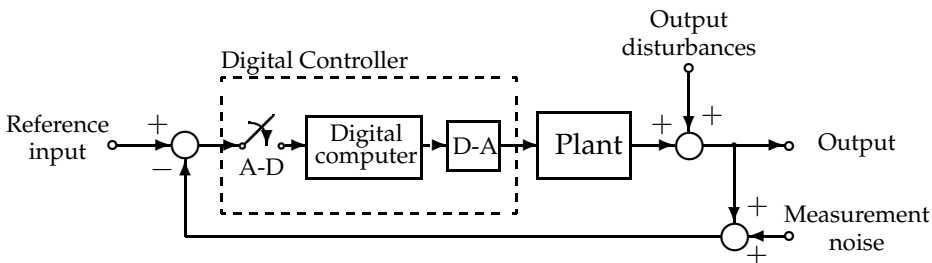


Figure 1.1: Typical sampled-data feedback configuration.

A digital controller can be idealized as consisting of three main elements: the analog-to-digital (A-D) interface, the digital computer, and the digital-to-analog (D-A) interface. The A-D interface, or *sampler*, acts on a physical variable, normally an electric voltage, and converts it into a sequence of binary numbers, which represent the values of the variable at the sampling instants. These numbers are then processed by the digital computer, which generates a new sequence

of binary numbers that correspond to the discrete control signal. This control signal is finally converted into an analog voltage by the D-A interface, also called the *hold device*.

The digital computer implements the control algorithm as a set of difference equations, which represent a dynamic system in the discrete-time domain. We shall refer to this system as the *discrete controller*. In general, the discrete controller will include nonlinearities and varying parameters in it; our discussion here is restricted to linear time-invariant controllers, which nevertheless constitute an useful and important case in analysis and design.

Essentially, two classic approaches are taken in engineering practice for the design of a discrete controller. The first technique, referred to as *emulation* [Franklin et al., 1990], is the most widely applied in industry. Emulation consists in first designing an analog controller such that the closed-loop system has satisfactory properties, and then translating the analog design into a discrete one using a suitable discretization method (see Keller and Anderson [1992] for a recent approach). This technique has the advantage that the synthesis is done in continuous-time, where the design goals are typically specified, and where most of the designer's experience and intuition resides. Also, the system's analog performance will in general be recovered for fast sampling. Yet, the hybrid performance cannot be expected to be better than the analog, and there may be a serious degradation if the sampling is not sufficiently fast. This is an important drawback, since the sampling rate is a critical constraint in many applications.

The second traditional technique consists in discretizing the plant and performing a *discrete design*. The main benefit of this approach is that the synthesis procedure is again simplified, since the discretized plant is linear time-invariant (LTI) in the discrete-time domain. However, a serious limitation of discrete design is that it is generally difficult to translate the analog specifications into discrete. Furthermore, the simple models obtained by discretization fail to represent the full response of the system, since *intersample behavior* is inherently lost or hidden¹.

In particular, neither of these approaches offers an adequate framework for analysis of the continuous-time time-varying hybrid system. Emulation is purely a method of synthesis, whereas discrete design gives a partial answer, since only the *sampled* behavior can be studied in the discretized model. On the other hand, the analysis of the hybrid system requires the consideration of both sampled *and* intersample behavior. This is crucial especially when considering robustness and sensitivity properties of the system, since *analog* uncertainties, disturbances and noise are frequently the issues of practical significance.

1.1 Recent Developments in Sampled-data Systems

Naturally, in view of the technological appeal of digital implementations, sampled-data systems have been the subject of many research works in recent years. Two

¹Some intersample information can still be handled in a discrete model by using the *modified Z-transform* introduced by Jury [1958]. However, this line of work seems to have been largely abandoned.

research directions in particular have generated much activity. First, various optimal control problems have been stated and solved for hybrid systems using frameworks that incorporate intersample behavior [e.g., Chen and Francis, 1991, Bamieh and Pearson, 1992, Dullerud and Francis, 1992, Tadmor, 1992, Kabamba and Hara, 1993, Bamieh et al., 1993]. Second, several researchers have explored the potential ability of nonstandard hold functions, periodic digital controllers, and multirate sampling to circumvent design limitations inherent to LTI systems [e.g., Khargonekar et al., 1985, Kabamba, 1987, Francis and Georgiou, 1988, Hagiwara and Araki, 1988, Das and Rajagopalan, 1992, Yan et al., 1994]. Within these two research avenues, we shall restrict the discussion here to optimal H_∞ sampled-data control, and control techniques using *generalized sampled-data hold functions* (GSHFs).

The earliest efforts to extend H_∞ control methods to sampled-data systems focused on the computation of the induced L_2 -norm. The L_2 -induced norm measures the maximum gain of an operator acting on spaces of square integrable, or “finite energy”, signals. For a LTI system, the optimization of the L_2 -induced norm is equivalent to the minimization of the H_∞ -norm of its transfer matrix. This is not trivial to extend to sampled-data systems, since they are time-varying due to the presence of the sampler, and hence we cannot describe their input-output behavior with ordinary transfer matrices. Therefore, special procedures have been developed. For example, Thompson et al. [1983], and Thompson et al. [1986] provided the first bounds for the norm of open-loop hybrid systems using conic sector techniques. Exact expressions of the L_2 -induced norms were later on obtained by Chen and Francis [1990] via frequency-domain methods. In 1991, Leung et al. derived a formula for sampled-data feedback systems with band-limited signals.

In recent years, different general frameworks to handle intersample behavior appeared on the scene, and led the way to the solution of certain hybrid optimal H_∞ control problems². These frameworks include *lifting techniques* [Bamieh et al., 1991, Toivonen, 1992, Bamieh and Pearson, 1992, Yamamoto, 1993, 1994], *descriptor system techniques* [Kabamba and Hara, 1993], and techniques based on *linear systems with jumps* [Sun et al., 1993, Sivashankar and Khargonekar, 1994]. More specifically, the lifting technique consists on transforming the original sampled-data system into an equivalent LTI discrete-time system with infinite-dimensional input-output signal spaces. Then, the L_2 -induced norm of the sampled-data system is shown to be less than one if and only if the H_∞ -norm of this equivalent discrete system is less than one. In the descriptor system approach, on the other hand, the system is represented by a hybrid state-space model, from which the descriptor system is formulated. The solution of the H_∞ sampled-data problem is then characterized by the solution of certain associated Hamiltonian equation. In contrast with these procedures, the theory of linear systems with jumps allows a direct characterization of the problem in similar — although more involved — terms to those of standard LTI H_∞ -control problems, and leads to a pair of Riccati equations. Despite the procedural differences in all these approaches, the results

²Yet, as pointed out by Glover [1995], practical design guidelines are still under development.

obtained are mathematically equivalent.

On the other hand, new control schemes using GSHFs were introduced to approach various problems that are insoluble with LTI control schemes. A GSHF reconstructs an analog signal from a discrete sequence of values, but instead of holding these values constant along the sample period — as it is the case of a classic *zero-order hold* (ZOH) — a GSHF scales a fixed suitable waveform. In particular, by selecting this waveform it is possible to assign the zeros of the discretized plant, and hence, e.g., convert a non-minimum phase (NMP) analog plant into a minimum phase discrete plant [Bai and Dasgupta, 1990]. This is the key technique of several applications of GSHFs. For example, Kabamba [1987] obtained simultaneous pole-assignment of an arbitrary finite number of plants using a single GSHF; and Yan et al. [1994] proposed the combination of a discrete controller with a GSHF to achieve arbitrary gain-margin improvement of continuous-time NMP linear systems. Other applications of GSHFs include decoupling, exact model-matching, and exact discrete loop transfer recovery of NMP plants [Liu et al., 1992, Paraskevopoulos and Arvanitis, 1994, Er and Anderson, 1994].

Besides the benefits offered by GSHFs, some authors have pointed out the existence of intersample difficulties and serious robustness and sensitivity problems associated with the use of these devices [Araki, 1993, Feuer and Goodwin, 1994, Zhang and Zhang, 1994]. For example, Feuer and Goodwin [1994] have argued that GSHF control relies on the generation of high-frequency harmonics, which tend to make the system more sensitive to high-frequency plant uncertainty, disturbances and noise. As a consequence, the potential utility of GSHFs in overcoming LTI design limitations seems still to be a matter of debate.

Despite these advances in synthesis, there is as yet no well-developed theory of inherent design limitations for hybrid feedback systems. For analog feedback systems, on the other hand, many results on design limitations are available. Bode first stated the sensitivity integral theorem in 1945, whose importance for feedback control was emphasized by Horowitz [1963]. Later extensions were obtained by several researchers; of particular relevance to the present discussion are the results of Freudenberg and Looze [1985] and Middleton [1991]. Briefly, the theory describes how plant properties such as NMP zeros, unstable poles, and time delays limit the achievable performance of a feedback system consisting of a LTI plant and a continuous-time controller. These limitations manifest themselves as tradeoffs between desirable system properties in different frequency ranges, and are expressed mathematically using Bode and Poisson integrals.

A parallel theory of inherent design limitations for purely discrete-time feedback systems is also available [Sung and Hara, 1988, Middleton and Goodwin, 1990, Mohtadi, 1990, Middleton, 1991]. Unfortunately, this theory is insufficient to describe fundamental limitations in hybrid systems. Indeed, discrete-time results do not consider intersample behavior, and therefore do not tell us the whole story (in particular, good sampled behavior is necessary but not sufficient for good overall behavior). The development of an equivalent theory for sampled-data systems is one of the main goals of this thesis.

1.2 Contributions of this Thesis

This thesis is aimed at analysis of sampled-data feedback systems. Our approach is in the frequency-domain, and stresses the study of sensitivity and complementary sensitivity operators. Our main contributions may be summarized as follows:

- (i) We expound a systematic frequency-domain framework to describe sampled-data systems considering full-time information. This framework allows us to study important properties of the system in a way that appears to be simpler than in alternative state-space approaches. There are two reasons why we believe the frequency-domain approach to be simpler. First, this frequency-domain setting has better links with classical frequency-domain analysis for analog control systems, in which a large heuristic knowledge is available. Second, the mathematics involved seems easier to understand and relate to the original plant model.
- (ii) We develop a theory of design limitations for sampled-data systems. This theory allows us to quantify the essential constraints imposed by NMP zeros of the hold function, and NMP zeros and unstable poles of the analog plant and discrete controller. As an application, we quantitatively analyze the sensitivity and robustness properties of control schemes that rely on GSHF discrete zero-shifting capabilities.
- (iii) We derive closed-form expressions to compute the L_2 -induced norms of the hybrid sensitivity and complementary sensitivity operators. These expressions have interesting interpretations in terms of signal spaces associated with the hold, the plant and the anti-aliasing filter. All our formulas admit straightforward implementation in a numerically reliable fashion.
- (iv) We study the frequency-domain properties of GSHFs, providing results that describe in detail their zero-distribution, and some integral relations that their frequency response must satisfy. In particular, these results show the source of some of the difficulties associated with the use of GSHFs.

The framework of (i), and the results of (iii) are valid for multiple-input multiple-output (MIMO) systems. The results in (ii) and (iv) are restricted to the single-input single-output (SISO) case. Due to the issue of directionality, the generalization of these results to multivariable is difficult — for (ii) this is so even in the analog case — and hence we have not pursued it here.

Many of the results referred to in (ii) have been developed in collaboration, and published in Freudenberg et al. [1995] and Freudenberg et al. [1994], with significant input from the first author. The results in (i) and (iii) have been partially communicated in Braslavsky et al. [1995b], while some of the results in (iv) will appear in Braslavsky et al. [1995a].

We now give an overview of the rest of the thesis.

Chapter 2: This chapter introduces most of our notation, main assumptions, and the basic preliminary results upon which the rest of the chapters will be

developed. Here, we define the mathematical representations of the A-D and D-A interfaces, the sampler, and the hold device. A distinctive feature of our approach is that the hold device is not restricted to the ZOH. Indeed, we shall consider that the hold is a GSHF of the type introduced by Kabamba [1987], which will allow us to develop a comprehensive framework to study sampled-data systems. We also present in this chapter a basic but key sampling formula concerning the Laplace transform of a sampled signal. This relation will be the starting point of our discussion on the frequency response of hybrid systems in the following chapters. We conclude with a review of two important results concerning the closed-loop stabilizability properties of sampled-data systems.

Chapter 3: The focus of this chapter is the frequency response of a GSHF. As opposed to that of a ZOH, the frequency response of a GSHF may have large high-frequency peaks that compromise the robustness properties of the system. It is also known that GSHFs may have zeros off the $j\omega$ -axis that pose discrete stabilizability difficulties. In this chapter we go deeper into the analysis of these issues by studying fundamental properties of the frequency response of GSHFs. Specifically, we describe their zero-distribution and the constraints that these zeros impose on the values on the $j\omega$ -axis. One of the main results of this chapter is that GSHFs with “asymmetric” pulse response function will necessarily have zeros off the $j\omega$ -axis.

Chapter 4: In this chapter, we study the frequency response of a sampled-data system, and develop a theory of design limitations wherein we consider the response of the analog system output. To do this, we use the fact that the steady-state response of a hybrid feedback system to a sinusoidal input consists of a fundamental component at the frequency of the input together with infinitely many harmonics, located at frequencies spaced integer multiples of the sampling frequency away from the fundamental. This fact allows us to define fundamental sensitivity and complementary sensitivity functions that relate the fundamental component of the response to the input signal. These sensitivity and complementary sensitivity functions must satisfy integral relations analogous to the Bode and Poisson integrals for purely analog systems. The relations show, for example, that design limitations due to NMP zeros of the analog plant constrain the response of the sampled-data feedback system regardless of whether the discretized system is minimum phase, and independently of the choice of hold function.

Chapter 5: This chapter deals with the analysis and computation of the L_2 -induced norm of operators in sampled-data systems. We first expound a *frequency-domain lifting* technique to derive “closed-form” expressions for the frequency gains of hybrid sensitivity operators in a MIMO setup. We show that these frequency-gains can be characterized by the maximum eigenvalue of certain finite-dimensional discrete transfer matrices; even in the case of the sensitivity operator, which — since it is known to be non-compact — presents extra difficulties for the analysis. The L_2 -induced norm is then

computed by searching the maximum of this eigenvalue over a finite range of frequencies. At the end of the chapter, we provide expressions from which the generation of numerical algorithms to compute these norms is straightforward.

Chapter 6: This chapter is about stability robustness of sampled-data systems. Dullerud and Glover [1993] have derived necessary and sufficient conditions for robust stability of hybrid systems against multiplicative perturbations in the analog system. These authors have used a frequency-domain formulation based on state-space lifting techniques. We show in this chapter that the same type of result may be obtained in a simpler way when the problem is directly formulated in the frequency-domain. We do this by using the frequency-domain lifting framework introduced in Chapter 5. We also give both necessary conditions and sufficient conditions for robust stability as simple expressions that emphasize the role played by the fundamental and harmonic sensitivity functions defined in Chapter 4. We conclude the chapter by showing that the same framework may be used to approach the problem of robust stability against divisive perturbations.

Chapter 7: As an application of the preceding results, in this chapter we study the difficulties associated with the zero-shifting capabilities of GSHFs. Many GSHF-based proposed schemes rely on zero-shifting, since this appears to circumvent fundamental limitations imposed by analog NMP zeros. We show that if the plant has a NMP zero with significant phase lag within the desired closed-loop bandwidth of the system, then zero-shifting will necessarily lead to serious robustness and sensitivity problems in both analog and discrete performances of the system.

Chapter 8: In this chapter we summarize the main results of the thesis, and give some concluding remarks and directions for future research.

2

Preliminaries

This chapter defines most of our notation, and introduces general assumptions and preliminary results required in the sequel. We present a key formula concerning the Laplace transform of a sampled signal that will play an important role in the rest of this thesis. This formula yields the well-known infinite summation expression showing that the response of the discretized plant at a given frequency depends upon that of the analog plant at infinitely many frequencies. We finish the chapter reviewing the basic conditions for closed-loop stability of sampled-data systems; i.e., a non-pathological sampling assumption, and the closed-loop stability of the discretized system.

2.1 Analog and Discrete Signals

2.1.1 Signal Spaces

We start introducing some standard signal spaces. We denote the set of complex numbers by \mathbb{C} . The open and closed right halves of \mathbb{C} are denoted by \mathbb{C}^+ and $\overline{\mathbb{C}^+}$ respectively, and sometimes we shall use the acronyms ORHP and CRHP. Correspondingly, we denote by \mathbb{C}^- and $\overline{\mathbb{C}^-}$ the open and closed left halves of \mathbb{C} , also referred as OLHP and CLHP, respectively. We denote the set of real numbers by \mathbb{R} , and by \mathbb{R}_0^+ we represent the set of non-negative real numbers, i.e., the segment $[0, \infty)$. The open and closed unit disks in \mathbb{C} are denoted by $\mathbb{D} \triangleq \{z : |z| < 1\}$ and $\overline{\mathbb{D}} \triangleq \{z : |z| \leq 1\}$ respectively; we denote their complements by \mathbb{D}^c and $\overline{\mathbb{D}}^c$.

As usual, $L_p^n(\mathbb{R}_0^+)$ denotes the space of Lebesgue measurable functions f from \mathbb{R}_0^+ to \mathbb{R}^n that satisfy

$$\|f\|_{L_p} \triangleq \left(\int_0^\infty |f(t)|^p dt \right)^{1/p} < \infty \quad \text{for } 1 \leq p < \infty,$$

and

$$\|f\|_{L_\infty} \triangleq \operatorname{ess\,sup}_{t \in \mathbb{R}_0^+} |f(t)| < \infty,$$

where $|\cdot|$ denotes the Euclidean norm in \mathbb{R}^n . We denote by $L_{pe}^n(\mathbb{R}_0^+)$ the extended space of $L_p^n(\mathbb{R}_0^+)$, i.e., the space of functions whose truncations to intervals $[0, a)$ are in $L_p^n(\mathbb{R}_0^+)$ for any finite real number a .

In a similar way, L_2^n denotes the space of functions $F(j\omega)$ defined on $j\mathbb{R}$ with values over \mathbb{C}^n and satisfying

$$\|F\|_{L_2} \triangleq \left(\int_{-\infty}^{\infty} |F(j\omega)|^2 d\omega \right)^{1/2} < \infty.$$

Here the Euclidean norm $|\cdot|$ is taken on \mathbb{C}^n , i.e., $|F| = \sqrt{F^*F}$, where F^* denotes the complex conjugate transpose of F . In general, we shall denote the transpose of a matrix M by M^T , and by \bar{M} its conjugate.

In discrete-time we represent by ℓ_p^n the space of sequences $\mathbf{u} \triangleq \{u_k\}_{k=-\infty}^{\infty}$ valued in \mathbb{C}^n and satisfying

$$\|\mathbf{u}\|_{\ell_p} \triangleq \left(\sum_{k=-\infty}^{\infty} |u_k|^p \right)^{1/p} < \infty \quad \text{for } 1 \leq p < \infty,$$

and

$$\|\mathbf{u}\|_{\ell_\infty} \triangleq \sup_k |u_k| < \infty.$$

We shall dispense with the superscript n in the above notations whenever the dimension of the spaces is clear from the context. We shall also omit the subindex that indicates the spaces in the notation of norms $\|\cdot\|$ when they are clear from the context.

We shall represent linear dynamic systems as input-output operators acting on L_p spaces. If \mathcal{M} is a linear operator defined by

$$\begin{aligned} \mathcal{M} &: L_p(\mathbb{R}_0^+) \rightarrow L_p(\mathbb{R}_0^+) \\ &: \mathbf{u} \mapsto \mathbf{y} = \mathcal{M}\mathbf{u}, \end{aligned}$$

the L_p -induced norm of the operator \mathcal{M} is defined as

$$\|\mathcal{M}\|_p \triangleq \sup \left\{ \frac{\|\mathcal{M}\mathbf{y}\|_{L_p}}{\|\mathbf{u}\|_{L_p}} : \text{for } \mathbf{u} \text{ in } L_p(\mathbb{R}_0^+), \text{ and } \|\mathbf{u}\|_{L_p} \neq 0 \right\}.$$

A quick-reference list of the above notations may be found on page 165.

2.1.2 Samplers and Holds

As discussed in Chapter 1, the implementation of a controller for a continuous-time system by means of a digital device, such as a computer, implies the process of sampling and reconstruction of analog signals. By sampling, an analog signal is converted into a sequence of numbers that can then be digitally manipulated. The hold device performs the inverse operation, translating the output of the digital controller into a continuous-time signal. We shall assume throughout that nonlinearities associated with the process of discretization, such as finite memory word-length, quantization, etc., have no significant effect on the sampled-data system.

We assume also that sampling is regular, i.e., if T is the *sampling period*, sampling is performed at instants $t = kT$, with $k = 0, \pm 1, \pm 2, \dots$. Associated with T , we define the *sampling frequency* $\omega_s = 2\pi/T$. By Ω_N we denote the *Nyquist range* of frequencies $[-\omega_s/2, \omega_s/2]$.

We consider an idealized model of the sampler. If y is an analog signal defined on the time set \mathbb{R}_0^+ with values over \mathbb{C}^n , we define the sampling operator with sampling period T , denoted by \mathcal{S}_T , as

$$\mathcal{S}_T\{y\} = \{y_k\}_{k=-\infty}^{\infty}, \quad (2.1)$$

where $\{y_k\}_{k=-\infty}^{\infty}$ is the sequence representing the sampled signal, and $y_k = y(kT^+)$ ¹. Thus, the sampler is a linear, periodically time-varying operator. Note that the sampler operator may be unbounded in many standard signal spaces, as for example from $L_p(\mathbb{R}_0^+)$ to ℓ_p when $1 \leq p < \infty$ Chen and Francis [1991]. Therefore, we need to specify with some care the class of signals that are “sampleable”.

A class of functions that guarantee that the sampling operator is well-defined is the class of functions of *bounded variation* (BV). These functions will be required to define the hold devices we shall deal with, and to assure the validity of a sampling formula that will be the starting point of our approach to sampled-data systems. The following definition is taken from Riesz and Sz.-Nagy [1990].

Definition 2.1.1 (Function of Bounded Variation)

A function f defined over a real interval (a, b) is of BV if the following sum is bounded,

$$\sum_{k=1}^n |f(t_k) - f(t_{k-1})| < \infty, \quad (2.2)$$

for every partition of the interval (a, b) into subintervals (t_k, t_{k-1}) , where $k = 1, 2, \dots, n$, and $t_0 = a, t_n = b$. The least upper bound of the sum in (2.2) is called the *total variation* of f in the interval (a, b) . \diamond

A function of BV is not necessarily continuous, but it is differentiable almost everywhere and its derivative is a function in $L_1(a, b)$ Rudin [1987]. Moreover, the limits $f(t^+)$ and $f(t^-)$ are well defined for every t in (a, b) , which means that f can have discontinuities of at most the *finite-jump* type.

The hold device that we shall consider is a GSHF *a la* Kabamba [1987], defined by the operation

$$u(t) = h(t - kT) u_k, \quad \text{for } kT \leq t < (k + 1)T, \quad (2.3)$$

where $\{u_k\}_{k=-\infty}^{\infty}$ is a discrete sequence, and h is a bounded function with support on the interval $[0, T)$. We consider the case in which the sequence $\{u_k\}_{k=-\infty}^{\infty}$ takes values in \mathbb{R}^p , and so h takes values in $\mathbb{R}^p \times \mathbb{R}^p$. We shall assume throughout that h satisfies the following technical conditions.

¹Here, $y(kT^\pm)$ denotes the *right (left) limit* of $y(\cdot)$ at $t = kT$, i.e.,

$$y(kT^\pm) \triangleq \lim_{\epsilon \downarrow 0} f(kT \pm \epsilon), \quad \text{for } \epsilon > 0,$$

whenever the limit exists.

Assumption 1

The hold function h is a function of BV on $[0, T)$. ◦

As discussed in Middleton and Freudenberg [1995], we can associate a *frequency response function* to this hold device, defined by

$$H(s) = \int_0^T e^{-st} h(t) dt. \quad (2.4)$$

Since h is supported on a finite interval, it follows that H is an entire function, i.e., analytic at every s in \mathbb{C} . For example, in the case of the ZOH we have the well-known response $H(s) = (1 - e^{-sT})/s$. Frequency responses of other types of holds will be studied in detail in Chapter 3.

We shall be particularly interested in the *zeros* of the response function H . These have transmission blocking properties, and may affect the stabilizability of the discretized system Middleton and Freudenberg [1995]. Furthermore, as we shall see in Chapter 4, they are an important factor in analysis of the achievable performance of the sampled-data system.

Definition 2.1.2 (Zeros of the Hold Middleton and Freudenberg [1995])

Consider a response function defined by (2.4) and suppose that $\det(H)$ is not identically zero. Then the *zeros* of H are those values s in \mathbb{C} for which $H(s)$ has less than full rank. ◊

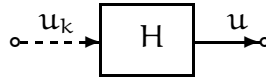


Figure 2.1: Response of a GSHF.

The frequency response of the hold defined in (2.4) is useful to compute the Laplace transform of the output of the hold device (see Figure 2.1). As described in Middleton and Freudenberg [1995], the i -th column of the frequency response function (2.4) represents the Laplace transform of the output of the hold to an unitary pulse in the i th input. More generally, if U_d is the \mathcal{Z} -transform of the input sequence $\{u_k\}_{k=-\infty}^{\infty}$, then we have the following Åström and Wittenmark [1990].

Lemma 2.1.1

Consider the hold defined by (2.3) and its associated frequency response (2.4). Then

$$U(s) = H(s) U_d(e^{sT}).$$

◦

GSHFs have been proposed as a more versatile alternative to the traditional ZOH [see for example Kabamba, 1987], and indeed, recent studies have shown that if a solution to the sampled-data H_∞ control problem exists, then it may be realized by a LTI discrete controller and a GSHF Sun et al. [1993]. Nevertheless, these devices certainly are much more complex to be implemented and — as some authors have suggested and we shall expand on — they may bring in serious intersample difficulties.

2.1.3 A Key Sampling Formula

Our approach to sampled-data systems is in the frequency-domain. We now present a result that is essential to the understanding of the frequency-domain properties of sampled-data systems and will play a central role throughout the following chapters. Unfortunately, despite the fact that the result is well-known and appears in many textbooks [e.g., Åström and Wittenmark, 1990, Franklin et al., 1990, Kuo, 1992, Ogata, 1987], it is difficult to find in the literature a proof that is rigorous and self-contained, and which clearly delineates the classes of signals to which it is applicable. Indeed, this fact has stimulated discussion in the past [cf. Pierre and Kolb, 1964, Carroll and W.L. McDaniel, 1966, Phillips et al., 1966, 1968].

Let g be a function of BV in every finite interval of \mathbb{R}_0^+ , and let G be its Laplace transform,

$$G(s) = \int_0^\infty e^{-st} g(t) dt.$$

If σ_G is the abscissa of absolute — and uniform — convergence of G , we denote by \mathcal{D}_G the strip

$$\mathcal{D}_G \triangleq \{s = x + jy, \text{ with } x > \sigma_G \text{ and } y \text{ in } \Omega_N\}.$$

Given a sequence $\{g_k\}_{k=0}^\infty$, we introduce the \mathcal{Z} -transform, $G_d = \mathcal{Z}\{\{g_k\}\}$, defined by

$$G_d(z) = \sum_{k=0}^{\infty} g_k z^{-k}. \quad (2.5)$$

For a continuous-time signal g defined on \mathbb{R}_0^+ , and $g(t) = 0$ for $t < 0$, we define the \mathcal{Z} -transform as the transformation of its sampled version,

$$\begin{aligned} G_d(z) &= \mathcal{Z}\{\mathcal{S}_T\{g\}\} \\ &= \sum_{k=0}^{\infty} g(kT^+) z^{-k}. \end{aligned}$$

Then we have the following lemma.

Lemma 2.1.2

If g is a function of BV in every finite interval of \mathbb{R}_0^+ , then for every s in \mathcal{D}_G

$$G_d(e^{sT}) = \frac{g(0^+)}{2} + \sum_{k=1}^{\infty} \frac{g(kT^+) - g(kT^-)}{2} e^{-skT} + \frac{1}{T} \sum_{n=-\infty}^{\infty} G(s + jn\omega_s). \quad (2.6)$$

Proof: See Appendix A, §A.1. \square

Lemma 2.1.2 shows the well-known fact that the frequency response of a sampled signal is built upon the superposition of infinitely many copies of the original frequency response of the signal. If the signal has finite discontinuities at the sampling instants, then correction terms of half of the jumps at the corresponding sampling instants have to be included — cf. the property of the Laplace and Fourier inverse transforms which converge to the average of the limits of the function from left and right at a jump discontinuity. In particular, (2.6) is closely related to an important identity in Fourier analysis known as the *Poisson Summation Formula*². See further remarks in Appendix A, §A.1.

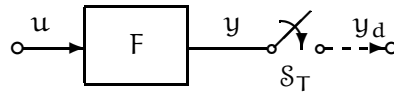


Figure 2.2: Filtered sampling.

represents a common practice in digital control engineering, i.e., to precede the sampler by an anti-aliasing filter, and is also required for the the sampling operation to be well-defined [e.g., Chen and Francis, 1991].

Corollary 2.1.3

Let u be a signal in $L_1e(\mathbb{R}_0^+)$, and let F be a strictly proper rational function. Then for every s in \mathcal{D}_{FU}

$$(FU)_d(e^{sT}) = \frac{1}{T} \sum_{n=-\infty}^{\infty} F(s + jn\omega_s)U(s + jn\omega_s).$$

Proof: Immediate from Lemma 2.1.2 by noting that the response of a FDLTI strictly proper system to an input in $L_1e(\mathbb{R}_0^+)$ is continuous [e.g., Desoer and Vidyasagar, 1975], so $y(t^+) = y(t^-)$ for every t . In particular, since $y(t) = 0$ for $t < 0$, this also implies that $y(0) = 0$, and the result then follows. \square

The second corollary deals with sampling the pulse response of a hold function followed by a FDLTI strictly proper system, and displays the relation between the discrete equivalent of this cascade and the corresponding continuous-time Laplace transforms (see Figure 2.3).

Corollary 2.1.4

Let H be a hold frequency-response function as described in Subsection 2.1.2 and P a strictly proper rational function. Let $(PH)_d$ denote the discrete equivalent of the cascade connection PH defined as

$$(PH)_d(z) = \mathcal{Z}\{S_T\{\mathcal{L}^{-1}\{P(s)H(s)\}\}\}.$$

²This is the following Rudin [1987]. If G is the Fourier transform of g , then

$$\sum_{k=-\infty}^{\infty} g(k\alpha) = \beta \sum_{k=-\infty}^{\infty} G(jk\beta),$$

where $\alpha > 0$, $\beta > 0$, and $\alpha\beta = 2\pi$. Although named after S.D. Poisson, this formula seems to have been first discovered by A.L. Cauchy in 1817 [Grattan-Guinness, 1990, p. 793].

Then for every s in \mathcal{D}_P ,

$$(\text{PH})_d(e^{sT}) = \frac{1}{T} \sum_{n=-\infty}^{\infty} P(s + jn\omega_s) H(s + jn\omega_s). \quad (2.7)$$

Proof: Since the pulse response of H is of BV by assumption, we then have that the output of P is continuous Desoer and Vidyasagar [1975]. The result then follows from Lemma 2.1.2. \square

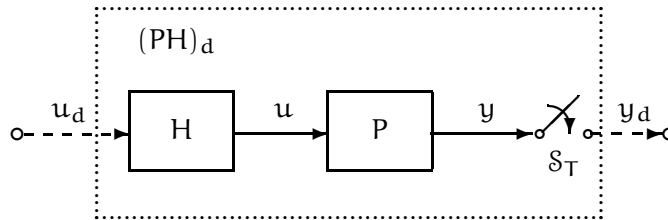


Figure 2.3: Discrete equivalent of the cascade of a hold and a FDLTI system.

Note that the domains of validity of these results can be further extended by analyticity of Laplace transforms.

Equation (2.7) appears in many digital control textbooks [e.g., Åström and Wittenmark, 1990, Franklin et al., 1990], and it has been the starting point of a number of recent frequency-domain approaches to sampled-data systems Goodwin and Salgado [1994], Araki and Ito [1993], Araki et al. [1993], Freudenberg et al. [1995]. Some authors refer to (2.7) as the *impulse modulation formula* [e.g., Araki and Ito, 1993, Araki et al., 1993].

2.2 Hybrid Systems

2.2.1 Basic Feedback Configuration

The basic feedback system of study is shown in Figure 2.4. The analog plant is a linear time-invariant system represented by the transfer matrix P , and the controller is given by the discrete transfer matrix C_d . The digital controller interfaces with the analog parts of the system by a sampler \mathcal{S}_T and a hold function H as described in Subsection 2.1.2. The transfer matrix F represents the anti-aliasing filter.

Signals in Figure 2.4 are as follows,

r reference input,	u_k discrete control sequence,
y plant output,	u analog control signal,
d output disturbance,	v analog output of the filter,
n sensor noise,	v_k sampled output of the filter.

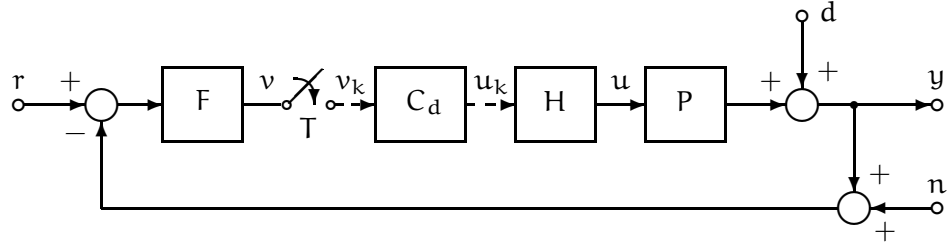


Figure 2.4: Sampled-data control system.

Analog signals are given as functions defined over t in \mathbb{R}_0^+ , while discrete signals are sequences defined at entire multiples k of the sampling time T . We shall assume that the input signals satisfy the following condition.

Assumption 2

The reference signal r , disturbance d , and noise n are functions in $L_{1e}(\mathbb{R}_0^+)$. \circ

It is straightforward to verify that this assumption is satisfied by signals that are steps, ramps, sinusoids or exponentials, and signals in $L_p(\mathbb{R}_0^+)$ for $1 \leq p \leq \infty$ Chen and Francis [1991]. Signals that contain impulses are excluded.

We shall assume throughout that the following conditions are satisfied by the plant, filter, and compensator.

Assumption 3

The plant, filter, and compensator are full column rank rational transfer matrices, each free of unstable hidden modes, and they satisfy the following additional hypotheses,

(i) $P(s) = P_0(s) e^{-s\tau}$, where P_0 is proper and $\tau \geq 0$,

(ii) F is strictly proper, stable and minimum-phase, and

(iii) C_d is proper. \circ

The assumption that the filter F is strictly proper is standard and guarantees that the sampling operation is well-defined [e.g., Chen and Francis, 1991, Sivashankar and Khargonekar, 1993]. The assumptions that F has no poles or zeros in $\overline{\mathbb{C}^+}$ may be removed, and are only invoked to facilitate discussion. In practice anti-aliasing filters will satisfy these assumptions.

We define the *discretized plant* as the discrete transfer function of the series connection of hold, plant, filter, and sampler,

$$(FPH)_d(z) \triangleq \mathcal{Z}\{\mathcal{S}_T\{\mathcal{L}^{-1}\{F(s)P(s)H(s)\}\}\}. \quad (2.8)$$

It follows from Assumptions 1 and 3, and Corollary 2.1.4 that the discretized plant satisfies the well-known relation

$$(\text{FPH})_d(e^{sT}) = \frac{1}{T} \sum_{k=-\infty}^{\infty} F_k(s) P_k(s) H_k(s), \quad (2.9)$$

where the notation $F_k(s)$ represents $F(s + jk\omega_s)$, i.e., the shift of $F(\cdot)$ by an entire number of times the sampling frequency in the direction of the imaginary axis. We shall use this notation throughout this thesis.

Suppose now that in the loop of Figure 2.4 we assume $r = 0$ and consider a disturbance x at the input of the plant. Introduce a fictitious hold at x , and shift the filter and sampler to the inputs at the summation point of n , as shown in Figure 2.5. From this diagram we obtain the discrete loop of Figure 2.6.

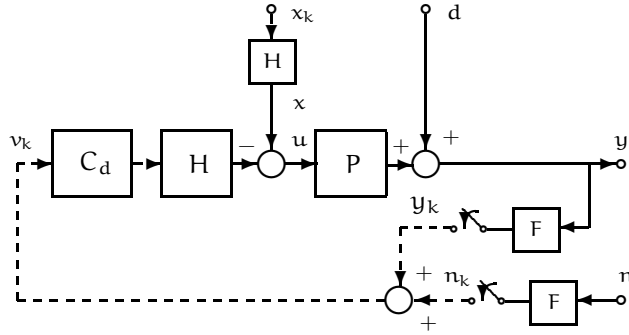


Figure 2.5: Sampled-data system with input disturbances.

We now define the discrete sensitivity and discrete complementary sensitivity functions. Since the setup is multiple-input multiple output, there are two pairs of functions corresponding to the scalar ones, depending where the loop is opened Freudenberg and Looze [1988]. We shall require only the following *input discrete sensitivity function*,

$$S_d(z) \triangleq [I + C_d(z)(\text{FPH})_d(z)]^{-1}, \quad (2.10)$$

and *output discrete complementary sensitivity function*,

$$T_d(z) \triangleq (\text{FPH})_d(z)S_d(z)C_d(z). \quad (2.11)$$

These functions map signals in the discrete loop of Figure 2.6 as

$$\tilde{U}_d(z) = S_d(z)X_d(z) \quad \text{and} \quad Y_d(z) = T_d(z)N_d(z),$$

where \tilde{U}_d , X_d , Y_d , and N_d correspond to the \mathcal{Z} -transforms of the signals \tilde{u}_x , x_k , y_k , and n_k , respectively.

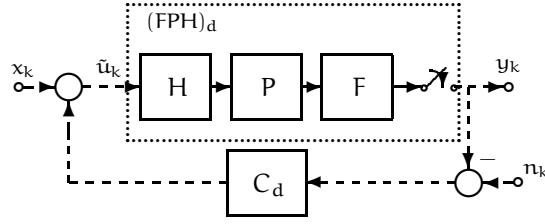


Figure 2.6: Discrete sensitivity functions.

2.2.2 Non-pathological Sampling and Internal Stability

As with the case of a ZOH, closed-loop stability is guaranteed by the assumptions that sampling is non-pathological and that the discretized system is closed-loop stable. The next result is a generalization of the well-known result of Kalman et al. [1963] to the case of GSHFs.

Lemma 2.2.1 (Non-pathological Sampling, Middleton and Freudenberg [1995]) Suppose that P and F are as defined in Subsection 2.2.1 and assume further that

(i) if λ_i and λ_k are CRHP poles of P , then

$$\lambda_i \neq \lambda_k + jn\omega_s, \quad n = \pm 1, \pm 2, \dots \quad (2.12)$$

(ii) if λ_i is a CRHP pole of P , then $H(s)$ has no zeros at $s = \lambda_i$.

Then the discretized plant (2.8) is free of unstable hidden modes. \circ

In particular, Lemma 2.2.1 says that since the response of a GSHF may have zeros in $\overline{\mathbb{C}^+}$, it may be necessary to require that none of these coincides with an unstable pole of the analog plant (note that this *is* necessary in the SISO case). Under the non-pathological sampling hypothesis, it is straightforward to extend the exponential and L_2 input-output stability results of Francis and Georgiou [1988] and Chen and Francis [1991] to the case of GSHF.

Lemma 2.2.2

Suppose that P , F , C_d , and H are as defined in Subsections 2.1.2 and 2.2.1, that the nonpathological sampling conditions (i) - (ii) are satisfied, that the product $(FPH)_d C_d$ has no pole-zero cancelations in \mathbb{D}^c , and that all poles of S_d lie in \mathbb{D} . Then the feedback system in Figure 2.4 is exponentially stable and L_2 input-output stable.

Proof: The proof may be obtained by simple modification of the proofs of Francis and Georgiou [1988, Theorem 4] and Chen and Francis [1991, Theorem 6]. \square

Lemma 2.2.2 establishes the conditions for the nominal stability of the sampled-data system of Figure 2.4, and will be required in most of the remaining chapters. In particular, this result guarantees that the operators mapping disturbances and noise to the output are bounded on L_2 . This will be the starting point for the analysis developed in Chapter 5.

2.3 Summary

This chapter has introduced the main notation, definitions, and preliminary results that will be required in the rest of this thesis.

Generalized Sampled-data Hold Functions

Generalized Sampled-data Hold Functions [e.g., Kabamba, 1987, Bai and Dasgupta, 1990, Yan et al., 1994, Er et al., 1994] have been proposed as an approach to several control problems that do not have answers with analog LTI, or traditional sampled-data settings based on the ZOH. GSHF-based control schemes are sampled-data systems where the D-A conversion is performed using a special waveform instead of the constant function generated by the ZOH (see Figure 3.1). The choice of this waveform is an additional degree of freedom incorporated to the design, and it seems to give a number of advantages over other control schemes. For example, it has been recently shown that if there exist a solution to the H_∞ control problem for sampled-data systems, then this solution can be implemented by a GSHF following a LTI discrete controller. [e.g., Sun et al., 1993].

However, serious robustness and sensitivity problems associated with the use of GSHFs have been pointed out by some authors Feuer and Goodwin [1994], Zhang and Zhang [1994] showing that many of the most impressive features of GSHFs come along with quite undesirable “side-effects”. For example, Feuer and Goodwin [1994] have shown that the arbitrary shaping of the sampled frequency response of a system by means of a GSHF necessarily relies on the generation of high frequency components in the continuous-time output. This exposes the mechanism by which sensitivity and robustness properties of the system are compromised, since in practice high frequency uncertainty is very common.

Furthermore, as we shall see in Chapter 4, there are essential continuous-time design limitations that are inherited by the sampled-data system, irrespective of the particular discretization method employed. Particularly linked to these issues are the frequency response and the zeros of the hold device. It turns out, for example, that “non-minimum phase” holds, i.e., holds with zeros in \mathbb{C}^+ , impose extra limitations in the achievable continuous-time performance of the system. These “non-minimum phase” zeros of the hold may also lead to poorly conditioned discretized systems, as has been discussed by Middleton and Freudenberg [1995] and Middleton and Xie [1995].

In this chapter, we study the frequency response and zero distribution of GSHFs. The results obtained here allow us to go deeper into the understanding

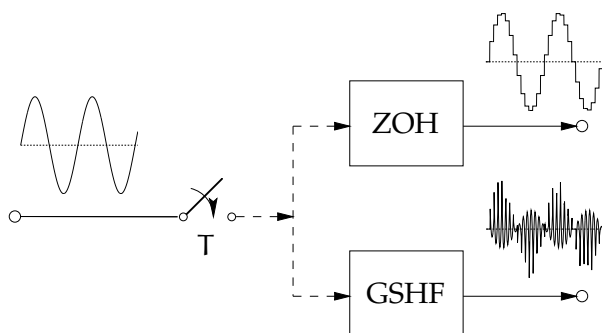


Figure 3.1: D-A conversion with ZOH and GSHF

of the design tradeoffs associated with the use of these devices. For example, one of the key results of this chapter is that holds with “asymmetric” pulse response will necessarily have zeros off the $j\omega$ -axis, which may lead to the aforementioned difficulties.

The organization of the chapter is as follows. In §3.1, we collect several properties of the frequency response of a GSHF. Among these properties are some interesting relations between the frequency response of a generalized hold and that of a ZOH. The distribution of zeros of GSHFs is the theme of §3.2. In §3.3, we establish some connections between these zeros and the values of the frequency response on the $j\omega$ -axis. Finally, we provide some concluding remarks in §3.4.

3.1 Frequency Response of Generalized Sampled-data Holds

The most standard and simplest D-A converter in digital control implementations is the ZOH. Given a discrete input sequence $\{u_k\}_{k=0}^{\infty}$, the ZOH is defined by

$$u(t) = u_k, \quad \text{for } kT \leq t < (k+1)T.$$

In particular, the ZOH can be seen as a particular case of the GSHF defined in (2.3) with the hold function

$$h(t) = \begin{cases} 1 & t \in [0, T) \\ 0 & \text{otherwise} \end{cases}$$

(see Figure 3.2).

The idea of a GSHF is to allow h to be some suitably chosen function instead of just holding the discrete values constant during the sampling interval. In this way a new degree of freedom is introduced in the sampled-data control design problem, in addition to the choice of the discrete controller.

In this section we present some preliminary results concerning the frequency response of a GSHF. In Subsections 3.1.1 and 3.1.2, we obtain some general properties of the frequency response of a GSHF, norms and reconstruction from boundary values. These properties are intimately linked to the fact that GSHF frequency

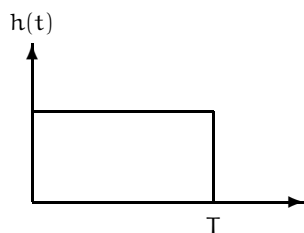


Figure 3.2: Pulse response of a ZOH.

responses are entire functions, as we noted in Subsection 2.1.2. In Subsection 3.1.3 we introduce two important characterizations of GSHFs common in the literature, namely, GSHFs where h is the truncated pulse response of a dynamic system, and GSHFs where h is a piecewise-constant function.

3.1.1 Norms and the Frequency Response of a GSHF

Let H be the frequency response of a GSHF defined by (2.4). Since h is of BV on $[0, T]$ by Assumption 1, then h is in $L_2(0, T)$, that is

$$\|h\|_2^2 = \int_0^T |h(t)|^2 dt < \infty.$$

A well-known result of Paley and Wiener [1934] says that the Laplace transform of a square integrable function vanishing outside the interval $(-T, T)$ is an entire function of order 1 and type¹ T . Moreover, since h actually vanishes outside $[0, T]$, the function H is uniformly bounded in the closed right half plane. Indeed, we can easily check this from the following inequalities, which follow as a trivial application of Cauchy-Schwarz Inequality.

$$\begin{aligned} |H(re^{j\theta})|^2 &\leq \left(\int_0^T |h(t)|^2 dt \right) \left(\int_0^T e^{-2rt \cos \theta} dt \right) \\ &= \|h\|_2^2 \left(\frac{1 - e^{-2rT \cos \theta}}{2r \cos \theta} \right). \end{aligned} \quad (3.1)$$

Now, we can see from (3.1) that if the angle θ is on the interval $[-\pi/2, \pi/2]$, then

$$|H(re^{j\theta})| \leq \sqrt{T} \|h\|_2. \quad (3.2)$$

In particular, (3.2) tells us that if the infinity norm, $\|H\|_\infty = \sup_\omega |H(j\omega)|$, is large, then the 2-norm,

$$\|H\|_2 = \left(\int_{-\infty}^{\infty} |H(j\omega)|^2 d\omega \right)^{1/2},$$

¹The order and type of an entire function quantify its growth properties, see Appendix B for a brief description.

will also be large, since by Parseval's Formula $\|H\|_2 = \sqrt{2\pi} \|h\|_2$.

Another interesting connection between frequency and time domain values is given by the following lemma [cf. Yamamoto and Araki, 1994, Lemma 3.3].

Lemma 3.1.1 (Parseval's Equality for Holds)

For any real number ω and any H defined by (2.4),

$$\frac{1}{T} \sum_{k=-\infty}^{\infty} |H(j\omega + jk\omega_s)|^2 = \|h\|_2^2 \quad (3.3)$$

Proof: Consider the function $f_\omega(t) = h(t) e^{-j\omega t}$, with support on the interval $[0, T)$. Its Fourier series representation is

$$f_\omega(t) = \sum_{k=-\infty}^{\infty} c_k e^{jk\omega_s t}, \quad \text{for } t \text{ in } [0, T)$$

where the Fourier coefficients are

$$\begin{aligned} c_k &= \frac{1}{T} \int_0^T f_\omega(t) e^{-jk\omega_s t} dt \\ &= \frac{1}{T} H(j\omega + jk\omega_s) \end{aligned} \quad (3.4)$$

Hence, by Parseval's Formula we have that

$$\frac{1}{T} \int_0^T |f_\omega(t)|^2 dt = \sum_{k=-\infty}^{\infty} |c_k|^2.$$

The result is then obtained by noting that $|f_\omega(t)| = |h(t)|$, and replacing c_k from (3.4). \square

An interpretation in terms of frequency aliasing can be given to the above result. Suppose that $H(0) \neq 0$, i.e., the hold has non-zero *DC-gain*, and (without loss of generality) assume that $H(0) = 1$. If $|H(j\omega)|$ has a large peak, say $\|H\|_\infty \gg 1$, then from (3.2) and (3.3) follows that

$$\sum_{k=-\infty}^{\infty} |H(j\omega + jk\omega_s)|^2 \gg 1. \quad (3.5)$$

Hence, evaluation of (3.5) at small values of ω still gives a large sum, and so there must be a significant number of other terms ($k \neq 0$) adding to $|H(j\omega)|$ to give a large 2-norm. Thus, a peak of $|H(j\omega)|$ necessarily implies a lot of frequency "folding" going on. In particular, note that since H_{ZOH} has zeros at integer multiples of the sampling frequency ω_s , then the ZOH has the minimum L_2 -norm over all the holds that satisfy $H(0) = 1$.

Yet a last property of GSHFs gives us the "gain" of the hold viewed as an input-output operator. Let \mathcal{H} denote the hold operator mapping ℓ_p to L_p , $1 \leq p \leq \infty$, defined by (2.3). The lemma below is a generalization to GSHFs of a result for the ZOH in Francis [1991].

Lemma 3.1.2 (Input-output norm of a hold operator)

The hold operator $\mathcal{H} : \ell_p \rightarrow L_p$ is bounded and of norm $\|\mathcal{h}\|_p$.

Proof: We prove this for $p < \infty$; the case $p = \infty$ follows similar steps. Let u be a function in L_p , and $v = \{v_k\}_{k=-\infty}^{\infty}$ a sequence in ℓ_p , such that $u = \mathcal{H}v$. Then,

$$\begin{aligned} \|u\|_p^p &= \int_{-\infty}^{\infty} |u(t)|^p dt \\ &= \sum_{k=-\infty}^{\infty} \int_{kT}^{(k+1)T} |h(t-kT)v_k|^p dt \\ &= \left(\int_0^T |h(t)|^p dt \right) \left(\sum_{k=-\infty}^{\infty} |v_k|^p \right) \\ &= \|\mathcal{h}\|_p^p \|v\|_p^p. \end{aligned}$$

□

In particular, Lemma 3.1.2 tells us that the induced norm of the hold operator in the case of bounded-input, bounded-output (BIBO) spaces ($p = \infty$) is precisely $\|\mathcal{h}\|_{\infty}$. Therefore, we see that a large value of $\|\mathcal{h}\|_{\infty}$ implies a “high gain” hold, viewed as a BIBO device. Combining (3.2) with the fact that $\|\mathcal{h}\|_2 \leq \sqrt{T} \|\mathcal{h}\|_{\infty}$, we obtain

$$\|\mathcal{H}\|_{\infty} \leq T \|\mathcal{h}\|_{\infty}.$$

So, we see that, for a given sampling rate, a large peak in $|H(j\omega)|$ also implies a large BIBO gain. Since the output of the hold is typically the input to the plant, such large gain may introduce serious difficulties due to actuator saturations, present in most real systems Gilbert [1992].

3.1.2 GS HF Frequency Responses from Boundary Values

Analytic functions can be reconstructed from their boundary values by means of integral formulas like Poisson’s or Cauchy’s [e.g., Hoffman, 1962]. Not surprisingly, since they are entire functions, GS HF frequency responses can be recovered from similar relations. The interesting fact is that the frequency response of a ZOH is involved in these reconstructions. In this subsection we present two results on reconstruction from boundary values of the frequency response of a GS HF.

Denote by H_{ZOH} the response of a ZOH,

$$H_{\text{ZOH}}(s) = \frac{1 - e^{-sT}}{s}.$$

The following lemma is a straightforward consequence of the Fourier representation of h [See also Feuer and Goodwin, 1996].

Lemma 3.1.3 (Hold Response from Boundary Values: “Discrete” Version)

For any complex number s and any H defined by (2.4),

$$H(s) = \frac{1}{T} \sum_{k=-\infty}^{\infty} H(jk\omega_s) H_{ZOH}(s - jk\omega_s) \quad (3.6)$$

Proof: Expand h into Fourier series,

$$h(t) = \sum_{k=-\infty}^{\infty} c_k e^{jk\omega_s t}, \quad \text{where } c_k = \frac{1}{T} \int_0^T h(t) e^{-jk\omega_s t} dt = H(jk\omega_s). \quad (3.7)$$

Then, the Laplace transform of (3.7) gives

$$H(s) = \frac{1}{T} \sum_{k=-\infty}^{\infty} H(jk\omega_s) \frac{1 - e^{-sT}}{s - jk\omega_s},$$

completing the proof. \square

Interestingly, there exists a — not so obvious — “continuous” version of the above formula, arising from properties of Paley-Wiener spaces of entire functions De Branges [1968].

Lemma 3.1.4 (Hold Response from Boundary Values: “Continuous” Version)

For any complex number s and any H defined by (2.4),

$$H(s) = \frac{1}{2\pi} \int_{-\infty}^{\infty} H(j\omega) H_{ZOH}(s - j\omega) d\omega \quad (3.8)$$

Proof: If f is a function that vanishes outside the interval $[-T/2, T/2]$, and its Laplace transform, F , is such that $\int_{-\infty}^{\infty} |F(j\omega)|^2 d\omega < \infty$, then F is an entire function of type $T/2$ [De Branges, 1968, p. 45]. Moreover, for any complex number s ,

$$F(s) = \int_{-\infty}^{\infty} F(j\omega) \frac{\sinh(j\omega T/2 - sT/2)}{\pi(j\omega - s)} d\omega. \quad (3.9)$$

Applying (3.9) to the function $H(s) e^{-sT/2}$ gives the result. \square

3.1.3 Two Simple Classes of GSHFs

To further study properties of the frequency responses of GSHFs we need to describe them in greater detail. In this subsection we present two different classes of GSHFs that are important for their simple mathematical description. These holds have been suggested by different authors, and were studied in the present formulation by Middleton and Freudenberg [1995].

The first class of GSHFs is characterized by a pulse response h generated as the response of a finite dimensional linear time-invariant system truncated to have support on the interval $[0, T)$ (see Figure 3.3). This family covers, for example, the type of GSHFs suggested by Kabamba [1987] to achieve simultaneous

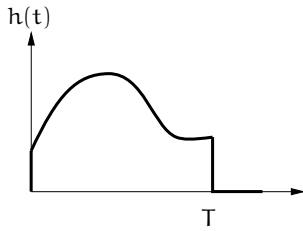


Figure 3.3: Pulse response of a FDLTI GSHF.

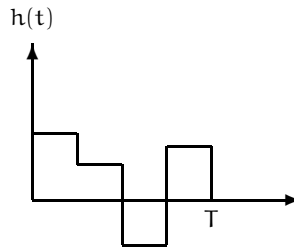


Figure 3.4: Pulse response of a PC GSHF.

stabilization of a finite number of continuous-time plants, decoupling, discrete model matching, discrete simultaneous optimal noise rejection, and arbitrary gain-margin improvement [See also Bai and Dasgupta, 1990, Liu et al., 1992, Had-dad et al., 1994, Yang and Kabamba, 1994, Paraskevopoulos and Arvanitis, 1994].

Definition 3.1.1 (Finite Dimensional Linear Time-invariant GSHF)

Given suitably dimensioned matrices K , L and M , we define a finite dimensional linear time-invariant GSHF (FDLTI GSHF) by the pulse response

$$h(t) = Ke^{L(T-t)}M, \quad \text{for } t \in [0, T]. \quad (3.10)$$

◇

FDLTI GSHFs have a simple and convenient model for analysis and design of GSHF-based control systems. Yet, this model still seems an impractical scheme for implementation.

The second class of GSHFs is characterized by a piecewise-constant pulse response function h , typically with a regular partition of N subintervals of the sampling interval $[0, T)$ (see Figure 3.4). Clearly [*e.g.* Yan et al., 1994], this type of holds can arbitrarily approximate any GSHF of the form (3.10) by taking N sufficiently large and, in addition, appears as a much more feasible alternative for a practical implementation. Holds of this class have been suggested for discrete loop transfer recovery, and arbitrary gain-margin improvement of continuous-time non-minimum phase linear systems [Yan et al., 1994, Er et al., 1994, Er and Anderson, 1994].

Definition 3.1.2 (Piecewise-constant GSHF)

A piecewise-constant GSHF (PC GSHF) is given by the following pulse response:

$$h(t) = \begin{cases} a_0 & \text{if } t \in [0, T/N), \\ a_1 & \text{if } t \in [T/N, 2T/N), \\ \dots & \dots \\ a_{N-1} & \text{if } t \in [(N-1)T/N, T). \end{cases} \quad (3.11)$$

◇

The frequency response functions for FDLTI and PC GSHFs can be easily computed from their definitions, and are given by the following lemmas taken from Middleton and Freudenberg [1995].

Lemma 3.1.5 (Frequency Response Function of a FDLTI GSHF)

The frequency response function of a FDLTI GSHF defined by (3.10) is:

$$H(s) = K(sI + L)^{-1}(e^{LT} - e^{-sT}I)M. \quad (3.12)$$

◦

Lemma 3.1.6 (Frequency Response Function of a PC GSHF)

The frequency response function of a PC GSHF defined by (3.11) is:

$$H(s) = \frac{1 - e^{-sT/N}}{s} A_d(e^{-sT/N}), \quad (3.13)$$

where $A_d(z)$ is the polynomial

$$A_d(z) \triangleq \sum_{k=0}^{N-1} a_k z^k. \quad (3.14)$$

◦

In the rest of the chapter we shall assume that the following additional condition is satisfied by the pulse response h .

Assumption 4

The hold function h is non-zero almost everywhere in neighborhoods of $t = 0$ and $t = T$. ◦

This is a technical condition required only for simplicity of analysis; it may be removed at the expense of more complexity in the notation. This assumption may be interpreted as that the hold pulse response h has “effective” support on the whole interval $[0, T)$, e.g., no pure time-delays. This is clearly satisfied by FDLTI GSHFs, as is easily seen from (3.12). For PC GSHFs Assumption 4 is equivalent to $a_0 \neq 0 \neq a_{N-1}$.

3.2 Distribution of Zeros of GSHFs

Zeros of a hold response function have important connections with fundamental properties of the sampled-data system. For example, Middleton and Freudenberg [1995] have shown that these zeros have transmission blocking properties and can also affect the stabilizability properties of the discretized system (cf. §2.2.2 in Chapter 2). Furthermore, zeros of the hold in \mathbb{C}^+ impose design tradeoffs in the achievable performance of the sampled-data system, as we shall see in Chapter 4.

This section focuses on the distribution of zeros of the hold frequency response H . In Subsection 3.2.1 we describe the precise location and asymptotic

distribution of the zeros of PC and FDLTI holds. Apart from the mentioned effects of “non-minimum phase” zeros on the system performance, it turns out — and we shall see it in §3.3 — that *all* zeros compromise the shape of the hold frequency response on the $j\omega$ -axis. In Subsection 3.2.2, we derive a necessary condition for these GSHFs to have frequency responses with all their zeros on the $j\omega$ -axis. We finish in Subsection 3.2.3 with an example that illustrates these results.

3.2.1 Zeros of PC and FDLTI GSHFs

It is difficult to make general statements about the distribution of the zeros of a GSHF. However, for important special cases, the locations and asymptotic distribution of these zeros can be described precisely. The following lemma characterizes exhaustively the zeros of PC holds, which are the GSHFs of greatest practical significance.

Lemma 3.2.1 (Zeros of a Piecewise-constant GSHF)

Consider a GSHF given by (3.11) with associated frequency response function H given by (3.13) and (3.14). Then the zeros of H are at

$$s = j\ell N\omega_s, \quad \text{where } \ell = \pm 1, \pm 2, \dots, \quad (3.15)$$

and

$$s = -\frac{N}{T} \log \xi_i + jkN\omega_s, \quad \text{with } k = 0, \pm 1, \pm 2, \dots, \quad (3.16)$$

where ξ_i , with $i = 1, 2, \dots, N$, is any zero of $A_d(z)$.

Proof: From Lemma 3.1.6, H can be written as (3.13). The zeros of

$$\frac{1 - e^{-sT/N}}{s}$$

are given by (3.15). It remains, therefore, to determine the zeros of $A_d(e^{-sT/N})$, which are given precisely by (3.16). The assumption that $a_0 \neq 0$ implies that $\xi_i \neq 0$ for every i , and hence $\log \xi_i$ is defined. \square

This result tells us that the zeros of a PC GSHF are essentially determined by those of the polynomial A_d , and the sampling period.

Zeros of FDLTI holds are harder to determine, but we can say something in particular cases. Consider a hold defined by (3.10), and suppose that h is not identically zero. Let m and n be the smallest nonnegative integers such that

$$h^{(m)}(0^+) \neq 0 \quad \text{and} \quad h^{(n)}(T^-) \neq 0, \quad (3.17)$$

where $h^{(k)}$ denotes the k th-derivative of h . We define

$$\eta \triangleq \frac{h^{(m)}(0^+)}{h^{(n)}(T^-)}, \quad (3.18)$$

which, for the particular case of FDLTI GSHFs, equals

$$\eta = \frac{K(-L)^m e^{L^T M}}{K(-L)^n M}.$$

Then we have the following result concerning the asymptotic locations of the zeros of FDLTI GSHFs.

Lemma 3.2.2 (High Frequency Zeros of a FDLTI GSHF)

If H is the frequency response of a FDLTI GSHF, then it has an unbounded sequence of zeros $\{\gamma_\ell\}_{\ell=1}^{\infty}$ “converging to infinity”. Furthermore, these zeros converge to the roots of the equation $\eta = e^{-\phi^T} \phi^{n-m}$. In particular, if $n = m$, the zeros converge to the sequence defined by

$$\phi_\ell = -\frac{1}{T} \log \eta + j\ell\omega_s, \quad \ell = 0, \pm 1, \pm 2, \dots \quad (3.19)$$

Proof: See §A.2 in Appendix A. □

A precise description of the zeros of a FDLTI hold is possible in a particular case, as we see in the following lemma.

Lemma 3.2.3 (Zeros of a FDLTI GSHF (Special Case))

Consider a FDLTI GSHF, and suppose that $KM \neq 0$. Assume that $L = \lambda I$, where I is the identity matrix and λ is a scalar. Then the zeros of H are located precisely at

$$\gamma_\ell = -\lambda + j\ell\omega_s, \quad \ell = \pm 1, \pm 2, \dots \quad (3.20)$$

Proof: Since $KM \neq 0$, H is not identically zero. The special structure of L implies that

$$H(s) = KM \frac{e^{\lambda T} - e^{-sT}}{s + \lambda},$$

and the result follows. □

Remark 3.2.1 (Approximation of the zeros of a FDLTI GSHF) Notice that since a FDLTI GSHF will most probably be implemented as a PC GSHF, the additional difficulty in characterizing zeros of FDLTI holds over PC holds is somehow deprived of practical significance². ◇

3.2.2 GSHFs with all Zeros on the $j\omega$ -axis

A well-known property of a hybrid control system using a ZOH in conjunction with a discrete integrator is the ability to asymptotically reject step disturbances. This arises from the fact that the ZOH frequency response has zeros at multiples of the sampling frequency $\omega_s = 2\pi/T$ on the $j\omega$ -axis,

$$H_{\text{ZOH}}(jk\omega_s) = 0, \quad \text{for } k = \pm 1, \pm 2, \dots$$

²See the example in Subsection 3.2.3.

In addition, these zeros contribute to diminish high frequency components of the plant response that are aliased down to low frequencies. This is particularly important in sampled-data control applications, where the low-frequency range is typically of great interest.

The response of a GSHF, on the other hand, need not have zeros at these frequencies, and thus high frequency plant behavior (and uncertainty) may have significant effect on the low-frequency range of the hybrid control system [cf. Feuer and Goodwin, 1994]. To get a preliminary intuitive view of this, compare for example the GSHF response with the response of a ZOH, plotted in Figure 3.5; this GSHF is taken from Kabamba [1987, Example 2].

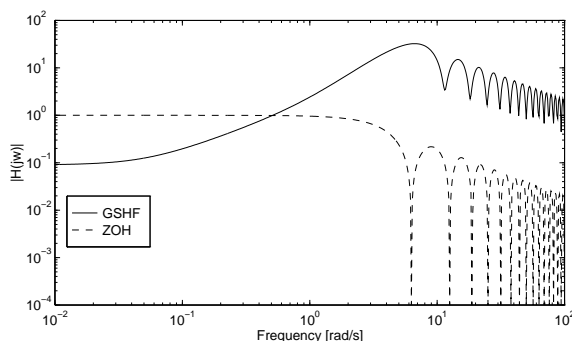


Figure 3.5: Frequency response of hold functions.

In addition, zeros of H close to unstable open-loop poles of the plant may render an ill-conditioned discrete-time system Middleton and Freudenberg [1995], Middleton and Xie [1995], due to an approximate pole-zero cancelation that tend to violate the non-pathological sampling assumption of Lemma 2.2.1. Moreover, as will become clear in §3.3, also zeros in \mathbb{C}^- compromise the frequency response of the hold, depending on the specifications that this frequency response is required to meet.

An interesting question then arises from the above observations: What is the class of GSHFs that, as the ZOH, have all their zeros on the $j\omega$ -axis? The following proposition gives a necessary condition that the hold frequency response must satisfy to have such a zero distribution.

Proposition 3.2.4

Let H be the frequency response function of a PC or a FDLTI GSHF; suppose that h satisfy Assumption 4. Then if H has all its zeros on the $j\omega$ -axis, either

$$H(s) = e^{-sT} H(-s), \quad (3.21)$$

or

$$H(s) = -e^{-sT} H(-s). \quad (3.22)$$

Proof: Suppose that $\{ja_k\}$ are the nonzero zeros of H repeated according to multiplicity, and that H has a zero at $z = 0$ of order $p \geq 0$ ($p = 0$ means that $H(0) \neq 0$). Since H is an entire function of exponential type T , using the Hadamard Factorization Theorem [e.g., Markushevich, 1965] we can represent it as

$$H(s) = s^p e^{g_0 + g_1 s} \prod_{k=1}^{\infty} \left(1 - \frac{s}{ja_k}\right) e^{s/ja_k}, \quad (3.23)$$

where g_0 and g_1 are real numbers. Without loss of generality we may assume $g_0 = 0$ (since otherwise we consider $H(s)e^{-g_0}$), and since the zeros are symmetric with respect to the real axis, (3.23) simplifies to

$$H(s) = s^p e^{g_1 s} \prod_{\ell=1}^{\infty} \left(1 + \frac{s^2}{a_{\ell}^2}\right), \quad (3.24)$$

where now $\{a_{\ell}\}$ denote the zeros in the upper (or lower) half of the $j\omega$ -axis.

As in Subsection 3.2.1 let m and n be the smallest integers such that (3.17) holds. Notice that both $h^{(m)}(0^+)$ and $h^{(n)}(T^+)$ are nonzero finite numbers for PC and FDLTI GSHFs with compact support on $[0, T)$. Hence, the number η defined in (3.18) is also nonzero and finite. Next we use the Initial Value Theorem [e.g., Zemanian, 1965] to compute $h^{(m)}(0^+)$ from (3.24). Thus, for x real we have that

$$\begin{aligned} h^{(m)}(0^+) &= \lim_{x \rightarrow \infty} x^{m+1} H(x) \\ &= \lim_{x \rightarrow \infty} x^{p+m+1} e^{g_1 x} \prod_{k=1}^{\infty} \left(1 + \frac{x^2}{a_{\ell}^2}\right). \end{aligned} \quad (3.25)$$

An analogous expression can be obtained for $h^{(n)}(T^-)$ following similar steps with $H(-s)e^{-sT}$,

$$\begin{aligned} h^{(n)}(T^-) &= \lim_{x \rightarrow \infty} (-x)^{n+1} e^{-xT} H(-x) \\ &= \lim_{x \rightarrow \infty} (-1)^{n+p} x^{p+n+1} e^{-(g_1+T)x} \prod_{k=1}^{\infty} \left(1 + \frac{x^2}{a_{\ell}^2}\right). \end{aligned} \quad (3.26)$$

Therefore, we can write from (3.25) and (3.26),

$$\begin{aligned} \eta &= \frac{h^{(m)}(0^+)}{h^{(n)}(T^-)} \\ &= \lim_{x \rightarrow \infty} (-1)^{n+p} x^{m-n} e^{(2g_1+T)x}. \end{aligned} \quad (3.27)$$

Since η is nonzero and finite, it necessarily follows from (3.27) that $m = n$ and $g_1 = -T/2$. With this value of g_1 in (3.24), it is easy to check that H verifies the required conditions (3.21) or (3.22) (the sign depending on the order of the zero at $s = 0$), completing the proof. \square

Notice in the proof above that the conditions $m = n$, and $g_1 = -T/2$ imply that $\eta = (-1)^{n+p}$, which in turn, by Lemma 3.2.2, tells us that the zeros of H approach asymptotically to the $j\omega$ -axis as the distance from the origin increases. We could say then that conditions (3.21) and (3.22) become also “sufficient” for large values of s .

The fact that $\eta = (-1)^{n+p}$ also suggests that if H has all its zeros on the $j\omega$ -axis, then h has some kind of symmetry with respect to the middle point of the interval $[0, T]$. For example, if $n = 1$ and $p = 0$ say, then $h(0^+) = 0 = h(T^-)$, and the corresponding derivatives are mirrored, $h'(0^+) = -h'(T^-)$. In fact, conditions (3.21) and (3.22) are *equivalent* to “symmetry” of h , as we shall prove next. Let us first make more precise what we mean by this.

Definition 3.2.1 (Symmetry of h)

We say that h has *even* (*odd*) symmetry if $h(t) = h(T - t)$ ($h(t) = -h(T - t)$). We say that h is *symmetric* if h has either even or odd symmetry. \diamond

The following corollary to Proposition 3.2.4 establishes that holds with all their zeros on the $j\omega$ -axis are necessarily symmetric in the sense just defined.

Corollary 3.2.5

If H has all its zeros on the $j\omega$ -axis, then h is symmetric. Moreover,

- (i) *if H has none or an even number of zeros at $s = 0$, then h is even symmetric;*
- (ii) *if H has an odd number of zeros at $s = 0$, then h is odd symmetric.*

Proof: We prove only (i); the proof of (ii) is obtained in a similar way. We know from Proposition 3.2.4 that if H has all its zeros on the $j\omega$ -axis — and none or an even number of them at $s = 0$, then condition (3.21) is satisfied. Write the Fourier Series representation of h ,

$$h(t) = \sum_{k=-\infty}^{\infty} c_k e^{jk\omega_s t}, \quad (3.28)$$

with

$$\begin{aligned} c_k &= \frac{1}{T} \int_0^T e^{-jk\omega_s t} h(t) dt \\ &= \frac{H(jk\omega_s)}{T}. \end{aligned}$$

We prove now that condition (3.21) is satisfied if and only if all c_k — i.e., $H(jk\omega_s)$ — are real. Indeed, if c_k is real for all k , then $H(jk\omega_s) = H(-jk\omega_s)$, and using

Lemma 3.1.3 we have that

$$\begin{aligned}
 H(s) &= \frac{1}{T} \sum_{k=-\infty}^{\infty} H(jk\omega_s) H_{\text{ZOH}}(s - jk\omega_s) \\
 &= \frac{1}{T} \sum_{\ell=-\infty}^{\infty} H(j\ell\omega_s) H_{\text{ZOH}}(s + j\ell\omega_s) \\
 &= \frac{e^{-sT}}{T} \sum_{\ell=-\infty}^{\infty} H(j\ell\omega_s) H_{\text{ZOH}}(-s - j\ell\omega_s) \\
 &= e^{-sT} H(-s).
 \end{aligned}$$

The converse is immediate. Finally, (i) follows easily from noting that h has all real Fourier coefficients if and only if it is even symmetric. \square

This corollary provides an easy way of determining whether the hold frequency response H may have zeros off the $j\omega$ -axis by just examining the shape of the hold function h ; i.e., an asymmetric h will necessarily imply zeros in either \mathbb{C}^+ or \mathbb{C}^- .

Remark 3.2.2 (A Conjecture for a General GSHF) Strictly, we have proved these results only for PC and FDLTI GSHFs; nevertheless, we could conjecture that they hold for the general case. Indeed, notice that any admissible h can be arbitrarily approximated by a piecewise-constant function h_{PC} , and then the zeros of H_{PC} will approximate the zeros of H . Then, it is clear that if H has all its zeros on the $j\omega$ -axis, we can build a sequence of symmetric PC functions whose zeros will approach to the $j\omega$ -axis. Since the result holds for H_{PC} , we can expect that, in the limit, it will hold also for H . A rigorous proof seems difficult, though. \diamond

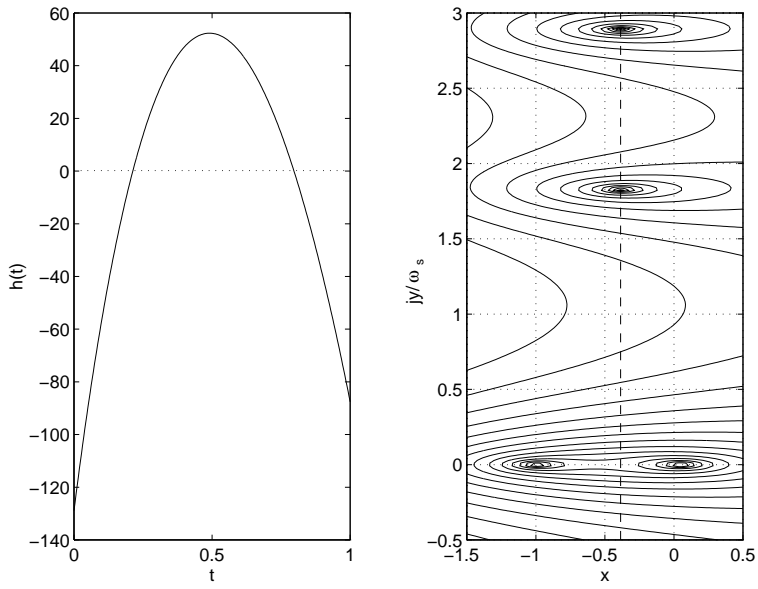
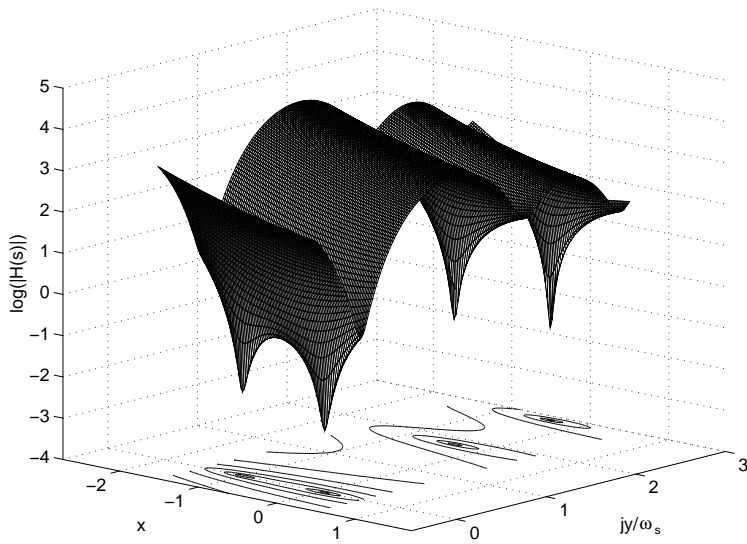
3.2.3 Example: Zeros of a FDLTI GSHF

In this example we illustrate the previous results on zero locations of GSHFs. We consider the FDLTI GSHF used in Kabamba [1987, Example 2] to simultaneously stabilize two continuous-time systems that violate the appropriate parity interlacing property (cf. Example 7.1.1). The matrices that define the hold function with the characterization given by Definition 3.1.1 are

$$K = \begin{bmatrix} 1 & 0 & 0 \end{bmatrix}, \quad L = \begin{bmatrix} 1 & 1 & 0 \\ 2 & 0 & 1 \\ 0 & 0 & 0 \end{bmatrix}, \quad M = \begin{bmatrix} 87.5619 \\ -616.4937 \\ 1322.6 \end{bmatrix}.$$

The sampling period is $T = 1s$, to which corresponds a sampling frequency $\omega_s = 2\pi$. The hold function h is shown on the left in Figure 3.6.

As we can see in the figure, h is not symmetric, so we know by Corollary 3.2.5 that the corresponding frequency response H *will* have zeros off the $j\omega$ -axis. Indeed, this can be seen in Figure 3.7, where we have plotted a section of the function $\log |H|$ for $s = x + jy$, with $-1.5 \leq x \leq 0.5$ and $-\omega_s/2 \leq y \leq 3\omega_s$. The zeros

Figure 3.6: Hold function h , and contour plot of H .Figure 3.7: Zeros of H .

are indicated by the negative peaks on this surface; a contour plot is given on the right in Figure 3.6.

Let us check the asymptotic behavior of the zeros of H . Following the notation of Lemma 3.2.2 we compute η from (3.18), which, for the values of K , L , and M given is $\eta = 1.4718$, with $n = 0 = m$. Then, by Lemma 3.2.2 we know that there is an infinite sequence of zeros that approach asymptotically to a sequence given by (3.19), which for this case is

$$\phi_\ell = -0.3865 + j\ell\omega_s. \quad (3.29)$$

This is can be anticipated already in Figure 3.6, where for reference we have drawn a vertical line at $x = -0.3865$.

As we discussed in Remark 3.2.1, the zeros of a FDLTI GSHF can be approximated by the zeros of a PC GSHF, which are completely characterized in Lemma 3.2.1. This is verified in Figures 3.8, 3.9, and 3.10, where we have depicted analogs to Figure 3.6 for PC approximations to h with 4, 32, and 256 partitions respectively. We can see there how the zeros approach to the locations given in Figure 3.6 as the number of partitions is increased. Notice, however, that the convergence is slow, particularly for those zeros on the real axis.

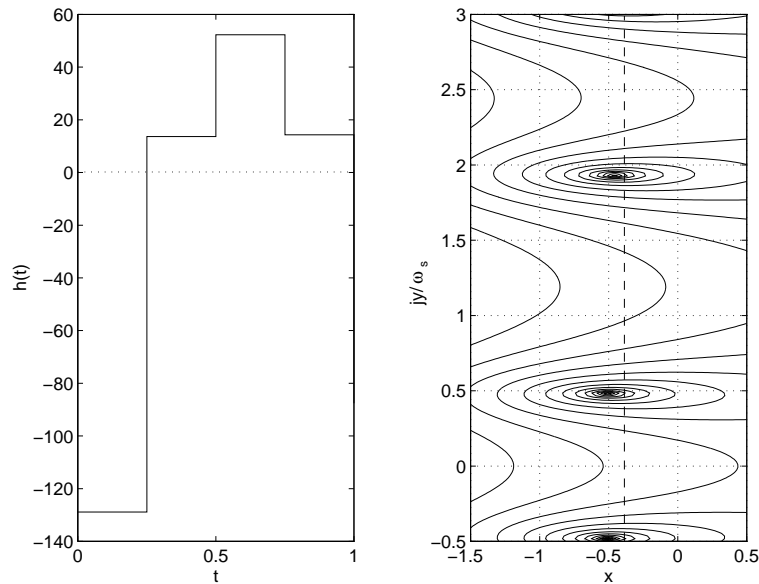
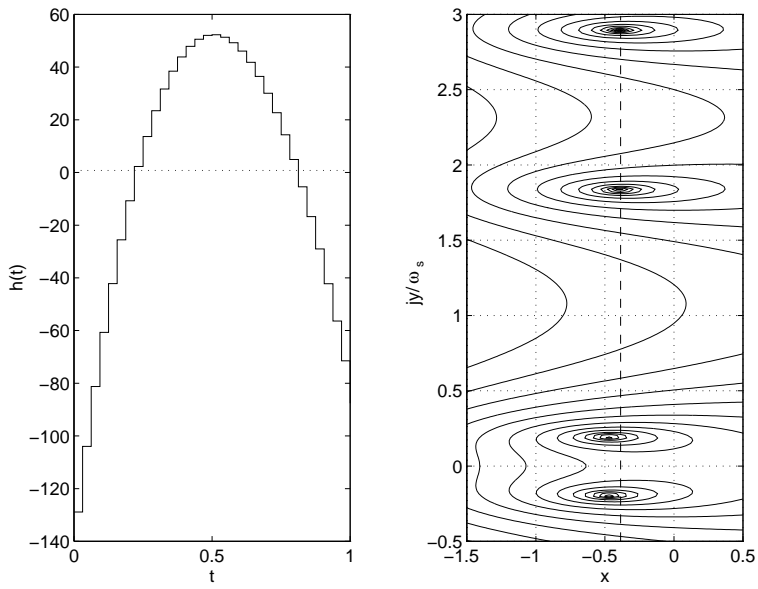
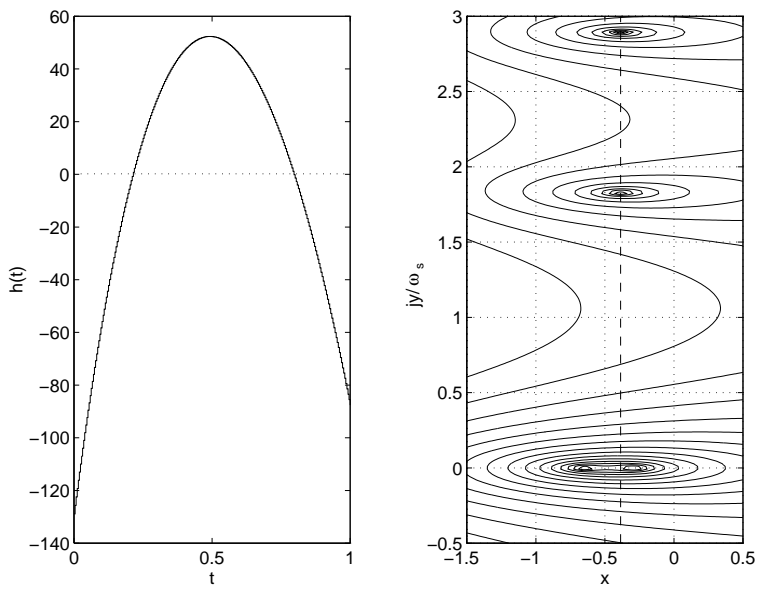


Figure 3.8: PC approximation to h , $N = 4$.

3.3 Integral Relations

Integral relations quantifying inherent limitations in the achievable performance of feedback control systems have been known for some time. Bode and Poisson

Figure 3.9: PC approximation to h , $N = 32$.Figure 3.10: PC approximation to h , $N = 256$.

integrals on the sensitivity and complementary sensitivity functions of continuous-time systems have been used to describe design tradeoffs arising from the feedback structure, and the requirement of closed-loop stability Freudenberg and Looze [1985]. Similar results have been also extended to discrete-time systems Sung and Hara [1988], Middleton and Goodwin [1990]. In Chapter 4 we shall study the case of sampled-data systems.

In this section, we present two types of integral relations for the frequency response of a GSHF. These integrals translate the connection between growth characteristics and the distribution of zeros into constraints that the magnitude of the frequency response of the GSHF must satisfy on the $j\omega$ -axis. We show how zeros off the $j\omega$ -axis impose tradeoffs over the values of the frequency response of the hold at all frequencies. In contrast, a zero *on* the $j\omega$ -axis only imposes a constraint at one point (namely, the frequency response is zero at that frequency).

3.3.1 Poisson Integral for GSHFs

Let H be the frequency response function of a GSHF defined by (2.4). Recall the definition of the Poisson kernel for the half plane, [e.g., Freudenberg and Looze, 1988]. Let $s = x + jy$, s in \mathbb{C} , and let ω be a real number. We define the Poisson kernel for the half plane, $\Psi(s, \omega)$, by

$$\Psi(s, \omega) \triangleq \frac{x}{x^2 + (\omega - y)^2} + \frac{x}{x^2 + (\omega + y)^2}. \quad (3.30)$$

The following proposition presents a Poisson integral relation for the function $1 - H$.

Proposition 3.3.1 (Poisson integral for $1 - H$)

Let $\xi = x + jy$ be a zero of H . Then

(i) if $x > 0$,

$$\int_0^\infty \log |1 - H(j\omega)| \Psi(\xi, \omega) d\omega \geq 0; \quad (3.31)$$

(ii) if $x < 0$,

$$\int_0^\infty \log |1 - H(j\omega) e^{j\omega T}| \Psi(-\xi, \omega) d\omega \geq 0. \quad (3.32)$$

Proof: We prove only (3.31); (3.32) is obtained in a similar way. Consider the function $F = 1 - H$. Since H is entire, so is F , and therefore, we may factorize it as

$$F = \tilde{F} B,$$

where \tilde{F} is an entire function without zeros in \mathbb{C}^+ , and B is the Blaschke product of the sequence of zeros of F , $\{\phi_k\}_{k=1}^{N_\phi}$ (with N_ϕ possibly infinite), in \mathbb{C}^+ ,

$$B = \prod_{k=1}^{N_\phi} \frac{\phi_k - s}{\phi_k + s}.$$

Note that $\log \tilde{F}$ is analytic in \mathbb{C}^+ , and furthermore, it satisfies the conditions for a Poisson Integral representation Freudenberg and Looze [1988]. Hence, we can write,

$$\begin{aligned} \int_0^\infty \log |\tilde{F}(j\omega)| \Psi(s, \omega) d\omega &= \pi \log |\tilde{F}(s)| \\ &= \pi \log |F(s)| - \pi \log |B(s)|. \end{aligned} \quad (3.33)$$

Evaluating (3.33) at a zero of H in \mathbb{C}^+ , and noting that $|\tilde{F}(j\omega)| = |F(j\omega)|$ and $-\log |B(s)| \geq 0$ for each s in \mathbb{C}^+ , we get inequality (3.31), completing the proof. Inequality (3.32) is obtained similarly by starting with the function $F(s) = 1 - H(-s)e^{-sT}$. \square

It follows from (3.31) and (3.32) that zeros of the hold off the $j\omega$ -axis impose design tradeoffs on its frequency response. More specifically, if we require that $|H(j\omega)|$ be close to 1 over some range of frequencies, $|H(j\omega)|$ will necessarily show a peak somewhere else. The extent of this difficulty is linked to the relative location of these zeros, and depends on the specifications that the hold frequency response is required to satisfy on the low-frequency range, as we see next.

Consider an interval of low frequencies $\Omega = [0, \omega_b]$, where $\omega_b \leq \omega_s/2$, and suppose that we require the hold response $H(j\omega)$ to be close to 1 over this interval. The interval Ω may be interpreted as the closed-loop bandwidth of a hybrid feedback system with hold H . Asking $H(j\omega)$ not too large on Ω is a reasonable specification in practice, since a “high gain” hold may bring in difficulties with actuator saturations (cf. Lemma 3.1.2 and the discussion following). We state this requirement as

$$|1 - H(j\omega)| < \alpha, \quad \text{for } \omega \text{ in } \Omega = [0, \omega_b], \quad (3.34)$$

where α is a small positive number.

Assume that H has a zero $\xi = x + jy$ in either \mathbb{C}^+ or \mathbb{C}^- . Let $\Theta(\xi, \Omega)$ denote the weighted length of the interval Ω with the Poisson kernel for the half plane,

$$\Theta(\xi, \Omega) \triangleq \int_0^{\omega_b} \Psi(\xi, \omega) d\omega, \quad (3.35)$$

It is not difficult to check that

$$\Theta(\xi, \Omega) = \arctan\left(\frac{\omega_b - y}{x}\right) + \arctan\left(\frac{\omega_b + y}{x}\right).$$

As discussed in Freudenberg and Looze [1985] and Freudenberg and Looze [1988], the weighted length $\Theta(\xi, \Omega)$ may also be interpreted as a phase lag introduced by the term of a Blaschke product corresponding to the zero ξ over Ω ; e.g., if ξ is real, then

$$\Theta(\xi, \Omega) = -\angle \frac{\xi - j\omega_s}{\xi + j\omega_s}; \quad (3.36)$$

i.e., the weighted length of the interval Ω equals the negative of the phase lag contributed by the Blaschke product $(\xi - s)/(\xi + s)$ at the upper end point of the interval.

The following result is a straightforward consequence of Proposition 3.3.1.

Corollary 3.3.2

Suppose that $|H(j\omega)|$ satisfies (3.34). Then, if $\xi = x + jy$ is a zero of H , with $x \neq 0$,

(i) if $x > 0$,

$$\sup_{\omega > \omega_b} |H(j\omega)| \geq \left(\frac{1}{\alpha}\right)^{M_{\Omega}(\xi)} - 1, \quad (3.37)$$

(ii) if $x < 0$,

$$\sup_{\omega > \omega_b} |H(j\omega)| \geq \left(\frac{1}{\alpha}\right)^{M_{\Omega}(-\xi)} - 1, \quad (3.38)$$

where

$$M_{\Omega}(\xi) = \frac{\Theta(\xi, \Omega)}{\pi - \Theta(\xi, \Omega)}$$

◦

Note from (3.37) and (3.38), that the effect of zeros in \mathbb{C}^- is as detrimental as the effect of zeros in \mathbb{C}^+ . To illustrate these bounds, suppose that we wish to design a hold satisfying specification (3.34), and that due to the type of hold chosen, there will be a real zero $\xi = x$. It follows that if the hold response has zeros off the $j\omega$ -axis, and we require $|H(j\omega)|$ very close to 1 on Ω , then $|H(j\omega)|$ will necessarily have a large peak at higher frequencies. The tradeoff relaxes as the zero tends to be located at relatively high frequencies. By contrast, if the zero gets closer to the $j\omega$ -axis, the constraint worsens. In the limit, when the zero is *on* the $j\omega$ -axis, then the Poisson integrals (3.31) and (3.32) collapse into an algebraic constraint³: $0 \leq \log |1 - H(\xi)| = 0$. Figure 3.11 shows plots of the bounds (3.37) and (3.38) vs. the location of the zero in Ω for different values of the specification α .

3.3.2 Middleton Integral for GSHFs

Another integral relation that evidences the penalties imposed by zeros and poles of an analytic function over its values on the $j\omega$ -axis has been proposed by Middleton and Goodwin [1990, Corollary 13.4.1]. This integral relation can be used to quantify the effect of zeros off the $j\omega$ -axis of the frequency response of holds with $H(0) \neq 0$. In contrast with the previous integral relation, here we obtain a single integral for both cases of zeros in \mathbb{C}^- and \mathbb{C}^+ .

Denote by $\{\lambda_k\}_{k=1}^{N_{\lambda}}$ and $\{\rho_k\}_{k=1}^{N_{\rho}}$ the sequence of zeros of H , counted with multiplicities, in \mathbb{C}^- and \mathbb{C}^+ , respectively. Typically, $N_{\lambda} + N_{\rho} = \infty$. Without loss of generality, we also assume $H(0) = 1$. Then, we have the following result.

³For which the specification (3.34) becomes incompatible unless $\alpha \geq 1$.

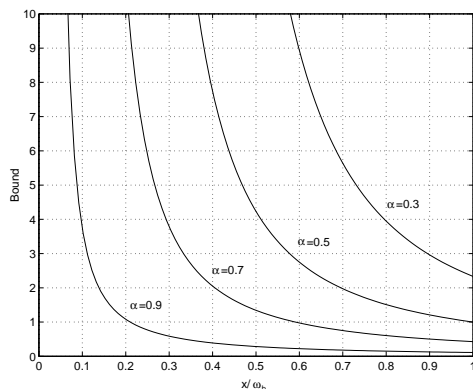


Figure 3.11: Lower bound (3.37) (or (3.38)) for a real zero.

Proposition 3.3.3 (Middleton Integral for H)

$$\int_0^\infty \frac{\log |H(j\omega)|}{\omega^2} d\omega = \frac{\pi}{4} \left(-T - 2 \sum_{k=1}^{N_\lambda} \frac{1}{\lambda_k} + 2 \sum_{k=1}^{N_\rho} \frac{1}{\rho_k} \right). \quad (3.39)$$

Proof: Factorize H as $H = \tilde{H} B_\rho$, where B_ρ is the Blaschke product of the zeros of H in \mathbb{C}^+ ,

$$B_\rho(s) = \prod_{k=1}^{N_\rho} \frac{\rho_k - s}{\bar{\rho}_k + s}.$$

From similar arguments to those in the proof of Proposition 3.3.1, we obtain the following Poisson Integral relation, which we evaluate at a real $s = x$, $x > 0$,

$$\int_0^\infty \log |H(j\omega)| \frac{2x}{x^2 + \omega^2} d\omega = \pi \log |H(x)| - \pi \log |B_\rho(x)|. \quad (3.40)$$

Dividing both sides of (3.40) by x , and taking the limit when $x \rightarrow 0$ yields⁴.

$$2 \int_0^\infty \frac{\log |H(j\omega)|}{\omega^2} d\omega = \lim_{x \rightarrow 0} \pi \frac{\log |H(x)|}{x} - \lim_{x \rightarrow 0} \pi \frac{\log |B_\rho(x)|}{x}. \quad (3.41)$$

The application of L'Hopital's rule to the limits on the RHS of (3.41), our assumption $H(0) = 1$, and the fact that zeros of H must occur in complex conjugate pairs, yield

$$2 \int_0^\infty \frac{\log |H(j\omega)|}{\omega^2} d\omega = \left. \frac{dH(s)}{ds} \right|_{s=0} + 2 \sum_{k=1}^{N_\rho} \frac{1}{\rho_k}. \quad (3.42)$$

⁴The interchange between limit and integration on the LHS is valid by the Lebesgue Dominated Convergence Theorem Riesz and Sz.-Nagy [1990]

From analogous arguments applied to $H(-s)e^{-sT}$, and noting that $|H(j\omega)| = |H(-j\omega)|$, we obtain an integral relation for the zeros of H in \mathbb{C}^- ,

$$2 \int_0^\infty \frac{\log |H(j\omega)|}{\omega^2} d\omega = -T - \left. \frac{dH(s)}{ds} \right|_{s=0} - 2 \sum_{k=1}^{N_\lambda} \frac{1}{\lambda_k}. \quad (3.43)$$

Finally, adding term-to-term (3.42) and (3.43) yields (3.39), completing the proof. \square

In the particular case of a PC hold, the location of zeros is well determined, and therefore, we obtain a more specific result. As it follows from Lemma 3.2.1, zeros off the $j\omega$ -axis for a PC hold are determined by the zeros of the discrete polynomial $A_d(z)$. Denote by $\{\phi_k\}_{k=1}^{N_\phi}$ and $\{\psi_k\}_{k=1}^{N_\psi}$ the set of zeros of $A_d(z)$ inside and outside the unit circle, respectively (note that there is a finite number of them, $N_\psi + N_\phi \leq N$). The following corollary states the analog to Proposition 3.3.3 for PC holds.

Corollary 3.3.4 (Middleton Integral for PC GSHFs)

$$\int_0^\infty \frac{\log |H(j\omega)|}{\omega^2} d\omega = \frac{\pi T}{4} \left(\frac{1}{N} \sum_{k=1}^{N_\psi} \frac{\psi_k + 1}{1 - \psi_k} + \frac{1}{N} \sum_{k=1}^{N_\phi} \frac{\phi_k + 1}{\phi_k - 1} - 1 \right). \quad (3.44)$$

Proof: From Lemma 3.2.1 we have that zeros of H in \mathbb{C}^+ are

$$\rho_{k,i} = -\frac{N}{T} \log \phi_i + jkN\omega_s, \quad \text{with } i = 1, \dots, N_\phi \text{ and } k = 0, \pm 1, \pm 2 \dots \quad (3.45)$$

and zeros in \mathbb{C}^- are

$$\lambda_{k,i} = -\frac{N}{T} \log \psi_i + jkN\omega_s, \quad \text{with } i = 1, \dots, N_\psi \text{ and } k = 0, \pm 1, \pm 2 \dots, \quad (3.46)$$

From (3.45) and (3.46), and using the identity [Rudin, 1987, p. 195]

$$\frac{e^{2\pi x} + 1}{e^{2\pi x} - 1} = \frac{1}{\pi} \sum_{k=-\infty}^{\infty} \frac{x}{x^2 + k^2},$$

in the form

$$\frac{e^{2\pi\alpha/\beta} + 1}{e^{2\pi\alpha/\beta} - 1} = \frac{\beta}{\pi} \sum_{k=-\infty}^{\infty} \frac{1}{\alpha + jk\beta},$$

we obtain the following closed forms for the series on the RHS of (3.39),

$$\sum_{i=1}^{N_\phi} \sum_{k=-\infty}^{\infty} \frac{1}{\lambda_{k,i}} = \frac{T}{2N} \sum_{i=1}^{N_\phi} \frac{\phi_k + 1}{\phi_k - 1},$$

and

$$\sum_{i=1}^{N_\psi} \sum_{k=-\infty}^{\infty} \frac{1}{\rho_{k,i}} = \frac{T}{2N} \sum_{i=1}^{N_\psi} \frac{\psi_k + 1}{\psi_k - 1}.$$

Replacing these in (3.39) yields (3.44), concluding the proof. \square

Proposition 3.3.3 and Corollary 3.3.4 show that if $|H(j\omega)| < 1$ over some frequency range, then it must necessarily be greater than one at other frequencies. This tradeoff is minimized if H has all its zeros on the $j\omega$ -axis, and can only worsen if there are zeros off the $j\omega$ -axis. Indeed, notice on the RHSs of (3.39) and (3.44) that the terms due to zeros off the $j\omega$ -axis are always positive. In particular, the RHSs of (3.39) and (3.44) can get arbitrarily large with real zeros of H approaching $s = 0$.

Remark 3.3.1 (Middleton Integral and Zero Density) There is an interesting connection between this integral relation and the results of §3.2. Let $\{a_k\}$ denote the infinite sequence of zeros of H repeated according to multiplicity. If $n(r)$ denotes the number of zeros of moduli not exceeding r , i.e., the number of a_k such that $|a_k| < r$, with r real positive, we define the *density of zeros* δ as

$$\delta \triangleq \lim_{r \rightarrow \infty} \frac{n(r)}{r}.$$

The following is a well-known result for entire functions of exponential type.

Proposition 3.3.5 (Boas [1954, Theorem 8.2.1])

If H is an entire function of exponential type with all its zeros on the $j\omega$ -axis, then the following two conditions

$$\lim_{R \rightarrow \infty} \int_{-R}^R \frac{|H(j\omega)|}{\omega^2} d\omega = -\pi^2 B, \quad (3.47)$$

and

$$\lim_{r \rightarrow \infty} \frac{n(r)}{r} = 2B \quad (3.48)$$

are equivalent. ◦

If we consider the integral relation (3.39) for a GSHF without zeros off the $j\omega$ -axis, we obtain

$$\int_0^\infty \frac{\log |H(j\omega)|}{\omega^2} d\omega = -\frac{\pi T}{4}. \quad (3.49)$$

Since $|H(j\omega)| = |H(-j\omega)|$ we can change the interval of integration on the LHS of (3.49) to $(-\infty, \infty)$ by multiplying by 2 its RHS. Then, according to (3.47) we have that $B = \omega_s^{-1}$, and therefore by Proposition 3.3.5 the density of zeros of H is

$$\delta = 2/\omega_s.$$

From this we can deduce that the number of zeros of H in a ball of radius $r = k\omega_s$ is approximately $2k$ when k is large, in agreement with our previous result of Lemma 3.2.2. ◊

3.3.3 Example: Tradeoffs in $H(j\omega)$

To illustrate the above results, we take an example from Er and Anderson [1994], where a PC hold of two steps is used to achieve discrete-time perfect loop transfer recovery of a non-minimum phase continuous plant. The zero-placement capabilities of GSHFs are used in their algorithm. The PC hold obtained for a sampling time $T = 0.04s$, is the following:

$$h(t) = \begin{cases} -1957 & \text{for } 0 \leq t < 0.02 \\ 1707 & \text{for } 0.02 \leq t < 0.04 \end{cases} \quad (3.50)$$

From Lemma 3.2.1 we see that there is an infinite sequence of zeros at

$$s = -6.8338 + jk\omega_s, \quad k = 0, \pm 1, \pm 2, \dots,$$

with $\omega_s = 157.0796$. Figure 3.12 shows the normalized magnitude of $H(j\omega)$ (such that $H(0) = 1$), compared to that of a ZOH. We can see that the frequency response of this GSHF displays large peaks both within and outside the Nyquist range of frequencies, peaks that will tend to amplify potential plant uncertainties and disturbances at those frequencies. The magnitude of these peaks may be estimated by considering the bound (3.38). In this case, the bandwidth of the closed loop system is given [from Er and Anderson, 1994] by $\omega_b = 15.3\text{rad/s}$, so we have that the ratio $\omega/\omega_b = 0.44$. This value in Figure 3.11 gives an indication of the peak expected in $|H(j\omega)|$ when we require that the specification (3.34) be satisfied on the interval $[0, \omega_b]$. \diamond

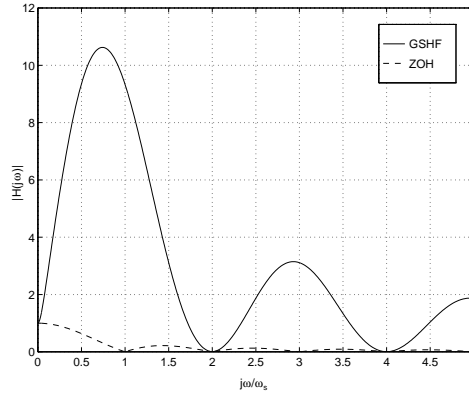


Figure 3.12: GSHF frequency response.

3.4 Summary

In this chapter, we have analyzed the frequency response and zero locations of non-traditional D-A devices known as GSHFs. We have presented general properties and results concerning norms and boundary values arising from the fact

that the frequency response of a GSHF is an entire function. In particular, we have shown that a frequency response with a large infinity-norm implies a hold device with large BIBO gain, which may bring in implementation difficulties in conjunction with the presence of plant input saturation.

Differently to the ZOH, GSHFs may have zeros off the $j\omega$ -axis, which — as we shall see in detail in the following chapter — may seriously damage sensitivity and robustness properties of the hybrid system. For two important classes of GSHFs, we have obtained exact and asymptotic characterizations of their zero locations in function of the hold response data. A key result of this chapter shows that if the hold has all its zeros on the $j\omega$ -axis, then necessarily its pulse response function has to meet certain condition of symmetry on its interval of definition.

In addition, we have derived integral relations displaying the connections between zero locations and the frequency response of the hold. Our results indicate there exist design tradeoffs that may imply frequency responses with relatively large values at high frequencies. This again, may be detriment on the sensitivity and robustness characteristics of the hybrid system, since these large values will amplify the effects of high frequency plant behavior and uncertainty on lower frequencies.

Frequency Response and Performance Limitations

In this chapter we develop a theory of inherent design limitations for sampled-data feedback systems wherein we consider full intersample behavior.

As pointed out in Chapter 1, a well-developed theory of design limitations is available for LTI feedback systems, both in continuous and discrete-time cases. Yet, this theory is insufficient to deal with hybrid systems, since they are periodically time-varying due to the action of the sampler. As explained in textbooks on sampled-data control, this fact implies that one cannot use transfer functions to describe system input-output properties¹. However, it is possible to calculate the Laplace transform of the response of a hybrid system to a particular input, and hence one may evaluate the steady-state response of a stable hybrid system to a sinusoidal input of given frequency. For analog systems, the response to such an input is a sinusoid of the same frequency as the input, but with amplitude and phase modified according to the transfer function of the system evaluated at the input frequency. The response of a stable hybrid system to an input signal, on the other hand, consists of a sum of infinitely many sinusoids spaced at integer multiples of the sampling frequency away from the frequency of the input. We shall refer to that component with the same frequency as the input as the *fundamental*, and the other components as the *harmonics*². Each of these components is governed by a *frequency-response function* with many properties similar to those of a transfer function. In particular, the response functions have sufficient structure to allow complex analysis to be applied to derive a set of formulas analogous to the Bode and Poisson integrals. As in the continuous-time case, these integrals describe tradeoffs between system properties in different frequency ranges.

Frequency response properties of hybrid systems have been discussed in several recent papers [e.g., Thompson et al., 1983, 1986, Leung et al., 1991, Araki and Ito, 1993, Araki et al., 1993, Yamamoto and Khargonekar, 1993, Goodwin and

¹An interesting notion of transfer function defined using lifting techniques is developed in Yamamoto and Araki [1994], and Yamamoto and Khargonekar 1993, 1996.

²In fact, the fundamental corresponds to the first harmonic. Our denomination is motivated by the fact that the first harmonic will be predominant in most applications, since the anti-aliasing filter should be designed to suppress higher frequency components.

Salgado, 1994, Feuer and Goodwin, 1994, Yamamoto and Araki, 1994]. The frequency response of periodic analog feedback systems was treated in Wereley and Hall [1990]. Particularly related to our setting are the works of Goodwin and Salgado [1994], Araki and Ito [1993], and Araki et al. [1993]. Goodwin and Salgado first introduced the idea of sensitivity functions to describe the fundamental response of a sampled-data system, and so give insights into the analysis of its intersample behavior. A frequency-domain framework to analyze both the fundamental and the harmonics, was communicated in Araki and Ito [1993] and Araki et al. [1993]. This framework introduced the concept of FR-operators, which are a hybrid system counterpart of transfer functions, and emphasized on the study of the sensitivity and complementary sensitivity operators. In this chapter, we develop similar methods to analyze fundamental properties of the frequency response of a sampled-data system.

The chapter is organized as follows. In §4.1 we define the hybrid fundamental sensitivity, fundamental complementary sensitivity, and the harmonic response functions. These functions have many common properties with transfer functions and govern the steady-state response of the hybrid system to sinusoidal disturbance and noise inputs. Using these functions we discuss the use of high-gain feedback, and describe differential sensitivity properties of the sampled-data system. §4.2 is devoted to a catalogue of interpolation constraints for these hybrid functions. As with their analog counterparts, the values of these functions at points in the ORHP is constrained by poles, zeros, and time delays in the plant and controller. Unlike the analog case, the constraints imposed by the compensator manifest themselves differently than do those imposed by the plant, and this fact leads to interesting design interpretations. Some of this interpretations are given in §4.3 in terms of steady-state disturbance rejection properties of the hybrid system. In §4.4, these interpolation constraints are used to derive generalizations of the Bode and Poisson integrals to the hybrid response functions. Design implications of these integrals are discussed in detail. Of particular interest is the fact that non-minimum phase zeros of the *analog* plant impose inherent tradeoffs upon the values of the fundamental sensitivity function on the $j\omega$ -axis. Non-minimum phase zeros of the *discretized* plant, on the other hand, do not. A summary discussion of the costs and benefits of sampled-data feedback is given in §4.5.

4.1 Frequency Response of a Sampled-data System

The steady-state response of a stable hybrid feedback system to a complex sinusoidal input consists of a fundamental component at the frequency of the input as well as additional harmonics located at integer multiples of the sampling frequency away from the fundamental. This well-known fact is discussed in textbooks [cf. Åström and Wittenmark, 1990, Franklin et al., 1990], and has been emphasized in several recent research papers³ Araki and Ito [1993], Araki et al.

³Similar results for systems with periodically time-varying *analog* controllers were derived by Wereley and Hall [1990].

[1993], Goodwin and Salgado [1994], Yamamoto and Araki [1994], Feuer and Goodwin [1994].

We now present expressions for the response of y in Figure 2.4 to disturbances and noise. Analogous expressions may be stated for the response to the reference input, and for the response of the control u to these signals. When evaluated along the $j\omega$ -axis, the following expressions are identical to those derived in Goodwin and Salgado [1994, Theorem 2.1] using Fourier transform techniques.

Recall the notation introduced in (2.9) on page 19, i.e., we write $F_k(s)$ to represent $F(s + jk\omega_s)$, for $k = 0, \pm 1, \pm 2, \dots$

Lemma 4.1.1

Denote the responses of y to each of d and n by y^d and y^n respectively. Then the Laplace transforms of these signals are given by

$$\begin{aligned} Y^d(s) &= \left[I - \frac{1}{T} P(s) H(s) S_d(e^{sT}) C_d(e^{sT}) F(s) \right] D(s) \\ &\quad - \sum_{\substack{k=-\infty \\ k \neq 0}}^{\infty} \left[\frac{1}{T} P(s) H(s) S_d(e^{sT}) C_d(e^{sT}) F_k(s) \right] D_k(s), \end{aligned} \quad (4.1)$$

and

$$\begin{aligned} Y^n(s) &= - \left[\frac{1}{T} P(s) H(s) S_d(e^{sT}) C_d(e^{sT}) F(s) \right] N(s) \\ &\quad - \sum_{\substack{k=-\infty \\ k \neq 0}}^{\infty} \left[\frac{1}{T} P(s) H(s) S_d(e^{sT}) C_d(e^{sT}) F_k(s) \right] N_k(s). \end{aligned} \quad (4.2)$$

Proof: These formulas may be derived using standard techniques from sampled-data control theory [e.g., Franklin et al., 1990, Åström and Wittenmark, 1990]. We present only a derivation of (4.2). Assume that r and d are zero. Block diagram algebra in Figure 2.4 and Lemma 2.1.1 yield

$$Y^n(s) = P(s) H(s) U_d(e^{sT}) \quad (4.3)$$

and

$$U_d(z) = -S_d(z) C_d(z) V_d(z). \quad (4.4)$$

The sampled output of the antialiasing filter can be written as

$$\begin{aligned} V_d(z) &= \mathcal{Z}\{\mathcal{S}_T\{\mathcal{L}^{-1}\{V(s)\}\}\} \\ &= \mathcal{Z}\{\mathcal{S}_T\{\mathcal{L}^{-1}\{F(s)N(s)\}\}\}. \end{aligned}$$

The assumptions that F is strictly proper and that n satisfies Assumption 2 allow Corollary 2.1.3 to be applied, yielding

$$V(e^{sT}) = \frac{1}{T} \sum_{k=-\infty}^{\infty} F_k(s) N_k(s). \quad (4.5)$$

Substituting (4.4) - (4.5) into (4.3) and rearranging yields the desired result. \square

If the feedback system is stable, then the preceding formulas may be used to derive the steady-state response of the system to a periodic input. As noted above, the response will be equal to the sum of infinitely many harmonics of the input frequency. The magnitude of each component is governed by a function analogous to the usual sensitivity or complementary sensitivity function for FDLTI systems.

Definition 4.1.1 (Hybrid Sensitivity Functions)

We define the *fundamental sensitivity* and *complementary sensitivity functions* by

$$S^0(s) \triangleq I - \frac{1}{T} P(s) H(s) S_d(e^{sT}) C_d(e^{sT}) F(s) \quad (4.6)$$

and

$$T^0(s) \triangleq \frac{1}{T} P(s) H(s) S_d(e^{sT}) C_d(e^{sT}) F(s) \quad (4.7)$$

respectively. For $k \neq 0$ define the *k-th harmonic response function* by

$$T^k(s) \triangleq \frac{1}{T} P_k(s) H_k(s) S_d(e^{sT}) C_d(e^{sT}) F(s) \quad (4.8)$$

◇

These hybrid response functions are not transfer functions in the usual sense, because they do not equal the ratio of the transforms of output to input signals. Moreover, note that they are not even rational functions, since their definition involves functions of the variable e^{sT} , like $H(s)$, $C_d(e^{sT})$, and $S_d(e^{sT})$. However, as the following result shows, these functions do govern the steady-state frequency response of the sampled-data system. We note that (4.6) and (4.7) are identical to the disturbance and reference gain functions defined in Goodwin and Salgado [1994].

From now and for the rest of this chapter, we confine our analysis to the case of a SISO system.

Lemma 4.1.2 (Steady-State Frequency Response)

Suppose that the hypotheses of Lemma 2.2.2 are satisfied and assume that $d(t) = e^{j\omega t}$, $t \geq 0$, and $n(t) = e^{j\omega t}$, $t \geq 0$. Then as $t \rightarrow \infty$, we have that

$$y^d(t) \rightarrow y_{ss}^d(t) \quad \text{and} \quad y^n(t) \rightarrow y_{ss}^n(t),$$

where

$$y_{ss}^d(t) = S^0(j\omega) e^{j\omega t} - \sum_{\substack{k=-\infty \\ k \neq 0}}^{\infty} T^k(j\omega) e^{j(\omega+k\omega_s)t}, \quad (4.9)$$

and

$$y_{ss}^n(t) = -T^0(j\omega) e^{j\omega t} - \sum_{\substack{k=-\infty \\ k \neq 0}}^{\infty} T^k(j\omega) e^{j(\omega+k\omega_s)t}. \quad (4.10)$$

Proof: The proof is a straightforward but tedious contour integration, so it is deferred to Subsection A.3.1 of Appendix A. \square

Note that the fundamental component of the disturbance response can potentially be reduced through use of feedback. The fundamental component of the noise response, on the other hand, is only increased by using feedback. These facts are analogous to the continuous-time case. Two other properties of (4.9)-(4.10) are unique to hybrid systems. First is the presence of harmonics at frequencies other than that of the input. The existence of these harmonics is due to the use of sampled-data feedback, and is a cost of feedback having no counterpart for analog systems. A second difference between analog and hybrid feedback systems is a limitation upon the ability of high-gain feedback to reduce the magnitude of the fundamental component of the disturbance response⁴.

Lemma 4.1.3 (High Compensator Gain)

Assume that $(FPH)_d(e^{j\omega T}) \neq 0$. Then, in the limit as $|C_d(e^{j\omega T})| \rightarrow \infty$, we have that $S^0(j\omega) \rightarrow S_{HG}(j\omega)$, where

$$S_{HG}(s) \triangleq 1 - \frac{F(s)P(s)H(s)}{T(FPH)_d(e^{sT})} \quad (4.11)$$

and

$$S_d(e^{j\omega T}) \rightarrow 0. \quad (4.12)$$

Furthermore, the steady-state responses of the system output and the sampler input to a disturbance $d(t) = e^{j\omega t}$, $t \geq 0$, satisfy

$$y_{ss}^d(kT) = \left[1 - \frac{F(j\omega) \sum_{n=-\infty}^{\infty} P_n(j\omega)H_n(j\omega)}{T(FPH)_d(e^{j\omega T})} \right] e^{j\omega kT} \quad (4.13)$$

and

$$v_{ss}^d(kT) = 0. \quad (4.14)$$

Proof: The formula (4.11) follows from (2.9) and the proof of Theorem 4.2.1 (vii). The limit (4.12) is obvious. Equation (4.13) follows by setting $t = kT$ in (4.9). Finally, (4.14) follows by first showing that

$$v_{ss}^d(t) = F(j\omega)S^0(j\omega)e^{j\omega t} - \sum_{\substack{k=-\infty \\ k \neq 0}}^{\infty} T^0(j(\omega + k\omega_s))F(j(\omega + k\omega_s))e^{j(\omega + k\omega_s)t}$$

yielding

$$v_{ss}^d(kT) = S_d(e^{j\omega T})F(j\omega)e^{j\omega kT}. \quad (4.15)$$

Together (4.12) and (4.15) yield (4.14). \square

⁴By contrast, recall that the disturbance response of an analog system can be made arbitrarily small at a given frequency provided that the plant gain is nonzero there.

It follows from (4.11) that use of high gain in the digital controller *does not* in general diminish the fundamental component of the disturbance response arbitrarily closely to zero⁵. For a disturbance lying in the Nyquist range, the obstruction to doing so is precisely the fact that the discrete frequency response depends upon the high frequency behavior of the plant, prefilter, and hold. It is true, of course, that the response of the sampler input may be reduced to zero at the sampling instants (cf. (4.14)). On the other hand, the sampled steady-state output due to a disturbance in the Nyquist range will be nonzero unless F is an ideal low pass filter, i.e., $F(j\omega) = 1$, for all $\omega \in \Omega_N$, and $F(j\omega) = 0$ otherwise.

The fundamental sensitivity and complementary sensitivity functions, together with the harmonic response functions, may be also used to describe differential sensitivity properties of a hybrid feedback system. It is well-known Bode [1945], that the sensitivity function of a continuous-time feedback system governs the relative change in the command response of the system with respect to small changes in the plant. Derivations similar to those of Lemma 4.1.2 show that the steady-state response of the system in Figure 2.4 to a command input $r(t) = e^{j\omega t}$, $t \geq 0$, is given by

$$y_{ss}^r(t) = T^0(j\omega)e^{j\omega t} - \sum_{\substack{k=-\infty \\ k \neq 0}}^{\infty} T^k(j\omega)e^{j(\omega+k\omega_s)t}. \quad (4.16)$$

Since $T^0(j\omega)$ depends upon $S_d(e^{j\omega T})$, it follows from (2.8) that the fundamental component of the command response at a particular frequency is sensitive to variations in the plant response at infinitely many frequencies.

Lemma 4.1.4 (Differential Sensitivity)

At each frequency ω , the relative sensitivity of the steady state command response (4.16) to variations in $P(j(\omega + \ell\omega_s))$ is given by

(i) For $\ell = 0$,

$$\frac{P(j\omega)}{T^0(j\omega)} \frac{\partial T^0(j\omega)}{\partial P(j\omega)} = S^0(j\omega). \quad (4.17)$$

(ii) For all $\ell \neq 0$,

$$\frac{P_\ell(j\omega)}{T^0(j\omega)} \frac{\partial T^0(j\omega)}{\partial P_\ell(j\omega)} = -T^0(j(\omega + \ell\omega_s)) \quad (4.18)$$

Proof: The proof is a straightforward calculation, keeping in mind the dependence of $S_d(e^{j\omega T})$ upon $P(s + j\ell\omega_s)$. \square

These results may best be interpreted by considering frequencies in the Nyquist range. Fix $\omega \in \Omega_N$. Then (4.17) states that the sensitivity of the fundamental component of the command response to small variations in the plant *at that frequency* is governed by the fundamental sensitivity function and hence may potentially

⁵However, see the remarks following Theorem 4.2.1 concerning the ZOH and use of integrators in C_d .

be reduced through use of feedback⁶. On the other hand, (4.18) states that the sensitivity of the fundamental component to *higher frequency* plant variations is governed by the fundamental complementary sensitivity function evaluated at the higher frequency, and thus *cannot* be reduced through the use of feedback. Further note that since

$$T^0(j(\omega + \ell\omega_s)) = \frac{1}{T} P(s + j\ell\omega_s) H(s + j\ell\omega_s) F(s + j\ell\omega_s) C_d(e^{j\omega T}) S_d(e^{j\omega T}),$$

the sensitivity of the command response at a frequency in the Nyquist range to higher frequency plant variations is proportional to the gain of the hold frequency response at the *higher* frequency, thus suggesting that the hold response should not be excessively large at high frequencies⁷.

4.2 Interpolation Constraints

It is well known that the sensitivity and complementary sensitivity functions of a stable, continuous-time feedback system must satisfy certain interpolation constraints at the CRHP poles and zeros of the plant and compensator. Specifically, the sensitivity function must equal zero at the CRHP poles, and the complementary sensitivity function must equal zero at the CRHP zeros.

As shown by Freudenberg and Looze [1985], these constraints may be used in conjunction with the Poisson integral to describe frequency dependent design tradeoffs. An entirely analogous set of interpolation constraints and design tradeoffs applies to the discrete-time part of a hybrid feedback system Sung and Hara [1988], Mohtadi [1990], Middleton [1991], Middleton and Goodwin [1990].

In this section we present a set of interpolation constraints that must be satisfied by the hybrid sensitivity functions defined in (4.6)-(4.8). Hybrid sensitivity responses have fixed values on $\overline{\mathbb{C}^+}$ that are determined by the open-loop zeros and poles of the plant, hold response, and digital compensator. As we shall see later, a significant difference between the hybrid case and the continuous-time only or discrete-time only cases is that the poles and zeros of the compensator yield different constraints than do those of the plant. The following theorem describe these interpolation relations for the fundamental sensitivity and complementary sensitivity functions.

Theorem 4.2.1 (Interpolation Constraints for S^0 and T^0)

Assume that P, F, H and C_d satisfy all conditions stated in Chapter 2 and that the hybrid feedback system of Figure 2.4 is stable. Then the following conditions are satisfied:

- (i) S^0 and T^0 have no poles in $\overline{\mathbb{C}^+}$.

⁶See the comments following Lemma 4.1.2.

⁷See also the preliminary remarks in Subsection 3.2.2, Chapter 3.

(ii) Let $p \in \overline{\mathbb{C}^+}$ be a pole of P . Then

$$\begin{aligned} S^0(p) &= 0, \\ T^0(p) &= 1. \end{aligned} \quad (4.19)$$

(iii) Let $\zeta \in \overline{\mathbb{C}^+}$ be a zero of P . Then

$$\begin{aligned} S^0(\zeta) &= 1, \\ T^0(\zeta) &= 0. \end{aligned} \quad (4.20)$$

(iv) Let $\gamma \in \overline{\mathbb{C}^+}$ be a zero of H . Then

$$\begin{aligned} S^0(\gamma) &= 1, \\ T^0(\gamma) &= 0. \end{aligned}$$

(v) Let $a \in \mathbb{D}^c$ be a zero of C_d . Define

$$a_m \triangleq \frac{1}{T} \log(a) + jm\omega_s, \quad m = 0, \pm 1, \pm 2, \dots$$

Then

$$\begin{aligned} S^0(a_m) &= 1, \\ T^0(a_m) &= 0. \end{aligned}$$

(vi) Let $p \in \overline{\mathbb{C}^+}$ be a pole of P . Define

$$p_m \triangleq p + jm\omega_s, \quad m = \pm 1, \pm 2, \dots$$

Then

$$\begin{aligned} S^0(p_m) &= 1, \\ T^0(p_m) &= 0. \end{aligned} \quad (4.21)$$

(vii) T^0 has no CRHP zeros other than those given by (iii) - (vi) above.

(viii) Let $b \in \mathbb{D}^c$ be a pole of C_d . Define

$$b_m \triangleq \frac{1}{T} \log(b) + jm\omega_s, \quad m = 0, \pm 1, \pm 2, \dots$$

Then

$$S^0(b_m) = 1 - \frac{P(b_m) H(b_m) F(b_m)}{T(\text{FPH})_d(b)}, \quad (4.22)$$

$$T^0(b_m) = \frac{P(b_m) H(b_m) F(b_m)}{T(\text{FPH})_d(b)}. \quad (4.23)$$

Proof: Introduce factorizations

$$P(s)F(s) = e^{-s\tau} \frac{N(s)}{M(s)},$$

where N and M are coprime rational functions with no poles in $\overline{\mathbb{C}^+}$, and

$$(\text{FPH})_d(z) = \frac{N_d(z)}{M_d(z)}, \quad (4.24)$$

where N_d and M_d are coprime rational functions with no poles in \mathbb{D}^c . By the Youla parameterization, all controllers C_d that stabilize (4.24) have the form⁸

$$C_d = \frac{Y_d + M_d Q_d}{X_d - N_d Q_d}, \quad (4.25)$$

where Q_d , X_d , and Y_d are stable, and X_d and Y_d satisfy the Bezout identity

$$M_d X_d + N_d Y_d = 1. \quad (4.26)$$

It follows that $S_d = M_d(X_d - N_d Q_d)$ and

$$C_d S_d = M_d(Y_d + M_d Q_d). \quad (4.27)$$

Using (4.27) in (4.6) and (4.7) yields

$$S^0(s) = 1 - \frac{1}{T} e^{-s\tau} \frac{N(s)H(s)}{M(s)} M_d(e^{sT}) [Y_d(e^{sT}) + M_d(e^{sT})Q_d(e^{sT})] \quad (4.28)$$

and

$$T^0(s) = \frac{1}{T} e^{-s\tau} \frac{N(s)H(s)}{M(s)} M_d(e^{sT}) [Y_d(e^{sT}) + M_d(e^{sT})Q_d(e^{sT})]. \quad (4.29)$$

- (i) T^0 is stable because each factor in the numerator of (4.29) is stable, and because the assumption of non-pathological sampling guarantees that any unstable pole of $1/M$ must be canceled by a corresponding zero of $M_d(e^{sT})$.
- (ii) It follows from (4.26) that $Y_d(e^{pT}) = 1/N_d(e^{pT})$. Using this fact, and evaluating (4.28) in the limit as $s \rightarrow p$ yields

$$S^0(s) \longrightarrow 1 - \lim_{s \rightarrow p} \frac{F(s)P(s)H(s)}{T(\text{FPH})_d(e^{sT})}.$$

Replace $(\text{FPH})_d(e^{sT})$ using (2.8):

$$S^0(s) \longrightarrow 1 - \lim_{s \rightarrow p} \frac{H(s)P(s)F(s)}{\sum_{k=-\infty}^{\infty} F(s + jk\omega_s) P(s + jk\omega_s) H(s + jk\omega_s)}. \quad (4.30)$$

By the assumptions that F is stable and that sampling is non-pathological, P and F have no poles at $p + jk\omega_s$, $k \neq 0$. Using this fact, and the fact that H has no finite poles, yields that each term in the denominator of (4.30) remains finite as $s \rightarrow p$ except the term $k = 0$. The result follows.

⁸We suppress dependence on the transform variable when convenient; the meaning will always be clear from context.

To prove (iii)-(vi), observe first that (4.29) implies T^0 can have CRHP zeros only at the CRHP zeros of N , H , $M_d(e^{sT})$, or $[Y_d(e^{sT}) + M_d(e^{sT})Q_d(e^{sT})]$.

(iii)-(vii) By Assumption 3, P , F , and PF are each free of unstable hidden modes.

Hence N and M can have no common CRHP zeros and (iii) follows. By the assumption of non-pathological sampling, neither can H and M . Hence (iv) follows. Note next that the zeros of $M_d(e^{sT})$ lie at $p + jk\omega_s$, $k = 0, \pm 1, \pm 2, \dots$, where p is any CRHP pole of P and hence a zero of M . It follows from this fact that the ratio $M_d(e^{sT})/M(s)$ can have zeros only for $k = \pm 1, \pm 2, \dots$. By the assumption of non-pathological sampling, no other cancelations occur, and all these zeros are indeed zeros of T^0 . This proves (vi). By (4.25), the CRHP zeros of $[Y_d(e^{sT}) + M_d(e^{sT})Q_d(e^{sT})]$ are identical to the CRHP zeros of $C_d(e^{sT})$. By the hypotheses of Lemma 2.2.2, none of these zeros can coincide with those of $M_d(e^{sT})$, and thus with those of M . This proves (v). Statement (vii) now follows because (iii)-(vi) exhaust all possibilities for T^0 to have CRHP zeros.

(viii) It follows from (4.27) that $C_d(b)S_d(b) = 1/(FPH)_d(b)$. Substitution of this identity into (4.6)-(4.7) yields (4.22)-(4.23). \square

A summary of the interpolation constraints satisfied by S^0 and T^0 is given in Table 4.1.

$\xi \in \overline{\mathbb{C}^+}$	Fundamental Sensitivity	Fundamental Complementary Sensitivity
Plant pole $P(\xi) = \infty$	$S^0(\xi) = 0$ $S^0(\xi + jk\omega_s) = 1$ $k \neq 0$	$T^0(\xi) = 1$ $T^0(\xi + jk\omega_s) = 0$ $k \neq 0$
Plant zero $P(\xi) = 0$	$S^0(\xi) = 1$	$T^0(\xi) = 0$
Controller pole $C_d(e^{\xi T}) = \infty$	$S^0(\xi) = 1 - \frac{F(\xi)P(\xi)H(\xi)}{T(FPH)_d(e^{\xi T})}$	$T^0(\xi) = \frac{F(\xi)P(\xi)H(\xi)}{T(FPH)_d(e^{\xi T})}$
Controller zero $C_d(e^{\xi T}) = 0$	$S^0(\xi) = 1$	$T^0(\xi) = 0$
Hold zero $H(\xi) = 0$	$S^0(\xi) = 1$	$T^0(\xi) = 0$

Table 4.1: Summary of interpolation constraints on S^0 and T^0 .

Harmonic response functions T^k also satisfy interpolation constraints, which are easily derived from the previous theorem.

Corollary 4.2.2 (Interpolation constraints for T^k)

Under the same hypotheses of Theorem 4.2.1 the following conditions are satisfied:

(i) T^k has no poles in $\overline{\mathbb{C}^+}$.

(ii) Let p be a pole of P with p in $\overline{\mathbb{C}^+}$. Then

$$T^k(p) = 0. \quad (4.31)$$

(iii) Let ζ be a zero of P with ζ in $\overline{\mathbb{C}^+}$. Then

$$T^k(\zeta - jk\omega_s) = 0. \quad (4.32)$$

(iv) Let γ be a zero of H with γ in $\overline{\mathbb{C}^+}$. Then

$$T^k(\gamma - jk\omega_s) = 0.$$

(v) Let a be a zero of C_d with a in \mathbb{D}^c , and a_m as defined in Theorem 4.2.1 (v). Then

$$T^k(a_m) = 0.$$

(vi) Let p be a pole of P with p in $\overline{\mathbb{C}^+}$, and p_m as defined in Theorem 4.2.1 (vi). Then

$$T^k(p_m) = \begin{cases} \frac{F(p_m)}{F(p)} & \text{if } m = -k, \\ 0 & \text{if } m \neq -k \end{cases} \quad (4.33)$$

(vii) T^k has no CRHP zeros other than those given by (iii) - (vi) above.

(viii) Let b be a pole of C_d with b in \mathbb{D}^c , and b_m as defined in Theorem 4.2.1 (viii). Then

$$T^k(b_{m-k}) = \frac{P(b_m) H(b_m) F(b_{m-k})}{T(\text{FPH})_d(b)}. \quad (4.34)$$

Proof: Note that the harmonic functions T^k can be expressed as

$$T^k(s - jk\omega_s) = \frac{F(s - jk\omega_s)}{F(s)} T^0(s). \quad (4.35)$$

By Assumption 3, F is minimum phase and stable, so F_{-k}/F is bistable. The result then follows straightforward from Theorem 4.2.1. \square

There are a number of differences between the interpolation constraints for the hybrid and the continuous-time cases; we now describe these in detail.

Remark 4.2.1 (CRHP Plant Poles) Each CRHP plant pole yields constraints (4.19) directly analogous to the continuous-time case. Furthermore, each of these poles yields the additional constraints (4.21), which arise from the periodically spaced zeros of $S_d(e^{sT})$ and the fact that non-pathological sampling precludes all but one of these zeros from being canceled by a pole of P . \diamond

Remark 4.2.2 (CRHP Plant Zeros) Each CRHP plant zero yields constraints (4.20) directly analogous to the continuous-time case. Note in particular that these constraints are present *independently* of the choice of the hold function. The zeros of the discretized plant lying in \mathbb{D}^c , on the other hand, do not impose any inherent constraints on S^0 . Indeed, suppose that $\nu \in \mathbb{D}^c$ is a zero of $(FPH)_d$. Then for each $\nu_k \triangleq \frac{1}{T} \log(\nu) + jk\omega_s$, $k = 0, \pm 1, \pm 2, \dots$, it follows that

$$S^0(\nu_k) = 1 - \frac{1}{T} P(\nu_k) H(\nu_k) C_d(\nu) F(\nu_k), \quad (4.36)$$

and thus the size of $S^0(\nu_k)$ is *not* independent of the choice of compensator. \diamond

Remark 4.2.3 (Unstable Compensator Poles) For analog systems, unstable plant and compensator poles yield identical constraints on the sensitivity and complementary sensitivity functions; namely, when evaluated at such a pole, sensitivity must equal zero and complementary sensitivity must equal one. Comparing (ii) and (vii) in Theorem 4.2.1, we see that in a hybrid system unstable plant and compensator poles will generally yield different constraints on sensitivity and complementary sensitivity. In particular, unstable compensator poles will yield corresponding zeros of S^0 only in special cases. \diamond

Remark 4.2.4 (Zeros of C_d) Each zero of the compensator lying in \mathbb{D}^c imposes infinitely many interpolation constraints upon the continuous-time system because there are infinitely many points in the s -plane that map to the location of the zero in the z -plane. These constraints are due to the fact that a pole at *any* of these points will lead to an unstable discrete pole-zero cancellation. \diamond

Remark 4.2.5 (Zeros of Hold Response) By Theorem 4.2.1 (iv), zeros of H lying in the CRHP impose constraints on the sensitivity function identical to those imposed by CRHP zeros of the plant. A ZOH has CRHP zeros only on the $j\omega$ -axis. As discussed in Chapter 3, GSHF response functions may have zeros in the *open* right half plane. \diamond

Remark 4.2.6 (Zeros of S^0) Our list of CRHP zeros for T^0 and T^k is exhaustive; however, our list for S^0 is not. It is interesting to contrast this situation with the analog case. For analog systems, the CRHP zeros of the sensitivity function consist precisely of the union of the CRHP poles of the plant and compensator. On the other hand, by Theorem 4.2.1 (ii) and (vii), unstable plant poles yield zeros of S^0 while unstable compensator poles generally do not. Furthermore, as the following example shows, S^0 may have CRHP zeros even if both plant and compensator are stable.

Example 4.2.1 Consider the plant $P(s) = 1/(s + 1)$. Discretizing with a ZOH, sample period $T = 1$, and no anti-aliasing filter (i.e., $F(s) = 1$) yields $(FPH)_d(z) = .6321/(z - .3670)$. A stabilizing discrete controller for this plant is

$$C_d(z) = \frac{(4.8158)(z^2 + .1z + 0.3988)}{(z^2 - 1.02657z + 0.9025)}.$$

Both plant and compensator are stable; yet it may be verified that S^0 has zeros at $s = 0.2 \pm j$ (see Figure 4.1).

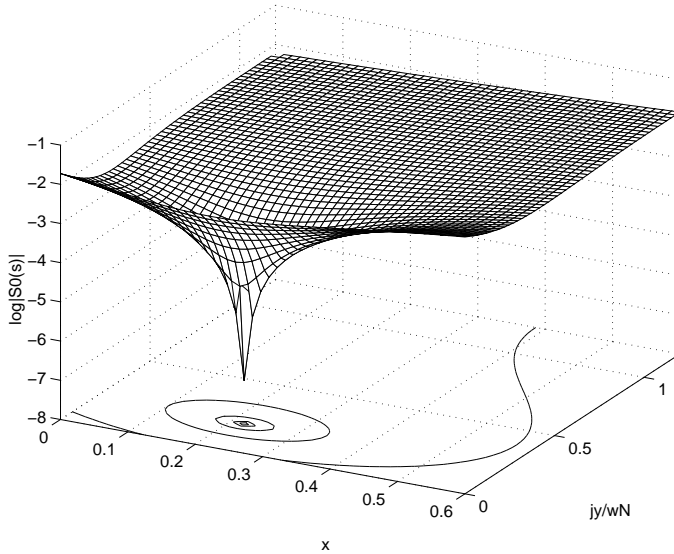


Figure 4.1: Fundamental sensitivity for Example 4.2.1

◇

4.3 Hybrid Disturbance Rejection Properties

In the last section we derived a set of interpolation constraints that must be satisfied by the hybrid sensitivity responses S^0 , T^0 , and T^k in the CRHP. As we shall see in this section, these constraints have interpretations in terms of steady-state disturbance rejection properties of the system. In particular, we analyze periodic disturbances of frequencies within and outside the Nyquist range, and the effect that corresponding unstable poles of the plant and compensator have on these rejection properties. For analog systems, it is well-known that, by the internal model principle, an input disturbance can be asymptotically rejected if the system includes the dynamics of the disturbance [e.g., Wonham, 1985]. As we shall see in this section, this is not generally the case for sampled-data systems.

We start analyzing those properties that are associated with unstable poles of the plant.

Corollary 4.3.1

Assume that P has a pole at $s = j\omega$, $\omega \in \Omega_N$. Then the steady-state response to a disturbance $d(t) = e^{j(\omega + \ell\omega_s)t}$, $t \geq 0$, $\omega \in \Omega_N$, $\ell = 0, \pm 1, \pm 2, \dots$, is given as follows.

(i) If $\ell = 0$, then

$$y_{ss}^d(t) = 0. \quad (4.37)$$

(ii) If $\ell \neq 0$, then

$$y_{ss}^d(t) = e^{j(\omega + \ell\omega_s)t} - \frac{F(j(\omega + \ell\omega_s))}{F(j\omega)} e^{j\omega t}. \quad (4.38)$$

Proof: By (4.9) the steady-state response is given by

$$y_{ss}^d(t) = S^0(j(\omega + \ell\omega_s)) e^{j(\omega + \ell\omega_s)t} - \sum_{\substack{k=-\infty \\ k \neq 0}}^{\infty} T^k(j(\omega + \ell\omega_s)) e^{j(\omega + (k+\ell)\omega_s)t}$$

(i) By (4.19) and (4.31), $S^0(j\omega) = 0$ and $T^k(j\omega) = 0$.

(ii) By (4.21), $S^0(j(\omega + \ell\omega_s)) = 1$. From (4.33) follows that $T^k(j(\omega + \ell\omega_s)) = 0$ if $k \neq -\ell$, and $T_{-\ell}(j(\omega + \ell\omega_s)) = F(j(\omega + \ell\omega_s))/F(j\omega)$ if $k = -\ell$. \square

It follows from (4.37) that a disturbance of frequency $\omega \in \Omega_N$ will be asymptotically rejected if the plant has a pole at $j\omega$ (if necessary, the pole may be augmented to the plant via an *analog* precompensator). However, any high frequency disturbance of frequency $\omega + \ell\omega_s$, $\omega \in \Omega_N$, $\ell \neq 0$ will be passed directly through to the output along with an alias of frequency ω whose amplitude is determined by the ratio of the gains of the anti-aliasing filter evaluated at the two frequencies.

As pointed out in Remark 4.2.4, unstable compensator poles do not yield the same type of constraints on S^0 as the unstable poles of the plant. Moreover, unstable compensator poles do not in general yield asymptotic disturbance rejection, as the following result shows.

Corollary 4.3.2

Assume that C_d has a pole at $z = e^{j\omega T}$, and that P has no poles at $s = j(\omega + k\omega_s)$, $k = 0, \pm 1, \pm 2, \dots$. Then the steady-state response to a disturbance input $d(t) = e^{j(\omega + \ell\omega_s)t}$, $t \geq 0$, $\omega \in \Omega_N$, $\ell = 0, \pm 1, \pm 2, \dots$, satisfies

$$y_{ss}^d(t) = S_\ell^0(j\omega) e^{j(\omega + \ell\omega_s)t} - \sum_{\substack{k=-\infty \\ k \neq 0}}^{\infty} T_\ell^k(j\omega) e^{j(\omega + (k+\ell)\omega_s)t}, \quad (4.39)$$

where

$$S_\ell^0(j\omega) = 1 - \frac{P(j(\omega + \ell\omega_s)) H(j(\omega + \ell\omega_s)) F(j(\omega + \ell\omega_s))}{T(\text{FPH})_d(e^{j\omega T})} \quad (4.40)$$

and

$$T_\ell^k(j\omega) = \frac{P(j(\omega + (k+\ell)\omega_s)) H(j(\omega + (k+\ell)\omega_s)) F(j(\omega + \ell\omega_s))}{T(\text{FPH})_d(e^{j\omega T})}. \quad (4.41)$$

o

Note that even for $\ell = 0$ the steady-state disturbance response is in general *nonzero*. For continuous-time systems, it is well known that a periodic disturbance may be asymptotically rejected by incorporating the dynamics of the disturbance into the system. For a hybrid system, Corollaries 4.3.1 and 4.3.2 show that for asymptotic disturbance rejection to be present, the dynamics should be augmented to the plant using an *analog precompensator*. Including a discretized version of these dynamics in the digital compensator will not, in general, achieve the desired result. Exceptions to this statement may be obtained by imposing additional structure on the hold response function.

Corollary 4.3.3

Let the hypotheses of Corollary 4.3.2 be satisfied. Choose $\omega \in \Omega_{\mathbb{N}}$. Assume that

$$P(j\omega) \neq 0 \quad (4.42)$$

$$H(j\omega) \neq 0 \quad (4.43)$$

and

$$H(j(\omega + k\omega_s)) = 0, \text{ for all } k = \pm 1, \pm 2, \dots \quad (4.44)$$

Then

- (i) the steady-state response to an input $d(t) = e^{j\omega t}$, $t \geq 0$ satisfies $y_{ss}^d(t) = 0$,
- (ii) the steady-state response to an input $d(t) = e^{j(\omega + \ell\omega_s)t}$, $t \geq 0$, $\ell = \pm 1, \pm 2, \dots$ satisfies

$$y_{ss}^d(t) = e^{j(\omega + \ell\omega_s)t} - \frac{F(j(\omega + \ell\omega_s))}{F(j\omega)} e^{j\omega t} \quad (4.45)$$

Proof:

- (i) The steady-state response to $e^{j\omega t}$ is given by (4.9). Hypotheses (4.42)-(4.43) imply that $(FPH)_d(e^{j\omega t}) = \frac{1}{T} F(j\omega)P(j\omega)H(j\omega) \neq 0$, and it follows from Theorem 4.2.1 (iv) that the coefficient of $e^{j\omega t}$ in (4.9) equals one. Using (4.44) in (4.41) shows that the coefficients of the higher frequency terms in (4.9) all equal zero.
- (ii) Hypotheses (4.42)-(4.44) imply that (4.40) equals one, (4.41) equals zero for $k + \ell \neq 0$, and that

$$T_{-\ell}(j(\omega + \ell\omega_s)) = \frac{F(j(\omega + \ell\omega_s))}{F(j\omega)}.$$

These facts, together with (4.39) yield (4.45). □

A consequence of Corollary 4.3.3 is the well known fact that a discrete integrator may be used in conjunction with a ZOH to achieve asymptotic rejection of constant disturbances. Related results for hybrid systems with a ZOH are found in Franklin and Emami-Naeini [1986] and Urikura and Nagata [1987]. A recent

and more general study of tracking problems in hybrid systems is given in Yamamoto [1994].

The role played by the hold frequency response function in the disturbance rejection properties of the system may be further explored by considering plant *input* disturbances. We shall now see that, in conjunction with a pole of the analog plant at the frequency of the disturbance, input disturbance rejection is essentially determined by the shape of the frequency response of the hold.

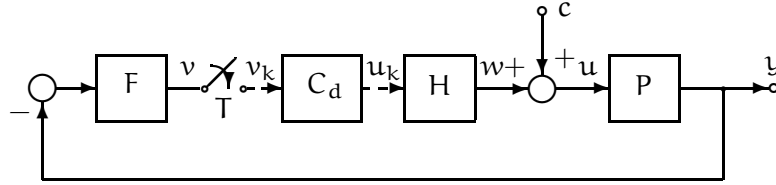


Figure 4.2: System with input disturbance.

Consider the SISO sampled-data system of Figure 4.2. In a similar way to the cases of output disturbance and noise, we can derive expressions describing the steady-state response of the plant input u to a periodic disturbance c . The following lemma, analogous to Lemma 4.1.2, shows this.

Lemma 4.3.4 (Steady-state Frequency Response to Input Disturbance)

Suppose the hypothesis of Lemma 2.2.2 are satisfied, and assume that $c(t) = e^{j\omega t}$, $t \geq 0$. Then as $t \rightarrow \infty$, $u(t) \rightarrow u_{ss}(t)$, where

$$u_{ss}(t) = S^0(j\omega)e^{j\omega t} - \sum_{\substack{k=-\infty \\ k \neq 0}}^{\infty} R^k(j\omega)e^{j(\omega+k\omega_s)t}, \quad (4.46)$$

and

$$R^k(s) \triangleq \frac{1}{T} H_k(s) S_d(e^{sT}) C_d(e^{sT}) F(s) P(s). \quad (4.47)$$

Proof: The proof is similar to that of Lemma 4.1.2. □

Note that, like the response to plant output disturbances, the fundamental component of u_{ss} is governed by S^0 , and so may also be potentially reduced by feedback. The main difference in this case lies on the harmonics, which are given by the responses R^k . From (4.47) we could foresee that the behavior of the hold response function at high frequencies will have a significant role in the relative magnitude of these harmonics. This is perhaps further clarified by the following result, which describes the steady-state disturbance rejection properties of the system in Figure 4.2 when the plant has an unstable pole at the frequency of the disturbance⁹.

⁹Compare with Corollary 4.3.1.

Lemma 4.3.5

Assume that P has a pole at $s = j\omega$, ω in Ω_N . Then the steady-state response to an input disturbance $c(t) = e^{j(\omega + \ell\omega_s)t}$, $t \geq 0$, $\ell = 0, \pm 1, \pm 2, \dots$, is given as follows:

(i) if $\ell = 0$

$$u_{ss}(t) = - \sum_{\substack{k=-\infty \\ k \neq 0}}^{\infty} \frac{H_k(j\omega)}{H(j\omega)} e^{j(\omega + k\omega_s)t}, \quad (4.48)$$

(ii) if $\ell \neq 0$

$$u_{ss}(t) = e^{j(\omega + \ell\omega_s)t}. \quad (4.49)$$

Proof: From Lemma 4.3.4 we have that the steady-state response is given by

$$u_{ss}(t) = S^0(j(\omega + \ell\omega_s)) e^{j(\omega + \ell\omega_s)t} - \sum_{\substack{k=-\infty \\ k \neq 0}}^{\infty} R^k(j(\omega + \ell\omega_s)) e^{j(\omega + (k+\ell)\omega_s)t}. \quad (4.50)$$

(i) By the assumption of non-pathological sampling $H(j\omega) \neq 0$ holds, and so comparing (4.47) and (4.7) we may alternatively write

$$R^k(j\omega) = \frac{H_k(j\omega)}{H(j\omega)} T^0(j\omega). \quad (4.51)$$

Replacing (4.51) in (4.50), and applying Theorem 4.2.1 (ii) gives $S^0(j\omega) = 0$ and $T^0(j\omega) = 1$, from which the result follows.

(ii) Theorem 4.2.1 (vi) yields $S^0(j(\omega + \ell\omega_s)) = 1$. Since $S_d(e^{j\omega T}) = 0$ and $s = j(\omega + \ell\omega_s)$ could not be a pole of P by the non-pathological sampling assumption, we have that

$$\begin{aligned} R^k(j(\omega + \ell\omega_s)) &= \frac{1}{T} H_{k+\ell}(j\omega) S_d(e^{j\omega T}) C_d(e^{j\omega T}) F_\ell(j\omega) P_\ell(j\omega) \\ &= 0. \end{aligned}$$

Equation (4.49) follows. □

Notice from (4.49) that harmonics are asymptotically rejected if the frequency of the disturbance is higher than the Nyquist frequency, but the fundamental component is passed directly to the input of the plant (cf. Corollary 4.3.1).

In the case of a disturbance of frequency ω within Ω_N , it follows from (4.48) that the fundamental component of the steady-state response will be asymptotically rejected if the plant has a pole at $s = j\omega$. However, harmonics of this frequency will pass with amplitudes proportional to the ratios $|H_k(j\omega)/H(j\omega)|$, with $k = \pm 1, \pm 2, \dots$

In practice, the system will have acceptable asymptotic rejection properties if the hold frequency response rolls off at frequencies higher than the Nyquist

frequency, as is the case of a ZOH¹⁰. If on the other hand the hold response is large at high frequencies, as from Chapter 3 we know it may happen with GSHFs, harmonics at those frequencies will be amplified, thereby degrading the input disturbance rejection properties of the hybrid system. In addition, the presence of these harmonics in conjunction with plant input saturation phenomena may compromise the system's overall performance¹¹.

The connection between the hold response and the "size" of the steady-state signals generated by a disturbance in case (i) of Lemma 4.3.5 is further illustrated by the following straightforward corollary. Let w denote the output of the hold device, i.e.,

$$w(t) = u_{ss}(t) - c(t). \quad (4.52)$$

From Lemma 4.3.5 follows that if $c(t) = e^{j\omega T}$, and the plant has a pole at $s = j\omega$, then w is given by

$$w(t) = \sum_{k=-\infty}^{\infty} \frac{H_k(j\omega)}{H(j\omega)} e^{j(\omega+k\omega_s)t}. \quad (4.53)$$

Notice that w is not necessarily periodic. However, its amplitude does correspond to that of a periodic function, since

$$|w(t)| = \left| \sum_{k=-\infty}^{\infty} \frac{H_k(j\omega)}{H(j\omega)} e^{jk\omega_s t} \right|. \quad (4.54)$$

We measure the size of the steady-state value of w by its 2-norm, over an interval of length T . From (4.54) it follows that this is the same as

$$\|w\|_2 = \left(\int_0^T |w(t)|^2 dt \right)^{\frac{1}{2}}.$$

We then have the following result.

Corollary 4.3.6

Assume the conditions of Lemma 4.3.5 are satisfied. Then for a disturbance $c(t) = e^{j\omega t}$, with ω in Ω_N ,

$$\frac{1}{T} \|w\|_2^2 = \frac{\|h\|_2^2}{|H(j\omega)|^2}. \quad (4.55)$$

Proof: From (4.53) we have that $w(t)e^{-j\omega T}$ is periodic with Fourier Series representation

$$w(t)e^{-j\omega T} = \sum_{k=-\infty}^{\infty} \frac{H_k(j\omega)}{H(j\omega)} e^{jk\omega_s t}. \quad (4.56)$$

¹⁰Notice then that the hold should have similar roll-off properties as those of the anti-aliasing filter. Further related comments are given in Chapter 5, Remark 5.2.3.

¹¹See remarks following Lemma 3.1.2 in Chapter 3.

Application of Parseval's Identity [e.g., Rudin, 1987] to the series (4.56) yields

$$\begin{aligned} \int_0^T |w(t)|^2 dt &= \sum_{k=-\infty}^{\infty} \left| \frac{H_k(j\omega)}{H(j\omega)} \right|^2 \\ &= \frac{T \|h\|_2^2}{|H(j\omega)|^2} \end{aligned}$$

where in the last equality we have used Lemma 3.1.1. The result follows. \square

Corollary 4.3.6 shows that the “average power” of the signal generated at the output of the hold device by a periodic disturbance in the Nyquist range Ω_N is proportional to the 2-norm of the hold pulse response h . Noting that

$$\begin{aligned} |H(j\omega)| &\leq \int_0^T |h(t)| dt \\ &= \|h\|_1, \end{aligned}$$

we obtain the lower bound

$$\|w\|_2 \geq \sqrt{T} \frac{\|h\|_2}{\|h\|_1}. \quad (4.57)$$

Since $\|h\|_1 \geq \sqrt{T} \|h\|_2$, we get that $\|w\|_2 \geq 1$ always. It is interesting to note that for a ZOH $\|h\|_1 = \sqrt{T} \|h\|_2$, and so it achieves the lowest bound for the size of the signal w .

We illustrate these results with a numerical example.

Example 4.3.1 (GSHF control of a harmonic oscillator) We consider Example 1 in Kabamba [1987], where a GSHF is designed to stabilize the plant

$$P(s) = \frac{1}{s^2 + 1}$$

by output feedback. The setup corresponds to the system in Figure 4.2 with $F(s) = 1$. This system cannot be made asymptotically stable by continuous-time direct output feedback. However, it can be asymptotically stabilized by a digital compensator and a ZOH, although the closed-loop eigenvalues cannot be arbitrarily assigned. The technique proposed by Kabamba allows the stabilization with just a GSHF (i.e., $C_d = 1$), and arbitrary closed-loop eigenvalues. The hold suggested is a FDLTI GSHF (Definition 3.1.1) given by the matrices

$$K = [0 \quad 1] \quad L = \begin{bmatrix} 0 & -1 \\ 1 & 0 \end{bmatrix} \quad M = \begin{bmatrix} -13.1682 \\ 7.0898 \end{bmatrix}.$$

The sampling period selected was $T = 1$. This GSHF sets the closed-loop discrete eigenvalues to $z = 0$, so the system is stabilized in two sampling periods. For comparison, we alternatively computed a stabilizing solution using a ZOH and

a discrete compensator. A constant compensator of gain $k = -0.9348$ renders a double real pole of the discretized system at $z = 0.7552$.

We computed the frequency response of this GSHF using the formula given by Lemma 3.1.5 in Chapter 3. This is plotted in Figure 4.3, together with the response of the ZOH for reference. We have indicated with dotted lines the abscissas corresponding to the frequencies ω , $\omega + \omega_s$, and $\omega + 2\omega_s$, where $\omega = 1$ is the frequency of the complex poles of the plant.

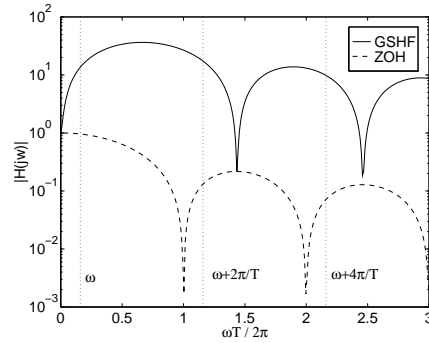


Figure 4.3: Frequency response of GSHF and ZOH.

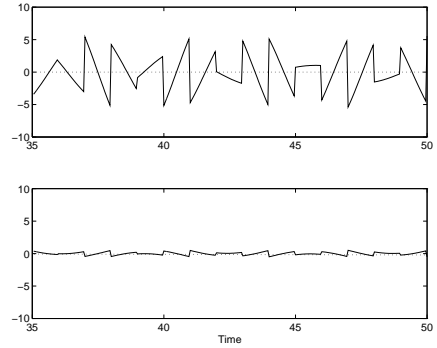


Figure 4.4: Response to input disturbance.

In reference to the summation of (4.48), we can see in this plots that the GSHF will have a larger number of terms with significant contribution than the ZOH. Therefore, we should expect from the GSHF solution a larger steady-state response to a sinusoidal input disturbance of frequency $\omega = 1$. This is illustrated in Figure 4.4, where we plotted the corresponding steady-state responses u for the GSHF system (above) and for the ZOH system (below). The amplitude of the signal produced in the GSHF case is approximately 10 times larger than that of the ZOH case. \diamond

4.4 Integral Relations

The interpolation constraints derived in the preceding section fix the values of the hybrid response functions at points of the CRHP. For continuous-time systems, the Poisson integral may be used to translate the interpolation constraints into equivalent integral relations that the sensitivity and complementary sensitivity functions must satisfy along the $j\omega$ - axis Freudenberg and Looze [1985]. In this section, we show that similar integral relations must be satisfied by the hybrid sensitivity functions. We also show that these functions must satisfy generalizations of the Bode sensitivity integral Bode [1945] and its dual for complementary sensitivity Middleton and Goodwin [1990], Middleton [1991].

4.4.1 Notation

Denote the non-minimum phase zeros of P by

$$\{\zeta_i; i = 1, \dots, N_\zeta\}, \quad (4.58)$$

the non-minimum phase zeros of H by

$$\{\gamma_i; i = 1, \dots, N_\gamma\}, \quad (4.59)$$

the non-minimum phase zeros of C_d by

$$\{a_i; i = 1, \dots, N_a\} \quad (4.60)$$

and the ORHP poles of P by

$$\{p_i; i = 1, \dots, N_p\}, \quad (4.61)$$

including multiplicities in each case. To each a_i and p_i , denote the associated NMP zeros of T^0 by

$$\{a_{ik} = \frac{1}{T} \log(a_i) + jk\omega_s, k = 0, \pm 1, \pm 2, \dots\} \quad (4.62)$$

and

$$\{p_{ik} = p_i + jk\omega_s, k = \pm 1, \pm 2, \dots\}, \quad (4.63)$$

respectively. As discussed in Chapter 3, it is possible that the hold function has a countable infinity of NMP zeros, and thus that N_γ in (4.59) equals infinity.

Denote the Blaschke products of NMP zeros of P and H by

$$B_\zeta(s) = \prod_{i=1}^{N_\zeta} \left(\frac{\zeta_i - s}{\bar{\zeta}_i + s} \right) \quad (4.64)$$

and¹²

$$B_\gamma(s) = \prod_{i=1}^{N_\gamma} \left(\frac{\gamma_i - s}{\bar{\gamma}_i + s} \right). \quad (4.65)$$

Denote the Blaschke product of ORHP plant poles by

$$B_p(s) = \prod_{i=1}^{N_p} \left(\frac{p_i - s}{\bar{p}_i + s} \right) \quad (4.66)$$

For each NMP zero of C_d and for each ORHP pole of P , denote the Blaschke products of associated NMP zeros of T^0 by¹²

$$B_{a_i}(s) = \prod_{k=-\infty}^{\infty} \left(\frac{a_{ik} - s}{\bar{a}_{ik} + s} \right) \quad (4.67)$$

¹²That the Blaschke product (4.65) converges even if N_γ is infinite follows from Hoffman [1962]. The same is valid for (4.67)-(4.68).

and

$$B_{p_i}(s) = \prod_{\substack{k=-\infty \\ k \neq 0}}^{\infty} \left(\frac{p_{ik} - s}{\bar{p}_{ik} + s} \right). \quad (4.68)$$

4.4.2 Poisson Sensitivity Integral

We now derive an integral *inequality* that must be satisfied by $\log |S^0(j\omega)|$.

Theorem 4.4.1 (Poisson integral for S^0)

Assume that the hypotheses of Lemma 2.2.2 are satisfied. Let $\xi = x + jy$ equal one of (4.58)-(4.59) or (4.62)-(4.63). Then

$$\int_0^{\infty} \log |S^0(j\omega)| \Psi(\xi, \omega) d\omega \geq \pi \log |B_p^{-1}(\xi)|, \quad (4.69)$$

where $\Psi(s, \omega)$ is the Poisson kernel for the half plane defined in (3.30).

Proof: Denote the NMP zeros of S^0 by μ_1, μ_2, \dots and define the Blaschke product

$$B_{\mu}(s) = \prod_i \frac{\mu_i - s}{\bar{\mu}_i + s}.$$

Then $S^0 = \check{S} B_{\mu}$ where \check{S} has no poles or zeros in the ORHP. The Poisson integral [Levinson and Redheffer, 1970, p. 225] implies that (4.69) holds with *equality* if $B_p(\xi)$ is replaced by $B_{\mu}(\xi)$. Since the set of NMP zeros of S^0 due to the ORHP poles of P is generally a *proper* subset of all such zeros (cf. Remark 4.2.6) inequality (4.69) follows. \square

Theorem 4.4.1 has several design implications, which we describe in a series of remarks.

Remark 4.4.1 (NMP Plant Zeros) As in the continuous time case, if the plant is non-minimum phase, then requiring that $|S^0(j\omega)| < 1$ over a frequency range Ω implies that, necessarily, $|S^0(j\omega)| > 1$ at other frequencies. The severity of this tradeoff depends upon the relative location of the NMP zero and the frequency range Ω . We now discuss this in more detail.

We recall the definition of the weighted length of an interval by the Poisson kernel for the half plane, introduced in Chapter 3, (3.35). Let $\xi = x + jy$ be a point lying in \mathbb{C}^+ , and consider the frequency interval $\Omega = [0, \omega_0)$. Then, we had that

$$\Theta(\xi, \Omega) \triangleq \int_0^{\omega_0} \Psi(\xi, \omega) d\omega.$$

We have seen in Subsection 3.3.1 that $\Theta(\xi, \Omega)$ equals the negative of the phase lag contributed by a Blaschke product of ξ at the upper end point of the interval Ω . With this notation, the following result is an immediate consequence of (4.69).

Corollary 4.4.2

Suppose that $\zeta = x + jy$ is a NMP zero of the plant, and suppose that

$$|S^0(j\omega)| \leq \alpha, \quad \text{for all } \omega \text{ in } \Omega.$$

Then

$$\sup_{\omega > \omega_0} |S^0(j\omega)| \geq (1/\alpha)^{\frac{\Theta(\zeta, \Omega)}{\pi - \Theta(\zeta, \Omega)}} |B_p^{-1}(\zeta)|^{\frac{\pi}{\pi - \Theta(\zeta, \Omega)}} \quad (4.70)$$

◊

The bound (4.70) shows that if disturbance attenuation is required throughout a frequency interval in which the NMP zero contributes significant phase lag, then disturbances will be greatly amplified at some higher frequency. The term due to the Blaschke product in (4.69) shows that plants with approximate ORHP pole-zero cancelations yield particularly sensitive feedback systems. ◊

Remark 4.4.2 (NMP Hold Zeros) A non-minimum phase zero of the hold response imposes precisely the same tradeoff as does a zero of the plant in the same location. This tradeoff is exacerbated if the NMP hold zero is near an unstable plant pole. Poor sensitivity in this case is to be expected, as an exact pole-zero cancelation yields an unstable hidden mode in the discretized plant¹³. ◊

Remark 4.4.3 (Unstable Plant Poles) Using an analog controller, the sensitivity function of a system with an unstable, but minimum phase, plant can be made arbitrarily small over an arbitrarily wide frequency range Zames and Bensoussan [1983] while maintaining sensitivity bounded outside this range. This is no longer true for digital controllers and the fundamental sensitivity function. The following result is an immediate consequence of (4.69). ◊

Corollary 4.4.3

(i) Assume that the plant has a real ORHP pole, $p = x$. Then

$$\|S^0\|_\infty \geq \sqrt{1 + \left(\frac{x}{\omega_N}\right)^2} \quad (4.71)$$

(ii) Assume that the plant has an ORHP complex conjugate pole pair, $p = x + jy$, $\bar{p} = x - jy$. Then for $k = \pm 1, \pm 2, \dots$

$$\|S^0\|_\infty \geq \sqrt{1 + \left(\frac{x}{k\omega_N}\right)^2} \sqrt{1 + \left(\frac{y}{y - k\omega_N}\right)^2} \quad (4.72)$$

◊

¹³See the conditions for non-pathological sampling in Lemma 2.2.1. An example of a poorly conditioned discretized system is given at the end of §7.1 in Chapter 7.

Proof: We show only (i); (ii) is similar. Evaluate (4.69) with ξ equal one of (4.63), i.e., $\xi = x + jk\omega_s$, with $k = \pm 1, \pm 2, \dots$. Then

$$\begin{aligned} \pi \log \|S^0\|_\infty &\geq \int_0^\infty \log |S^0(j\omega)| \Psi(\xi, \omega) d\omega \\ &\geq \pi \log \left| \frac{2x + jk\omega_s}{-jk\omega_s} \right|. \end{aligned} \quad (4.73)$$

From (4.73) follows

$$\begin{aligned} \|S^0\|_\infty &\geq \sqrt{1 + \left(\frac{x}{k\omega_N}\right)^2} \\ &\geq \sqrt{1 + \left(\frac{x}{\omega_N}\right)^2}. \end{aligned}$$

□

In either case of Corollary 4.4.3, the fundamental sensitivity function necessarily has a peak strictly greater than one.

For a real pole, achieving good sensitivity requires that the sampling rate be sufficiently fast with respect to the time constant of the pole; e.g., achieving $\|S^0\|_\infty < 2$ requires that $\omega_N > x/\sqrt{3}$. This condition is also necessary for a complex pole pair. Furthermore, sensitivity will be poor if $y \approx k\omega_N$ for some $k \neq 0$. The reason for poor sensitivity in this case is clear; if $y = k\omega_N$, then the complex pole pair violates the non-pathological sampling condition (2.12), and the discretized plant will have an unstable hidden mode.

More generally, we have

Corollary 4.4.4

Assume that the plant has unstable poles p_i and p_ℓ with $p_i \neq \bar{p}_\ell$. Then

$$\|S^0\|_\infty \geq \max_{k \neq 0} \left| \frac{\bar{p}_i + p_\ell + jk\omega_s}{p_i - p_\ell - jk\omega_s} \right| \quad (4.74)$$

and

$$\|S^0\|_\infty \geq \max_{k \neq 0} \left| \frac{p_i + p_\ell + jk\omega_s}{\bar{p}_i - p_\ell - jk\omega_s} \right| \quad (4.75)$$

◦

It follows that if sampling is “almost pathological”, in that $p_i - p_\ell \approx jk\omega_s$, or $\bar{p}_i - p_\ell \approx jk\omega_s$, then sensitivity will be large.

Remark 4.4.4 (Approximate Discrete Pole Zero Cancellations) Suppose that the discrete compensator has an NMP zero a_i . Then (4.69) holds with ξ equal to one of the points a_{ik} (4.62) in the s -plane that map to a_i in the z -plane. If the plant has an unstable pole near one of these points, then the right hand side of (4.69) will be large, and S^0 will have a large peak. Poor sensitivity is plausible, because this situation corresponds to an approximate pole-zero cancellation between a NMP zero of the compensator and a pole of the discretized plant. ◊

4.4.3 Poisson Complementary Sensitivity Integral

We now derive a result for T^0 dual to that for S^0 obtained in the previous section. An important difference is that we can characterize *all* NMP zeros of T^0 , and thus obtain integral *equalities*.

First, we note an additional property of the hold response function.

Lemma 4.4.5

The hold response function (2.4) may be factored as

$$H(s) = \check{H}(s)e^{-s\tau_H}B_\gamma(s), \quad (4.76)$$

where $\tau_H \geq 0$, B_γ is given by (4.65), and $\log |\check{H}|$ satisfies the Poisson integral relation.

Proof: Follows from Hoffman [1962, pp. 132-133]. \square

As we discussed in Chapter 3, page 30, for a FDLTI GSHE, $\tau_H = 0$. For a PC GSHE, defined by (3.11), if \bar{k} denotes the smallest value of k for which $a_k \neq 0$, then is easily seen from (3.13)-(3.14) that $\tau_H = \bar{k}T/N$.

We have seen in Chapter 3 explicit expressions for the zeros of a piecewise constant hold with $\alpha_0 \neq 0$ and approximations to the zeros of a FDLTI hold. We remark that, in each case, H possesses infinitely many zeros which approach infinity along well defined paths which may lie in the ORHP (See §3.2).

Theorem 4.4.6 (Poisson integral for T^0)

Assume that the hypotheses of Lemma 2.2.2 are satisfied. Let $p_\ell = x + jy$ be an ORHP pole of P . Then

$$\begin{aligned} \int_0^\infty \log |T^0(j\omega)| \Psi(p_\ell, \omega) d\omega &= \pi x \tau_p + \pi x \tau_H + \pi x N_C T \\ &+ \pi \log |B_\zeta^{-1}(p_\ell)| + \pi \log |B_\gamma^{-1}(p_\ell)| \\ &+ \pi \sum_{i=1}^{N_p} \log |B_{p_i}^{-1}(p_\ell)| + \pi \sum_{i=1}^{N_a} \log |B_{a_i}^{-1}(p_\ell)| \end{aligned} \quad (4.77)$$

where $\Psi(s, \omega)$ is the Poisson kernel for the half plane defined in (3.30).

Proof: Note that T^0 has an inner-outer factorization

$$T^0(s) = \check{T}(s) e^{-s\tau_p} e^{-s\tau_H} e^{-s\tau N_C T} B_\zeta(s) B_\gamma(s) \prod_{i=1}^{N_p} B_{p_i}(s) \prod_{i=1}^{N_a} B_{a_i}(s)$$

where $\log |\check{T}|$ satisfies the Poisson integral Levinson and Redheffer [1970]. Since $\log |\check{T}(j\omega)| = \log |T^0(j\omega)|$, the result follows. \square

We comment on the design implications of Theorem 4.4.6 in a series of remarks.

Remark 4.4.5 The first three terms on the right hand side of (4.77) show that $|T^0(j\omega)|$ will display a large peak if there is a long time delay in the plant, digital controller, or hold function. \diamond

Remark 4.4.6 The fourth and fifth terms on the right hand side of (4.77) show that $|T^0(j\omega)|$ will display a large peak if there is an approximate unstable pole-zero cancelation in the plant, or between the plant and the hold function. By the non-pathological sampling condition (ii) in Lemma 2.2.1, the latter peak corresponds to an approximate unstable pole-zero cancelation in the *discretized* plant. \diamond

The following result is analogous to Corollary 4.4.4 for T^0 .

Corollary 4.4.7

(i) Assume that $p_\ell = x$, a real pole. Then

$$\|T^0\|_\infty \geq \frac{\sinh\left(\frac{\pi x}{\omega_N}\right)}{\left(\frac{\pi x}{\omega_N}\right)}. \quad (4.78)$$

(ii) Assume that $p_\ell = x + jy$, a complex pole. Then

$$\|T^0\|_\infty \geq \frac{\sinh\left(\frac{\pi x}{\omega_N}\right)}{\left(\frac{\pi x}{\omega_N}\right)} \left| \frac{\sinh\left(\frac{\pi p_\ell}{\omega_N}\right)}{\left(\frac{\pi p_\ell}{\omega_N}\right)} \right| \left| \frac{\left(\frac{\pi y}{\omega_N}\right)}{\sin\left(\frac{\pi y}{\omega_N}\right)} \right|. \quad (4.79)$$

Proof: By rearranging definition (4.68), we have

$$B_{p_i}(s) = \prod_{k=1}^{\infty} \frac{1 - \left(\frac{p_i - s}{jk\omega_s}\right)^2}{1 - \left(\frac{\bar{p}_i + s}{jk\omega_s}\right)^2}$$

Using the identities [Levinson and Redheffer, 1970, p. 387],

$$\frac{\sin \pi \alpha}{\pi \alpha} = \prod_{k=1}^{\infty} \left(1 - \frac{\alpha^2}{k^2}\right)$$

and $\sin j\alpha = j \sinh \alpha$ yields

$$B_{p_i}(s) = \frac{\sinh \pi \left(\frac{p_i - s}{\omega_s}\right)}{\pi \left(\frac{p_i - s}{\omega_s}\right)} \frac{\pi \left(\frac{\bar{p}_i + s}{\omega_s}\right)}{\sinh \pi \left(\frac{\bar{p}_i + s}{\omega_s}\right)} \quad (4.80)$$

Note that the first factor on the right hand side of (4.80) converges to one as $s \rightarrow p_i$. It follows that

$$B_{p_\ell}(p_\ell) = \frac{\left(\frac{\pi x}{\omega_N}\right)}{\sinh\left(\frac{\pi x}{\omega_N}\right)} \quad (4.81)$$

Inverting yields (4.78). Furthermore

$$B_{\bar{p}_\ell}(p_\ell) = \frac{\sin\left(\frac{\pi y}{\omega_N}\right)}{\left(\frac{\pi y}{\omega_N}\right)} \frac{\left(\frac{\pi p_\ell}{\omega_N}\right)}{\sinh\left(\frac{\pi p_\ell}{\omega_N}\right)} \quad (4.82)$$

Together (4.81)-(4.82) yield (4.79). \square

Figure 4.5(a) give plots of the bound (4.79) versus $\Re\{p_\ell\}$ for various values of $\Im\{p_\ell\}$, and Figure 4.5(b) give plots of the bound (4.79) versus $\Im\{p_\ell\}$ for various values of $\Re\{p_\ell\}$. The pole location has been normalized by the Nyquist frequency. Note in Figure 4.5(b) that for a complex pole $\|T^0\|_\infty$ will become arbitrarily large as $y \rightarrow k\omega_N$, $k = \pm 1, \pm 2, \dots$, because sampling becomes pathological at such frequencies. It follows from these plots that to achieve good robustness the Nyquist frequency should be chosen several times larger than the radius of any unstable pole.

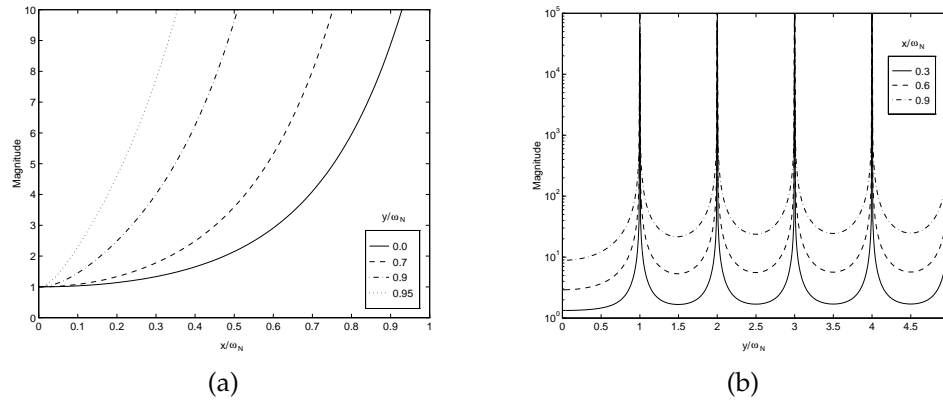


Figure 4.5: Lower bounds on $\|T^0\|_\infty$.

4.4.4 Poisson Harmonic Response Integral

Harmonic response functions (4.8) also satisfy Poisson integral relations. As for the case of T^0 , in this case we also obtain an integral *equality*, since *all* the zeros of

T^k in $\overline{\mathbb{C}^+}$ are characterized. The result follows as a straightforward corollary to Theorem 4.4.6.

Corollary 4.4.8 (Poisson Integral for T^k)

Assume that the hypotheses of Lemma 2.2.2 are satisfied. Let $p_\ell = x + jy$ be an ORHP pole of P . Then

$$\begin{aligned} \int_0^\infty \log |T^k(j\omega)| \Psi(p_\ell - jk\omega_s, \omega) d\omega &= \pi \log \left| \frac{F_{-k}(p_\ell)}{F(p_\ell)} \right| + \pi x \tau_P + \pi x \tau_H + \pi x N_C T \\ &\quad + \pi \log |B_C^{-1}(p_\ell)| + \pi \log |B_Y^{-1}(p_\ell)| \\ &\quad + \pi \sum_{i=1}^{N_p} \log |B_{p_i}^{-1}(p_\ell)| \\ &\quad + \pi \sum_{i=1}^{N_a} \log |B_{a_i}^{-1}(p_\ell)| \end{aligned} \quad (4.83)$$

where $\Psi(s, \omega)$ is the Poisson kernel for the half plane defined in (3.30).

Proof: Immediately from relation (4.35),

$$\begin{aligned} \int_0^\infty \log |T^k(j\omega)| \Psi(p_\ell - jk\omega_s, \omega) d\omega &= \int_0^\infty \log \left| \frac{F(j\omega)}{F_k(j\omega)} \right| \Psi(p_\ell - jk\omega_s, \omega) d\omega \\ &\quad + \int_0^\infty \log |T^0(j(\omega + k\omega_s))| \Psi(p_\ell - jk\omega_s, \omega) d\omega. \end{aligned}$$

The first integral on the RHS of the equation above gives the first term on the RHS of (4.83), since by our assumptions on F , $\log(F(s)/F(s - jk\omega_s))$ satisfies a Poisson integral relation. The second integral is the Poisson Complementary Sensitivity Integral of (4.77). The result follows. \square

The implications of this integral constraint are similar to those for T^0 , since — except for the first — all terms on the RHS of (4.83) are the same on the RHS of (4.77). Hence $|T^k(j\omega)|$ will display a large peak if there are long time delays in the plant, digital controller, or hold function. There will be also large peaks if there are approximate unstable pole-zero cancelations in the plant or between the plant and the hold function. Differently in this case, these constraints are relaxed by the presence of the first term on the RHS of (4.83), which will be generally negative since the anti-aliasing filter is normally designed to roll off at high frequencies. The following corollary, corresponding with Corollary 4.4.7, shows this.

Corollary 4.4.9

(i) Assume that $p_\ell = x$, a real pole. Then

$$\|T^k\|_\infty \geq \frac{\sinh\left(\frac{\pi x}{\omega_N}\right)}{\left(\frac{\pi x}{\omega_N}\right)} \left| \frac{F_{-k}(x)}{F(x)} \right|.$$

(ii) Assume that $p_\ell = x + jy$, a complex pole. Then

$$\|T^k\|_\infty \geq \frac{\sinh\left(\frac{\pi x}{\omega_N}\right)}{\left(\frac{\pi x}{\omega_N}\right)} \left| \frac{\sinh\left(\frac{\pi p_\ell}{\omega_N}\right)}{\left(\frac{\pi p_\ell}{\omega_N}\right)} \right| \left| \frac{\left(\frac{\pi y}{\omega_N}\right)}{\sin\left(\frac{\pi y}{\omega_N}\right)} \right| \left| \frac{F_{-k}(p_\ell)}{F(p_\ell)} \right|.$$

◦

4.4.5 Bode Sensitivity Integral

The following is a generalization of the classical sensitivity integral theorem of Bode [1945]. As in the case of the Poisson sensitivity integral, we only obtain an *inequality*, because S^0 may possess NMP zeros in addition to those associated with ORHP plant poles.

Theorem 4.4.10

Assume that the hypotheses of Lemma 2.2.2 are satisfied.

$$\int_0^\infty \log |S^0(j\omega)| d\omega \geq \pi \sum_{i=1}^{N_p} \Re\{p_i\} \quad (4.84)$$

Proof: Assumption 1 implies that $|sH(s)|$ is bounded on $\overline{\mathbb{C}^+}$ (see (A.12) in Chapter A). This fact, together with the assumption that F is strictly proper, imply that

$$\lim_{\substack{s \rightarrow \infty \\ \Re\{s\} \geq 0}} |sT^0(s)| = 0.$$

Hence the technique used in Freudenberg and Looze [1985] to derive the continuous-time version of (4.84) may be applied. \square

The sensitivity integral states that if $|S^0(j\omega)| < 1$ over some frequency range, then necessarily $|S^0(j\omega)| > 1$ at other frequencies. Hence there is a tradeoff between reducing and amplifying the fundamental component of the response to disturbances at different frequencies. This tradeoff is exacerbated if the plant has ORHP poles. As in the analog cases, (4.84) does not impose a meaningful design limitation unless an additional bandwidth constraint is imposed [e.g., Freudenberg and Looze, 1985]. The need to prevent aliasing in hybrid systems implies that bandwidth constraints are potentially more severe than in the analog case. Design implications remain to be worked out, but it should be noted that the frequency response of the hold function as well as that of the anti-aliasing filter will need to be considered.

4.4.6 Middleton Complementary Sensitivity Integral

We here derive an integral relation for T^0 that is dual to the Bode sensitivity integral obtained for S^0 in the preceding section. This result is a generalization to hybrid systems of the complementary sensitivity integral introduced in Middleton

and Goodwin [1990], and Middleton [1991]. As in the case of the Poisson complementary sensitivity integral, exhaustive knowledge of the zeros of T^0 yields an integral equality.

Theorem 4.4.11

Assume that the hypotheses of Lemma 2.2.2 are satisfied. Suppose also that $T^0(0) \neq 0$. Define $\dot{T}^0(0) = dT^0/ds|_{s=0}$. Then

$$\begin{aligned} \int_0^\infty \log \left| \frac{T^0(j\omega)}{T^0(0)} \right| \frac{d\omega}{\omega^2} &= \frac{\pi}{2}(\tau_P + \tau_H + N_C T) + \pi \sum_{k=1}^{N_\zeta} \frac{1}{\zeta_k} + \pi \sum_{k=1}^{N_\gamma} \frac{1}{\gamma_k} - \pi \sum_{k=1}^{N_p} \frac{1}{p_k} \\ &+ \frac{\pi T}{2} \sum_{k=1}^{N_p} \coth\left(\frac{p_k T}{2}\right) + \frac{\pi T}{2} \sum_{k=1}^{N_a} \coth\left(\frac{a_k T}{2}\right) \\ &+ \frac{\pi \dot{T}^0(0)}{2 T^0(0)}. \end{aligned} \tag{4.85}$$

Proof: See §A.3 in Appendix A. □

This result states that if the ratio $|T^0(j\omega)/T^0(0)| < 1$ over some frequency range, then necessarily this ratio must exceed one at other frequencies. Hence, there is a tradeoff between reducing and amplifying the fundamental component of the response to noise in different frequency ranges. Further comments are found in the following series of remarks.

Remark 4.4.7 The first term on the right hand side of (4.85) show that the tradeoff worsens if the plant, hold, or compensator has a time delay. The second three terms show that the tradeoff worsens if the plant, hold, or compensator has NMP zeros. It is easy to verify that the sum of the fifth and sixth terms is positive, and thus the tradeoff also worsens if the plant has ORHP poles. For an interpretation of the seventh term, see Remark 4.4.9 below. ◇

Remark 4.4.8 One difference between (4.85) and the analogous results in Middleton and Goodwin [1990], Middleton [1991] is that the latter references assume the presence of an integrator in the system. We avoid this requirement by instead assuming that $T^0(0) \neq 0$ and normalizing T^0 by its DC value. This approach could also have been taken in Middleton and Goodwin [1990], Middleton [1991]; we have adopted it here to obtain a more general result. If there is indeed an integrator in the system, then the following corollary, which follows from Corollaries 4.3.1 and 4.3.2, shows that the normalization factor is unnecessary. ◇

Corollary 4.4.12

Assume that

- (i) P contains at least one integrator, and/or

(ii) C_d contains at least one integrator and H is a ZOH.

Then $T^0(0) = 1$. ◦

Remark 4.4.9 We now provide an interpretation for the ninth term in (4.85). To do this, we consider the hybrid system depicted in Figure 4.6.

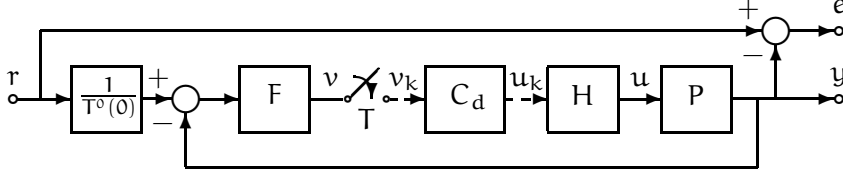


Figure 4.6: Hybrid system.

The proof of the following result is straightforward, and hence omitted.

Lemma 4.4.13

Suppose that the hypotheses of Lemma 2.2.2 are satisfied.

(i) Consider the response of the system to a unit step input. Then, as $t \rightarrow \infty$, $e \rightarrow e_{ss}$, where

$$e_{ss}(t) = \sum_{\substack{\ell=-\infty \\ \ell \neq 0}}^{\infty} -\frac{P(j\ell\omega_s)H(j\ell\omega_s)}{P(0)H(0)} e^{j\ell\omega_s t} \quad (4.86)$$

Furthermore, if H is a ZOH and/or if P contains an integrator, then $e_{ss} = 0$.

(ii) Consider the response of the system to a unit ramp input. Then as $t \rightarrow \infty$, $e \rightarrow e_{ss}$, where

$$e_{ss}(t) = -\frac{\dot{T}^0(0)}{T^0(0)} - \sum_{\substack{\ell=-\infty \\ \ell \neq 0}}^{\infty} [\alpha_\ell + \beta_\ell t] e^{j\ell\omega_s t}, \quad (4.87)$$

with

$$\alpha_\ell = \frac{d}{ds} \left[\frac{T^0(s)}{T^0(0)} \frac{F(s + j\ell\omega_s)}{F(s)} \right] \Big|_{s=-j\ell\omega_s} \quad (4.88)$$

and

$$\beta_\ell = \frac{P(-j\ell\omega_s)H(-j\ell\omega_s)}{P(0)H(0)}. \quad (4.89)$$

Furthermore, if H is a ZOH and/or if P contains an integrator, then $\beta_\ell = 0$ and e_{ss} is bounded. If both these conditions are satisfied, then $\alpha_\ell = 0$ and

$$e_{ss}(t) = -\frac{\dot{T}^0(0)}{T^0(0)}. \quad (4.90)$$

◦

It follows from part (ii) of Lemma 4.4.13 that the constant $\dot{T}^0(0)/T^0(0)$ plays a role similar to that played by the reciprocal of the velocity constant in a Type-1 analog feedback system¹⁴. Hence the ninth term on the right hand side of (4.85) can ameliorate the severity of the design tradeoff *only* if the steady-state error to a ramp input is large and positive, so that the output lags the reference input significantly. ◊

4.5 Summary

We conclude this chapter with a brief summary of inherent design limitations for hybrid feedback systems.

Perhaps most important is the fact that those plant properties such as non-minimum phase zeros, unstable poles, and time delays that pose design difficulty for analog feedback systems continue to pose difficulty when the controller is implemented digitally. Furthermore, the existence of such a difficulty is independent of the type of hold function used. It is important, however, that the intersample behavior be examined if the problems are to be detected. Examining system response only at the sampling instants may be misleading.

There are also a number of design limitations unique to digital controller implementations. First, there are limits upon the ability of high compensator gain to achieve disturbance rejection unless the hold function satisfies additional constraints. Second, there are design limitations due to potential non-minimum phase zeros of the hold function. Perhaps most interesting are the design limitations due to unstable plant poles. If the sample rate is “almost pathological” and/or is slow with respect to the time constant of the pole, then sensitivity, robustness, and response to exogenous inputs will all be poor.

Furthermore, as it is apparent from the results in Araki and Ito [1993], Leung et al. [1991], and Thompson et al. [1983], the fundamental and harmonic response functions introduced here have connections with the L_2 -induced norm of the system, and therefore with its robustness properties against linear time-varying perturbations. We shall deal with these issues in depth in the forecoming chapter.

Perhaps most interesting is the observation that the hold response function plays a role identical to that of the anti-aliasing filter in mapping high frequency plant behavior, including uncertainty, into the response of the discretized plant. This will be the main subject of Chapter 7.

¹⁴For an analog version of (4.90), see Truxal [1955, p. 286]

Sensitivity Operators on L_2

This chapter studies the computation of L_2 -induced norms of sampled-data sensitivity operators. The L_2 -induced norm is the operator norm when inputs and outputs belong to the space of square-integrable signals L_2 , and it is closely related to important control problems. Indeed, for LTI systems, the L_2 -induced norm of a system's operator is the H_∞ -norm of its transfer matrix, which represents an extremely useful measure in many applications of modern control theory [e.g., Francis, 1991].

Concepts and methods associated with LTI H_∞ control bear no immediate equivalent for sampled-data systems, since in this case the operators are time-varying and no transfer functions are associated with them. In view of this, considerable research during the last years has focused on the study of L_2 -norms and H_∞ related problems for sampled-data systems.

Early works considering L_2 -norms for hybrid systems studied restricted classes of sampled-data systems Thompson et al. [1983, 1986], Chen and Francis [1990], Leung et al. [1991]. Conic sectors were applied by Thompson et al. [1983] and Thompson et al. [1986] to obtain upper bounds for the L_2 -norm of cascade connections involving a sampler and a ZOH. Exact expressions for these open-loop systems appeared later on in Chen and Francis [1990]. A formula for the L_2 -norm of hybrid operators in a general feedback configuration was derived by Leung et al. [1991] for the case of band-limited signals.

More recent works introduced the use of *lifting* techniques for the H_∞ analysis and synthesis of sampled-data systems Bamieh and Pearson [1992], Toivonen [1992], Yamamoto [1990, 1993]. As mentioned in Chapter 1, the lifting technique transforms the sampled-data system into a discrete time-invariant equivalent system acting over infinite-dimensional signals. Time-invariance comes as a consequence of periodicity, but in contrast to the classical pure discrete approach, intersample behavior is built in the model, which is reflected in the infinite dimensionality of the transformed signals. Sampled-data H_∞ -norm computation and optimization Bamieh and Pearson [1992], Toivonen [1992], Yamamoto [1993], robust stabilization to LTI perturbations Dullerud and Glover [1993], and tracking Yamamoto [1994] are some recent results obtained via lifting.

Other time-domain approaches include the formulation of an associated Hamiltonian descriptor system Kabamba and Hara [1993], and the solution of continuous and discrete Riccati equations derived using the theory of linear systems with

jumps Sivashankar and Khargonekar [1994], Sun et al. [1993], Tadmor [1991].

An interesting and novel application derived from the computation of L_2 -norms is the extension of the LTI concept of frequency-gain to sampled-data systems Araki and Ito [1993], Araki et al. [1993], Yamamoto and Khargonekar [1996], Hagiwara et al. [1995], Yamamoto and Araki [1994]. The so-called frequency-gain of a sampled-data system is equivalent to the magnitude of a Bode plot of certain discrete transfer function associated with the hybrid system. In Yamamoto and Khargonekar [1996] lifting techniques were used to compute the frequency-gain of a sampled-data system. In Hagiwara et al. [1995] the same issue was addressed using a frequency-domain framework that uses the notion of FR-operators Araki and Ito [1993], Araki et al. [1993].

Our approach in this chapter evolves from the frequency-domain formulation introduced in Chapter 4. In §5.1 we expound a *frequency-domain lifting* framework, which further exposes the harmonic structure of the sampled-data system, yielding a compact description of the operators that govern its behavior. This framework is equivalent to that of FR-operators introduced by Araki and Ito [1993] and Araki et al. [1993]. Yet, our formulation builds up on spaces of Fourier transforms of the original signals, while the FR-operators are defined on special spaces of time-domain signals called SD-sinusoids. The advantages of both methods over time-domain alternatives are similar, and arise from the simplicity of the frequency-domain description.

In §5.2 we exploit the benefits of the frequency-domain lifting to compute the L_2 -induced norms and frequency-gains of sampled-data sensitivity and complementary sensitivity operators. Note that the complementary sensitivity operator is a finite-rank operator — and therefore compact — which implies that its norm can be computed relatively easily. On the other hand, the sensitivity operator is non-compact, which imposes a greater difficulty in the computation of its norm Yamamoto and Khargonekar [1996]. We show that either norm and the frequency-gains can be computed in a straightforward way from finite dimensional discrete transfer functions. The expressions derived are easily implemented in numerically reliable algorithms, as we show in §5.2.2.

5.1 A Frequency-domain Lifting

Many important concepts and methods for LTI systems have no immediate extension to sampled-data systems for the simple fact that sampled-data systems are time-varying. Nevertheless, they belong to a particular class of time-varying systems that have a lot of structure, namely, they can be represented by periodic operators. Most of recent advances in sampled-data control theory have been based on mathematical frameworks that profit from this periodic characteristic. An example of this is the time-domain lifting technique of Bamieh and Pearson [1992] and Yamamoto 1990, 1994. By lifting, a signal valued in a finite dimensional space is bijectively mapped into a signal valued in infinite dimensional spaces. The great attractiveness of the transformation lies on the fact that in the new spaces the operators are represented as LTI operators, which allow a simpler

treatment of many important problems.

In this section we describe a similar mathematical formalism that we call the *frequency-domain lifting*¹. The lifting of Bamieh and Pearson [1992] and Yamamoto [1994] is done over signals in the time-domain, which leads to state-space representations of the sampled-data system. The main difference in our approach is that we lift signals directly in frequency-domain, which — as we shall see in the remaining sections of this chapter — may allow a simpler and more intuitive treatment² of problems that are naturally formulated in input-output scenarios.

Consider a signal y in the space $L_2(0, \infty)$. Then, its Fourier transform $Y(j\omega)$ is known to belong to $L_2(-\infty, \infty)$. Introduce the following sequence of functions constructed from $Y(j\omega)$,

$$Y_k(j\omega) = Y(j(\omega + k\omega_s)), \quad (5.1)$$

for ω in the Nyquist range Ω_N and k integer. We arrange this sequence in an infinite vector, and we denote it by

$$\mathbf{y}(\omega) \triangleq \begin{bmatrix} \vdots \\ Y_1(j\omega) \\ Y_0(j\omega) \\ Y_{-1}(j\omega) \\ \vdots \end{bmatrix}. \quad (5.2)$$

We say that the infinite vector $\mathbf{y}(\omega)$ is the — frequency-domain — *lifting* of the signal $Y(j\omega)$. Figure 5.1 illustrates the action of the lifting operation, which chops up the function $Y(j\omega)$ defined on $(-\infty, \infty)$ into a sequence of functions $Y_k(j\omega)$, $k = 0, \pm 1, \pm 2, \dots$ defined on Ω_N .

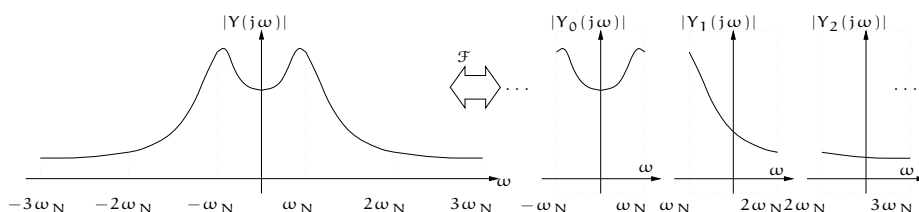


Figure 5.1: Action of the frequency-domain lifting operation.

Thus, $\mathbf{y}(\omega)$ can be seen as a function defined a.e.³ over Ω_N taking values in ℓ_2 . Moreover, the space of such functions is a Hilbert space under the norm

$$\|\mathbf{y}\| \triangleq \left(\int_{\Omega_N} \|\mathbf{y}(\omega)\|_{\ell_2}^2 d\omega \right)^{1/2}, \quad (5.3)$$

¹The concept of frequency-domain lifting is not new; it was developed in the signal processing literature for linear discrete-time periodic systems [e.g., Shenoy et al., 1994].

²Simpler and more intuitive in the sense explained in Chapter 1, §1.2 (i).

³With respect to the standard Lebesgue measure.

and inner product

$$\langle \mathbf{y}, \mathbf{x} \rangle \triangleq \int_{\Omega_N} \langle \mathbf{y}(\omega), \mathbf{x}(\omega) \rangle_{\ell_2} d\omega. \quad (5.4)$$

We denote this space by $L_2(\Omega_N; \ell_2)$ [cf. Balakrishnan, 1981]. Since the signals in $L_2(\Omega_N; \ell_2)$ are basically rearrangements of signals in $L_2(-\infty, \infty)$, it is not difficult to see that both spaces are isomorphic with preservation of norm, as the following lemma asserts.

Lemma 5.1.1

The space $L_2(\Omega_N; \ell_2)$ is isometrically isomorphic to $L_2(-\infty, \infty)$.

Proof: See Appendix A, §A.4. □

Lemma 5.1.1 tells us that there is a bijective relation between elements in $L_2(-\infty, \infty)$ and elements in $L_2(\Omega_N; \ell_2)$, and moreover, they have the same measure, i.e.,

$$\|\mathbf{y}\|_{L_2(\Omega_N; \ell_2)} = \|\mathbf{Y}\|_{L_2(-\infty, \infty)}.$$

We formalize this relationship by defining the *frequency-domain lifting operator*, \mathcal{F} , mapping

$$\begin{aligned} \mathcal{F} : L_2(-\infty, \infty) &\rightarrow L_2(\Omega_N; \ell_2) \\ Y(j\omega) &\mapsto \mathbf{y}(\omega). \end{aligned}$$

Evidently from Lemma 5.1.1, \mathcal{F} is invertible, and moreover, $\|\mathcal{F}\| = 1 = \|\mathcal{F}^{-1}\|$. In particular, if \mathcal{M} is a bounded linear operator from $L_2(-\infty, \infty)$ to $L_2(-\infty, \infty)$, then the lifted operator $\mathcal{M} = \mathcal{F} \mathcal{M} \mathcal{F}^{-1}$ is a bounded linear operator from $L_2(\Omega_N; \ell_2)$ to $L_2(\Omega_N; \ell_2)$ with the same operator norm. A key observation at this point is that it will be in general easier and numerically more tractable to compute $\|\mathcal{M}\|$ rather than $\|\mathcal{M}\|$.

The representation of sampled-data operators by their liftings also reveals structure with interesting similarities to ordinary LTI operators and their corresponding transfer matrices. Indeed, it turns out that the lifted operator \mathcal{M} is a *multiplication operator* in ℓ_2 sense, so it has an associated representation as an infinite-dimensional “transfer matrix”. In other words, we can write $(\mathcal{M}\mathbf{y})(\omega) = \mathbf{M}_\omega \mathbf{y}(\omega)$, where \mathbf{M}_ω is a bounded linear operator in ℓ_2 at (almost) every fixed ω in Ω_N . An important consequence of this fact is that the L_2 -induced norm of the operator can be computed as [cf. Yamamoto and Khargonekar, 1996]

$$\|\mathcal{M}\| = \sup_{\omega \in \Omega_N} \|\mathbf{M}_\omega\|_{\ell_2}, \quad (5.5)$$

where $\|\mathbf{M}_\omega\|_{\ell_2}$ denotes the induced ℓ_2 -norm of the operator \mathbf{M}_ω . Notice the similarity of (5.5) to the familiar expression of the L_2 -induced norm of an operator in a LTI system, i.e., the H_∞ -norm of its associated transfer matrix.

In particular, we shall be concerned with *compact* and *approximable* operators on these spaces, so we finish the section with a brief discussion of these concepts. This follows Willis [1994].

Recall that a set K in a metric space is *compact* if each sequence in K has a convergent subsequence. Equivalently, for any collection of open sets $\{V_k\}$ that covers K , then K is compact if and only if $\{V_k\}$ has a finite subcollection that covers K . To say that a set is compact is to say that it is “small” in some sense. The Heine-Borel Theorem [e.g., Rudin, 1987] asserts that a set in a finite-dimensional space is compact if and only if it is closed and bounded.

Definition 5.1.1 (Compact Operator)

Let X and Y be metric spaces, and let B_X denote the unit ball in X . Then the operator $T : X \rightarrow Y$ is said to be compact if the closure of $T(B_X)$ is a compact set. \diamond

Compact operators are very close to finite-rank operators, i.e., operators whose range is finite-dimensional. Since $T(B_X)$ is bounded if T is a bounded operator, it follows from the Heine-Borel Theorem that each finite-rank operator is compact. In a sense, a “converse” of this is also true in the spaces we are interested in. Namely, a compact operator on these spaces is *approximable* by sequences of finite-rank operators; i.e., if $\{E_n\}$ is a sequence of finite-rank operators, then $\lim_{n \rightarrow \infty} \|E_n - T\| = 0$, where $\|\cdot\|$ denotes the induced operator norm.

5.2 L_2 -induced Norms and Frequency-gains

5.2.1 Sensitivity Operators

We study the sensitivity and complementary sensitivity operators for the sampled-data system of Figure 2.4. As for LTI systems, we define these operators as the mappings relating output disturbance d and noise n to the output y , and denote them respectively by

$$\begin{aligned} \mathcal{S} : L_2 &\rightarrow L_2 & \text{and} & & \mathcal{T} : L_2 &\rightarrow L_2 \\ \mathcal{S}d &\mapsto y & & & \mathcal{T}n &\mapsto y. \end{aligned}$$

Under the assumptions of closed-loop L_2 -stability, \mathcal{S} and \mathcal{T} are bounded operators on L_2 .

The actions of the sensitivity and complementary sensitivity operators are respectively defined in frequency-domain by the steady-state responses (4.1) and (4.2) introduced in Chapter 4, §4.1. From the definition of frequency-domain lifting in §5.1, it is straightforward to alternatively write (4.1) and (4.2) evaluated at $s = j\omega$ in a very compact form as

$$\mathbf{y} = \mathbf{S}_\omega \mathbf{d} \quad \text{and} \quad \mathbf{y} = -\mathbf{T}_\omega \mathbf{n}, \quad (5.6)$$

where \mathbf{T}_ω and \mathbf{S}_ω are the following infinite-dimensional transfer matrices defined on Ω_N

$$\mathbf{T}_\omega = \begin{bmatrix} \ddots & \vdots & \vdots & & \\ \cdots & G_k F_k & G_k F_{k-1} & \cdots & \\ \cdots & G_{k-1} F_k & G_{k-1} F_{k-1} & \cdots & \\ & \vdots & \vdots & \ddots & \end{bmatrix}, \quad (5.7)$$

$$\mathbf{S}_\omega = \begin{bmatrix} \ddots & \vdots & \vdots & \vdots & \vdots \\ \cdots & 1 - G_k F_k & -G_k F_{k-1} & \cdots & \vdots \\ \cdots & -G_{k-1} F_k & 1 - G_{k-1} F_{k-1} & \cdots & \vdots \\ \vdots & \vdots & \vdots & \ddots & \ddots \end{bmatrix}, \quad (5.8)$$

where, to ease notation, we have omitted the explicit dependence of the variable $j\omega$ in the entries of the matrices. Keep also in mind the notation $F_k(j\omega)$ representing $F(j(\omega + k\omega_s))$, which will be profusely used in the sequel. Here $F(j\omega)$ is the transfer matrix of the anti-aliasing filter, and the function $G(j\omega)$ denotes the product

$$G(j\omega) \triangleq \frac{1}{T} P(j\omega)H(j\omega)S_d(e^{j\omega T})C_d(e^{j\omega T}). \quad (5.9)$$

Associated with $F(j\omega)$ and $G(j\omega)$ we define the following discretized transfer matrices that will be required to formulate our results,

$$G_d(e^{j\omega T}) \triangleq \sum_{k=-\infty}^{\infty} G_k^*(j\omega)G_k(j\omega), \quad (5.10)$$

and

$$F_d(e^{j\omega T}) \triangleq \sum_{k=-\infty}^{\infty} F_k(j\omega)F_k^*(j\omega), \quad (5.11)$$

where F^* denotes the conjugated transpose of F . Note that if y , n , and d are valued in \mathbb{R}^m , then $G_d(e^{j\omega T})$ and $F_d(e^{j\omega T})$ are $m \times m$ discrete transfer matrices.

Operators \mathbf{S}_ω and \mathbf{T}_ω are infinite-dimensional transfer matrix representations of the hybrid sensitivity and complementary sensitivity operators \mathcal{S} and \mathcal{T} , and verify the complementarity relation $\mathbf{S}_\omega + \mathbf{T}_\omega = \mathbf{I}$ [cf. Araki and Ito, 1993, Araki et al., 1993, Yamamoto and Araki, 1994]. From (5.5) their induced norms are given by

$$\|\mathcal{T}\| = \sup_{\omega \in \Omega_N} \|\mathbf{T}_\omega\|_{\ell_2} \quad \text{and} \quad \|\mathcal{S}\| = \sup_{\omega \in \Omega_N} \|\mathbf{S}_\omega\|_{\ell_2}, \quad (5.12)$$

and so, they can be evaluated by computing the functions $\|\mathbf{T}_\omega\|_{\ell_2}$ and $\|\mathbf{S}_\omega\|_{\ell_2}$ — the so-called *frequency-gains* of the hybrid operators [e.g., Hagiwara et al., 1995] — and then searching for suprema over the finite interval Ω_N .

An important fact about the complementary sensitivity operator \mathcal{T} is that it has finite rank (and therefore is compact, as discussed in §5.1). We show this in the following lemma.

Lemma 5.2.1

If the inputs to the system in Figure 2.4 are valued in \mathbb{R}^m , then \mathcal{T} has at most rank m .

Proof: Partition $F(j\omega)$ by rows, and $G(j\omega)$ by columns, i.e.,

$$F(j\omega) = \begin{bmatrix} f_1(j\omega) \\ f_2(j\omega) \\ \vdots \\ f_m(j\omega) \end{bmatrix}, \quad \text{and} \quad G(j\omega) = [g_1(j\omega) \quad g_2(j\omega) \quad \cdots \quad g_m(j\omega)].$$

Introduce the liftings for $F^*(j\omega)$ and $G(j\omega)$,

$$\mathbf{f}(\omega) \triangleq \begin{bmatrix} \vdots \\ F_1^*(j\omega) \\ F_0^*(j\omega) \\ F_{-1}^*(j\omega) \\ \vdots \end{bmatrix}, \quad \text{and} \quad \mathbf{g}(\omega) \triangleq \begin{bmatrix} \vdots \\ G_1(j\omega) \\ G_0(j\omega) \\ G_{-1}(j\omega) \\ \vdots \end{bmatrix}. \quad (5.13)$$

Using the partitions above, we can alternatively write

$$\mathbf{f}(\omega) = [\mathbf{f}_1(\omega) \quad \mathbf{f}_2(\omega) \quad \dots \quad \mathbf{f}_m(\omega)],$$

and

$$\mathbf{g}(\omega) = [\mathbf{g}_1(\omega) \quad \mathbf{g}_2(\omega) \quad \dots \quad \mathbf{g}_m(\omega)],$$

where each column $\mathbf{f}_i = \mathcal{F}f_i^*$ in \mathbf{f} , and $\mathbf{g}_i = \mathcal{F}g_i$ in \mathbf{g} is certainly a vector in $L_2(\Omega_N; \ell_2)$, since F and G are both stable and strictly proper from our assumptions in Chapter 2. Using this notation, the action of \mathbf{T}_ω can be alternatively written as

$$\mathbf{T}_\omega \mathbf{n} = \sum_{i=1}^m \mathbf{g}_i \langle \mathbf{n}, \mathbf{f}_i \rangle_{\ell_2}, \quad (5.14)$$

where, $\langle \mathbf{n}, \mathbf{f}_i \rangle_{\ell_2}$ is a scalar-valued function defined a.e. on Ω_N ⁴. Equation (5.14) shows that \mathbf{T}_ω is the sum of m rank-one operators on $L_2(\Omega_N; \ell_2)$. Hence it has at most rank m , and so does \mathcal{T} . \square

The fact that \mathcal{T} is compact — and so approximable — suggests a way of numerically computing the norm of \mathcal{T} by truncating \mathbf{T}_ω between harmonics $-n$ and n , say, and evaluating the maximum singular value of the finite dimensional transfer matrix so obtained Araki et al. [1993]. The convergence of this sequence of computations could be slow, though, since in general $G(j\omega)$ and $F(j\omega)$ decay as $1/\omega^p$, where p is some integer depending on the relative degrees of the transfer matrices involved.

Actually, since \mathcal{T} is of finite-rank, more efficient ways of numerically evaluating the induced norm of \mathbf{T}_ω are possible and already available. Using frequency-domain techniques similar to ours, Hagiwara et al. [1995] have shown that the computation of the frequency-gain of a compact operator can be obtained as the magnitude of an associated discrete-time transfer matrix. For the case of ZOH, they show how to implement their procedures in a numerically reliable fashion.

The following theorem is analogous to the result of Hagiwara et al. [1995] for the case of the hybrid complementary sensitivity operator \mathcal{T} . The pattern of our proof is quite different though, and importantly, we shall use the same pattern for the more difficult case of the hybrid sensitivity operator, which is non-compact. Our results extend to the case of GSHF, and are also implementable in a numerically reliable way, as we shall see in Subsection 5.2.2.

⁴Often, we shall drop the dependence of the independent variable when convenient; meaning will always be clear from context.

We denote by $\lambda_{\max}[M]$ the maximum eigenvalue of a square matrix M . Then we have the following result.

Theorem 5.2.2 (L_2 -induced Norm of the Complementary Sensitivity Operator)
If the hybrid system of Figure 2.4 is L_2 -input-output stable, then

$$\|\mathcal{T}\|^2 = \sup_{\omega \in \Omega_N} \lambda_{\max} [G_d(e^{j\omega T})F_d(e^{j\omega T})]. \quad (5.15)$$

Proof: Using (5.13) write \mathbf{T}_ω as a dyadic product

$$\mathbf{T}_\omega = \mathbf{g}(\omega)\mathbf{f}(\omega)^*,$$

where \mathbf{f}^* denotes the conjugate transpose of \mathbf{f} (i.e., \mathbf{f}^* is composed of “row” vectors of $L_2(\Omega_N, \ell_2)$). From (5.12) we have that $\|\mathcal{T}\| = \sup_{\omega \in \Omega_N} \|\mathbf{T}_\omega\|_{\ell_2}$. Fix ω in Ω_N , and decompose ℓ_2 into

$$\ell_2 = P_F \oplus P_F^\perp,$$

where P_F is the subspace of ℓ_2 spanned by the range of \mathbf{f} , and P_F^\perp its orthogonal complement. Hence, if \mathbf{v} is a vector in P_F^\perp then $\mathbf{T}_\omega \mathbf{v} = 0$. So,

$$\begin{aligned} \|\mathbf{T}_\omega\|_{\ell_2} &= \sup_{\substack{\mathbf{v} \in \ell_2 \\ \mathbf{v} \neq 0}} \frac{\|\mathbf{T}_\omega \mathbf{v}\|_{\ell_2}}{\|\mathbf{v}\|_{\ell_2}} \\ &= \sup_{\substack{\mathbf{v} \in P_F \\ \mathbf{v} \neq 0}} \frac{\|\mathbf{T}_\omega \mathbf{v}\|_{\ell_2}}{\|\mathbf{v}\|_{\ell_2}}. \end{aligned}$$

Vectors of ℓ_2 in P_F can be finitely parameterized as

$$\mathbf{v} = \mathbf{f}\alpha,$$

where α belongs to \mathbb{C}^m , with m the number of inputs of F . Thus, we have

$$\begin{aligned} \|\mathbf{T}_\omega\|_{\ell_2}^2 &= \sup_{\substack{\alpha \\ \mathbf{f}\alpha \neq 0}} \frac{\alpha^* \mathbf{f}^* \mathbf{g}^* \mathbf{g} \mathbf{f} \alpha}{\alpha^* \mathbf{f}^* \mathbf{f} \alpha} \\ &= \lambda_{\max} [(\mathbf{f}^* \mathbf{f})^{1/2} (\mathbf{g}^* \mathbf{g}) (\mathbf{f}^* \mathbf{f})^{1/2}]. \end{aligned} \quad (5.16)$$

Notice that both $(\mathbf{g}^* \mathbf{g})$ and $(\mathbf{f}^* \mathbf{f})$ are finite $m \times m$ matrices, and particularly, $\mathbf{f}^* \mathbf{f}$ is non-singular since F was assumed full column rank.

Since eigenvalues are invariant under similarity transformations, (5.16) yields

$$\|\mathbf{T}_\omega\|_{\ell_2}^2 = \lambda_{\max} [(\mathbf{g}^* \mathbf{g}) (\mathbf{f}^* \mathbf{f})].$$

The proof is finished by noting that

$$(\mathbf{g}^* \mathbf{g})(\omega) = G_d(e^{j\omega T})$$

and

$$(\mathbf{f}^* \mathbf{f})(\omega) = F_d(e^{j\omega T})$$

are the discrete transfer matrices defined in (5.10) and (5.11). \square

The case of \mathcal{S} has to be considered more carefully, since this is a non-compact operator, and as such, it may not be in principle approximable by sequences of finite-rank operators (which means that the norms of progressive truncations of \mathbf{S}_ω would not necessarily converge to the norm of the operator). Frequency-gains of possibly non-compact sampled-data operators have been discussed in Yamamoto and Khargonekar [1996]. Their method computes the frequency-gain γ_ω at the frequency ω by searching for the maximum value γ such that a γ -dependent generalized eigenvalue problem has an eigenvalue $e^{j\omega T}$. Yet, the procedure seems in general very hard to be implemented numerically in a reliable fashion Hagiwara et al. [1995].

The following theorem gives an expression for the frequency-gain and L_2 -induced norm of the hybrid sensitivity operator \mathcal{S} . Our result relies on the fact that \mathcal{S} verifies the complementarity relation

$$\mathcal{S} = \mathcal{J} - \mathcal{T},$$

and since \mathcal{T} is of finite rank, it is also possible to reduce the computation of the frequency-gain of \mathcal{S} to a finite-dimensional eigenvalue problem. As for Theorem 5.2.2, these results admit a simple and reliable numerical implementation.

Theorem 5.2.3 (L_2 -induced Norm of the Sensitivity Operator)

If the hybrid system of Figure 2.4 is L_2 -input-output stable, then

$$\|\mathcal{S}\|^2 = 1 + \sup_{\omega \in \Omega_N} \lambda_{\max} \begin{bmatrix} F_d(e^{j\omega T}) G_d(e^{j\omega T}) - T_d(e^{j\omega T}) & -F_d(e^{j\omega T}) \\ T_d(e^{-j\omega T}) G_d(e^{j\omega T}) - G_d(e^{j\omega T}) & -T_d(e^{-j\omega T}) \end{bmatrix}. \quad (5.17)$$

Proof: The same idea for the proof of Theorem 5.2.2 works here. Again, for a fixed ω in Ω_N , decompose ℓ_2 into

$$\ell_2 = P_{(F,G)} \oplus P_{(F,G)}^\perp,$$

where $P_{(F,G)}$ denotes the subspace spanned by both \mathbf{f} and \mathbf{g} , and $P_{(F,G)}^\perp$ its orthogonal complement. Since \mathbf{S}_ω is block diagonal in these spaces,

$$\begin{aligned} \|\mathbf{S}_\omega\|_{\ell_2} &= \max \left\{ \sup_{\substack{\mathbf{v} \in P_{(F,G)} \\ \mathbf{v} \neq 0}} \frac{\|\mathbf{S}_\omega \mathbf{v}\|_{\ell_2}}{\|\mathbf{v}\|_{\ell_2}}, \sup_{\substack{\mathbf{v} \in P_{(F,G)}^\perp \\ \mathbf{v} \neq 0}} \frac{\|\mathbf{S}_\omega \mathbf{v}\|_{\ell_2}}{\|\mathbf{v}\|_{\ell_2}} \right\} \\ &= \max \left\{ \sup_{\substack{\mathbf{v} \in P_{(F,G)} \\ \mathbf{v} \neq 0}} \frac{\|\mathbf{S}_\omega \mathbf{v}\|_{\ell_2}}{\|\mathbf{v}\|_{\ell_2}}, 1 \right\}. \end{aligned} \quad (5.18)$$

Now, any vector \mathbf{v} in $P_{(F,G)}$ can be finitely parameterized as

$$\begin{aligned} \mathbf{v} &= \mathbf{f}\alpha + \mathbf{g}\beta \\ &= [\mathbf{f}, \mathbf{g}] \gamma, \end{aligned} \quad (5.19)$$

with γ in C^{2m} . Denote $\mathbf{h} \triangleq [\mathbf{f}, \mathbf{g}]$, and $M \triangleq \mathbf{h}^* \mathbf{h}$. Notice that M is a finite-dimensional Hermitian matrix and, moreover, since for any vector η in C^{2m} we have that $\eta^* M \eta = \eta^* \mathbf{h}^* \mathbf{h} \eta = \|\mathbf{h}\eta\|_2$, M is also non-negative definite, i.e., $M \geq 0$. Using the notation introduced in (5.10) and (5.11), and the definition of the discrete output complementary sensitivity function (2.11) (i.e., notice that $T_d = \mathbf{f}^* \mathbf{g}$), we can write M as

$$M = \begin{bmatrix} F_d & T_d \\ T_d^* & G_d \end{bmatrix}.$$

Introduce also the matrix N ,

$$N \triangleq \begin{bmatrix} G_d & -I \\ -I & 0 \end{bmatrix}.$$

It then follows that $\mathbf{h}^*(\mathbf{I} - \mathbf{f}\mathbf{g}^*)(\mathbf{I} - \mathbf{g}\mathbf{f}^*)\mathbf{h} = (\mathbf{I} + \mathbf{M}\mathbf{N})\mathbf{M}$, and hence we obtain from (5.19) that

$$\begin{aligned} \sup_{\substack{\mathbf{v} \in P_{(F, G)} \\ \mathbf{v} \neq 0}} \frac{\|\mathbf{S}_\omega \mathbf{v}\|_{\ell_2}^2}{\|\mathbf{v}\|_{\ell_2}^2} &= \sup_{\gamma \in C^{2m}} \frac{\gamma^* M \gamma + \gamma^* M N M \gamma}{\gamma^* M \gamma} \\ &= 1 + \lambda_{\max} \left[M^{1/2} N M^{1/2} \right] \end{aligned} \quad (5.20)$$

$$= 1 + \lambda_{\max} [MN] . \quad (5.21)$$

Since in (5.21) the product MN is

$$MN = \begin{bmatrix} F_d G_d - T_d & -F_d \\ T_d^* G_d - G_d & -T_d^* \end{bmatrix},$$

from (5.18) and (5.21) we see that it remains to show that $\lambda_{\max} [MN]$ is nonnegative to complete the proof. This follows easily from the fact that $M \geq 0$. Indeed, if M is positive definite, i.e., $M > 0$, then

$$\delta = \begin{bmatrix} F_d & T_d \\ T_d^* & G_d \end{bmatrix}^{-1/2} \begin{bmatrix} I \\ 0 \end{bmatrix},$$

gives $\delta^* M^{1/2} N M^{1/2} \delta = G_d \geq 0$. Thus λ_{\max} in (5.20) is nonnegative. If otherwise M is not positive definite it is then necessarily singular, and therefore 0 must be in the spectrum of $M^{1/2} N M^{1/2}$, which then shows that $\lambda_{\max} [MN] \geq 0$. The proof is now complete. \square

Remark 5.2.1 (L_2 -norms and Hybrid Sensitivity Functions) As anticipated at the end of Chapter 4, the L_2 -induced norm of these operators may be linked to certain measure of the hybrid sensitivity functions S^0 , T^0 , and T^k . In fact, this connection establishes that large harmonics will necessarily imply a large norm of the operator on L_2 , as we shall see next. We define first the *hybrid* (k, m)-*harmonic response*

$$T^{k, m} \triangleq G_k F_m.$$

Notice that $T^{k,m}$ for $k, m = \pm 1, \pm 2, \dots$ appear as the off-diagonal entries of the infinite-dimensional transfer matrices \mathbf{T}_ω and \mathbf{S}_ω in (5.7) and (5.8). In particular, $T^{k,0} = T^k$ and $T^{0,0} = T^0$, the harmonic and fundamental complementary sensitivity responses of Chapter 4. We require the following preliminary lemma.

Lemma 5.2.4

Let $A, B_1, B_2, \dots, B_k, \dots$ be square hermitian positive-definite matrices. Then

$$\lambda_{\max} \left[\sum_k B_k A \right] \geq \max_k \lambda_{\max} [B_k A].$$

Proof:

$$\begin{aligned} \lambda_{\max} \left[\sum_k B_k A \right] &= \lambda_{\max} \left[\sum_k [A^{\frac{1}{2}} B_k A^{\frac{1}{2}}] \right] \\ &= \max_{\nu, \|\nu\|=1} \sum_k [\nu^* A^{\frac{1}{2}} B_k A^{\frac{1}{2}} \nu] \\ &\geq \max_k \max_{\nu, \|\nu\|=1} \nu^* A^{1/2} B_k A^{1/2} \nu \\ &= \max_k \lambda_{\max} [B_k A] \end{aligned}$$

□

Now we have the following result.

Proposition 5.2.5

Assume the conditions of Lemma 2.2.2 are satisfied. Then

$$\|\mathcal{T}\| \geq \max_{k,m} \|T_{k,m}\|_\infty$$

Proof: From Theorem 5.2.2,

$$\|\mathcal{T}\|^2 = \frac{1}{T^2} \sup_{\omega \in \Omega_N} \lambda_{\max} \left[\left(\sum_k G_k^* G_k \right) \left(\sum_m F_m F_m^* \right) \right].$$

Use Lemma 5.2.4 with $A = (\sum_k G_k^* G_k)$, and $B_m = F_m F_m^*$ to get

$$\|\mathcal{T}\|^2 \geq \frac{1}{T^2} \sup_{\omega \in \Omega_N} \max_m \lambda_{\max} \left[\sum_k G_k^* G_k F_m F_m^* \right],$$

and once more with $A = F_m F_m^*$, and $B_k = G_k^* G_k$. This yields

$$\begin{aligned} \|\mathcal{T}\|^2 &\geq \frac{1}{T^2} \sup_{\omega \in \Omega_N} \max_{k,m} \lambda_{\max} [G_k^* G_k F_m F_m^*] \\ &= \max_{k,m} \sup_{\omega \in \Omega_N} \left\| \frac{1}{T} G_k F_m \right\|_2^2 \\ &= \max_{k,m} \|T_{k,m}\|_\infty^2. \end{aligned}$$

□

This result establishes that a peak in any of the harmonics will increase the L_2 -induced norm of \mathcal{T} , reducing the system's stability robustness properties against T -periodic perturbations Sivashankar and Khargonekar [1993]. \diamond

In the particular case of SISO systems, we can derive simpler formulas from Theorems 5.2.2 and 5.2.3. The operator \mathcal{T} is then of rank one, and so the computation of its norm and the norm of \mathcal{S} reduces to a single-eigenvalue problem.

Corollary 5.2.6

If the hybrid system of Figure 2.4 is SISO, then

$$\|\mathcal{T}\| = \sup_{\omega \in \Omega_N} \Phi_d(e^{j\omega T}) |T_d(e^{j\omega T})|, \quad (5.22)$$

and

$$\begin{aligned} \|\mathcal{S}\| = \sup_{\omega \in \Omega_N} \frac{1}{2} & \left(\sqrt{(\Phi_d^2(e^{j\omega T}) - 1) |T_d(e^{j\omega T})|^2 + (|S_d(e^{j\omega T})| + 1)^2} \right. \\ & \left. + \sqrt{(\Phi_d^2(e^{j\omega T}) - 1) |T_d(e^{j\omega T})|^2 + (|S_d(e^{j\omega T})| - 1)^2} \right), \quad (5.23) \end{aligned}$$

where

$$\Phi_d^2(e^{j\omega T}) = \frac{F_d(e^{j\omega T}) G_d(e^{j\omega T})}{|T_d(e^{j\omega T})|^2}. \quad (5.24)$$

Proof: The proof of (5.22) follows immediately from Theorem 5.2.2. Formula (5.23) is obtained by computing λ_{\max} in (5.17) and after some algebraic manipulation. \square

The function Φ_d may be given some interesting interpretations that we consider in the following remarks.

Remark 5.2.2 (Φ_d as a Measure of Intersample Activity) The function Φ_d may be given an interpretation as a “fidelity function”, that is, a measure of the amount of intersample behavior in the sampled-data system. Indeed, note that Φ_d is always greater than or equal to 1, since by Cauchy-Schwarz

$$\begin{aligned} |(FPH)_d(e^{j\omega T})|^2 &= \left| \frac{1}{T} \sum_{k=-\infty}^{\infty} F_k(j\omega) P_k(j\omega) H_k(j\omega) \right|^2 \\ &\leq \left(\sum_{k=-\infty}^{\infty} |F_k(j\omega)|^2 \right) \left(\frac{1}{T^2} \sum_{k=-\infty}^{\infty} |P_k(j\omega) H_k(j\omega)|^2 \right). \end{aligned}$$

Thus, from (5.22) we can see that

$$\|\mathcal{T}\| \leq \|\Phi_d\|_{\infty} \|T_d\|_{\infty},$$

so $\|\Phi_d\|_{\infty}$ is an upper bound of the quotient between the L_2 -induced norms considering full-time information, and sampled behavior respectively.

Also notice that since $\Phi_d \geq 1$, for all ω in Ω_N , then $\|\mathcal{J}\| \geq \|\mathsf{T}_d\|_\infty$; i.e., the L_2 -induced norm of the discretized system gives a lower bound for the L_2 -induced norm of the sampled-data system, as should be expected. The following result formalizes this observation.

Corollary 5.2.7

Under the assumptions of Corollary 5.2.6,

$$\lim_{\Phi_d \rightarrow 1} \|\mathcal{J}\| = \|\mathsf{T}_d\|_\infty \quad (5.25)$$

$$\lim_{\Phi_d \rightarrow 1} \|\mathcal{S}\| = \|\mathsf{S}_d\|_\infty \quad (5.26)$$

Proof: Proof of (5.25) is immediate from (5.22). For (5.26) we have the following from (5.23):

$$\begin{aligned} \lim_{\Phi_d \rightarrow 1} \|\mathcal{S}\| &= \lim_{\Phi_d \rightarrow 1} \sup_{\omega \in \Omega_N} \frac{|S_d(e^{j\omega T})| + 1 + |S_d(e^{j\omega T})| - 1}{2} \\ &= \max\{\|\mathsf{S}_d\|_\infty, 1\} \\ &= \|\mathsf{S}_d\|_\infty. \end{aligned} \quad (5.27)$$

□

Hence, for example, if $\|\Phi_d\|_\infty$ is close to 1, then $\|\mathcal{J}\| \approx \|\mathsf{T}_d\|_\infty$ and $\|\mathcal{S}\| \approx \|\mathsf{S}_d\|_\infty$, and we should expect little intersample activity. ◇

Remark 5.2.3 (An Alignment Condition) Notice that Φ_d is independent of the controller, but depends on the prefilter, plant, and hold function. This suggests a possibly interesting way of looking at an optimization problem; i.e., selecting a suitable discrete complementary sensitivity function T_d , and then choosing the prefilter and hold to minimize Φ_d . In particular, when $\Phi_d = 1$ the matrix on the RHS of (5.17) becomes singular, since the vectors \mathbf{f} and \mathbf{g} “align”. Therefore, minimization of the intersample behavior may be interpreted as an “alignment condition” between the hold, plant, and prefilter. This remains as a topic for future investigation. Further related comments may be found in Hagiwara and Araki [1995]. ◇

5.2.2 Numerical Implementation

The expressions for the frequency-gains and L_2 -induced norms obtained in the last section can be readily numerically implemented by computing G_d and F_d from (5.10) and (5.11). These computations can be approached as “special discretizations” by considering relations similar to (2.8). In this way, the arguments of $\sup_{\omega \in \Omega_N}$ in (5.15) and (5.17) are expressed by two rational transfer functions in $z = e^{j\omega T}$ — the frequency-gains of the sampled-data sensitivity operators. The induced norms can then be computed by a straightforward search of maxima over the finite interval Ω_N ⁵.

⁵Similar formulas have been derived for the case of ZOH in Leung et al. [1991, Theorem 3].

Computation of $F_d(e^{j\omega T})$

We compute (5.11) from the discretization $F_d(z) = \mathcal{TZ}\{\mathcal{S}_T\{\mathcal{L}^{-1}\{F(s)\tilde{F}(s)\}\}\}$ (see Figure 5.2), where $\tilde{F}(s)$ denotes $F(-s)^T$. Since F is a strictly proper rational function, the sampling of the output of $\tilde{F}\tilde{F}$ is well-defined.

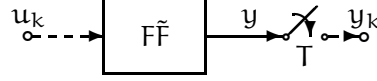


Figure 5.2: Scheme to compute $F_d(e^{j\omega T})$.

Let $\{a, b, c, 0\}$ be a minimal state-space realization of F . Then, a minimal realization for $\tilde{F}\tilde{F}$ is given by

$$A = \begin{bmatrix} a & bb^T \\ 0 & -a^T \end{bmatrix}, \quad B = \begin{bmatrix} 0 \\ -c^T \end{bmatrix}, \quad C = [c \quad 0].$$

We then have the following.

Lemma 5.2.8 (Computation of $F_d(e^{j\omega T})$)

The function $F_d(e^{j\omega T})$ is given by

$$F_d(e^{j\omega T}) = TC(e^{j\omega T}I - e^{AT})^{-1}B.$$

Proof: At the sampling instants the state response of $\tilde{F}\tilde{F}$ is given by

$$\begin{aligned} x_{k+1} &= e^{AT}x_k + \int_0^T e^{A(T-\tau)}B u(\tau) d\tau \\ &= e^{AT}x_k + \int_0^T e^{A(T-\tau)}B \delta(\tau - T) d\tau u_k, \end{aligned} \quad (5.28)$$

where δ is Dirac's delta, since there is no hold device at the input of the system. From (5.28) we get the discrete system

$$\begin{aligned} x_{k+1} &= A_d x_k + B_d u_k \\ y_k &= C x_k, \end{aligned}$$

where $A_d = e^{AT}$ and $B_d = B$. The result then follows from application of Lemma 2.1.2. \square

Computation of $G_d(e^{j\omega T})$

The case of G_d is slightly more complicated than the previous one, but can be approached in a similar fashion. From (5.10) we have

$$\begin{aligned} G_d(e^{j\omega T}) &= \sum_{k=-\infty}^{\infty} G_k^*(j\omega)G_k(j\omega) \\ &= \frac{1}{T}C_d^*(e^{j\omega T})S_d^*(e^{j\omega T})E_d(e^{j\omega T})S_d(e^{j\omega T})C_d(e^{j\omega T}), \end{aligned}$$

where

$$E_d(e^{j\omega T}) \triangleq \frac{1}{T} \sum_{k=-\infty}^{\infty} H_k^*(j\omega) P_k^*(j\omega) P_k(j\omega) H_k(j\omega). \quad (5.29)$$

Hence, to compute G_d we need to evaluate $E_d(e^{j\omega T})$. We do this by discretizing the system depicted in Figure 5.3, i.e., the cascade of the hold \tilde{H} , the system $\tilde{P}P$, and the hold H . Since H is proper by definition, so is the cascade, and therefore the sampling operation is again well-defined.

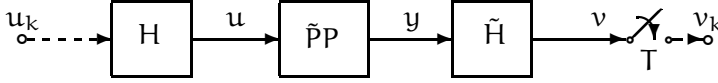


Figure 5.3: Scheme for computing (5.29).

Suppose that the plant P has a minimal realization $\{a, b, c, d\}$. Then, a minimal realization for $\tilde{P}P$ is given by

$$A = \begin{bmatrix} a & 0 \\ c^T c & -a^T \end{bmatrix}, \quad B = \begin{bmatrix} b \\ c^T d \end{bmatrix}, \quad C = [d^T c \quad -b^T], \quad D = [d^T d]$$

We consider the case of a FDLTI GSHP; similar derivations are also valid for a PC GSHP. As seen in Chapter 3, a LTI GSHP is defined by a pulse response h ,

$$h(t) = \begin{cases} Ke^{L(T-t)}M & \text{if } t \in [0, T) \\ 0 & \text{otherwise} \end{cases}, \quad (5.30)$$

for matrices K, L , and M of appropriate dimensions. The following lemma gives a formula for the computation of $E_d(e^{j\omega T})$ given the matrices A, B, C, D , and K, L, M .

Lemma 5.2.9 (Computation of $E_d(e^{j\omega T})$)

The function $E_d(e^{j\omega T})$ in (5.29) is given by

$$E_d(e^{j\omega T}) = C_d(e^{j\omega T}I - A_d)B_d + D_d, \quad (5.31)$$

where

$$A_d = e^{AT}$$

$$B_d = \int_0^T e^{A\tau} B K e^{L\tau} M \, d\tau$$

$$C_d = \int_0^T M^T e^{L^T(T-\tau)} K^T C e^{A\tau} \, d\tau$$

$$D_d = \int_0^T M^T e^{L^T\tau} K^T D K e^{L\tau} M \, d\tau + \int_0^T M^T e^{L^T(T-\tau)} K^T C \int_0^\tau e^{A(\tau-\sigma)} B K e^{L(T-\sigma)} M \, d\sigma \, d\tau$$

Proof: We discretize the system of Figure 5.3 in four steps. Suppose t is in the interval $[kT, (k+1)T]$. First we compute the continuous-time response of the hold H to a pulse in u_k . This is

$$u(t) = Ke^{L((k+1)T-t)}Mu_k. \quad (5.32)$$

Second, feed u from (5.32) into $P\tilde{P}$ to get

$$x(t) = e^{A(t-kT)}x_k + \int_0^{t-kT} e^{A(t-kT-\sigma)}BKe^{L(T-\sigma)}Md\sigma u_k \quad (5.33)$$

$$y(t) = Cx(t) + DKe^{L((k+1)T-t)}Mu_k. \quad (5.34)$$

Third, compute the response of the hold \tilde{H} to the output y given by (5.34) above. By Lemma 3.1.5 we know that the frequency response of the LTI GSHF is $H(s) = K(sI+L)^{-1}(e^{LT} - e^{-sT})M$. Let \tilde{h} denote the impulse response of the “conjugated” hold whose frequency response is $\tilde{H}(s) = M^T(sI-L^T)^{-1}(e^{-L^TT} - e^{-sT})e^{L^TT}e^{sT}K^T$. Here, we neglect for the moment the “advance” of one sampling period due to the non-causality of \tilde{H} , i.e., we are considering $e^{-sT}\tilde{H}(s)$ instead. It follows then that

$$\tilde{h}(t) = \begin{cases} M^Te^{L^Tt}K^T & \text{if } t \in [0, T) \\ 0 & \text{otherwise} \end{cases}. \quad (5.35)$$

We get

$$\begin{aligned} v(t) &= \int_{kT}^t \tilde{h}(t-\tau)y(\tau) d\tau \\ &= \int_0^{t-kT} M^Te^{L^T(t-kT-\tau)}K^TCx(\tau+kT) d\tau \\ &\quad + \int_0^{t-kT} Ke^{L^T(t-kT-\tau)}K^TDu(\tau+kT) d\tau. \end{aligned} \quad (5.36)$$

Denote the first integral on the RHS of (5.36) by v_1 , and the second by v_2 . Replace $x(\tau+kT)$ and $u(\tau+kT)$ in (5.36) using (5.33) and (5.32) to obtain

$$\begin{aligned} v_1(t) &= \left(\int_0^{t-kT} M^Te^{L^T(t-kT-\tau)}K^TCe^{A\tau} d\tau \right) x_k \\ &\quad + \left(\int_0^{t-kT} M^Te^{L^T(t-kT-\tau)}K^TC \int_0^{\tau} e^{A(\tau-\sigma)}BKe^{L(\tau-\sigma)}Md\sigma d\tau \right) u_k, \end{aligned} \quad (5.37)$$

and

$$v_2(t) = \left(\int_0^{t-kT} M^Te^{L^T(t-kT-\tau)}K^TDKe^{L(T-\tau)}M d\tau \right) u_k. \quad (5.38)$$

Finally, we evaluate $v = v_1 + v_2$ at $t = (k+1)T$, which renders

$$\begin{aligned} x_{k+1} &= A_d x_k + B_d u_k \\ v_{k+1} &= C_d x_k + D_d u_k, \end{aligned} \quad (5.39)$$

where A_d, B_d, C_d and D_d are as claimed. To conclude, compute the \mathcal{Z} -transform of the expressions in (5.39) above, and eliminate X to get

$$zV(z) = (C_d(zI - A_d)^{-1}B_d + D_d)U(z). \quad (5.40)$$

If we introduce now the advance of one sampling period neglected before, the factor z on the RHS of (5.40) is canceled, rendering $E_d(z) = V(z)/U(z) = C_d(zI - A_d)^{-1}B_d + D_d$. Application of Lemma 2.1.2 gives the result. \square

Remark 5.2.4 Matrices B_d, C_d and D_d in the above expressions can be easily numerically evaluated using matrix exponential formulas suggested by Van Loan [1978]. So, we have

$$\begin{aligned} B_d &= [e^{A^T} \ 0] \exp \left\{ \begin{bmatrix} -A & BK \\ 0 & L \end{bmatrix}^T \right\} \begin{bmatrix} 0 \\ M \end{bmatrix}, \\ C_d &= [M^T \ 0] \exp \left\{ \begin{bmatrix} L^T & K^T C \\ 0 & A \end{bmatrix}^T \right\} \begin{bmatrix} 0 \\ I \end{bmatrix}, \\ D_d &= [M^T e^{L^T} \ 0] \exp \left\{ \begin{bmatrix} -L^T & K^T D K \\ 0 & L \end{bmatrix}^T \right\} \begin{bmatrix} 0 \\ M \end{bmatrix} \\ &\quad + [M^T \ 0] \exp \left\{ \begin{bmatrix} L^T & K^T C & 0 \\ 0 & A & BK \\ 0 & 0 & -L \end{bmatrix}^T \right\} \begin{bmatrix} 0 \\ e^{L^T} M \end{bmatrix}. \end{aligned}$$

\diamond

Example 5.2.1 (Sensitivity of gain-margin improvement with GSHFs) The use of these formulas is illustrated by computing the “frequency gain” of a system from an example in Yang and Kabamba [1994]. In this paper the authors present a technique based on GSHFs to achieve arbitrary gain-margin improvement of a feedback system.

The plant considered in the example is the following,

$$P(s) = \frac{s - 2}{(s - 1)(s + 2)}.$$

Since the plant is non-minimum phase, there is a limit to the gain-margin achievable by LTI compensation Khargonekar et al. [1985], which in this case is 4.

Using the technique suggested by Yang and Kabamba, this plant can be stabilized by a FDLTI GSHF (Definition 3.1.1) determined by the matrices

$$K = [0 \ 1], \quad L = \begin{bmatrix} 0 & 2 \\ 1 & -1 \end{bmatrix}, \quad M = \begin{bmatrix} -12616 \\ 312.8194 \end{bmatrix},$$

and a sampling period of $T = 0.05$, yielding a gain-margin of 10. However, this improvement of gain-margin comes at the cost of a very large sensitivity to input disturbances. Indeed, consider the feedback loop of Figure 5.4, where we have introduced a plant input disturbance c . Figure 5.5 shows the frequency-gain of

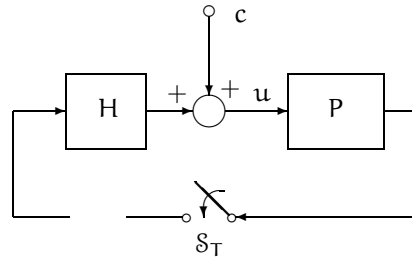


Figure 5.4: System with plant input disturbance.

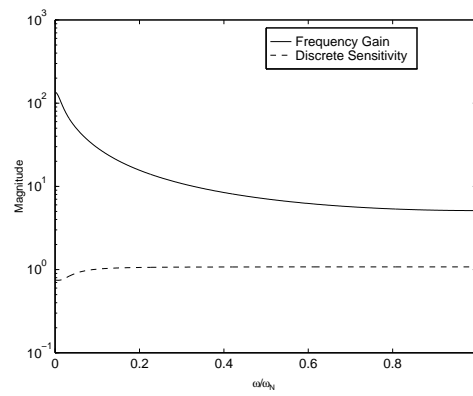


Figure 5.5: Hybrid frequency gains.

the hybrid operator on L_2 mapping c to u . For comparison we also plotted the frequency response of the discrete sensitivity function S_d .

The corresponding L_2 -induced norms are

$$\begin{aligned}\|S\| &= 134.69 \\ \|S_d\|_\infty &= 1.0785,\end{aligned}$$

which display a great difference. In a sense, this says that the discretized model does not represent the true behavior of the system. Indeed, these norms show that taking in account just the sampled behavior in this system gives only a very conservative lower bound of the actual L_2 -gain of the hybrid system. As a consequence, a significant part of the system's dynamics is "hidden" from a sampled analysis as intersample activity. A large $\|S\|$ means high sensitivity to L_2 plant input disturbances, which is particularly problematic if in addition there exist plant input saturations. Furthermore, a large $\|S\|$ will also imply poor robustness properties to time-varying perturbations Sivashankar and Khargonekar [1993]. \diamond

5.3 Summary

This chapter has considered the hybrid sensitivity and complementary sensitivity operators on L_2 . We have described a mathematical framework called "frequency-domain lifting", which provides a representation of these operators as infinite dimensional "transfer matrices". Based on this representation we have characterized the frequency-gains of these operators as the maximum eigenvalue of an associated finite dimensional discrete transfer matrix. The L_2 -induced norm of the operators is then computed by performing a search of maxima of these eigenvalues over a finite interval of frequencies. The expressions obtained can be easily implemented numerically to any desired degree of accuracy in a reliable fashion.

Similar expressions have been communicated in the literature for the case of the compact operators, like the complementary sensitivity operator [e.g., Hagiwara and Araki, 1995]. Hybrid non-compact operators impose additional difficulties in the evaluation of frequency-gains and L_2 -induced norms Yamamoto and Khargonekar [1993]. Perhaps most interesting in our results is the fact that also the sensitivity operator, which is non-compact, can be characterized as a finite dimensional eigenvalue problem feasible of a numerically reliable implementation.

These formulas have immediate application in the analysis of stability robustness for LTV unstructured perturbations, and H_∞ control synthesis problems. Particularly, since our expressions allow the use of GSHFs, they provide a reliable computational tool for the evaluation of performance of a general class of sampled-data designs.

Stability Robustness

Since no mathematical model can completely describe the exact behavior of a physical system, the consideration of model uncertainty in the analysis and design of feedback systems is an issue of unarguable theoretical and practical significance. In this respect, one of the fundamental problems is the analysis of the *stability robustness* of the control system, i.e., the property by which the closed-loop system remains stable under perturbations. This is a well-studied problem for FDLTI systems, where several useful tools, like H_∞ and μ methods, have proven successful.

The analysis of stability robustness for sampled-data systems is more difficult, again due to their time-varying characteristics, and has attracted the attention of a number of researchers in recent years. For example, Thompson et al. [1983] and Thompson et al. [1986] have used conic sector techniques to obtain sufficient conditions for robust stability. Similar results have been derived by Hara et al. [1991] using the L_2 -induced norm and the Small-gain Theorem. More recently, Sivashankar and Khargonekar [1993] have shown that the L_2 -induced norm actually gives both necessary and sufficient conditions for robust stability when the class of unstructured perturbations include periodic time-varying perturbations. However, as illustrated in Dullerud and Glover [1993], the L_2 -induced norm may be a very conservative measure of robust stability under LTI perturbations, which are a more natural class of uncertainties to consider since the plant is normally assumed LTI. Indeed, under the assumption of stable LTI perturbations, Dullerud and Glover [1993] have shown that the necessary and sufficient condition for robust stability reduces to a μ type of test. This result has now been generalized to the case of unstable perturbations by Hagiwara and Araki [1995], who used Nyquist type of arguments and the frequency-domain framework suggested in Araki and Ito [1993] and Araki et al. [1993].

The approach followed in Dullerud and Glover [1993] is based on a state-space representation of the sampled-data system, and uses time-domain lifting techniques and a generalization of the \mathcal{Z} -transform to obtain a representation of the operators in frequency-domain. As pointed out by Yamamoto and Khargonekar [1996], this detour through state-space to describe input-output operators might complicate the analysis.

In this chapter, we show how these results can be obtained in a very intu-

itive and simple way — almost entirely by block-diagram manipulation — if the problem is set up directly in frequency-domain. In §6.1 we consider stable LTI multiplicative perturbations on the analog plant. Using the frequency-domain framework introduced in Chapter 5, we derive a μ -test that corresponds with the results of Dullerud and Glover. In the particular case of SISO systems, this test can be reduced to an ℓ_1 -type condition involving the *fundamental complementary sensitivity function*, $T^0(s)$, introduced in §4.1. This has an important link with the results of Chapter 4, since it shows that peaks of T^0 will have direct deleterious effects on the stability robustness properties of the system.

It is interesting to note that under our framework, the problem is easily brought to the classical *basic perturbation model* of Figure 6.1 [see also Hagiwara and Araki, 1995]. Moreover — and perhaps unsurprisingly too — we shall see that the *interconnection matrix* G will be \mathbf{T}_ω , the infinite matrix representation of the *sampled-data complementary sensitivity operator* introduced in §5.2. Note that this is in complete analogy with the corresponding LTI case, where the interconnection matrix is the complementary sensitivity function [e.g., Doyle et al., 1992].

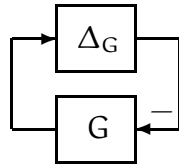


Figure 6.1: Basic perturbation model.

Moreover, we shall see in §6.2 that this carries over to the problem of robust stability under a divisive perturbation model. Again in analogy with the LTI case, this time G is \mathbf{S}_ω , the infinite matrix representation of the *sampled-data sensitivity operator*. The corresponding μ -test, though, will be only conjectured, since the sensitivity operator is *non-compact*, a fact that makes the analysis much more

intricate than the multiplicative case. Nevertheless, a necessary condition for robust stability with the divisive perturbation model is easily obtained in the SISO case. This shows that peaks in the fundamental sensitivity function S^0 will necessarily reduce the stability margin of the hybrid system respect to this type of perturbations.

6.1 Multiplicative Perturbation

Consider the multivariable sampled-data system depicted in Figure 6.2. The perturbed plant is represented by the multiplicative uncertainty model

$$\tilde{P}(s) = (I + W(s)\Delta(s))P(s), \quad (6.1)$$

where $\Delta(s)$ is a FDLTI perturbation given by a stable rational function satisfying $\|\Delta\|_\infty < 1$; we call such Δ and *admissible* perturbation. The weighting function $W(s)$ is assumed a fixed stable, minimum-phase rational function, and such that $F(s)W(s)P(s)$ is proper. This type of uncertainty model is useful to represent high frequency plant uncertainty Doyle and Stein [1981].

Assuming closed loop stability of the nominal hybrid system, i.e., for $\Delta(s) = 0$, we shall determine necessary and sufficient conditions for the perturbed system to remain stable under the class of admissible perturbations.

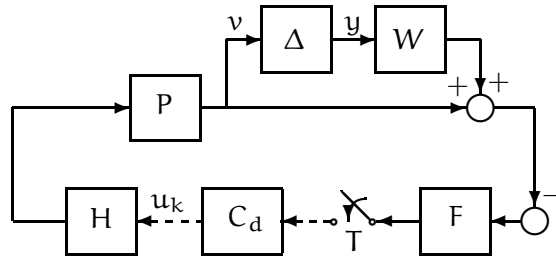


Figure 6.2: System with multiplicative uncertainty.

Suppose that we discretize the system of Figure 6.2 by opening the loop at the input and output of the discrete controller C_d . Then, we obtain the simplified discrete diagram of Figure 6.3, where $(\tilde{F}\tilde{P}H)_d$ is the discretized series of hold, perturbed plant and anti-aliasing filter. Applying Corollary 2.1.4 to $(\tilde{F}\tilde{P}H)_d$ yields the infinite sum representation

$$(\tilde{F}\tilde{P}H)_d(e^{sT}) = \frac{1}{T} \sum_{k=-\infty}^{\infty} F_k(s)(I + W_k(s)\Delta_k(s))P_k(s)H_k(s). \quad (6.2)$$

Equation (6.2) displays the multi frequency structure induced by the sampling operation. This relation can be translated directly into the block diagram of Figure 6.4. Note in this picture that although the sampler is not represented explicitly, its action is structurally embedded in the block diagram as the parallel of an infinite number of direct paths where each harmonic component of the signals operates. We use this representation to derivate an expression where all the perturbations Δ_k are blocked together.

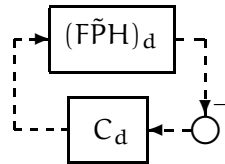


Figure 6.3: Discretized perturbed system.

Take the k -harmonic direct path in Figure 6.4. Then, we can write

$$V_k(s) = \frac{1}{T} P_k(s) H_k(s) U_d(e^{sT}), \quad (6.3)$$

where U_d is the \mathcal{Z} -transform of the output of the controller. To ease notation, we shall drop the independent variables in the sequel of this derivation, understanding that all signals and transfer functions are functions of s , save for the discrete ones, like C_d and U_d , which are functions of e^{sT} . Now, we have that U_d is given

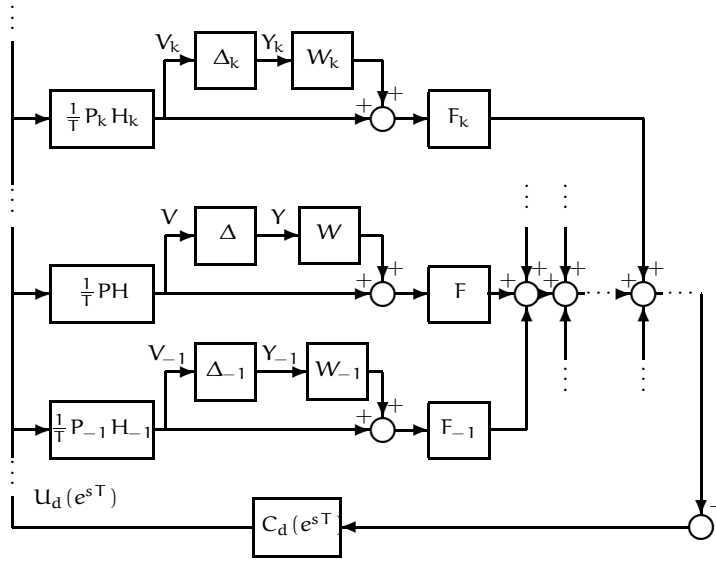


Figure 6.4: Harmonic structure of the perturbed system.

by

$$\begin{aligned} U_d &= -C_d \sum_{k=-\infty}^{\infty} F_k \left(W_k Y_k + \frac{1}{T} P_k H_k U_d \right) \\ &= -C_d \sum_k F_k W_k Y_k - C_d \left(\frac{1}{T} \sum_k F_k P_k H_k \right) U_d. \end{aligned} \quad (6.4)$$

Noting that by Corollary 2.1.4 $1/T \sum_k F_k P_k H_k$ is the nominal discretized plant $(FPH)_d$, from (6.4) we get

$$U_d = -S_d C_d \sum_k F_k W_k Y_k, \quad (6.5)$$

where

$$S_d(z) = [I + C_d(z)(FPH)_d(z)]^{-1} \quad (6.6)$$

is the nominal discrete Sensitivity Function. Now, replacing U_d from (6.5) and $Y_k = \Delta_k V_k$ into (6.3) yields

$$V_k = \frac{1}{T} P_k H_k S_d C_d \sum_m F_m W_m \Delta_m V_m. \quad (6.7)$$

In the lifted domain, (6.7) can be written as

$$(\mathbf{I} + \mathbf{T}_\omega \mathbf{W}_\omega \Delta_\omega) \mathbf{v} = 0, \quad (6.8)$$

where \mathbf{I} is the infinite identity matrix (the identity operator in ℓ_2) and \mathbf{T}_ω is the infinite matrix representation of the complementary sensitivity operator, defined in (5.7). \mathbf{W}_ω and Δ_ω are infinite-dimensional block diagonal matrices,

$$\mathbf{W}_\omega \triangleq \text{diag}[\dots, W_k(j\omega), W_{k-1}(j\omega), \dots],$$

and

$$\Delta_\omega \triangleq \text{diag}[\dots, \Delta_k(j\omega), \Delta_{k-1}(j\omega), \dots],$$

while \mathbf{v} is the lifted vector

$$\mathbf{v}(\omega) \triangleq \begin{bmatrix} \vdots \\ V_1(\omega) \\ V_0(\omega) \\ V_{-1}(\omega) \\ \vdots \end{bmatrix}. \quad (6.9)$$

Equation (6.8) collects system knowns and perturbations in two separated blocks, as in the basic perturbation model of Figure 6.5. Thus, we can see clearly in the form of Δ_ω how the original time-varying problem with unstructured analog perturbations conduces to a time-invariant, infinite-dimensional, problem with a very structured class of perturbations. From this setup it is standard to derive the conditions for the internal stability of the loop of Figure 6.5 as a μ -test.

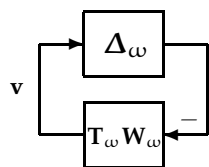


Figure 6.5: Basic perturbation model for multiplicative uncertainty.

Before proceeding, we need to recall a few definitions relative to the structured singular value μ required to state the results; we refer for example to Packard and Doyle [1993] for more details. The structured singular value of a given $n \times n$ complex matrix M is a nonnegative real number defined with respect to a set Δ of perturbation matrices Δ in $\mathbb{C}^{n \times n}$ of prescribed structure. Denote by $\bar{\sigma}\{\Delta\}$ the maximum singular value of Δ . Then we define $\mu_\Delta(M)$ as

$$\mu_\Delta(M) \triangleq \frac{1}{\min_{\Delta \in \Delta} \{\bar{\sigma}\{\Delta\} : \det(I - M\Delta) = 0\}},$$

unless no $\Delta \in \Delta$ makes $(I - M\Delta)$ singular, in which case $\mu_\Delta(M) \triangleq 0$. The perturbation set Δ is defined as the set of perturbations Δ of the form

$$\Delta = \text{diag}[\delta_1 I_{r_1}, \delta_2 I_{r_2}, \dots, \delta_S I_{r_S}, \Delta_{S+1}, \dots, \Delta_{S+F}], \quad (6.10)$$

where $\delta_i \in \mathbb{C}$, $\Delta_{S+j} \in \mathbb{C}^{m_j \times m_j}$, for $i = 1, 2, \dots, S$, and $j = 1, 2, \dots, F$. With I_{r_i} we denote $\mathbb{C}^{r_i \times r_i}$ identity matrices. Note that for dimensional consistency it is necessary that $\sum_{i=1}^S r_i + \sum_{j=1}^F m_j = n$.

With these definitions, we can now state necessary and sufficient conditions for robust stability of the hybrid system of Figure 6.2, adapted from the result obtained by Dullerud and Glover [1993]. The result reduces to a μ -problem on the infinite dimensional matrices of Figure 6.5, and it is expressed as a sequence of all the finite dimensional μ -problems obtained by truncating the original matrices. Denote by $[\mathbf{T}_\omega]^n$, $[\mathbf{W}_\omega]^n$ and $[\Delta_\omega]^n$ the corresponding truncations keeping all harmonics between $-n$ and n , for some positive integer n . For each ω in Ω_N , $[\Delta_\omega]^n$ has a block diagonal structure, where each block $\Delta_k(j\omega)$ is as in (6.10). Let Δ^n denote the set of all these finite dimensional block diagonal matrix perturbations, $\Delta^n \triangleq \{\text{diag}[\Delta_n, \dots, \Delta_{-n}] : \Delta_i \in \Delta\}$. Then, we have the following proposition.

Proposition 6.1.1 (Dullerud and Glover [1993])

For all Δ such that $\|\Delta\|_\infty < 1$ the system of Figure 6.2 is internally stable if and only if for each integer $n > 0$ the following inequality is satisfied

$$\max_{\omega \in \Omega_N} \mu_{\Delta^n}([\mathbf{T}_\omega]^n [\mathbf{W}_\omega]^n) \leq 1. \quad (6.11)$$

◦

As mentioned before, although we started with unstructured perturbations on the analog plant, they are mapped into a very structured type of perturbations in the lifted space $L_2(\ell_2; \Omega_N)$. In general, assuming also Δ_ω unstructured Sivashankar and Khargonekar [1993] will lead to a small-gain type of test in terms of the L_2 -induced norm

$$\|\mathbf{T}_\omega \mathbf{W}_\omega\| \leq 1.$$

This small-gain condition is only sufficient for LTI perturbations, and it may be quite conservative. This has been analyzed by means of example by Dullerud and Glover [1993]. Other interesting related remarks are given in Hagiwara and Araki [1995].

A necessary condition for robust stability may be stated in terms of the fundamental complementary sensitivity function of Chapter 4.

Theorem 6.1.2 (Necessary Condition for Robust Stability)

A necessary condition for the the system of Figure 6.2 to remain stable for all Δ such that $\|\Delta\|_\infty < 1$ is that

$$\|T^0(j\omega)W(j\omega)\|_\infty \leq 1. \quad (6.12)$$

Proof: It is necessary for closed loop stability that

$$\tilde{S}_d(z) = [I + C_d(z)(F\tilde{P}H)_d(z)]^{-1} \quad (6.13)$$

have no poles in \mathbb{D}^c . Rearranging yields

$$\tilde{S}_d(z) = [I + S_d(z)C_d(z)(FW\Delta PH)_d(z)]^{-1}S_d(z). \quad (6.14)$$

Since the nominal system is stable, then \tilde{S}_d will have no poles in \mathbb{D}^c if and only if

$$\det[I + S_d(e^{j\omega T})C_d(e^{j\omega T})(FW\Delta PH)_d(e^{j\omega T})] \neq 0 \quad \text{for all } \omega. \quad (6.15)$$

The proof proceeds by contradiction, following that in Chen and Desoer [1982, Theorem 2]. Denote $Q(j\omega) \triangleq T^0(j\omega)W(j\omega)$, and suppose that (6.12) is violated. Then there exists a frequency ω_1 such that $\sigma_1 \triangleq \bar{\sigma}\{Q(j\omega_1)\} > 1$, where $\bar{\sigma}\{\cdot\}$, recall, denotes the maximum singular value. Performing a singular value decomposition of $Q(j\omega_1)$ yields

$$Q(j\omega_1) = U \text{diag}[\sigma_1 \dots] V^*,$$

where $U \triangleq \{u_{ij}\}$ and $V \triangleq \{v_{ij}\}$ are unitary matrices. Now assume for the moment that there exists an admissible $\check{\Delta}$ that also satisfies

$$\begin{aligned} \check{\Delta}(j\omega_1) &= \begin{bmatrix} v_{11} \\ \vdots \\ v_{n1} \end{bmatrix} (-\sigma_1)^{-1} [u_{11}^* \quad \dots \quad u_{n1}^*] \\ &= V \text{diag}[(-\sigma_1)^{-1}, 0, \dots, 0] U^*, \end{aligned} \quad (6.16)$$

and

$$\check{\Delta}(j(\omega_1 + k\omega_s)) = 0 \quad \text{for } k = \pm 1, \pm 2, \dots, \text{ and } k \neq -2\omega_1/\omega_s. \quad (6.17)$$

The assumptions on W , and Δ , imply that Corollary 2.1.4 may be used to calculate $(FW\check{\Delta}PH)_d$. Using (6.16) and (6.17) yields

$$(FW\check{\Delta}PH)_d(e^{j\omega_1 T}) = -\frac{1}{T}F(j\omega_1)W(j\omega_1)V \text{diag}\left[-\frac{1}{\sigma_1}, 0, \dots, 0\right] U^*P(j\omega_1)H(j\omega_1), \quad (6.18)$$

and therefore¹

$$\begin{aligned} \det[I + S_d(e^{j\omega_1 T})C_d(e^{j\omega_1 T})(FW\check{\Delta}PH)_d(e^{j\omega_1 T})] \\ &= \det[I + S_d C_d \frac{1}{T} F W V \text{diag}[(-\sigma_1)^{-1}, 0, \dots, 0] U^* P H] \\ &= \det[I + V \text{diag}[(-\sigma_1)^{-1}, 0, \dots, 0] U^* \frac{1}{T} P H S_d C_d F W] \\ &= \det[I + V \text{diag}[(-\sigma_1)^{-1}, 0, \dots, 0] U^* Q(j\omega_1)] \\ &= [I + V \text{diag}[-1, 0, \dots, 0] V^*] \\ &= \det[V] \det[\text{diag}[0, 1, 1, \dots, 1]] \det[V^*] \\ &= 0. \end{aligned}$$

¹We suppress dependence on the transform variable when convenient, meaning will be clear from context.

Hence, (6.15) fails and so the perturbed system is unstable.

It remains to show that $\check{\Delta}$ satisfying the required properties exists. We do this following a construction in Chen and Desoer [1982]. Consider

$$\check{\Delta}(s) \triangleq \begin{bmatrix} \alpha_1(s) \\ \vdots \\ \alpha_n(s) \end{bmatrix} \left(-\frac{1}{\sigma_1} \right) f_q(s)^{k'} z(s) [\beta_1(s), \dots, \beta_n(s)]$$

where k' is a natural number, and

$$\begin{aligned} f_q(s) &\triangleq \frac{\omega_1 s}{q(s^2 + \omega_1^2) + \omega_1 s}, \quad q > 0 \\ \alpha_i(s) &\triangleq \frac{s}{\omega_1} \text{Im}\{v_{i1}\} + \text{Re}\{v_{i1}\} \\ \beta_i(s) &\triangleq -\frac{s}{\omega_1} \text{Im}\{u_{i1}\} + \text{Re}\{u_{i1}\} \\ z(s) &\triangleq \frac{H_{\text{ZOH}}(s - j\omega_1) H_{\text{ZOH}}(s + j\omega_1)}{T |H_{\text{ZOH}}(j2\omega_1)|} \eta(s), \\ \eta(s) &\triangleq \left(-\frac{s}{\omega_1} \sin(\angle H_{\text{ZOH}}(j2\omega_1)) + \cos(\angle H_{\text{ZOH}}(j2\omega_1)) \right), \end{aligned}$$

where $H_{\text{ZOH}}(s)$ is the frequency response function of the ZOH, and \angle denotes the phase of a complex number. It is then straightforward to verify that

- (i) $\check{\Delta}(j\omega_1)$ satisfies (6.16) and (6.17), and
- (ii) by choosing both k' and q large enough, $\check{\Delta}$ is exponentially stable and, for all $\omega \neq \pm\omega_1$, $\lim_{\omega \rightarrow \infty} \bar{\sigma}\{\check{\Delta}(j\omega)\} \rightarrow 0$, i.e., $\|\check{\Delta}\|_\infty < 1$ is satisfied. \square

In relation to the results of Chapter 4, for SISO systems follows that if $|T^0(j\omega)|$ is very large at any frequency, then the hybrid system will exhibit poor robustness to uncertainty in the analog plant at that frequency.

The necessary and sufficient condition of Proposition 6.1.1 yields an explicit expression that also involves T^0 in the SISO case. We state this in the following corollary.

Corollary 6.1.3 (Robust Stability Test — SISO case)

If the system of Figure 6.2 is SISO, then, for all Δ satisfying $\|\Delta\|_\infty < 1$, the system is internally stable if and only if

$$\sum_{k=-\infty}^{\infty} |T^0(j(\omega + k\omega_s)) W(j(\omega + k\omega_s))| \leq 1 \quad \text{for all } \omega \text{ in } \Omega_N \quad (6.19)$$

Proof: By Proposition 6.1.1, the system will be robustly stable if and only if all truncated systems satisfy μ -condition (6.11). Fix an integer $n > 0$ and ω in Ω_N .

The standard approach to evaluate $\mu_{\Delta^n}([\mathbf{T}_\omega]^n[\mathbf{W}_\omega]^n)$ is through the computation of upper and lower bounds. Define the sets

$$\mathcal{Q} \triangleq \{\mathbf{Q} \in \Delta^n : \mathbf{Q}^* \mathbf{Q} = \mathbf{I}\} \quad (6.20)$$

$$\mathcal{D} \triangleq \{\mathbf{D} \in \Delta^n : \mathbf{D} = \mathbf{D}^* > 0 \text{ and } \mathbf{D} \Delta_\omega^n = \Delta_\omega^n \mathbf{D} \text{ for all } \Delta_\omega^n \in \Delta^n\}. \quad (6.21)$$

Then we have the following inequalities Packard and Doyle [1993]

$$\max_{\mathbf{Q} \in \mathcal{Q}} \rho(\mathbf{Q}[\mathbf{T}_\omega]^n[\mathbf{W}_\omega]^n) \leq \mu_{\Delta^n}([\mathbf{T}_\omega]^n[\mathbf{W}_\omega]^n) \leq \inf_{\mathbf{D} \in \mathcal{D}} \bar{\sigma}\{\mathbf{D}[\mathbf{T}_\omega]^n[\mathbf{W}_\omega]^n \mathbf{D}^{-1}\}. \quad (6.22)$$

Note that the structure of the uncertainty in this case is diagonal,

$$\Delta_\omega^n = \text{diag}[\delta_n(j\omega), \dots, \delta_{-n}(j\omega)],$$

with $\delta_i(j\omega)$ in \mathbb{C} . As the truncated $[\mathbf{T}_\omega]^n[\mathbf{W}_\omega]^n$ is rank-one, we can work out in closed form the values of $\rho(\mathbf{Q}[\mathbf{T}_\omega]^n[\mathbf{W}_\omega]^n)$ and $\bar{\sigma}\{\mathbf{D}[\mathbf{T}_\omega]^n[\mathbf{W}_\omega]^n \mathbf{D}^{-1}\}$ in (6.22). We show that there exist matrices \mathbf{Q}_0 and \mathbf{D}_0 such that upper and lower bounds in (6.22) coincide, yielding the expression for $\mu_{\Delta^n}([\mathbf{T}_\omega]^n[\mathbf{W}_\omega]^n)$. To lighten notation we write in the remaining $\mathbf{T}\mathbf{W}$ for $[\mathbf{T}_\omega]^n[\mathbf{W}_\omega]^n$.

We compute first the lower bound, i.e., the spectral radius $\rho(\mathbf{Q}\mathbf{T}\mathbf{W})$. Since in the SISO case the complementary sensitivity operator is rank-one, so is $\mathbf{T}\mathbf{W}$, and its matrix may then be written as a dyad, i.e., in an outer product form, $\mathbf{T}\mathbf{W} = \mathbf{g} \mathbf{w}^*$, where the vectors

$$\mathbf{g} = \frac{1}{T} S_d C_d \begin{bmatrix} P_n H_n \\ P_{n-1} H_{n-1} \\ \vdots \\ P_{-n} H_{-n} \end{bmatrix} \quad \text{and} \quad \mathbf{w} = \begin{bmatrix} F_n^* W_n^* \\ F_{n-1}^* W_{n-1}^* \\ \vdots \\ F_{-n}^* W_{-n}^* \end{bmatrix}.$$

Then, $\mathbf{Q}\mathbf{T}\mathbf{W}$ is also a rank-one matrix, and its only eigenvalue is $\lambda = \mathbf{w}^* \mathbf{Q} \mathbf{g}$, so $\rho(\mathbf{Q}\mathbf{T}\mathbf{W}) = |\mathbf{w}^* \mathbf{Q} \mathbf{g}|$.

Consider the particular matrix $\mathbf{Q}_0 = \text{diag}[Q_n, Q_{n-1}, \dots, Q_{-n}]$, with

$$Q_i \triangleq \begin{cases} \frac{P_i^* H_i^* C_d^* S_d^* F_i^* W_i^*}{|P_i H_i C_d S_d F_i W_i|} & \text{if } P_i H_i C_d S_d F_i W_i \neq 0 \\ 1 & \text{otherwise} \end{cases}$$

Then

$$\rho(\mathbf{Q}_0 \mathbf{T}\mathbf{W}) = \sum_{i=-n}^n |P_i H_i C_d S_d F_i W_i|, \quad (6.23)$$

and \mathbf{Q}_0 is certainly in \mathcal{Q} .

We now consider the upper bound $\bar{\sigma}\{\mathbf{D}\mathbf{T}\mathbf{W}\mathbf{D}^{-1}\}$. The 2-norm of a rank-one matrix $\mathbf{T}\mathbf{W} = \mathbf{g} \mathbf{w}^*$ is given by $\bar{\sigma}\{\mathbf{T}\mathbf{W}\} = \rho(\mathbf{T}\mathbf{W}^* \mathbf{T}\mathbf{W})^{1/2} = \bar{\sigma}\{\mathbf{g}\} \bar{\sigma}\{\mathbf{w}\}$. Consider $\bar{\sigma}\{\mathbf{D}_0 \mathbf{T}\mathbf{W} \mathbf{D}_0^{-1}\}$ with $\mathbf{D}_0 = \text{diag}[D_n, D_{n-1}, \dots, D_{-n}]$ and let

$$D_i \triangleq \begin{cases} \left| \frac{F_i W_i}{P_i H_i C_d S_d} \right|^{1/2} & \text{if } P_i H_i C_d S_d F_i W_i \neq 0, \\ 1 & \text{otherwise.} \end{cases}$$

Therefore,

$$\bar{\sigma}\{\mathbf{D}_0 \mathbf{T} \mathbf{W} \mathbf{D}_0^{-1}\} = \sum_{i=-n}^n |P_i H_i C_d S_d F_i W_i|, \quad (6.24)$$

with \mathbf{D}_0 in \mathcal{D} .

From (6.22), (6.23), and (6.24), we conclude that

$$\mu_{\Delta^n}(\mathbf{Q} \mathbf{T} \mathbf{W}) = \sum_{i=-n}^n |P_i H_i C_d S_d F_i W_i|. \quad (6.25)$$

Note that (6.25) is valid for an arbitrary integer $n > 0$ and ω in Ω_N .

The proof is completed by recalling that

$$\mathbf{T}^0(s) = \frac{1}{\mathbf{T}} P(s) H(s) C_d (e^{sT}) S_d (e^{sT}) F(s)$$

and using Proposition 6.1.1. □

Again, as for Theorem 6.1.2, we see from this result that a large value of \mathbf{T}^0 at any frequency reduces the stability robustness properties of the system at that frequency. Notice that in this case the condition is an ℓ_1 -type condition on the lifted vector representing \mathbf{T}^0 , in contrast to that of Theorem 6.1.2, which is an ℓ_∞ -type condition. Hence, for the SISO case, the condition of Theorem 6.1.2 is straightforwardly implied by condition (6.19), since $\ell_1 \subset \ell_\infty$.

Remark 6.1.1 This result may also be obtained dispensing with the μ -framework, in a similar way to Theorem 6.1.2. An outline of this alternative proof is provided in Appendix A, §A.5. ◇

6.2 Divisive Perturbation

We now consider the stability robustness properties of the sampled-data system of Figure 6.6, i.e., with a divisive type of uncertainty model. We assume that Δ and W satisfy the conditions stated in §6.1. The perturbed plant is represented by

$$\tilde{P}(s) = (I + W(s)\Delta(s))^{-1} P(s). \quad (6.26)$$

The derivation of necessary and sufficient conditions for robust stability of the hybrid system with this class of perturbations is considerably more difficult than the multiplicative case, and remains as a challenging open problem. In this section we show that the problem can be also represented by a basic perturbation model, where the infinite dimensional matrix \mathbf{S}_ω appears in the interconnection matrix. A small-gain type sufficient condition follows immediately from this representation. We also provide a necessary condition for the SISO case, that imposes a bound on the values of the fundamental sensitivity function of Chapter 4 on the $j\omega$ -axis.

k -harmonic of the input to the uncertainty block, V , getting this time

$$V_k = -W_k \Delta_k V_k + \frac{1}{T} P_k H_k S_d C_d \sum_m F_m W_m \Delta_m V_m . \quad (6.28)$$

The lifted version of (6.28) is then

$$(\mathbf{I} + \mathbf{S}_\omega \mathbf{W}_\omega \Delta_\omega) \mathbf{v} = 0 , \quad (6.29)$$

with the same notation used in the preceding subsection. As could have been intuitively expected, now the *sensitivity operator* appears in the formula through its infinite matrix representation \mathbf{S}_ω , defined in (5.8). As before, the underlying μ -problem is evident from (6.29), also represented in the basic perturbation model of Figure 6.8.

A sufficient condition for stability of the perturbed system is evident from (6.29). Indeed, if the following inequality is satisfied,

$$\|\mathbf{S}_\omega \mathbf{W}_\omega\| \leq 1 ,$$

then the operator $(\mathbf{I} + \mathbf{S}_\omega \mathbf{W}_\omega \Delta_\omega)$ is non-singular, which implies internal stability of the basic perturbation model.

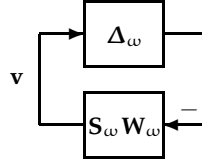


Figure 6.8: Basic perturbation model for divisive uncertainty.

Remark 6.2.1 (Robust Stability Test under Divisive Perturbations) We conjecture that a result analogous to Proposition 6.11 will be valid in this case also, i.e., the system will be robust stable under divisive perturbation if and only if all the truncated μ -problems corresponding to Figure 6.8 satisfy a stability condition. In other words, if and only if for all admissible LTI perturbations and each integer $n > 0$

$$\max_{\omega \in \Omega_N} \mu_{\Delta^n}(\mathbf{S}_\omega^n \mathbf{W}_\omega^n) \leq 1 . \quad (6.30)$$

A proof for this result is not obvious to us at present, and it remains as a topic for future research. We can foresee a greater difficulty in this case since the sensitivity operator is *non-compact*, and non-compact operators are not necessarily *approximable* by a sequence of finite-rank operators. Therefore, special care should be taken to show that the infinite sequence of μ -problems in (6.30) indeed converges when $n \rightarrow \infty$.

Nevertheless, a hint that a proof for this conjecture could be possible is perhaps suggested by the same fact that allowed us to compute a “closed form” for

the frequency-gain of this operator in Chapter 5, i.e., the sensitivity operator \mathcal{S} is not an arbitrary non-compact operator, since it can be written as

$$\mathcal{S} = \mathcal{J} - \mathcal{T},$$

where \mathcal{T} is always finite-rank. Moreover, notice that a condition like (6.30) would in principle be valid if we impose additional restrictions on the weighting function W , e.g., if it is assumed stable and strictly proper. In this case the corresponding infinite matrix \mathbf{W}_ω represents a compact operator, which also makes the product $\mathbf{S}_\omega \mathbf{W}_\omega$ compact. \diamond

A necessary condition for robust stability is easily obtained in the SISO case. In parallel with the result of Theorem 6.1.2, this condition involves the fundamental sensitivity function S^0 , as we see next.

Lemma 6.2.1

A necessary condition for the the system of Figure 6.6 to remain stable for all Δ such that $\|\Delta\|_\infty < 1$ is that

$$\|S^0(j\omega)W(j\omega)\|_\infty \leq 1. \quad (6.31)$$

Proof: The proof follows the same lines of that of Theorem 6.1.2 after noting that we can alternatively write the perturbed discrete sensitivity function as

$$\begin{aligned} \tilde{S}_d &= [1 + C_d(\tilde{F}\tilde{P}H)_d]^{-1} \\ &= \left[1 + C_d(FPH)_d - C_d \left(\frac{F\Delta WPH}{1 + W\Delta}_d \right) \right]^{-1} \\ &= \left[1 - S_d C_d \left(\frac{F\Delta WPH}{1 + W\Delta}_d \right) \right]^{-1} S_d. \end{aligned} \quad (6.32)$$

That the nonsingularity of the term between brackets in (6.32) implies (6.31) may be shown by a contrapositive argument similar to that for the proof of Theorem 6.1.2, and is omitted here to avoid repetition. \square

In connection with the results of Chapter 4, this lemma shows that if $|S^0(j\omega)|$ is large at any frequency, then the system will have poor robustness to divisive uncertainties in the analog plant at that frequency.

6.3 Summary

In this chapter we have considered the stability robustness of a hybrid system to unstructured LTI perturbations of the analog plant.

Using the frequency-domain lifting introduced in Chapter 5, we have derived a robust stability test in the form of a structured singular value for the case of multiplicative perturbations. The expression obtained was first given by Dullerud and Glover [1993] based on time-domain lifting techniques. Our procedures,

though, are considerably simplified by the use of the frequency-domain lifting technique.

For the case of divisive perturbations, our framework allows the problem to be easily recasted as a basic perturbation model, from which a small-gain type sufficient condition for robust stability is directly obtained. The derivation of necessary and sufficient conditions for this type of perturbation model is a much harder problem than that of multiplicative perturbations, and is left as subject of ulterior research.

For both types of perturbation models, we have drawn important connections with the discussion of Chapter 4 by obtaining necessary conditions for robust stability of the hybrid system in terms of the fundamental sensitivity and complementary sensitivity functions S^0 and T^0 . A key conclusion of these results is that large peaks in either S^0 or T^0 will necessarily degrade the robustness stability properties of the hybrid system respect to uncertainty in the analog plant.

An Application: Design Implications of Discrete Zero-placement

Non-minimum phase zeros of a linear time invariant plant impose inherent design limitations that cannot be overcome by any linear time invariant controller [see Freudenberg and Looze, 1985, Middleton, 1991]. This fact suggests that more general compensation schemes, such as periodic linear time-varying control, may prove useful in controlling NMP systems. Sampled-data control, wherein an analog plant is controlled by a digital computer through the use of periodic sample and hold, is one class of periodic controllers. Indeed, several authors have noted that the zeros of a discretized plant (unlike the poles) bear no straightforward relationship to the zeros of the original analog plant [e.g., Kabamba, 1987, Åström and Wittenmark, 1990]. In particular, use of a GSHF with a linear time invariant digital controller allows the zeros of the discretized plant to be placed arbitrarily Kabamba [1987], Åström and Wittenmark [1990], Yan et al. [1994]. Hence it is tempting to conclude that design limitations due to non-minimum phase zeros of an analog plant may be circumvented by assigning the zeros of the discretized plant to be minimum phase Bai and Dasgupta [1990], Er and Anderson [1994].

On the other hand, several authors have pointed out potential disadvantages to the use of GSHF control. In Åström and Wittenmark [1990, p. 75] the authors note that “the control signal may become highly irregular”. Kabamba [1987] notes that systems with GSHF control can sometimes exhibit intersample ripple. Furthermore, Feuer and Goodwin [1994] present analyses and simulations that suggest that systems with GSHF controllers are prone to robustness difficulties in addition to poor intersample behavior. Hence the potential utility of GSHF control in overcoming linear time invariant design limitations is still a matter of debate Feuer and Goodwin [1992], Araki [1993].

We have shown in Chapter 4 that design limitations imposed by NMP zeros of the analog plant remain present when the plant is discretized using a GSHF hold, *even if the discretized plant is minimum phase*. In this chapter we shall provide further interpretations to this fact by analyzing robustness properties of sampled-

data feedback designs that rely on GSHF zero-placement capabilities.

Let us now consider a common procedure by which a digital compensator is designed to control an analog plant. Namely, one discretizes the plant at an appropriate sample rate and designs the compensator so that the discretized feedback system has acceptable properties. As a consequence, the behavior of the analog signals in the resulting hybrid feedback system will be acceptable *at the sampling instants*. One then simulates the hybrid system to verify that the intersample behavior is also acceptable. If the plant is discretized with a ZOH, and if an appropriate sample rate and anti-aliasing filter are used, then this is very often the case.

As noted above, an interesting feature of GSHF control is its ability to locate the zeros of the discretized plant arbitrarily. Suppose that the analog plant has a NMP zero within the desired closed loop bandwidth, but that the discretized plant does not. Suppose also that the discrete closed loop system possesses feedback properties that would be unachievable if the discretized plant also had a problematic NMP zero. It follows as a straightforward corollary to the results of Chapter 4 that these feedback properties *cannot* also be present in the intersample behavior of the hybrid system.

A more intriguing question is whether the use of GSHF control to relocate zeros is responsible for sensitivity and robustness difficulties in the resulting feedback system above and beyond those due to the NMP zero of the analog plant. It was argued in Feuer and Goodwin [1994] that the poor robustness properties of GSHF control are due to the way in which components of the high frequency plant response are aliased down into the Nyquist range to form the frequency response of the discretized plant. In this chapter we shall investigate this phenomenon in detail by developing a framework in which the robustness difficulties associated with zero-shifting may be studied quantitatively.

The remainder of this chapter is organized as follows. §7.1 presents a preliminary result that implies that the use of GSHFs to locate discrete zeros, introduce serious limitations in the continuous-time response and stabilizability properties of certain hybrid systems. This section motivates the more general discussion of Sections 7.2 and 7.3. In §7.2 we state and resolve the first of two Gedanken experiments. The first experiment shows that if one is concerned about the quality of the intersample response, then GSHF control cannot circumvent design limitations due to an analog NMP zero. In §7.3 we state the second Gedanken experiment; unlike the first, this experiment is concerned only with performance at the sampling instants. Indeed, the analog plant enters only as a source of modeling uncertainty in the discretized system. This experiment shows that if the analog plant has at least one NMP zero with significant phase-lag contribution on the closed-loop bandwidth of the system, then there is a tradeoff between requiring (i), high performance of the discrete system, and (ii), stability robustness with respect to high-frequency *analog* plant uncertainty.

7.1 Discrete Zero-placement and ORHP Zeros of GSHFs

This section analyzes some preliminary implications of discrete zero-placement with GSHFs. Based on a property of real pole-zero parity preservation under discretization, we shall see that GSHF discrete zero-placement, as used for the strong stabilization of certain systems, will require a GSHF with zeros in the ORHP. In view of the results of Chapters 3 and 4, these zeros may bring in stabilizability difficulties and serious limitations to the continuous-time response of the hybrid system.

Even in the case of a ZOH, a simple classification of the zeros of a discretized system is not possible, except in special cases. Åström et al. [1984] have given asymptotic formulae for slow and fast sampling rates. Hara et al. [1989] examined parity interlacing properties of real zeros and poles. The key result of their work is that the parity¹ of the number of real zeros between any two real poles is preserved under discretization — except possibly for cases of *pathological sampling* Kalman et al. [1963].

At first glance, it might be expected that since GSHFs are capable of zero assignment in the discretized plant [Bai and Dasgupta, 1990, Er and Anderson, 1994, *e.g.*], that no similar property holds. The proposition below, however, shows that there is a generalization of the result of Hara et al. [1989] to the case of GSHFs.

Consider the strictly proper SISO plant P , and a GSHF H of Figure 7.1. Denote by $(PH)_d$ the discretized plant with sampling period T ,

$$(PH)_d(z) = \mathcal{Z}\{\mathcal{S}_T\{\mathcal{L}^{-1}\{P(s)H(s)\}\}\}, \quad (7.1)$$

where $\mathcal{L}\{\cdot\}$ and $\mathcal{Z}\{\cdot\}$ denote the Laplace and \mathcal{Z} -transforms, respectively, and $\mathcal{S}_T\{\cdot\}$ the sampling operation. We assume that P and H satisfy the conditions for non-pathological sampling stated in Lemma 2.2.1.

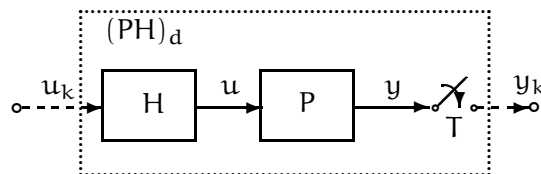


Figure 7.1: Discrete plant configuration.

Proposition 7.1.1 (Real Pole, Zero Parity Preservation in GSHF Systems)

Suppose that the plant P has simple real poles at $s = p_1$ and $s = p_2$. Then the parity of the number of real zeros of PH on the interval (p_1, p_2) is the same as the parity of the number of real zeros of the discretized plant $(PH)_d$ on the interval $(e^{p_1 T}, e^{p_2 T})$. \circ

¹Parity is even (odd) if there is an even (odd) number of zeros between the two poles.

Before proving Proposition 7.1.1, we require the following lemma from Middleton and Freudenberg [1995].

Lemma 7.1.2 (Discretized Plant by Partial Fractions Expansion)

Suppose P has only simple poles, and thus let

$$P(s) = \sum_{i=1}^n \frac{r_i}{s - p_i}.$$

Then,

$$(PH)_d(z) = \sum_{i=1}^n r_i H(p_i) \frac{e^{p_i T}}{z - e^{p_i T}}.$$

◦

Proof of Proposition 7.1.1: From Lemma 7.1.2,

$$\begin{aligned} \lim_{z \rightarrow (e^{p_1 T})^+} \text{sign} (PH)_d(z) &= \text{sign } r_1 H(p_1) \\ &= \lim_{s \rightarrow p_1^+} \text{sign } P(s)H(s). \end{aligned}$$

Similarly,

$$\lim_{z \rightarrow (e^{p_2 T})^-} \text{sign} (PH)_d(z) = \lim_{s \rightarrow p_2^-} \text{sign } P(s)H(s),$$

from which the result follows. ◻

Note that for the ZOH case, H has no real zeros, and so we recover the result of Hara et al. [1989]. Also note that alteration of the zero parity of the discretized plant — e.g., as required for strong stabilization of some systems — can only be achieved at the cost of introducing non-minimum phase zeros in the hold.

The implications of a NMP hold function in the sampled-data system are important. First, it follows from the discussion in Chapter 4 that NMP zeros of the hold worsen the tradeoffs on design by adding extra limitations to the achievable analog performance of the system. Second, and perhaps more critically, even the stabilizability properties of the system could be seriously affected by a NMP hold if its NMP zero happens to be too close to an unstable pole of the analog plant, rendering sampling “almost pathological”. This is illustrated by the following example.

Example 7.1.1 (Simultaneous stabilization by GSHF) In Kabamba [1987, Example 2] a FDLTI GSHF is designed to simultaneously stabilize the two systems given by the transfer functions

$$P_1(s) = \frac{1}{s+1} \quad \text{and} \quad P_2(s) = \frac{s-1.5}{s(s-2)}, \quad (7.2)$$

in the parallel configuration of Figure 7.2.

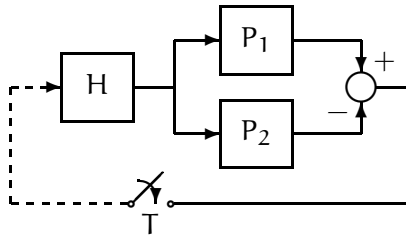


Figure 7.2: Simultaneous stabilization via GSHP.

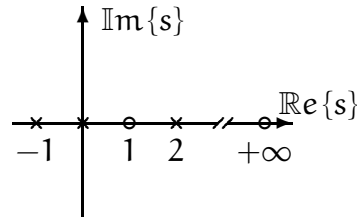


Figure 7.3: Pole-zero map of the combined system.

Note that the combined system,

$$P_1(s) - P_2(s) = \frac{-1.5(s-1)}{s(s+1)(s-2)}, \quad (7.3)$$

does not satisfy the conditions for strong stabilizability, namely, there is an odd number of positive real poles (one at $s = 2$) between two positive real zeros (at $s = 1$ and $s = +\infty$); see Figure 7.3. Hence simultaneous stabilization is impossible [Vidyasagar, 1985, § 5.4, Corollary 12]. Following the procedures suggested by Kabamba, we design a FDLTI hold with sampling time $T = 1$ to simultaneously stabilize the parallel. The matrices K , L , and M corresponding to this hold were given in the example of Subsection 3.2.3.

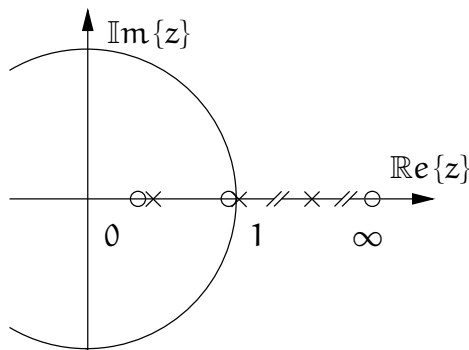


Figure 7.4: Discrete pole-zero map.

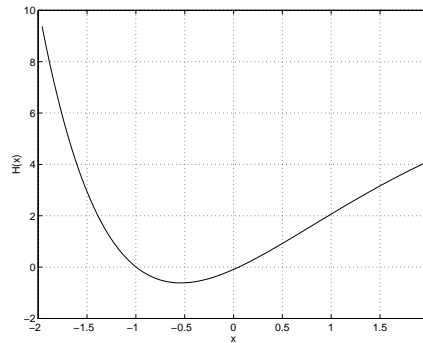


Figure 7.5: H on the real axis.

The discretized combined plant with this hold is

$$((P_1 - P_2)H)_d(z) = \frac{(z - 0.9433)(z - 0.3641)}{(z - 1)(z - e^{-1})(z - e^2)}.$$

Notice that it is minimum phase, and so strongly stabilizable. There is also one real zero between the real poles $z = e^{-1}$ and $z = 1$; see Figure 7.4. Hence, by

Lemma 7.1.1, the product $(P_1 - P_2)H$ will have an even number of zeros in the interval $(0, 2)$, and an odd number of zeros in the interval $(-1, 0)$. By inspecting $(P_1 - P_2)$ in (7.3), we conclude that H necessarily has an odd number of zeros in those intervals. Indeed, as we see in Figure 7.5, H has zeros at $s = -0.9967$ and $s = 0.0518$.

Notice that since the NMP zero of H is very close to the open loop pole of the continuous plant at the origin, by Lemma 2.2.1 sampling is almost pathological, and so we should expect the discretized plant to be almost non-stabilizable/non-detectable. Indeed, this may be checked by computing the singular values of the Hankel matrix for the discretized system, which are

$$\Sigma = [23163 \quad 0.1178 \quad 0.0005].$$

◇

7.2 Gedanken Experiment No. 1: Analog Performance

We have seen in the previous section that discrete zero-placement, as used in some applications of GSHF for strong stabilization, may bring in extra limitations to the achievable analog performance of the system. In this section we broaden this discussion by showing that if the analog plant is NMP, then the analog performance of the system is subject to constraints that are inescapable to GSHF sampled-data control.

Consider the following scenario. We wish to design a digital compensator for an analog plant having a problematic NMP zero. Suppose that a GSHF is used so that the discretized plant is minimum phase, or has NMP zeros only at less problematic locations. Then one can design a digital controller so that the discrete sensitivity function satisfies the specification

$$|S_d(e^{j\omega T})| \leq \beta_1, \quad 0 \leq \omega \leq \omega_1 \quad (7.4)$$

$$|S_d(e^{j\omega T})| \leq \gamma, \quad \omega_1 < \omega \leq \omega_N, \quad (7.5)$$

where $\beta_1 < 1$ and γ satisfies the lower bound (C.3) imposed by the discrete Bode sensitivity integral (see Appendix C). On the other hand, the intersample behavior of the hybrid system must satisfy constraints due to the analog NMP zero. We now present a Gedanken experiment whose result shows that these constraints manifest themselves as limitations upon the ability of the analog response to approximate that of the discretized system.

Gedanken Experiment No. 1: Suppose that we wish to design a digital controller for an analog plant. Then the following three questions (among others) are of interest:

- (A1) Is the nominal response of the discretized system satisfactory? Equivalently, is the response of the sampled-data system satisfactory *at the sampling instants*?

- (A2) Does the nominal analog response approximate that of the discrete system, so that a satisfactory discrete response will correspond to satisfactory inter-sample behavior?
- (A3) Is the analog response *insensitive* to plant uncertainty, disturbances, and sensor noise?

Clearly it is desirable that the answers to all three questions be affirmative. *The proposed experiment is to determine whether affirmative answers to all three of these questions can be obtained simultaneously.* ◦

We shall consider that the answer to (A1) is affirmative if the discrete sensitivity and complementary sensitivity functions are well behaved. Specifically, we require that $S_d(e^{sT})$ satisfy bounds of the form (7.4)-(7.5). It follows from the identity

$$S_d(e^{sT}) + T_d(e^{sT}) = 1 \quad (7.6)$$

that if the bounds (7.4)-(7.5) are satisfied, then $|T_d(e^{j\omega T})|$ is also bounded.

To quantify the answer to (A2), define the *fidelity function*.

$$\begin{aligned} S_f(s) &\triangleq S^0(s) - S_d(e^{sT}) \\ &= -T^0(s) + T_d(e^{sT}) \end{aligned} \quad (7.7)$$

If $|S_f(e^{j\omega T})| \ll 1$, then at frequency ω the fundamental component of the analog response to disturbances, noise, and commands will closely approximate that of the discretized system.

Since the discrete frequency response is periodic in ω , it is clearly not possible (nor desirable) that $S^0(j\omega)$ and $T^0(j\omega)$ closely approximate the discrete responses at all frequencies. Hence we shall consider that the answer to (A2) is affirmative if fidelity is achieved over a low frequency range:

$$|S_f(j\omega)| \leq \beta_2, \quad \text{for } 0 \leq \omega \leq \omega_2 < \omega_N. \quad (7.8)$$

Finally, as discussed in Chapter 4, it is necessary to keep the fundamental sensitivity and complementary sensitivity functions bounded at all frequencies to prevent large intersample response to disturbances and noise, as well as to keep differential sensitivity from being poor. Moreover, from the results in Chapter 6 (particularly Theorem 6.1.2 and Lemma 6.2.1), this is also required to prevent stability robustness from being poor. Hence an affirmative answer to (A3) will require that $S^0(j\omega)$ and $T^0(j\omega)$ satisfy upper bounds of the form

$$|S^0(j\omega)| \leq M_S(\omega) \quad (7.9)$$

and

$$|T^0(j\omega)| \leq M_T(\omega) \quad (7.10)$$

at all frequencies.

It follows immediately from Theorem 4.4.1 that the analog NMP zero imposes a limitation upon our ability to achieve affirmative answers to all of questions (A1)-(A3).

Corollary 7.2.1

Suppose that the hybrid feedback system is stable and that (7.4) and (7.8) both hold. Define $\omega^* \triangleq \min\{\omega_1, \omega_2\}$, and $\Omega^* = [0, \omega^*)$. If the analog plant has a NMP zero at ξ , it follows that

$$\sup_{\omega > \omega^*} |S^0(j\omega)| \geq \left(\frac{1}{\beta_1 + \beta_2} \right)^{\frac{\Theta(\xi, \Omega^*)}{\pi - \Theta(\xi, \Omega^*)}} |B_p^{-1}(\xi)|^{\frac{\pi}{\pi - \Theta(\xi, \Omega^*)}}, \quad (7.11)$$

where B_p is the Blaschke product of the unstable poles of the plant (cf. Subsection 4.4.1), and $\Theta(\xi, \Omega^*)$ is the weighted length of the interval Ω^* , defined in Chapter 3, (3.35).

Proof: It follows as a direct application of Corollary 4.4.2, taking into account bounds (7.4) and (7.8). \square

The peak in $|S^0(j\omega)|$ associated with making both β_1 and β_2 small will tend to violate the bounds (7.9)-(7.10) *unless* ω^* is sufficiently small that the NMP zero does not contribute significant phase lag at this frequency.

7.3 Gedanken Experiment No. 2: Discrete Response

We argued in the preceding section that GSHF control is ineffective at removing the design limitations due to analog NMP zeros. Indeed, there exists a tradeoff between the quality of the response at sampling instants and that of the intersample behavior. Specifically, if $|S_d(e^{j\omega T})|$ is made small over a wide frequency band relative to the location of the NMP zero, then $|S^0(j\omega)|$ cannot closely approximate the discrete response over this band without incurring large peaks at higher frequencies.

In the present section, we shall argue that use of GSHF control to shift zeros so that the discrete sensitivity function can be made small over a wide frequency range may lead to unacceptable robustness difficulties *even if no requirement is imposed upon the analog response*. The source of these difficulties is the necessity to maintain stability robustness against the contribution of high frequency aliases to the discrete plant response.

7.3.1 Formulation of Gedanken Experiment No. 2

Consider the formula (2.9), which shows that the response of the discretized plant at a frequency $\omega \in \Omega_N$ depends upon the response of the analog plant, prefilter, and hold function at infinitely many frequencies $\omega + k\omega_s$, $k = 0, \pm 1, \pm 2, \dots$

To explore this phenomenon further, let us rewrite (2.9) as

$$(FPH)_d(e^{sT}) = \frac{1}{T} F(s)P(s)H(s) + \frac{1}{T} \Upsilon(s), \quad (7.12)$$

where

$$\Upsilon(s) \triangleq \sum_{k \neq 0} F_k(s)P_k(s)H_k(s). \quad (7.13)$$

It follows from (7.12)-(7.13) that if for some value of s the analog plant has a zero, $P(s) = 0$, but the discretized plant does not, $(FPH)_d(e^{sT}) \neq 0$, then *necessarily* the response of the discretized plant at $z = e^{sT}$ must depend upon the response of the analog plant at one or more of the frequencies $s + jk\omega_s$, $k \neq 0$. As a corollary, the response of the discretized system will be potentially sensitive to uncertainty in the analog plant at these frequencies. This fact is significant in that uncertainty in the plant model generally increases at higher frequencies. Hence if a strong dependence upon high frequency plant behavior is required to shift a zero, then one might suspect that the sensitivity and robustness of the resulting design would be poor. We now propose another Gedanken experiment whose result should serve to clarify this issue.

Gedanken Experiment No. 2: Suppose that we wish to design a digital controller for an analog plant. Then the following two questions (among others) are of interest:

(D1) Is the nominal response of the discrete system satisfactory?

(D2) Is the *discrete* response insensitive to uncertainty in the analog plant?

Clearly, it is desirable that the answers to both questions be affirmative. *The proposed experiment is to determine whether affirmative answers to both of these questions can be obtained simultaneously.* ◦

Note that we are now concerned solely with the response of the system *at the sampling instants* and are imposing no requirement that the nominal or robust intersample behavior be satisfactory. The only requirement concerning the analog system is that the behavior at sampling instants be robust against uncertainty in the analog plant.

Let us now revisit the problem of achieving robust stability against linear time invariant uncertainty in the *analog* plant. Motivated by the discussion surrounding (7.12)-(7.13), we shall consider separately uncertainty in the two terms on the right hand side of (7.12). In particular since uncertainty in the analog plant tends to increase with frequency, it follows that for $\omega \in \Omega_N$ uncertainty in the term $F(j\omega)P(j\omega)H(j\omega)$ will tend to be dominated by uncertainty in the term $\Upsilon(j\omega)$ due to the high frequency aliases.

Consider uncertainty in the discretized plant due to analog plant uncertainty of the form

$$\tilde{P}(s) = P(s) (1 + W(s)\Delta(s)), \quad (7.14)$$

where Δ is stable and proper, with $|\Delta(j\omega)| < 1$ for all ω , and W is a stable, minimum phase weighting function used to represent frequency dependence of the modeling error. A necessary and sufficient condition for the sampled-data system to remain stable under uncertainty of the form (7.14) was derived in Dullerud and Glover [1993], and was discussed in Chapter 6. This condition concerns an infinite sequence of μ -tests, but in the case of SISO systems simplifies to the ex-

pression

$$\sup_{\omega \in \Omega_N} \sum_{k=-\infty}^{\infty} |T_k^0(j\omega)W_k(j\omega)| \leq 1, \quad (7.15)$$

as we stated in Corollary 6.1.3. We have also seen in Chapter 6, Theorem 6.1.2, that a necessary condition for robust stability was

$$|T^0(j\omega)W(j\omega)| \leq 1 \quad \text{for all } \omega \text{ in } \mathbb{R}. \quad (7.16)$$

Typically, $|W(j\omega)|$ becomes unbounded at high frequencies, and thus it is necessary that $|T^0(j\omega)| \rightarrow 0$ sufficiently rapidly as $\omega \rightarrow \infty$. An inspection of the proof of this result in Chapter 6 reveals that the effects of aliases in (7.12) are ignored in deriving (7.16). We now develop a stronger necessary condition that does take aliases into account. Define

$$\underline{w} = \inf_{\omega \notin \Omega_N} |W(j\omega)|. \quad (7.17)$$

Then, we have the following.

Corollary 7.3.1

A necessary condition for robust stability of the sampled-data system is that

$$|T^0(j\omega)W(j\omega)| + \underline{w}|S_f(j\omega)| \leq 1, \quad \text{for all } \omega \text{ in } \Omega_N. \quad (7.18)$$

Proof: It follows immediately from (7.15) and (7.7), since

$$\begin{aligned} \sum_k |T_k^0(j\omega)W_k(j\omega)| &\geq |T^0(j\omega)W(j\omega)| \\ &\quad + \frac{\underline{w}}{T} \sum_{k \neq 0} |F_k(j\omega)P_k(j\omega)H_k(j\omega)S_d(e^{j\omega T})C_d(e^{j\omega T})| \\ &\geq |T^0(j\omega)W(j\omega)| + \underline{w}|S_f(j\omega)|. \end{aligned}$$

□

Since relative uncertainty in the analog plant (7.14) typically becomes large at high frequencies, and since the Nyquist frequency is usually chosen to be around 5 times the desired closed loop bandwidth, it is not unreasonable to assume that \underline{w} in (7.17) is greater than 1. Hence (7.18) requires that $|S_f(j\omega)| < 1$ over the Nyquist range. This fact is significant since, as we shall see in the next subsection, S_f must satisfy a Poisson integral relation.

7.3.2 Interpolation Constraints and an Integral Relation

We now state a set of interpolation constraints and an integral relation that must be satisfied by the fidelity function, S_f . We first require an additional assumption that will hold generically.

Assumption 5

If ξ is a CRHP zero of P or H , then $e^{\xi T}$ is not a zero of $(FPH)_d$. \circ

Proposition 7.3.2 (Interpolation Constraints for the Fidelity Function)

Suppose that the sampled-data feedback system is stable, and that P , F , H , and C_d satisfy all assumptions stated in Chapter 2 as well as Assumption 5. Then the following conditions are satisfied:

(i) Let ζ be a CRHP zero of P . Then

$$S_f(\zeta) = T_d(e^{\zeta T}). \quad (7.19)$$

(ii) Let γ be a CRHP zero of H . Then

$$S_f(\gamma) = T_d(e^{\gamma T}). \quad (7.20)$$

(iii) Let a be a zero of C_d with $a \in D^c$. Define

$$a_k \triangleq \frac{1}{T} \log(a) + jk\omega_s, \quad \text{with } k = 0, \pm 1, \pm 2, \dots \quad (7.21)$$

Then

$$S_f(a_k) = 0, \quad \text{for all } k. \quad (7.22)$$

(iv) Let p be a CRHP pole of P . Define

$$p_k \triangleq p + jk\omega_s, \quad \text{with } k = \pm 1, \pm 2, \dots \quad (7.23)$$

Then

$$S_f(p) = 0 \quad \text{and} \quad S_f(p_k) = 1 \quad (7.24)$$

(v) Let δ be a CRHP zero of Υ . Then

$$S_f(\delta) = 0. \quad (7.25)$$

(vi) S_f has no CRHP zeros other than those given in (iii), (iv), and (v).

Proof: From (7.7) and (7.13) we can alternatively write

$$S_f(s) = \frac{\frac{1}{T}\Upsilon(s)}{(FPH)_d(e^{sT})} T_d(e^{sT}). \quad (7.26)$$

Conditions (i) and (ii) follow then from Assumption 5, and the identity (7.26). Condition (iii) follows from the identity

$$S_f(s) = \frac{1}{T}\Upsilon(s)S_d(e^{sT})C_d(e^{sT}). \quad (7.27)$$

Condition (iv) follows from (7.26). Condition (v) follows from (7.27). Finally, (7.27) shows that the zeros of S_f are restricted to those of $\Upsilon(s)$, $S_d(e^{sT})$, and $C_d(e^{sT})$, and condition (vi) follows. \square

These interpolation constraints fix the values of the fidelity function at some points of the CRHP. As we have seen in Chapter 4, the Poisson integral may be used to translate the interpolation constraints into an equivalent integral relation. The following result shows this.

Theorem 7.3.3 (Poisson Integral for the Fidelity Function)

Let $\xi = x + jy$ equal one of the NMP zeros of P or H . Then

$$\int_0^\infty \log |S_f(j\omega)| \Psi(\xi, \omega) d\omega \geq \pi \log |T_d(e^{\xi T})| \quad (7.28)$$

where $\Psi(\xi, \omega)$ is the Poisson kernel for the half plane defined in (3.30).

Proof: Note that we can write

$$S_f(s) = \check{S}_f(s) B_p(s) B_a(s) B_\rho(s) B_\delta(s) e^{-s\tau_\Delta} e^{-sN_e T},$$

where \check{S}_f satisfies the Poisson integral relation Hoffman [1962], and²

B_p is the Blaschke product of the poles of P in \mathbb{C}^+ ,

B_a is the Blaschke product of the poles of $C_d(e^{sT})$ in \mathbb{C}^+ ,

B_ρ is the Blaschke product of the poles of $(FPH)_d(e^{sT})$ in \mathbb{C}^+ , and

B_δ is the Blaschke product of the zeros of Υ in \mathbb{C}^+ .

This fact, together with the identities $|S_f(j\omega)| = |\check{S}_f(j\omega)|$ and $S_f(\xi) = T_d(\xi)$, yield the desired results. \square

The integral (7.28) imposes a constraint upon values of $|S_f(j\omega)|$. Analysis of design implications is deferred to the next section.

7.3.3 Result of Gedanken Experiment No. 2

Suppose that the analog plant has at least one NMP zero and is subject to large modeling uncertainty at high frequencies. Using the Poisson integrals for $S_d(e^{j\omega T})$ (see Appendix C), and $S_f(j\omega)$ given by (7.28), we now show that there exists a limitation upon the ability of a sampled-data feedback system to satisfy, with affirmative answers, questions (D1) and (D2) of this Gedanken experiment. Specifically, we shall show that there exists a tradeoff between requiring (i) high performance in the discrete system and (ii) stability robustness with respect to the analog plant uncertainty. The severity of this tradeoff is determined by the relative location of the analog NMP zero, and is *independent of whether or not the discretized plant is minimum phase*. Furthermore, the tradeoff exists *even if no performance requirements are imposed upon intersample behavior*.

We shall state performance requirements in terms of bounds upon the discrete sensitivity function:

$$|S_d(e^{j\omega T})| \leq \beta, \quad \text{for all } \omega \text{ in } \Omega_\epsilon \triangleq [0, \epsilon\omega_N) \quad (7.29)$$

$$|S_d(e^{j\omega T})| \leq \gamma, \quad \text{with } \epsilon\omega_N < \omega \leq \omega_N, \text{ for } \epsilon < 1, \quad (7.30)$$

²Compare with Subsection 4.4.1 in Chapter 4.

where $\beta < 1$, and γ satisfies the lower bound $\gamma > (1/\beta)^{\epsilon/(1-\epsilon)}$ imposed by the discrete version of the Bode sensitivity integral, (C.3) in Appendix C.

If the discretized plant is minimum phase, then any such specification can be achieved. Note that the bounds (7.29)-(7.30) imply that $|T_d(e^{j\omega T})|$ is also bounded. We now show that requiring $S_d(e^{j\omega T})$ to satisfy bounds such as (7.29)-(7.30) imposes constraints upon the values of $T_d(e^{sT})$ off the unit circle.

Lemma 7.3.4

Assume that S_d is stable and that $S_d(e^{j\omega T})$ satisfies the bounds (7.29)-(7.30). Consider $v = e^{\xi T}$, where $\xi \in \text{ORHP}$. Then

$$|T_d(e^{\xi T})| \geq F_T(\xi, \beta, \gamma, \epsilon), \quad (7.31)$$

where

$$F_T(\xi, \beta, \gamma, \epsilon) \triangleq 1 - \beta \frac{\Theta_d(\xi, \Omega_\epsilon)}{\pi} \gamma \frac{\pi - \Theta_d(\xi, \Omega_\epsilon)}{\pi} \quad (7.32)$$

Proof: It follows from Corollary C.1.4 in Appendix C that

$$|T_d(e^{\xi T}) - 1| \leq \beta \frac{\Theta_d(\xi, \Omega_\epsilon)}{\pi} \gamma \frac{\pi - \Theta_d(\xi, \Omega_\epsilon)}{\pi} |B_\xi(e^{\xi T})|, \quad (7.33)$$

from which the result follows. \square

This result shows that if the specification imposed upon $|S_d(e^{j\omega T})|$ is very stringent (i.e., if $\beta \ll 1$) then the lower bound on $|T_d(e^{\xi T})|$ will nearly equal one. Proximity to one is determined by the relative location of the zero with respect to the interval Ω_ϵ . This point is illustrated for a real zero, $\xi = x$, in Figure 7.6, wherein we plot $F_T(\xi, \beta, \gamma, \epsilon)$ vs. the ratio $x/\epsilon\omega_N$ for $\gamma = 2$, $\epsilon = 0.2$, and various values of β . For each β , the lower bound on $|T_d(e^{xT})|$ increases monotonically as the zero location decreases relative to the frequency interval Ω_ϵ .

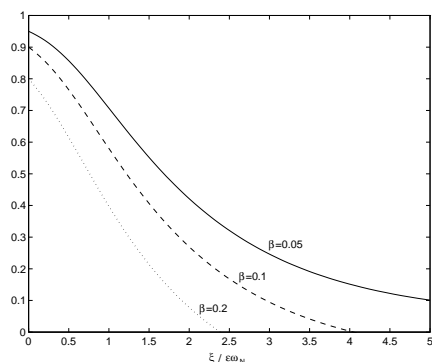


Figure 7.6: Bound (7.31) on T_d .

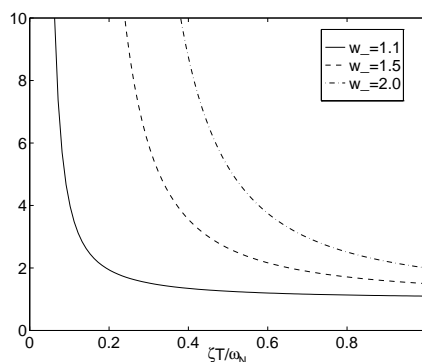


Figure 7.7: $F_S(\underline{w}, x)$ vs. x .

We shall suppose that the analog plant is subject to uncertainty of the form (7.14), where Δ is arbitrary save for the bound $|\Delta(j\omega)| < 1$, and $|W(j\omega)| \rightarrow \infty$

as $\omega \rightarrow \infty$. Let $\underline{\omega}$ be given by (7.17). It follows from Theorem 6.1.2 and Corollary 7.3.1 that *necessary* conditions for robust stability are that

$$|S_f(j\omega)| < 1/\underline{\omega}, \quad \text{for all } \omega \text{ in } \Omega_N, \quad (7.34)$$

and

$$|T^0(j\omega)| < 1/\underline{\omega}, \quad \text{for all } \omega \notin \Omega_N \quad (7.35)$$

Our next result is an immediate corollary to Theorem 7.3.3.

Corollary 7.3.5

Assume that the feedback system of Figure 2.4 is stable. Let ζ denote a NMP zero of P . Suppose that S_f satisfies the bound (7.34). Then

$$\sup_{\omega > \omega_N} |S_f(j\omega)| \geq F_S(\underline{\omega}, \zeta) |T_d(e^{\zeta T})|^{\frac{\pi}{\pi - \Theta(\zeta, \omega_N)}}, \quad (7.36)$$

where

$$F_S(\underline{\omega}, \zeta) \triangleq (\underline{\omega})^{\frac{\Theta(\zeta, \omega_N)}{\pi - \Theta(\zeta, \omega_N)}}. \quad (7.37)$$

Furthermore,

$$\sup_{\omega > \omega_N} |T^0(j\omega)| \geq F_S(\underline{\omega}, \zeta) |T_d(e^{\zeta T})|^{\frac{\pi}{\pi - \Theta(\zeta, \omega_N)}} - \left| |S_d(e^{j\omega T})| - 1 \right| \quad (7.38)$$

Proof: The bound (7.36) follows from (7.28) by imposing (7.34), exponentiating both sides, and rearranging the result. The bound (7.38) follows from this and (7.7). \square

Consider Figure 7.7, which contains plots of $F_S(\underline{\omega}, \zeta)$ vs. the location of a real zero, $\zeta = x$, for various values of $\underline{\omega}$. These plots show that, for a fixed value of $\underline{\omega}$, $F_S(\underline{\omega}, \zeta)$ is large when ζ is at a relatively low frequency with respect to ω_N . In this case $|S_f(j\omega)|$ will have a large peak outside the Nyquist range *unless* the value of $|T_d(e^{\zeta T})|$ is sufficiently small. If $|S_d(e^{j\omega T})|$ satisfies bounds as (7.29)-(7.30), then (7.38) shows that there exists a corresponding peak in $|T^0(j\omega)|$. The latter peak will, in turn, imply that (7.35) will be violated, and thus that the system will not be robustly stable. These remarks imply that to satisfy the stability robustness requirements (7.34)-(7.35) it is *necessary* that $|T_d(e^{\zeta T})|$ be small. However, as Lemma 7.3.4 shows, requiring $|T_d(e^{\zeta T})|$ to be small imposes a limitation upon the response of the discretized system *even if the discrete plant is minimum phase*. Specifically, for a given interval Ω_ϵ , the value of β cannot be required to be very small, and this limitation worsens as ϵ approaches 1. Indeed, the following is a straightforward corollary of Lemma 7.3.4.

Corollary 7.3.6

Suppose that ϵ and γ are fixed and that we require

$$|T_d(e^{\xi T})| < c < 1. \quad (7.39)$$

Then necessarily the value of β in (7.29) must satisfy

$$\beta > (1 - c) \frac{\pi}{\Theta_d(\xi, \Omega_\epsilon)} \gamma \frac{\Theta_d(\xi, \Omega_\epsilon) - \pi}{\Theta_d(\xi, \Omega_\epsilon)} \quad (7.40)$$

◦

This result shows that if $|T_d(e^{\xi T})|$ is required to be very small to prevent large peaks in $|S_f(j\omega)|$ and $|T^0(j\omega)|$, then there is a lower limit on the level of discrete sensitivity reduction that may be required by (7.29).

It follows from the above discussion that design limitations due to analog NMP zeros *must* be taken into account in the design of the discretized feedback system even if no performance requirement is imposed upon the intersample behavior. Neglecting such limitations will lead to poor robustness properties against uncertainty in the analog plant. We illustrate these results with an example in the following subsection.

7.3.4 Example: Robustness of Zero-placement

In this section, we analyze robustness properties of a design application of GSHFs to loop transfer recovery (LTR). The procedure of LTR, originally developed by Doyle and Stein [1979], 1981, briefly consists on suitably tuning a parameter in a dynamic output-feedback compensator to “recover” the properties of a state-feedback design. This design technique has become very popular in recent years [e.g., Zhang and Freudenberg, 1990, Fu, 1990, Shi et al., 1994, Turan and Mingori, 1995].

A crucial requirement for satisfactory LTR is that the plant has to be minimum phase, since this procedure renders a controller that essentially involves an inverse of the plant. Design limitations imposed by NMP zeros have been analyzed by Zhang and Freudenberg [1990] in the continuous-time case. In sampled-data implementations these limitations are even more severe. Indeed, since the system operates “open-loop” between samples, analog disturbances can never be completely rejected (see §4.3 in Chapter 4), and therefore perfect LTR is impossible if intersample behavior is considered Shi et al. [1993].

Nevertheless, a technique to achieve perfect *discrete* LTR “irrespective of whether the underlying continuous-time plant is minimum phase or not” has been suggested by Er and Anderson [1994]. The basic idea of this paper is first to use a GSHF to relocate the discrete zeros so that the discretized plant is minimum phase, and then apply a standard discrete-time LTR procedure. Naturally, perfect LTR *at the sampling times* is then feasible independently of the zero distribution of the analog plant. Unfortunately, as we have seen in the previous section, such a technique is inherently non-robust to uncertainty in the analog plant, *even if just*

the sampled behavior is of concern. We show this on the design example provided by Er and Anderson.

The system structure for GSHF-based LTR is shown in Figure 7.3.4. The plant considered was stable but non-minimum phase, and is given by

$$P(s) = \frac{s - 5}{(s + 1)(s + 3)}.$$

The target state-feedback design satisfied the following specifications:

- Rise time, $t_r = 0.1\text{s}$
- Settling time, $t_s \leq 0.5\text{s}$
- Maximum overshoot, $M_p \leq 15\%$.

According to these requirements, the sampling time was selected $T = 0.04\text{s}$, and the closed-loop bandwidth $\omega_b = 15.3\text{ rad/s}$, approximately a 20% of the Nyquist range. Notice that these choices leave the NMP zero of the plant well inside the closed-loop bandwidth, which, according to our results, will have a significant incidence in the sensitivity and robustness properties of the system.

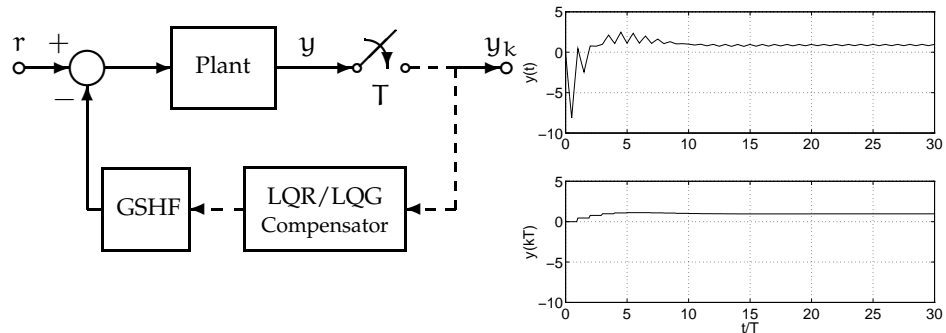


Figure 7.8: Structure for GSHF-based LTR.

Figure 7.9: Analog and discrete step response with $q = 3$.

The GSHF proposed was PC type with two steps, and was given by (3.50) on page 46. The LQR/LQG compensator for the system discretized with this GSHF is parameterized with the weight $R = 1/q^2$, with $q \geq 0$, and yields asymptotic LTR as $q \rightarrow \infty$. Figure 7.9 shows the analog and discrete step responses of the closed-loop system with $q = 3$, as suggested by the authors. We see that for this value of q the specifications are satisfied by the discrete response, although the continuous-time response shows large oscillations. This can be predicted from Figure 7.10 by analyzing the plot of the corresponding fidelity function $S_f(j\omega)$,

which displays significantly large values over the system's closed-loop bandwidth. Notice that this is even worse for larger values of q , which will give better discrete recovery of the loop.

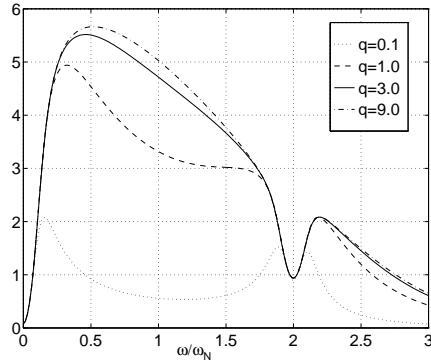


Figure 7.10: $S_f(j\omega)$ for different values of recovery q .

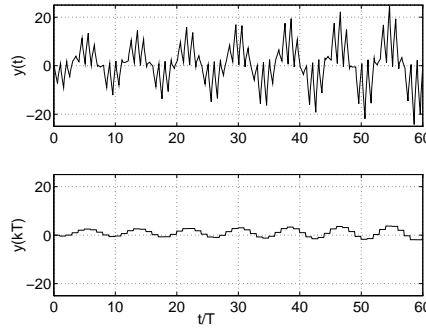


Figure 7.11: System destabilized by a time delay $\theta = 0.0023$ s.

More critically, it follows from the discussion in Subsection 7.3.3 that the system is prone to stability problems under plant uncertainty, since $S_f(j\omega)$ has important peaks on the Nyquist band. Indeed, suppose that there is a small unmodeled time delay θ , with $\theta \geq 0$, in the analog plant. This may be represented by a multiplicative perturbation model as in (7.14), with

$$\Delta(s) = \frac{1 - e^{-s\theta}}{s\theta}(1 + \delta), \quad \text{and} \quad W(s) = \frac{-\theta s}{(1 + \delta)},$$

where $0 < \delta \ll 1$. Notice that both Δ and W satisfy the conditions required in Subsection 7.3.1, so they are admissible. Consider the plots in Figure 7.10 for $q = 3$. From (7.34) we see that if

$$\inf_{\omega \notin \Omega_N} |W(j\omega)| > \frac{1}{5.52},$$

then the condition for stability of the perturbed system will be violated, since

$$\sup_{\omega \in \Omega_N} |S_f(j\omega)| = 5.52$$

from the plots. Equivalently, since $\inf_{\omega \notin \Omega_N} |W(j\omega)| = \theta(1 + \delta)\omega_N$, it follows for this perturbation — assuming $\delta \approx 0$ — that if the delay θ is greater than $\theta_0 = T/5.52\pi \approx 0.0023$ s, then condition (7.34) is violated. The system actually becomes unstable. This may be appreciated in Figure 7.11, where we plotted the step responses for the system perturbed with a delay $\theta = \theta_0$.

7.4 Summary

This chapter has studied robustness and sensitivity properties of a sampled-data system with a GSHF. Based on the results of previous chapters, we have shown here that shifting NMP zeros with GSHF control may lead to serious robustness difficulties in both the analog and discrete performances of the system.

In particular when the plant has NMP zeros, we have presented two instances in which GSHF zero-placement is generally prejudicial:

- (i) If good nominal *discrete* performance is required, then necessarily the discrete response will be sensitive to uncertainty in the *analog* plant.
- (ii) If good nominal *discrete* performance *and* satisfactory intersample behavior is required, then necessarily the *analog* response will be sensitive to plant uncertainty, disturbances and sensor noise.

In addition, we have shown that GSHF zero-placement, as used for robust stabilization of certain systems, will necessarily require a GSHF with NMP zeros. From the results in Chapters 3 and 4, these zeros yield extra limitations in analog performance, and moreover, may render sampling “almost pathological”, which in turn implies a discretized system with poor stabilizability properties.

Conclusions

We have provided a frequency-domain framework to study sampled-data feedback control systems. This framework incorporates full information of the continuous-time response of the system, and has emphasized the description of the hybrid operators governing the steady-state response to output disturbances and measurement noise. Using this framework,

- (i) We have developed a theory of design limitations for SISO sampled-data systems. This theory allows the quantification of performance limitations that are inherent to open-loop properties of the plant and hold function. Briefly, we found that
 - Hybrid systems *inherit* the difficulty imposed upon analog feedback design by those plant properties such as NMP zeros, unstable poles, and time-delays. Furthermore, such difficulty is independent of the type of hold used.
 - Hybrid systems are subject to *extra* design limitations due to potential NMP zeros of the hold. In particular, if there is a hold zero close to a plant pole in the ORHP, sampling is “almost pathological”, and then system’s sensitivity, robustness, and response to disturbances will be poor.
 - Hybrid systems, unlike the analog case, are subject to limits upon the ability of high compensator gain to achieve disturbance rejection. This limits can be overcome in some cases by imposing additional constraints on the structure of the hold.
- (ii) We have derived MIMO closed-form expressions for the frequency-gains and L_2 -induced norms of hybrid sensitivity and complementary sensitivity operators. These expressions characterize the frequency-gain of both operators as the maximum eigenvalue of an associated finite-dimensional discrete transfer matrix. The induced norm is then computed by performing a search of maximum over a finite range of frequencies. The results admit straightforward implementation in a numerically reliable fashion.
- (iii) We have shown that certain robust stability tests for sampled-data systems

may be derived in simpler and more intuitive way with a pure frequency-domain approach than with alternative state-space based formulations.

- (iv) We have analyzed GSHFs and GSHF-based feedback control systems. From our results we conclude that control schemes relying on GSHF zero-placement capabilities cannot circumvent fundamental limitations imposed by analog NMP plant zeros. Furthermore, if the analog plant has a NMP zero within the desired system's closed-loop bandwidth, and GSHF zero-shifting is used to attempt removing the limitations imposed by this zero, then the following design tradeoffs arise:
- (a) If good nominal *discrete* performance is required, then necessarily the discrete response will be sensitive to uncertainty in the *analog* plant.
 - (b) If good nominal *discrete* performance *and* satisfactory intersample behavior is required, then necessarily the *analog* response will be sensitive to plant uncertainty, disturbances and sensor noise.

From the above discussion, it seems that only a marginal improvement in performance may be expected from using a GSHF instead of a ZOH. In any case, it should be noted that the potential advantages of GSHFs may altogether evaporate at the time of a practical implementation. Indeed, it is not obvious how to actually construct a LTI GSHF other than as an approximation by a PC GSHF, and even in this case, the realization will be considerably more demanding than that of the simpler ZOH.

A number of other issues remain as topics for future research. Perhaps an obvious first step would be the application of the analysis tools developed in this thesis to synthesis of discrete controllers. In this direction, the frequency-domain methods presented may prove useful, offering clear interpretations, and reliable numerical algorithms.

For example, a potential line of research is connected with the expressions derived in Chapter 5 for operator frequency-gains and L_2 -induced norms. In Corollary 5.2.6 we introduced the discrete function Φ_d , which was indicated as a measure of intersample activity, since it serves to quantify the difference in L_2 -induced norms between hybrid and discrete sensitivity operators. For example, Φ_d could be useful to perform hybrid H_∞ loop shaping, i.e., by considering the frequency-gain of the hybrid complementary sensitivity operator, and then "shaping" the responses of Φ_d and the discrete complementary sensitivity function. This function has some other intriguing interpretations that might be worthwhile analyzing further:

- (i) Φ_d may be seen as a "distance" between the spaces spanned by the plant, hold, and anti-aliasing filter in the lifted domain (cf. Remark 5.2.3). The minimization of this distance might be considered, for example, to draw alternative design guidelines for the anti-aliasing filter.
- (ii) Φ_d is linked to the degree of conservativeness of the L_2 -induced norm as a measure of hybrid stability robustness against LTI uncertainties [Hagiwara and Araki, 1995]. In relation to this, we might consider the problem of

mapping analog uncertainties to discrete, and devise a procedure to reduce a hybrid robust stability problem to a simpler discrete one. More concretely, suppose that Δ is some admissible uncertainty in the analog plant P ,

$$\tilde{P} = P(1 + \Delta).$$

Then, if F is the anti-aliasing filter, and H the hold, we may write the discretized perturbed plant as

$$(\tilde{P}\tilde{H})_d = (FPH)_d \left(1 + \frac{(FP\Delta H)_d}{(FPH)_d} \right).$$

Let us then define the discrete perturbation by $\Delta_d \triangleq (FP\Delta H)_d / (FPH)_d$. Thus, if $\|\Delta\|_\infty \leq \gamma$, then it is not difficult to see that

$$\|\Delta_d\|_\infty \leq \gamma \|\Phi_d\|_\infty,$$

which characterizes a class of uncertainties for an associated discrete-time robust stability problem. The conditions obtained from this discrete problem will be conservative, but this may be quantified from the analysis of Φ_d .

An extension of our theory of hybrid performance limitations to a multivariable setting is also a path worth pursuing in the future. This could be approached, for example, by combining our results with those obtained by Freudenberg and Looze [1988], and more recently by Gómez and Goodwin [1995], for analog multivariable linear systems.

In relation to the possible improvement in performance obtained from using GSHFs, it would be indeed interesting to compare the different optimal H_∞ solutions to the sampled-data control problem; as for example those given by Bamieh and Pearson [1992] and Sun et al. [1993]. Bamieh and Pearson solve the problem assuming that the hold is a ZOH, whereas Sun et al. do not make this assumption, and thus obtain a more general solution that involves a discrete controller and a GSHF. The loss of performance arising from the use of the ZOH may well be quantified by using our formulas for the L_2 -induced norms, which consider GSHFs, and are easily programmable.

In a wider perspective for further work, one of the issues that comes to mind is to examine how pervasive these fundamental design limitations are. For some time, we have known that NMP zeros and unstable poles of the plant impose design constraints on analog systems. We have now shown that these limitations carry over to sampled-data systems. It seems that this would also follow to some extent to related control schemes such as periodic and multirate, which are subjects of current research. Do these limitations apply to *any* linear controller? Or even perhaps to *any controller whatsoever*?

At present, no answer to these general questions seems to be known, but it is expected that different analysis techniques would need to be applied.

A

Proofs of Some Results in the Chapters

A.1 Proofs for Chapter 2

In this section we prove Lemma 2.1.2. A proof for the strict conditions we stated may be found in Henrici [1977, Theorem 10.10a]¹; we shall give here a more compact version under an additional hypothesis.

We start with a few definitions and preliminary results. Given a function G (the Laplace transform of a function g) we introduce the following sequence of functions defined over the domain \mathcal{D}_G .

$$\Gamma_N(s) \triangleq \frac{1}{T} \sum_{n=-N}^N G(s + jn\omega_s), \quad \text{for } N = 0, 1, 2, \dots \quad (\text{A.1})$$

We shall assume the following, which is required for our proof of Lemma 2.1.2.

Assumption 6

The sequence $\{\Gamma_N\}_{N=0}^{\infty}$ is uniformly convergent in the strip \mathcal{D}_G . \circ

The convergence of the sequence $\{\Gamma_N\}_{N=0}^{\infty}$ established above delineates the conditions under which the RHS of (2.6) is mathematically meaningful.

Remark A.1.1 The uniform convergence of the series $\frac{1}{T} \sum_{n=-\infty}^{\infty} G(s + jn\omega_s)$ is also the condition required by the proof of Doetsch [1971]. We suspect that assuming that g is a function of BV should imply the uniform convergence of the series, and then allow a reasonably compact proof of Lemma 2.1.2 without resorting to the Poisson Summation Formula Henrici [1977]. However, we could not complete this proof by the time of writing this monograph. This assumption on g would then be a more restrictive condition, although somehow more insightful if one is interested in a time-domain characterization. That this condition is in fact sufficient to prove Lemma 2.1.2 follows from Henrici [1977]. \diamond

¹Henrici refers to this result as the Polya Formula, and derives it as a corollary of the Poisson Summation Formula.

Many of the proofs for results related to Lemma 2.1.2 available in the literature rely on the introduction of the “function”

$$\delta_T(t) = \sum_{k=-\infty}^{\infty} \delta(t - kT),$$

defined as an infinite series of impulses, or Dirac’s deltas Pierre and Kolb [1964], Carroll and W.L. McDaniel [1966], Phillips et al. [1966], Åström and Wittenmark [1990]. A Dirac’s delta is *not* well-defined as a function; it is in fact a *distribution*, and so special care must be taken regarding the sense in which certain mathematical manipulations are performed [cf. Zemanian, 1965].

Our approach dispenses with the use of δ_T , and instead resources to the *Dirichlet Kernel*, a classical tool in proving convergence of Fourier series. The Dirichlet Kernel is defined by

$$D_N(t) = \frac{\sin((2N + 1)t)}{\sin(t)},$$

where N is a positive integer. D_N is periodic and its integral on $[0, \pi/2]$ has a fixed value independent of N ,

$$\int_0^{\pi/2} D_N(t) dt = \frac{\pi}{2}.$$

A key property of the Dirichlet Kernel is related to the following *Dirichlet Integral* [e.g., Carslaw, 1950, § 94].

Lemma A.1.1 (Dirichlet Integral.)

If f is a function of BV on the interval $[0, \pi]$, then

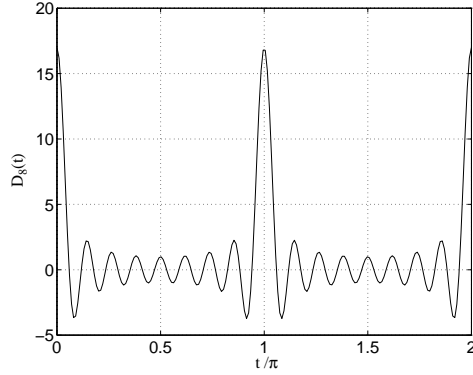
$$\lim_{N \rightarrow \infty} \int_0^{\pi} f(t) D_N(t) dt = \frac{\pi}{2} [f(0^+) + f(\pi^-)]$$

◦

Note that D_N is very much like an approximation to δ_T , with many similar properties, but is well-defined as a function (see Figure A.1).

Proof of Lemma 2.1.2 Consider the finite series $\sum_{|n| \leq N} G(s + jn\omega_s)$ for some s in \mathcal{D}_G . Then, we have:

$$\begin{aligned} \sum_{|n| \leq N} G(s + jn\omega_s) &= \sum_{|n| \leq N} \int_0^{\infty} e^{-(s+jn\omega_s)t} g(t) dt \\ &= \sum_{|n| \leq N} \sum_{k=0}^{\infty} \int_{kT}^{(k+1)T} e^{-(s+jn\omega_s)t} g(t) dt \\ &= \sum_{|n| \leq N} \sum_{k=0}^{\infty} \int_0^T e^{-s(t+kT)} e^{-jn\omega_s t} g(t + kT) dt \\ &= \sum_{k=0}^{\infty} \int_0^T e^{-s(t+kT)} g(t + kT) \left(\sum_{|n| \leq N} e^{-jn\omega_s t} \right) dt \quad (\text{A.2}) \end{aligned}$$

Figure A.1: Dirichlet Kernel for $N = 8$.

Note that the summation inside the integral in (A.2) is precisely the Dirichlet Kernel introduced before, since

$$\sum_{|n| \leq N} e^{-jn\omega_s t} = D_N(\omega_s t/2).$$

Hence, for each k we obtain a Dirichlet Integral on $e^{-s(t+kT)} g(t+kT)$,

$$\sum_{|n| \leq N} G(s + jn\omega_s) = \sum_{k=0}^{\infty} \int_0^T e^{-s(t+kT)} g(t+kT) D_N(\omega_s t/2) dt. \quad (\text{A.3})$$

Take limits on both sides of (A.3) and, since the series on the LHS is uniformly convergent, we can interchange limit and summation, which yields

$$\begin{aligned} \lim_{N \rightarrow \infty} \sum_{|n| \leq N} G(s + jn\omega_s) &= \sum_{k=0}^{\infty} \lim_{N \rightarrow \infty} \int_0^T e^{-s(t+kT)} g(t+kT) D_N(\omega_s t/2) dt. \\ &= \frac{T}{2} \sum_{k=0}^{\infty} (g(kT^+) + g((k+1)T^-)) e^{-skT}. \end{aligned} \quad (\text{A.4})$$

Adding and subtracting $\sum_{k=0}^{\infty} g(kT^+) e^{-skT}/2$, we obtain $T F_d(e^{sT})$ on the RHS of (A.4). Finally, noting that $g(0^-) = 0$, expression (2.6) follows, completing the proof. \square

A.2 Proofs for Chapter 3

This section provides the proof of Lemma 3.2.2, on the asymptotic location of the zeros of a FDLTI GSHF.

Proof of Lemma 3.2.2 We first prove, by contradiction, that $n, m < N - 1$, where $L \in \mathbb{R}^{N \times N}$. Suppose $n \geq N - 1$. Then $KL^i M = 0$ for $i = 1, 2, \dots, N - 1$.

By the Cayley-Hamilton Theorem Chen [1984], $KL^iM = 0$ for all i . However, since $d^i h/dt^i|_{t=T} = KL^iM$, this implies that h is identically zero [Chen, 1984, Appendix B]. This argument also shows that the coefficient of e^{-sT} in (3.12) is nonzero. A similar argument shows that $m < N - 1$.

Consider next the ratio

$$F(s) = \frac{K(sI + L)^{-1}Me^{-sT}}{K(sI + L)^{-1}e^{LT}M}.$$

Note that F is analytic in a neighborhood of infinity and has an essential singularity at infinity (the latter is due to the presence of e^{-sT} with a nonzero coefficient). It follows from the Great Picard Theorem [Conway, 1973, p. 302] that in each neighborhood of infinity F assumes each complex number with one possible exception, infinitely many times. Because of the term e^{-sT} , this exceptional value must equal zero. Hence there exists a sequence $\{\gamma_\ell\}_{\ell=1}^\infty$ converging to infinity such that $F(\gamma_\ell) = 1$, and thus $H(\gamma_\ell) = 0$ for all ℓ .

We now show that if $n = m$, then the γ_ℓ 's necessarily converge to the values given in (3.19). To do this note that for each integer k ,

$$(sI + L)^{-1} = \frac{1}{s} \left(\left(\frac{-L}{s} \right)^{k+1} \left(I + \frac{L}{s} \right)^{-1} + \sum_{i=0}^k \left(\frac{-L}{s} \right)^i \right)$$

Using this identity and the definitions of m and n yields

$$H(s) = \frac{1}{s^{m+1}} (Q(s) - R(s) e^{-sT} s^{m-n}),$$

where

$$Q(s) = K(-L)^m e^{LT}M + \frac{1}{s} K(-L)^{m+1} \left(I + \frac{L}{s} \right)^{-1} e^{LT}M,$$

and

$$R(s) = K(-L)^n M + \frac{1}{s} K(-L)^{n+1} \left(I + \frac{L}{s} \right)^{-1} M.$$

For γ_ℓ a zero of H , we have $Q(\gamma_\ell) = \gamma_\ell^{m-n} R(\gamma_\ell) e^{\gamma_\ell T}$. Note that for ℓ sufficiently large, $Q(\gamma_\ell)$ and $R(\gamma_\ell)$ are both nonzero and constant. Taking logarithms and rearranging shows that there exists k such that

$$\gamma_\ell = -\frac{1}{T} \log \frac{Q(\gamma_\ell)}{R(\gamma_\ell)} + \frac{m-n}{T} \log \gamma_\ell + jk\omega_s.$$

If $n = m$, then taking limits yields

$$\gamma_\ell \rightarrow -\frac{1}{T} \log \eta + jk\omega_s.$$

Noting that zeros must occur in conjugate pairs yields (3.19). \square

A.3 Proofs for Chapter 4

This section provides an sketch of a proof for Lemma 4.1.2 on the steady-state frequency response of the hybrid system to input disturbances and noise. We also give here a proof for the complementary sensitivity integral constraint of Theorem 4.4.11.

A.3.1 Proof of Lemma 4.1.2

We consider only the disturbance response, calculations for the noise response being entirely analogous. To evaluate the steady-state response to $d(t) = e^{j\omega t}$, we must first evaluate the inverse Laplace transform of Y^d , and then discard all terms due to those poles lying in \mathbb{C}^- . Inverting the Laplace transform requires that we evaluate the Bromwich integral Levinson and Redheffer [1970]

$$y^d(t) = \frac{1}{2\pi j} \int_{\gamma-j\infty}^{\gamma+j\infty} e^{st} Y^d(s) ds, \quad (\text{A.5})$$

where $\gamma > 0$. This integral may be evaluated using the residue theorem.

It follows from (4.1) that Y^d has poles due to the disturbance located along the imaginary axis at $s = j(\omega + k\omega_s)$, $k = 0, \pm 1, \pm 2, \dots$. By the assumption of closed loop stability all other poles of Y^d lie in the \mathbb{C}^- . Using (4.1), it may be shown that these poles have the following properties:

- (i) they all lie to the right of some vertical line $\text{Re}[s] = c < 0$,
- (ii) there are finitely many poles due to P and no poles due to H , and
- (iii) there are finitely many sequences of poles due to $C_d(e^{sT})$, $S_d(e^{sT})$, and $F(s + jk\omega_s)$, $k = 0, \pm 1, \pm 2, \dots$ lying on vertical lines and spaced at intervals equal to ω_s .

Next, it is straightforward to verify that the residues of $e^{st} Y^d$ at the $j\omega$ -axis poles are given by

$$\lim_{s \rightarrow j(\omega + k\omega_s)} (s - j(\omega + k\omega_s)) e^{st} Y^d(s) = \begin{cases} S^0(j\omega) e^{j\omega t} & \text{if } k = 0 \\ -T_k(j\omega) e^{j(\omega + k\omega_s)t} & \text{if } k \neq 0 \end{cases}. \quad (\text{A.6})$$

We need not calculate explicitly the residues at the other poles; as we shall show, they do not contribute to the steady-state response.

Consider the contours of integration \mathcal{C}_n , $n = 1, 2, 3, \dots$ depicted in Figure A.2, and chosen so that (i) \mathcal{C}_1 encloses only that $j\omega$ -axis pole lying in Ω_N , (ii) the horizontal line $\text{Im}[s] = R_1$ does not contain any OLHP poles of Y^d , and (iii) $R_{n+1} = R_n + \omega_s$.

Figure A.2 and subsequent calculations are appropriate for the case that ω is in Ω_N (modifications to the general case are straightforward). Our construction

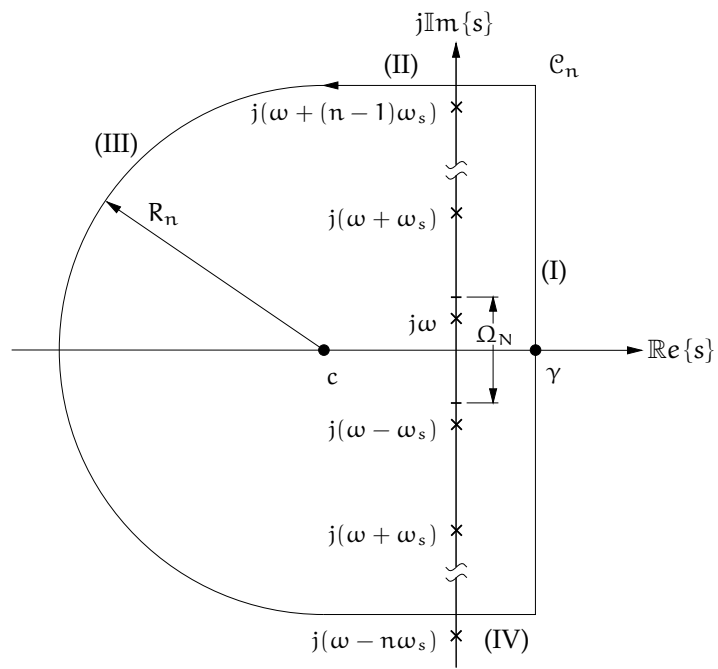


Figure A.2: Contours of integration.

of the contour of integration guarantees that for n sufficiently large no poles of Y^d will lie on \mathbb{C}_N . Hence the residue theorem may be applied to yield

$$\begin{aligned} & \frac{1}{2\pi j} \left\{ \int_{\text{I}} e^{st} Y^d(s) ds + \int_{\text{II}} e^{st} Y^d(s) ds + \int_{\text{III}} e^{st} Y^d(s) ds + \int_{\text{IV}} e^{st} Y^d(s) ds \right\} \\ & = S^0(j\omega) e^{j\omega t} - \sum_{\substack{k=-N \\ k \neq 0}}^N T_k(j\omega) e^{j(\omega+k\omega_s)t} + \Psi(t), \end{aligned} \quad (\text{A.7})$$

where $\Psi(t)$ denotes the contribution of the poles in \mathbb{C}^- .

We now sketch a proof that as $t \rightarrow \infty$, $\Psi(t) \rightarrow 0$. First, it is clear that the contribution to Ψ from each pole of P converges to zero. Consider next the contribution of one of the finitely many sequences of poles described in (iii) above. Let this sequence be denoted $\rho_k \triangleq \rho + jk\omega_s$, $k = 0, \pm 1, \pm 2, \dots$, and $\Re\{\rho\} < 0$. We shall assume that ρ is real for notational simplicity, and shall also assume for simplicity that each ρ_k is a simple pole. Then, for any fixed value of t , the contribution to Ψ from this sequence of poles is given by

$$y^\rho(t) \triangleq e^{\rho t} \lim_{K \rightarrow \infty} \sum_{k=-K}^K \text{Res}(\rho_k) e^{jk\omega_s t}, \quad (\text{A.8})$$

where $\text{Res}(\rho_k) = \lim_{s \rightarrow \rho_k} (s - \rho_k) Y^d(s)$. By the Riesz-Fischer Theorem [Riesz and Sz.-Nagy, 1990, p.70], if it may be shown that the sequence $\{\text{Res}(\rho_k)\}$ is square-summable, then the series in (A.8) will converge to a bounded periodic function of t . Since $\rho < 0$, it thus follows that $y^\rho(t) \rightarrow 0$ as $t \rightarrow \infty$. Since there are only finitely many sequences of the form (A.8), we then have that $\Psi(t) \rightarrow 0$.

We now show that the sequence $\{\text{Res}(\rho_k)\}$ is square-summable. From the (4.1), we have that

$$Y^d(s) = D(s) - P(s)H(s)C_d(e^{sT})S_d(e^{sT})V_d(e^{sT}), \quad (\text{A.9})$$

where $V_d(e^{sT})$ is given by (cf. the proof of Lemma 4.1.1)

$$V_d(e^{sT}) = \frac{1}{T} \sum_{k=-\infty}^{\infty} F_k(s) D_k(s).$$

Hence

$$\text{Res}(\rho_k) = -P(\rho_k)H(\rho_k) \lim_{s \rightarrow \rho_k} (s - \rho_k) C_d(e^{sT}) S_d(e^{sT}) V_d(e^{sT}). \quad (\text{A.10})$$

Because $C_d(e^{sT})$, $S_d(e^{sT})$, and $V_d(e^{sT})$ are each periodic in s along vertical lines, it may be shown that the limit on the right hand side of (A.10) is independent of k . Denote the common value of this limit by L_ρ . Then (A.8) becomes

$$y^\rho(t) = e^{\rho t} L_\rho \lim_{K \rightarrow \infty} \sum_{k=-K}^K P(\rho_k) H(\rho_k) e^{jk\omega_s t}. \quad (\text{A.11})$$

By Assumption 3, $|P(\rho_k)|$ converges to a finite constant as $k \rightarrow \infty$. Next, using the definition of H (2.4) and integration by parts write for s in \mathbb{C}^-

$$\begin{aligned} |sH(s)| &= \left| h(0^+) - e^{-sT}h(T^-) + \int_0^T e^{-st}\dot{h}(t) dt \right| \\ &\leq |h(0^+)| + |h(T^-)|e^{-\Re\{s\}T} + e^{-\Re\{s\}T} \int_0^T |\dot{h}(t)| dt. \end{aligned} \quad (\text{A.12})$$

Since h is of BV by Assumption 1, \dot{h} is integrable on $[0, T)$, and then from (A.12)

$$|H(\rho_k)| \leq \frac{c_1 + c_2 e^{-\rho T}}{|\rho_k|}.$$

It follows that the sequence $\{P(\rho_k)H(\rho_k)\}$ is square summable, thus completing the proof that $\Psi(t) \rightarrow 0$.

The desired result (4.9) will hold if it may be shown that the last three integrals in (A.7) converge to zero as $N \rightarrow \infty$. We now show that the integral (II) converges to zero; similar calculations apply to (IV). Consider values of s such that $s = x + jR_n$, $c \leq x \leq \gamma$, and R_n is sufficiently large that $R_n > \omega$ and that \mathcal{C}_n encloses all poles of P . It may be shown that there exists constants M and M_p , independent of n , such that $|C_d(e^{sT})S_d(e^{sT})V_d(e^{sT})| \leq M$ and $|P(s)| \leq M_p$ for all such s . Furthermore, it is not difficult to see from similar arguments as those in (A.12) that for $t \geq T$ there exists a constant M_γ with

$$|se^{st}H(s)| \leq M_\gamma, \quad \text{for all } s \text{ with } \Re\{s\} \leq \gamma. \quad (\text{A.13})$$

Using these bounds in (A.8) yields

$$|e^{st}Y^d(s)| \leq e^{\gamma t}(R_n - \omega)^{-1} + MM_p M_\gamma (R_n - \omega)^{-1} \quad (\text{A.14})$$

Using this bound in (II) yields that the integral converges to zero as $R_n \rightarrow \infty$.

It remains to show that the integral (III) converges to zero. This follows by (i) parameterizing (III) by $s = c + R_n e^{j\theta}$, with $\pi/2 \leq \theta \leq 3\pi/2$, and defining $\sigma = s - c$; contour (III) is then a semicircle φ_n centered at the origin of the σ -plane and extended into the left half plane; (ii) showing that Y^d is bounded on φ_n ; and (iii) using Jordan's Lemma [Levinson and Redheffer, 1970, p. 199] to obtain a bound on the integral

$$\int_{\varphi_n} |e^{\sigma T} d\sigma|.$$

Hence, for $t > T$, integral (III) converges to zero as $R_n \rightarrow \infty$. \square

A.3.2 Proof of Theorem 4.4.11

This result is analogous to the integral constraint we proved for holds in Chapter 3, Proposition 3.3.3. The proof is in a similar pattern. We need the following preliminary result.

Lemma A.3.1

Suppose that G is an analytic function bounded in the CRHP; suppose that $G(0) = 1$. Then

$$\lim_{x \rightarrow 0} \int_0^{\infty} \frac{\log |G(j\omega)|}{x^2 + \omega^2} d\omega = \int_0^{\infty} \frac{\log |G(j\omega)|}{\omega^2} d\omega \quad (\text{A.15})$$

Proof: The result follows from the Lebesgue Dominated Convergence Theorem [e.g., Riesz and Sz.-Nagy, 1990, p. 37]. To apply this result, it suffices to

- note that $|\log |G(j\omega)|/(x^2 + \omega^2)| \leq |\log |G(j\omega)|/\omega^2|$ for all x and ω , and
- show that the integral on the right hand side of (A.15) is finite.

The latter follows by noting that

- (i) $|\log |G(j\omega)||$ is bounded on the $j\omega$ -axis except at zeros of $G(j\omega)$,
- (ii) these zeros, including a possible zero at infinity, are removable singularities Levinson and Redheffer [1970] and thus do not cause the integral to become unbounded, and
- (iii) the integral approaches a finite limit as $\omega \rightarrow 0$.

Statement (iii) follows by using L'Hospital's Rule to show that

$$\lim_{\omega \rightarrow 0} \frac{\log G(j\omega)}{\omega^2} = \frac{G'(0)^2 - G''(0)}{2},$$

where $G'(0) = dG(s)/ds|_{s=0}$ and $G''(0) = d^2G(s)/ds^2|_{s=0}$. \square

Proof of Theorem 4.4.11 We begin by applying the Poisson integral to the fundamental complementary sensitivity function for an arbitrary real $x > 0$. Subtracting $\log |T^0(0)|$ from both sides yields

$$\begin{aligned} \frac{2}{\pi} \int_0^{\infty} \log \left| \frac{T^0(j\omega)}{T^0(0)} \right| \frac{x}{x^2 + \omega^2} d\omega &= x(\tau_p + \tau_H + N_c T) + \log |B_c^{-1}(x)| \\ &+ \log |B_\gamma^{-1}(x)| + \sum_{k=1}^{N_p} \log |B_{p_k}^{-1}(x)| \quad (\text{A.16}) \\ &+ \sum_{k=1}^{N_a} \log |B_{a_k}^{-1}(x)| + \log \left| \frac{T^0(x)}{T^0(0)} \right|, \end{aligned}$$

where the terms on the right hand side are as defined in Subsection 4.4.1. Dividing both sides by x , taking the limit as $x \rightarrow 0$, and applying Lemma A.3.1

yields

$$\begin{aligned}
\frac{2}{\pi} \int_0^\infty \log \left| \frac{T^0(j\omega)}{T^0(0)} \right| \frac{1}{x^2 + \omega^2} d\omega &= \tau_P + \tau_H + N_c T + \lim_{x \rightarrow 0} \frac{1}{x} \log |B_\zeta^{-1}(x)| \\
&+ \lim_{x \rightarrow 0} \frac{1}{x} \log |B_Y^{-1}(x)| + \lim_{x \rightarrow \omega} \frac{1}{x} \sum_{k=1}^{N_p} \log |B_{p_k}^{-1}(x)| \quad (\text{A.17}) \\
&+ \lim_{x \rightarrow 0} \frac{1}{x} \sum_{k=1}^{N_a} \log |B_{a_k}^{-1}(x)| + \lim_{x \rightarrow 0} \frac{1}{x} \log \left| \frac{T^0(x)}{T^0(0)} \right|.
\end{aligned}$$

We now use L'Hospital's rule and the fact that the zeros and poles (4.58)-(4.63) must occur in complex conjugate pairs to evaluate the various limits on the right hand side of (A.17):

(i)

$$\begin{aligned}
\lim_{x \rightarrow 0} \frac{1}{x} \log |B_\zeta^{-1}(x)| &= \lim_{x \rightarrow 0} \frac{1}{x} \sum_{k=1}^{N_\zeta} \log \left| \frac{\bar{\zeta}_k + x}{\zeta_k - x} \right| \\
&= \sum_{k=1}^{N_p} \lim_{x \rightarrow 0} \frac{d}{dx} \left(\frac{1}{x} \log \left[\frac{\bar{\zeta}_k + x}{\zeta_k - x} \right] \right) \\
&= \sum_{k=1}^{N_p} \frac{2\text{Re}(\zeta_k)}{|\zeta_k|^2} \\
&= 2 \sum_{k=1}^{N_p} \frac{1}{\zeta_k}. \quad (\text{A.18})
\end{aligned}$$

(ii) A calculation similar to (i) applies to the fifth term in the RHS of (A.17) if it may be shown that the possibly infinite sum $\sum_{k=1}^{N_p} 1/\gamma_k$ converges. Convergence of this series follows from: (i) the fact that $T^0(0) \neq 0 \Rightarrow H(0) \neq 0$ and (ii) applying arguments based on properties of zeros of functions analytic in the CRHP (cf. p. 132 of Hoffman [1962]).

(iii)

$$\lim_{x \rightarrow 0} \frac{1}{x} \sum_{k=1}^{N_a} \log |B_{a_k}^{-1}(x)| = \lim_{x \rightarrow 0} \frac{1}{x} \sum_{k=1}^{N_a} \log \prod_{\ell=-\infty}^{\infty} \left| \frac{\bar{a}_{k\ell} + x}{\zeta_\ell - x} \right|. \quad (\text{A.19})$$

It follows from p. 175 of Conway [1973] that

$$\prod_{\ell=-\infty}^{\infty} \left| \frac{\bar{a}_{k\ell} + x}{a_{k\ell} - x} \right| = \left| \frac{\sinh((\bar{a}_k + x)\frac{T}{2})}{\sinh((a_k - x)\frac{T}{2})} \right| \quad (\text{A.20})$$

Substituting (A.20) into (A.19) and applying L'Hospital's rule yields the desired result.

(iv) A calculation similar to (iii) applies to the sixth term on the RHS of (A.17), keeping in mind that the factor $\ell = 0$ is not present in the infinite product that corresponds to (A.20).

(v) Applying L'Hospital's rule yields

$$\begin{aligned} \lim_{x \rightarrow 0} \frac{1}{x} \log \left| \frac{T^0(x)}{T^0(0)} \right| &= \lim_{x \rightarrow 0} \frac{d}{dx} \left(\frac{1}{2} \log \left(\frac{T^0(x)}{T^0(0)} \right)^2 \right) \\ &= \frac{T^{\prime 0}(0)}{T^0(0)} \end{aligned}$$

□

A.4 Proofs for Chapter 5

In this section we prove that the frequency-domain lifting transformation defined in Chapter 5 is an isometric isomorphism between the spaces $L_2(-\infty, \infty)$ and $L_2(\ell_2; \Omega_N)$.

Proof of Lemma 5.1.1 Let $Y(j\omega)$ be in L_2 . Then we have that

$$\|Y\|^2 = \int_{-\infty}^{\infty} |Y(j\omega)|^2 d\omega \quad (\text{A.21})$$

$$= \sum_{k=-\infty}^{\infty} \int_{(2k-1)\omega_N}^{(2k+1)\omega_N} |Y(j\omega)|^2 d\omega$$

$$= \sum_{k=-\infty}^{\infty} \int_{-\omega_N}^{\omega_N} |Y(j(\omega + k\omega_s))|^2 d\omega. \quad (\text{A.22})$$

As $\|Y\|^2$ is finite by assumption, the series $\sum \int |Y_k(j\omega)|^2 d\omega$ is convergent. Then, by Levi's Theorem Riesz and Sz.-Nagy [1990], we can interchange summation and integration in (A.22), and using (5.1), we have that

$$\sum_{k=-\infty}^{\infty} \int_{-\omega_N}^{\omega_N} |Y_k(j\omega)|^2 d\omega = \int_{-\omega_N}^{\omega_N} \sum_{k=-\infty}^{\infty} |Y_k(j\omega)|^2 d\omega \quad (\text{A.23})$$

$$= \|y\|^2 \quad (\text{A.24})$$

From (A.21)-(A.24) it follows that there is an isometry between $L_2(-\infty, \infty)$ and $L_2(\Omega_N; \ell_2)$. To see that the isometry is isomorphic, we have to show that it is *onto*, that is, *each* function in $L_2(\Omega_N; \ell_2)$ is the image of a function in $L_2(-\infty, \infty)$. Actually, it suffices to show that this is the case for each element in a basis for $L_2(\Omega_N; \ell_2)$, and so we shall do next.

Let $\{\gamma_k\}_{k=-\infty}^{\infty}$ be an orthonormal basis for ℓ_2 , and $\{\psi_k(\omega)\}_{k=-\infty}^{\infty}$ an orthonormal basis for $L_2(\Omega_N)$. It is not difficult to prove that the double sequence

$$\{\psi_n(\omega) \gamma_m\}_{n,m=-\infty}^{\infty}$$

is an orthonormal base on $L_2(\Omega_N; \ell_2)$. Now, take for example $\psi_n(\omega) \gamma_m$, for fixed integers n, m . This element of $L_2(\Omega_N; \ell_2)$ is precisely

$$\begin{bmatrix} \vdots \\ 0 \\ \psi_n(\omega) \\ 0 \\ \vdots \end{bmatrix} \begin{matrix} \vdots \\ m+1 \\ m \\ m-1 \\ \vdots \end{matrix}, \quad (\text{A.25})$$

which corresponds to the function

$$\psi(\omega) = \begin{cases} \psi_n(\omega) & \text{if } \omega \in [-\omega_N + m\omega_s, \omega_N + m\omega_s] \\ 0 & \text{otherwise} \end{cases}. \quad (\text{A.26})$$

But $\psi(\omega)$ is obviously in $L_2(-\infty, \infty)$, since it is a function of finite support and integrable there. Therefore, every element in $L_2(\Omega_N; \ell_2)$ is the image of an element in $L_2(-\infty, \infty)$ and the proof is completed. \square

A.5 Proofs for Chapter 6

In this section we include the sketch of an alternative proof for Corollary 6.1.3 that dispenses with the μ -framework. The arguments are similar to those in Theorem 6.1.2.

Proof of Corollary 6.1.3 We start by noting that the perturbed discrete sensitivity function can be written as

$$\begin{aligned} \tilde{S}_d &= \frac{S_d}{1 + (\text{FPW}\Delta H)_d S_d C_d} \\ &= \frac{S_d}{1 + \sum_{n=-\infty}^{\infty} T_k^0 W_k \Delta_k} \end{aligned} \quad (\text{A.27})$$

We prove both implications in Corollary 6.1.3 by contrapositive arguments.

(\Leftarrow) Suppose that there exist an admissible Δ such that \tilde{S}_d is unstable. Then, by continuity arguments there also exist some admissible Δ' such that \tilde{S}_d is *marginally* stable, i.e., it has a pole at $s = j\omega_0$, for some ω_0 . From (A.27) it follows that

$$\sum_{n=-\infty}^{\infty} T_k^0(\omega_0) W_k(\omega_0) \Delta'_k(\omega_0) = -1.$$

Hence,

$$\sum_{n=-\infty}^{\infty} |T_k^0(\omega_0) W_k(\omega_0) \Delta'_k(\omega_0)| \geq 1,$$

but as $\|\Delta'\|_\infty < 1$, then

$$\sum_{n=-\infty}^{\infty} |T_k^0(\omega_0)W_k(\omega_0)| > 1.$$

(\Rightarrow) Suppose that there exists ω_0 in Ω_N such that

$$\sum_{n=-\infty}^{\infty} |T_k^0(\omega_0)W_k(\omega_0)| = \alpha > 1.$$

Then, it is possible to find an admissible perturbation Δ that interpolates

$$\Delta(j(\omega_0 + k\omega_s)) = -1/\alpha e^{-j\theta_k},$$

where $\theta_k \triangleq \angle T_k^0(\omega_0)W_k(\omega_0)$. Then \tilde{S}_d has a pole at $z = e^{j\omega_0 T}$ and so the perturbed system is not asymptotically stable. \square

B

Order and Type of an Entire Function

This appendix provides a brief description of the concepts of *order* and *type* of entire functions; for further reference see Markushevich [1965]. We recall that an entire function, F , is a function defined and analytic for all finite values of the complex variable s . An entire function that is not a polynomial is called an entire *transcendental* function. For such a function F , define the *maximum modulus* as

$$M(r) = \max_{|s|=r} |F(s)|.$$

It can be seen [e.g., Markushevich, 1965] that, since F is analytic everywhere, $M(r)$ is a strictly increasing function, and, moreover, $\lim_{r \rightarrow \infty} M(r) = \infty$. An entire function is said to be of *finite order* if there exists a positive number μ such that as $|s| = r \rightarrow \infty$, we have that¹

$$F(s) = O(e^{r^\mu}). \quad (\text{B.1})$$

Clearly, if (B.1) is satisfied for some μ , it will also be satisfied for any $\mu' > \mu$. The infimum of the numbers satisfying (B.1) is defined as the *order*, ρ , of the entire function F . We shall be interested in entire functions of *exponential type*, i.e., of finite order 1 for which there exists a positive constant K such that as $|s| = r \rightarrow \infty$,

$$F(s) = O(e^{Kr}). \quad (\text{B.2})$$

The lower bound σ of numbers K for which (B.2) is true is called the *type* of the entire function. We say then that F is of exponential type σ .

¹Here we use the notation $F(s) = O(e^{r^\mu})$, which means that $M(r) < ke^{r^\mu}$ for some constant k when r is near to some given limit.

C

Discrete Sensitivity Integrals

Discrete sensitivity functions satisfy analytic constraints in the form of Bode and Poisson integral relations analogous to those satisfied by their continuous-time counterparts. The results in this section are adapted from Sung and Hara [1988], to which we refer for further details.

Let $d_i, i = 1, \dots, N_d$ denote the poles of $(FPH)_d C_d$ lying in $\overline{\mathbb{D}}^c$. Then we have the following.

Proposition C.1.1 (Bode Discrete Sensitivity Integral)

Assume that S_d is stable and that $(FPH)_d C_d$ is strictly proper. Then

$$\int_0^{\omega_N} \log |S_d(e^{j\omega T})| d\omega = \omega_N \sum_{i=1}^{N_d} \log |d_i|. \quad (C.1)$$

◦

For a fixed sampling period, this integral implies a non-trivial sensitivity trade-off even if no bandwidth constraint is imposed. The next corollary is a straightforward consequence of Proposition C.1.1.

Corollary C.1.2

Assume the conditions of Proposition C.1.1. Suppose in addition that

$$|S_d(e^{j\omega T})| \leq \beta \quad \text{for } \omega \text{ in } [0, \omega_0], \text{ with } \omega_0 < \omega_N. \quad (C.2)$$

Then necessarily

$$\sup_{\omega_0 < \omega < \omega_N} |S_d(e^{j\omega T})| \geq \left(\frac{1}{\beta}\right)^{\frac{\omega_0}{\omega_N - \omega_0}} \left| \prod_{i=1}^{N_d} d_i \right|^{\frac{\omega_N}{\omega_N - \omega_0}}. \quad (C.3)$$

◦

Denote by $\rho_i, i = 1, \dots, N_\rho$ the poles of $(FPH)_d$ in $\overline{\mathbb{D}}^c$, and denote by B_ρ the associated Blaschke product

$$B_d(z) \triangleq \prod_{i=1}^{N_d} \frac{z - d_i}{1 - \bar{d}_i z}.$$

Define also the Poisson kernel $\Psi_d(re^{j\theta}, \omega)$,

$$\Psi_d(re^{j\theta}, \omega) \triangleq \frac{\frac{T}{2}(r^2 - 1)}{1 - 2r \cos(\omega T + \theta) + r^2} + \frac{\frac{T}{2}(r^2 - 1)}{1 - 2r \cos(\omega T - \theta) + r^2}. \quad (\text{C.4})$$

Then S_d satisfy the following Poisson integral relation.

Proposition C.1.3 (Poisson Discrete Sensitivity Integral)

Assume that S_d is stable. Let $\nu = re^{j\theta}$ lie in \mathbb{D}^c . Then

$$\int_0^{\omega_N} \log |S_d(e^{j\omega T})| \Psi_d(\nu, \omega) d\omega \geq \pi \log |B_\rho^{-1}(\nu)| + \pi \log |S_d(\nu)|. \quad (\text{C.5})$$

o

Note that equality may be achieved in (C.5) by incorporating terms due to unstable poles of the compensator into the Blaschke product B_ρ .

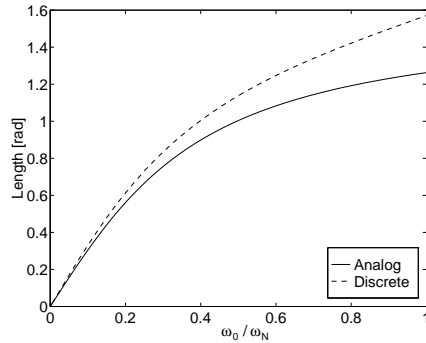


Figure C.1: Weighted lengths of intervals.

We shall require the weighted length of an interval by the Poisson kernel (C.4) (cf. the corresponding for the Poisson kernel for the half plane, in Chapter 3, (3.35)). Consider an interval $\Omega = [0, \omega_0)$, where $\omega_0 \leq \omega_N$, and a point $\xi = x + jy$ in the open right half plane. The image of the interval Ω under the mapping $z = e^{sT}$ is an arc, $\Omega_d = (1, e^{j\omega_0 T})$, of the unit circle, and the image of ξ is a point $e^{\xi T}$ in \mathbb{D}^c . Define the length of Ω_d , as weighted by $e^{\xi T}$, to be

$$\Theta_d(\xi, \Omega) \triangleq \int_0^{\omega_0} \Psi_d(e^{\xi T}, \omega) d\omega. \quad (\text{C.6})$$

In the case that ξ is real, we then have that

$$\Theta_d(\xi, \Omega) = -\angle \prod_{k=-\infty}^{\infty} \frac{\xi - j(\omega_0 - k\omega_s)}{\xi + j(\omega_0 + k\omega_s)} \quad (\text{C.7})$$

$$= -\angle \frac{\sinh\left(\frac{(\xi - j\omega_0)T}{2}\right)}{\sinh\left(\frac{(\xi + j\omega_0)T}{2}\right)}; \quad (\text{C.8})$$

i.e., the weighted length of the interval Ω equals the negative of the *sum* of the phase lags contributed by the Blaschke product $(\xi - s)/(\xi + s)$ at each of the points $\omega_0 + k\omega_s$, $k = 0, \pm 1, \pm 2, \dots$, that are mapped to the upper end point of the interval. It is straightforward to verify that the length of the discrete arc Ω_d weighted by the point $e^{\xi T}$ is *greater* than that of the corresponding analog interval $\Omega = [0, \omega_0)$ as weighted by the point ξ (cf. (3.36)). As an example, see Figure C.1, which contains plots of $\Theta(\xi, \Omega)$ and $\Theta_d(\xi, \Omega)$ for the point $\xi = 1/T$ and values of ω_0 ranging from 0 to ω_N . Similar remarks apply to the case of a complex ξ .

The following result is derived immediately from Proposition C.1.3.

Corollary C.1.4

Suppose that

$$|S_d(e^{j\omega T})| \leq \alpha, \quad \text{for all } \omega \text{ in } \Omega = [0, \omega_0), \quad (\text{C.9})$$

where $\omega_0 \leq \omega_N$, and let $\nu = e^{\xi T}$, where ξ lies in \mathbb{C}^+ . Then

$$\sup_{\omega \in [\omega_0, \omega_N)} |S_d(e^{j\omega T})| \geq (1/\alpha) \frac{\Theta_d(\xi, \Omega)}{\pi - \Theta_d(\xi, \Omega)} |B_\rho^{-1}(\nu)|^{\frac{\pi}{\pi - \Theta_d(\xi, \Omega)}} |S_d(\nu)|^{\frac{\pi}{\pi - \Theta_d(\xi, \Omega)}} \quad (\text{C.10})$$

o

If ν is a NMP zero of the discretized plant, then $S_d(\nu) = 1$ and $|S_d(e^{j\omega T})|$ is guaranteed to have a peak greater than one. Since $\Theta_d(\xi, \omega_0) \geq \Theta(\xi, \omega_0)$ it follows that the infimum of this peak is *guaranteed* to be greater than that given by (C.8) in the analog case.

Bibliography

- M. Araki. Recent developments in digital control theory. In *Proceedings of the 12th World Congress of the IFAC*, pages IX–251, 1993.
- M. Araki, T. Hagiwara, and Y. Ito. Frequency response of sampled-data systems II: Closed-loop consideration. In *Proceedings of the 12th World Congress*, pages VII–293, Sydney, 1993. IFAC.
- M. Araki and Y. Ito. Frequency response of sampled-data systems I: Open-loop consideration. In *Proceedings of the 12th World Congress*, pages VII–289, Sydney, 1993. IFAC.
- K.J. Åström, P. Hagander, and J. Sternby. Zeros of sampled-data systems. *Automatica*, 20(1):31–38, 1984.
- K.J. Åström and B. Wittenmark. *Computer-Controlled Systems: Theory and Design*. Prentice Hall, Englewood Cliffs NY, 2nd edition, 1990.
- E.-W. Bai and S. Dasgupta. A note on generalized hold functions. *Systems and Control Letters*, 14:363–368, 1990.
- A.V. Balakrishnan. *Applied functional analysis*. Springer-Verlag New York Inc., 1981.
- B.A. Bamieh, M.A. Dahleh, and J.B. Pearson. Minimization of the l_∞ -induced norm for sampled-data systems. *IEEE Trans. on Automatic Control*, AC-38(5): 717–732, May 1993.
- B.A. Bamieh and J.B. Pearson. A general framework for linear periodic systems with applications to H^∞ sampled-data control. *IEEE Trans. on Automatic Control*, AC-37(4):418–435, April 1992.
- B.A. Bamieh, J.B. Pearson, B.A. Francis, and A. Tannenbaum. A lifting technique for linear periodic systems with applications to sampled-data control. *Systems and Control Letters*, 17:79–88, 1991.
- R.P. Boas. *Entire functions*. Academic Press, 1954.
- H.W. Bode. *Network Analysis and Feedback Amplifier Design*. D. van Nostrand, New York, 1945.
- J.H. Braslavsky, R.H. Middleton, and J.S. Freudenberg. Frequency response of generalized sampled-data hold functions. In *Proceedings of the 34th CDC*, New Orleans, LO, December 1995a.

- J.H. Braslavsky, R.H. Middleton, and J.S. Freudenberg. Sensitivity and robustness of sampled-data control systems: a frequency domain viewpoint. In *Proceedings of the 1995 ACC*, pages 1040–1044, Seattle, WA, June 1995b.
- S.N. Carroll and Jr. W.L. McDaniel. Use of convolution integral in sampled-data theory. *IEEE Trans. on Automatic Control*, AC-11:328–329, April 1966.
- H.S. Carslaw. *Theory of Fourier's series and integrals*. Dover, 3rd edition, 1950. Reprint. Orig. McMillan, 1930.
- C.T. Chen. *Introduction to linear system theory*. Holt Rinehart and Winston, NY, 1984.
- M.J. Chen and C.A. Desoer. Necessary and sufficient condition for robust stability of linear distributed feedback systems. *Int. J. of Control*, 35(2):255–267, 1982.
- T. Chen and B.A. Francis. On the L_2 -induced norm of a sampled-data system. *Systems and Control Letters*, 15:211–219, 1990.
- T. Chen and B.A. Francis. Input-output stability of sampled-data systems. *IEEE Trans. on Automatic Control*, AC-36(1):50–58, January 1991.
- J.B. Conway. *Functions of One Complex Variable*. Springer-Verlag, New York, 1973.
- S.K. Das and P.K. Rajagopalan. Periodic discrete-time systems: Stability analysis and robust control using zero placement. *IEEE Trans. on Automatic Control*, AC-37(3):374–378, March 1992.
- L. De Branges. *Hilbert spaces of entire functions*. Prentice-Hall, Inc., Englewood Cliffs, N.J., 1968.
- C.A. Desoer and M. Vidyasagar. *Feedback systems: input-output properties*. Academic Press, 1975.
- Gustav Doetsch. *Guide to the Applications of Laplace and Z-transforms*. D. van Nostrand, Princeton NJ, 2nd. edition, 1971.
- J.C. Doyle, B.A. Francis, and A.R. Tannenbaum. *Feedback Control Theory*. Macmillan Publishing Company, New York, 1992.
- J.C. Doyle and G. Stein. Robustness with observers. *IEEE Trans. on Automatic Control*, AC-24(4):607–611, August 1979.
- J.C. Doyle and G. Stein. Multivariable feedback design: concepts for a classical/modern synthesis. *IEEE Trans. on Automatic Control*, AC-26, 1981.
- G. Dullerud and B. Francis. l_1 analysis and design of sampled-data systems. *IEEE Trans. on Automatic Control*, AC-37(4):436–446, April 1992.
- G. Dullerud and K. Glover. Robust stabilization of sampled-data systems to structured LTI perturbations. *IEEE Trans. on Automatic Control*, AC-38(10):1497–1508, October 1993.

- M.J. Er and B.D.O. Anderson. Discrete-time loop transfer recovery via generalized sampled-data hold functions based compensators. *Int. J. of Robust and Nonlinear Control*, 4:741–756, 1994.
- M.J. Er, B.D.O. Anderson, and W.-Y. Yan. Gain margin improvement using generalized sampled-data hold function based multirate output compensator. *Automatica*, 30(3):461–470, 1994.
- A. Feuer and G.C. Goodwin. Generalized sample hold functions: Facts and fallacies. In *Proceedings of the 31st. CDC*, Tucson, AZ, 1992.
- A. Feuer and G.C. Goodwin. Generalized sample hold functions: Frequency domain analysis of robustness, sensitivity, and intersample difficulties. *IEEE Trans. on Automatic Control*, AC-39(5):1042, May 1994.
- A. Feuer and G.C. Goodwin. *Sampling in Digital Signal Processing and Control*. Birkhauser, 1996.
- B. Francis. Lectures on H_∞ control and sampled-data systems. In C. Foias, E. Mosca, and L. Pandolfi, editors, *H_∞ -control theory: lectures given at the 2nd. session of the CIME*, Lecture notes in mathematics, pages 37–105. Springer-Verlag, 1991.
- B.A. Francis and T.T. Georgiou. Stability theory for linear time-invariant plants with periodic digital controllers. *IEEE Trans. on Automatic Control*, AC-33(9): 820–832, January 1988.
- G.F. Franklin and A. Emami-Naeini. Design of ripple-free multivariable servomechanisms. *IEEE Trans. on Automatic Control*, AC-31(7):661–664, July 1986.
- G.F. Franklin, J.D. Powell, and M.L. Workman. *Digital Control of Dynamic Systems*. Addison-Wesley, Reading, MA, 2nd edition, 1990.
- J.S. Freudenberg and D.P. Looze. Right half plane poles and zeros and design tradeoffs in feedback systems. *IEEE Trans. on Automatic Control*, AC-30(6):555–565, June 1985.
- J.S. Freudenberg and D.P. Looze. *Frequency Domain Properties of Scalar and Multivariable Feedback Systems*, volume 104 of *Lecture Notes in Control and Information Sciences*. Springer-Verlag, 1988.
- J.S. Freudenberg, R.H. Middleton, and J.H. Braslavsky. Robustness of zero-shifting via generalized sampled-data hold functions. In *Proceedings of the 33th CDC*, pages 231–235, Florida, December 1994.
- J.S. Freudenberg, R.H. Middleton, and J.H. Braslavsky. Inherent design limitations for linear sampled-data feedback systems. *International Journal of Control*, 61(6):1387–1421, June 1995.
- M. Fu. Exact, optimal, and partial loop transfer recovery. In *Proceedings of the 29th CDC*, pages 1841–1846, Honolulu, December 1990.

- E.G. Gilbert. Linear control systems with pointwise-in-time constraints: What do we do about them? In *Proceedings of the 1992 ACC*, 1992.
- K. Glover. Progress in applied robust control. In A. Isidori, editor, *Trends in control: A European perspective*. Springer-Verlag, 1995.
- G.I. Gómez and G.C. Goodwin. Vectorial sensitivity constraints for linear multi-variable systems. In *Proceedings of the 34th CDC*, New Orleans, LO, December 1995.
- G.C. Goodwin and M. Salgado. Frequency domain sensitivity functions for continuous time systems under sampled data control. *Automatica*, 30(8):1263, August 1994.
- I. Grattan-Guinness. *Convolutions in French mathematics, 1800-1840*, volume 2. Birkhäuser Verlag, 1990.
- W.M. Haddad, H.H. Huang, and D.S. Bernstein. Sampled-data observers with generalized holds for unstable plants. *IEEE Trans. on Automatic Control*, 39(1): 229–234, January 1994.
- T. Hagiwara and M. Araki. Design of a stable state feedback controller based on the multirate sampling of the plant output. *IEEE Trans. on Automatic Control*, AC-33(9):812–819, September 1988.
- T. Hagiwara and M. Araki. Robust stability of sampled-data systems under possibly unstable additive/multiplicative perturbations. In *Proceedings of the 1995 ACC*, pages 3893–3898, June 1995.
- T. Hagiwara, Y. Ito, and M. Araki. Computation of the frequency response gains and H_∞ -norm of a sampled-data system. *Systems and Control Letters*, 25:281–288, 1995.
- S. Hara, H. Katori, and R. Kondo. The relationship between real poles and real zeros in SISO sampled-data systems. *IEEE Trans. on Automatic Control*, 34(6): 632–635, 1989.
- S. Hara, M. Nakajima, and P.T. Kabamba. Robust stabilization in digital control systems. In *Proceedings*, pages 481–486, Japan, 1991. MTNS.
- P. Henrici. *Applied and computational complex analysis*, volume 2. John Wiley & Sons, 1977.
- K. Hoffman. *Banach spaces of analytic functions*. Dover, New York, 1962.
- I.M. Horowitz. *Synthesis of feedback systems*. Academic Press, New York, 1963.
- E.I. Jury. *Sampled-data control systems*. John Wiley & Sons, 1958.
- P.T. Kabamba. Control of linear systems using generalized sampled-data hold functions. *IEEE Trans. on Automatic Control*, pages 772–783, September 1987.

- P.T. Kabamba and S. Hara. Worst-case analysis and design of sampled-data control systems. *IEEE Trans. on Automatic Control*, 38:1337–1357, 1993.
- R. Kalman, B.L. Ho, and K. Narendra. Controllability of linear dynamical systems. In *Contributions to differential equations*. Interscience, 1963. Vol.1.
- J.P. Keller and B.D.O. Anderson. A new approach to the discretization of continuous-time controllers. *IEEE Trans. on Automatic Control*, AC-37(2):214–233, 1992.
- P. Khargonekar, K. Poolla, and A. Tannenbaum. Robust control of linear time-invariant plants using periodic compensation. *IEEE Trans. on Automatic Control*, AC-30(11):1088–1096, November 1985.
- B.C. Kuo. *Digital control systems*. Saunders College Publishing, Harcourt Brace Jovanovich, Ft. Worth, TX, 2nd. edition, 1992.
- G.M.H. Leung, T.P. Perry, and B.A. Francis. Performance analysis of sampled data control systems. *Automatica*, 27(4):699–704, 1991.
- N. Levinson and R.M. Redheffer. *Complex Variables*. Holden-Day, Inc., 1970.
- J.S. Liu, Y.S. Chou, and F.R. Chang. Decoupling of continuous-time linear time-invariant systems using generalized sampled-data hold functions. *Systems and Control Letters*, 19:61–69, 1992.
- A.I. Markushevich. *Theory of functions of a complex variable*, volume 2. Prentice-Hall, Inc., Englewood Cliffs, N.J., 1965.
- R.H. Middleton. Trade-offs in linear control systems design. *Automatica*, 27(2): 281–292, March 1991.
- R.H. Middleton and J.S. Freudenberg. Non-pathological sampling for generalised sampled-data hold functions. *Automatica*, 31(2), February 1995.
- R.H. Middleton and G.C. Goodwin. *Digital control and estimation. A unified approach*. Prentice-Hall, Inc., 1990.
- R.H. Middleton and J.Q. Xie. Non-pathological sampling for high order generalised sampled-data hold functions. In *Proceedings of the ACC*, Seattle, WA, June 1995.
- C. Mohtadi. Bode's Integral Theorem for discrete-time systems. *IEEE Proceedings*, 137 Pt. D(2):57–66, March 1990.
- K. Ogata. *Discrete-time control systems*. Prentice Hall, Englewood Cliffs, NJ, 1987.
- A. Packard and J. Doyle. The complex structured singular value. *Automatica*, 29 (1):71–109, 1993.
- R.E.A.C. Paley and N. Wiener. *Fourier transforms in the complex domain*. American Mathematical Society, Providence, 1934.

- P.N. Paraskevopoulos and K.G. Arvanitis. Exact model matching of linear systems using generalized sampled-data hold functions. *Automatica*, 30(3):503–506, 1994.
- C.L. Phillips, J.L. Lowry, and III R.K. Calvin. On the starred transform. *IEEE Trans. on Automatic Control*, AC-11:760, October 1966.
- C.L. Phillips, III R.K. Calvin, and D.L. Chenoweth. A note on the Laplace transform of discrete functions. *IEEE Trans. on Automatic Control*, AC-13:118–119, February 1968.
- D.A. Pierre and R.C. Kolb. Concerning the Laplace transform of sampled signals. *IEEE Trans. on Automatic Control*, AC-9:191–192, April 1964.
- F. Riesz and B. Sz.-Nagy. *Functional Analysis*. Dover, New York, 1990.
- W. Rudin. *Real and complex analysis*. McGraw-Hill Book Co., 3rd. edition, 1987.
- R.G. Shenoy, D. Burnside, and T.W. Parks. Linear periodic systems and multirate filter design. *IEEE Trans. on Signal Processing*, 42(9):2242–2256, September 1994.
- P. Shi, M. Fu, and C. De Souza. Loop transfer recovery for systems under sampled measurements. Technical Report EE9331, Dept of E&CE, The University of Newcastle, 1993. Submitted to IEEE Proceedings.
- P. Shi, M. Fu, and C. De Souza. Loop transfer recovery for sampled-data systems. In *Proceedings of the ACC*, pages 3232–3233, Baltimore, June 1994.
- N. Sivashankar and P. Khargonekar. Robust stability and performance analysis for sampled-data systems. *IEEE Trans. on Automatic Control*, 39(1):58–69, January 1993.
- N. Sivashankar and P. Khargonekar. Characterization of the L_2 -induced norm for linear systems with jumps with applications to sampled-data systems. *SIAM J. Control and Optimization*, 32(4):1128–1150, July 1994.
- W. Sun, K. Nagpal, and P. Khargonekar. \mathcal{H}_∞ control and filtering for sampled-data systems. *IEEE Transactions on Automatic Control*, AC-38(8):1162–1175, August 1993.
- H.-K. Sung and S. Hara. Properties of sensitivity and complementary sensitivity functions in single-input single-output digital control systems. *Int. J. of Control*, 48(6):2429–2439, 1988.
- G. Tadmor. \mathcal{H}_∞ optimal sampled data control in continuous time systems. In *Proceedings 1991 American Control Conference, Boston, MA*, pages 1658–1663, 1991.
- G. Tadmor. \mathcal{H}_∞ optimal sampled data control in continuous time systems. *Int. J. of Control*, 56(1):99, July 1992.
- P.M. Thompson, R.L. Daily, and J.C. Doyle. New conic sectors for sampled-data feedback systems. *Systems and Control Letters*, 7:395–404, 1986.

- P.M Thompson, G. Stein, and M. Athans. Conic sectors for sampled-data feedback systems. *Systems and Control Letters*, 3:77–82, 1983.
- H.T. Toivonen. Sampled-data control of continuous-time systems with an H_∞ optimality criterion. *Automatica*, 28(1):45–54, 1992.
- J.G. Truxal. *Control System Synthesis*. McGraw-Hill, New York, 1955.
- L. Turan and D.L. Mingori. A unified loop transfer recovery approach to robust control using H_∞ optimization methods. *Automatica*, 31(7):1045–1052, 1995.
- S. Urikura and A. Nagata. Ripple-free deadbeat control for sampled-data systems. *IEEE Trans. on Automatic Control*, AC-32(6):474–482, June 1987.
- C.F. Van Loan. Computing integrals involving the matrix exponential. *IEEE Trans. on Automatic Control*, AC-23(3):395–404, June 1978.
- M. Vidyasagar. *Control System Synthesis, A Factorization Approach*. MIT Press, Cambridge, 1985.
- N.M. Wereley and S.R. Hall. Frequency response of linear time-periodic systems. In *Proceedings*, pages 3650–3655, Honolulu, December 1990. 29th CDC.
- G. Willis. *Functional analysis. Lecture Notes*, The University of Newcastle, NSW, Australia, 1994.
- W.M. Wonham. *Linear multivariable control: A geometric approach*. Springer-Verlag, 3rd edition, 1985.
- Y. Yamamoto. New approach to sampled-data systems: a function space method. In *Proceedings of the 29th CDC*, pages 1882–1887, 1990.
- Y. Yamamoto. On the state space and frequency domain characterization of H^∞ -norm of sampled-data systems. *Systems and Control Letters*, 21:163–172, 1993.
- Y. Yamamoto. A function space approach to sampled data control systems and tracking problems. *IEEE Trans. on Automatic Control*, 39(4):703–713, April 1994.
- Y. Yamamoto and M. Araki. Frequency responses for sampled-data systems - Their equivalence and relationships. *Linear Algebra and its Applications*, 206: 1319–1339, 1994.
- Y. Yamamoto and P. Khargonekar. Frequency response of sampled-data systems. In *Proceedings of the 32nd CDC*, pages 799–804, December 1993. Also *IEEE Trans. on Automatic Control*, vol. 39, pp. 166–176, February 1996.
- Y. Yamamoto and P. Khargonekar. Frequency response of sampled-data systems. *IEEE Trans. on Automatic Control*, 41(2):166–176, 1996.
- W. Yan, B.D.O. Anderson, and R.R. Bitmead. On the gain margin improvement using dynamic compensation based on generalized sampled-data hold functions. *IEEE Trans. on Automatic Control*, 39(11):2347, November 1994.

-
- C. Yang and P.T. Kabamba. Multi-channel output gain margin improvement using generalized sampled-data hold functions. *IEEE Trans. on Automatic Control*, 39(3):657–661, March 1994.
- G. Zames and D. Bensoussan. Multivariable feedback, sensitivity, and decentralized control. *IEEE Trans. on Automatic Control*, AC-28(11):1030–1035, November 1983.
- A.H. Zemanian. *Distribution theory and transform analysis*. McGraw-Hill, 1965.
- J. Zhang and C. Zhang. Robustness analysis of control systems using generalized sample hold functions. In *Proceedings of the 33th CDC*, Lake Buena Vista, FL, December 1994.
- Z. Zhang and J.S. Freudenberg. Loop transfer recovery for nonminimum phase plants. *IEEE Trans. on Automatic Control*, AC-35(5):547–553, May 1990.

Notation

For purposes of reference, we include here a brief list of special symbols used in this thesis.

\mathbb{R}, \mathbb{C}	The sets of real and complex numbers.
\mathbb{R}_0^+	The set of real non-negative numbers; $[0, \infty)$.
$\mathbb{R}^n, \mathbb{C}^n$	The sets of n -dimensional real and complex vectors.
$\mathbb{C}^+, \overline{\mathbb{C}^+}, \mathbb{C}^-, \overline{\mathbb{C}^-}$	The open and closed right halves of the complex plane, the open and closed left halves of the complex plane.
\bar{M}, M^T, M^*	The conjugate, transpose, and conjugate transpose of a matrix M .
$ v $	The Euclidian norm of a vector v in \mathbb{R}^n ; $ v = (v^*v)^{1/2}$.
$\mathbb{D}, \bar{\mathbb{D}}$	The open and closed unit disks in \mathbb{C} ; $\mathbb{D} \triangleq \{z \in \mathbb{C} : z < 1\}$ and $\bar{\mathbb{D}} \triangleq \{z \in \mathbb{C} : z \leq 1\}$.
X^c, X^\perp	The complement and orthogonal complement of a space X .
$L_p^n(\mathbb{R}_0^+)$	The space of Lebesgue measurable functions $f : \mathbb{R}_0^+ \rightarrow \mathbb{R}^n$ that satisfy $\int_0^\infty f(t) ^p dt < \infty$ for a finite positive number p .
$L_\infty^n(\mathbb{R}_0^+)$	The space of Lebesgue measurable functions $f : \mathbb{R}_0^+ \rightarrow \mathbb{R}^n$; that satisfy $\text{ess sup}_{t \in \mathbb{R}} f(t) < \infty$.
$L_{pe}^n(\mathbb{R}_0^+)$	The extended space $L_p^n(\mathbb{R}_0^+)$; i.e., the space of functions $f : \mathbb{R}_0^+ \rightarrow \mathbb{R}^n$ that satisfy $\int_0^a f(t) ^p dt < \infty$ for any finite real number a .
L_2^n	The space of square Lebesgue integrable functions $f : \mathbb{R} \rightarrow \mathbb{C}^n$; $\int_0^a f(t) ^2 dt < \infty$.
ℓ_p^n	The space of sequences $u = \{u_k\}_{k=-\infty}^\infty$, with u_k in \mathbb{C}^n , satisfying $\ u\ _{\ell_2} \triangleq (\sum_{k=-\infty}^\infty u_k ^p)^{1/p} < \infty$.
T, ω_s	The sampling period and the sampling frequency; $\omega_s = 2\pi/T$.

Ω_N	The Nyquist range of frequencies; $\{\omega : \omega \in [-\omega_s/2, \omega_s/2]\}$.
$L_2(\Omega_N; \ell_2)$	The space of functions $f : \Omega_N \rightarrow \ell_2$ that satisfy $\int_{\Omega_N} \ f(\omega)\ _{\ell_2}^2 d\omega < \infty$.
$\mathcal{Z}\{\cdot\}, \mathcal{L}\{\cdot\}$	The Z and Laplace transform operators.
$\mathcal{S}_T\{\cdot\}$	The sampling operator with period T .
$F_k(\cdot)$	$F(\cdot + jk\omega_s)$.
$(F)_d$	The discretization of the function F ; $(F)_d = \mathcal{Z}\{\mathcal{S}_T\{\mathcal{L}^{-1}\{F\}\}\}$.
σ_F	The abscissa of absolute and uniform convergence of the Laplace transform $F = \mathcal{L}\{f\}$.
\mathcal{D}_F	The domain $\{s = x + jy, \text{ with } x > \sigma_F \text{ and } y \text{ in } \Omega_N\}$.
S^0, T^0, T^k	The fundamental sensitivity, fundamental complementary sensitivity, and harmonic hybrid responses.

Index

- A-D interface, 4, 13
- actuator saturations, 27, 66, 99
- admissible perturbation, 102
- aliasing, 26, 77
- alignment, 93
- analog vs. sampled-data, 53, 59, 80
- analog performance, 120–122
- analog plant, *see* plant
- anti-aliasing filter, 18, 76
 - and hold device, 66n
- approximable operator, 85, 87
- approximate pole-zero cancellation, 76
- approximate pole-zero cancellation, 72, 118, 120

- band-limited signals, 5, 81
- baseband, *see* Nyquist range
- basic perturbation model, 102, 105
- Bezout Identity, 57
- Blaschke Products, 42, 69, 126, 154
- Bode Integral
 - analog, 6
 - discrete, 153
 - for the fundamental sensitivity, 77
- bounded variation, 13, 15, 138
- bounds
 - for robust stability, 121
 - on L_2 induced operator norms, 93
 - on GSHF frequency responses, 42
 - on intersample behavior, 92
 - on the discrete sensitivity, 120
 - on the fundamental complementary sensitivity, 74
 - on the fundamental sensitivity, 70
 - on the harmonic response functions, 76
- Bromwich Integral, 141

- Cauchy & Poisson, 16n
- Cauchy-Schwarz Inequality, 25, 92
- closed-loop stability, 20
- compact operator, 85, 87
- compact set, 85
- complementary sensitivity
 - discrete function, 19
- complementary sensitivity
 - analog function, 55
 - hybrid fundamental function, 52
 - and robust stability, 108, 110
 - and velocity constant, 80
 - lower bounds, 74
 - Middleton Integral, 77–80
 - Poisson Integral, 73–75
 - hybrid operator on L_2 , 85–93
 - frequency gain, 88
- conic sector techniques, 5, 81, 101
- controller
 - design
 - classic procedures, 4, 116
 - digital implementation, 3
 - discrete, 4
 - high-gain, *see* high-gain feedback
 - LQR/LQG, 131
 - non-minimum phase zeros, 60, 69
 - unstable poles, 60, 62
- costs and benefits of sampled-data feedback, 80

- D-A interface, 4, 13
- descriptor system techniques, 5, 82
- design tradeoffs
 - analog, 6, 55

- discrete, 6, 132
- GSHF, 41
- hybrid, 70–72, 78–80, 132
 - from GSHF NMP zeros, 71
 - from plant NMP zeros, 70
 - from plant unstable poles, 71
- differential sensitivity, 55
- differential sensitivity, 54
- Dirac's Delta, 138
- Dirichlet Integral, 138
- Dirichlet Kernel, 138
- discrete design, 4
- discrete response, 122–129
- discrete sensitivity functions, 19
- discretized plant, 19
 - by partial fractions expansion, 118
- disturbance
 - rejection, 61–68
 - steady-state response, 52
- divisive perturbation model, 110–113
- emulation, 4
- entire function, 25, 28, 45, 151
- essential singularity, 140
- exponential stability, 20
- fidelity, 92, 121
- fidelity function, 121
 - integral constraints, 126
 - interpolation constraints, 124
- filter, *see* anti-aliasing filter
- finite-rank operators, 85, 86
- Fourier transform, 16n
- FR-operators, 82
- frequency gain of a hybrid operator, 82
- frequency-domain lifting, 82–85
 - isomorphism, 84
 - operation, 83
 - operator, 84
- fundamental
 - hybrid complementary sensitivity, 52
 - lower bounds, 74
 - Middleton Integral, 77–80
 - Poisson Integral, 73–75
- hybrid sensitivity, 52
 - Bode Integral, 77
 - lower bounds, 70
 - Poisson Integral, 70–72
 - zeros, 60
- fundamental response, 49
 - integral constraints, 68–80
 - interpolation constraints, 55–58
- gain-margin improvement via GSHF, 97
- Gedanken experiment
 - analog performance, 120–122
 - discrete response, 122–129
- generalized hold function, *see* GSHF
- Great Picard Theorem, 140
- GSHF, 13, 23–47
 - a la Kabamba, *see* FDLTI GSHF
 - and analog performance, 120–122
 - and discrete response, 122–129
 - DC-gain, 26
 - design tradeoffs, 41, 45, 46, 132
 - disturbance rejection properties, 64
 - FDLTI, 29, 32
 - frequency response function, 14, 24–30
 - boundary values, 27–28
 - bounds on, 42
 - Middleton Integral, 42–45
 - Parseval Equality, 26
 - peaks in, 27, 41, 42, 46
 - Poisson Integral, 40–42
 - gain-margin improvement, 97
 - input-output operator, 27
 - loop transfer recovery, 131
 - loop transfer recovery, 46, 129
 - non-minimum phase, 24, 31, 71, 78, 118
 - norms, 25–27
 - output feedback, 67
 - piecewise constant, 29, 31, 46
 - simultaneous stabilization, 36, 118–120
 - symmetry, 35

- transmission blocking properties, 14, 33
- undesirable side-effects, 23, 115, 131
- wonderful capabilities, 23, 115
- zero placement, 46, 115–132
 - design tradeoffs, 132
- zeros, 14, 31–38, 45, 60, 69, 71
- Hadamard Factorization Theorem, 34
- Hankel singular values, 120
- harmonic oscillator, 67
- harmonics, 49
 - and L_2 -induced norms, 90
 - hybrid response function, 52
 - interpolation constraints, 58
 - lower bounds, 76
 - Poisson Integral, 75–77
- Heine-Borel Theorem, 85
- high-gain feedback, 53–54
- H_∞ -control of hybrid systems, 5
- H_∞ -methods, 101
- H_∞ -norm, 84
- hold device, *see* GSHF
- hybrid, *see* sampled-data
- hybrid sensitivity functions, 52
 - and L_2 norms, 90
 - integral constraints, 68–80
 - interpolation constraints, 55–61
- impulse modulation formula, 17
- Initial Value Theorem, 34
- inner-outer factorization, 73
- input disturbance, 64
- input saturations, 27, 66, 99
- instability due to plant variations, 131
- integral relations, 68–80, 126
- interpolation constraints, 55–61, 125
- intersample behavior, 4, 68, 80, 92
- isometry, 147
- isometry between L_2 and $L_2(\Omega_N; \ell_2)$, 84, 147
- Jordan's Lemma, 144
- jump discontinuities, 13, 16
- L'Hopital's Rule, 43
- L'Hospital's Rule, 145–147
- Laplace transform, 15
 - inversion, 141
- Laplace transform of a sampled signal, 16
- Lebesgue Dominated Convergence, 43n, 145
- Levi Theorem, 147
- lifting techniques
 - and robust stability, 101
- lifting operation, 83
- lifting techniques, 5, 81–85
- limitations in sampled-data systems, 80, 132
- linear time-invariant perturbations, 101
- linear systems with jumps, 5, 82
- loop transfer recovery, 46, 129–131
- L_p , 11
 - extended spaces, 11
 - induced operator norms, 12
- l_p signal spaces, 12
- LQR/LQG compensator, 131
- L_2 , 12, 83
 - induced operator norms, 81, 84, 85
 - and hybrid sensitivity functions, 90
 - and stability robustness, 99
 - hybrid complementary sensitivity, 88
 - hybrid sensitivity, 89
 - lower bounds, 93
 - numerical implementation, 93–99
 - input-output stability, 20
- $L_2(\Omega_N; \ell_2)$, 84, 147
- matrix exponential formulas, 97
- Middleton Integral
 - for GSHF, 42–45
 - for the fundamental complementary sensitivity, 77–80
 - interpretations, 78–80
- modified Z-transform, 4n
- μ , 101, 105

- multiplicative perturbation model, 102–110
- multirate sampling, 5
- noise steady-state response, 52
- non-minimum phase
 - GSHF, 31
- non-minimum phase
 - GSHF, 24, 71, 78, 118
 - plant, 70, 78, 118, 130, 132
- non-pathological sampling, 20, 33
- non-robustness of zero placement, 131
- Nyquist range, 55
- Nyquist range, 13, 54
- order of an entire function, 25n, 151
- output feedback by GSHF, 67
- Paley & Wiener, 25
- Paley-Wiener spaces, 28
- Parseval's Formula, 26
- peaks
 - in GSHF frequency responses, 27, 41, 42, 46
 - in the harmonic response functions, 76
 - in the fidelity function, 131
 - in the fundamental complementary sensitivity response, 74 and robust stability, 114
 - in the fundamental sensitivity response, 71, 72, 122 and robust stability, 114
 - in the harmonic response functions and L_2 -induced norms, 92
- periodic controllers, 5
- periodic disturbances, 63, 64, 66
- periodic systems, 50, 51n
- periodic time-varying perturbations, 101
- perturbation
 - linear time-invariant, 101, 131
 - periodic time-varying, 101
- plant, 18
 - non-minimum phase zeros, 60, 69, 70, 78, 118, 130, 132
 - unstable poles, 59, 61, 64, 69
- plant uncertainty, 102, 110, 127, 131
 - sensitivity, 54
- Poisson & Cauchy, 16n
- Poisson Integral
 - analog, 6, 55
 - discrete sensitivity, 154
 - for GSHF, 40–42
 - for harmonic response functions, 75–77
 - for the fidelity function, 126
 - for the fundamental complementary sensitivity, 73–75
 - for the fundamental sensitivity, 70–72
 - interpretations, 70, 73–75
- Poisson Kernel, 154
 - for the half plane, 41, 70
- Poisson Summation Formula, 16, 137n
- pole-zero parity preservation, 118
- poles
 - and disturbance rejection, 61
 - interpolation constraints, 59
- Polya Formula, 137n
- prefilter, *see* anti-aliasing filter
- Riccati Equations, 6, 82
- Riesz-Fischer Theorem, 143
- robust stability, 81, 101–113
 - and fundamental complementary sensitivity, 108, 110
 - necessary and sufficient conditions, 106, 108
 - necessary conditions, 106, 124
 - small-gain condition, 106
 - via Nyquist criterion, 101
- robustness of zero-placement, 129–131
- sampled-data, 3
 - vs. analog, 53, 59, 80
 - vs. discrete, 99
 - basic feedback system, 3, 17
 - frameworks, 6
 - frequency gains, 82
 - frequency response, 50–55

- harmonic structure, 103
- H_∞ -control, 5, 81
- infinite-dimensional transfer matrices, 84, 86
- input-output stability, 20
- L_2 -induced operator norms, 85–99
- robust stability, 81, 101–113
- sensitivity operators, 85–93
- tracking, 64, 80, 81
- transfer function, 49n
- sampler, 4, 13
 - unbounded operator, 13
- sampling formula, 15–17, 137–139
 - domain of validity, 17
- sampling frequency, 13
- sampling period, 13
- saturations, *see* actuator saturations
- sensitivity
 - analog function, 55
 - differential, 54–55
 - discrete function, 19
 - hybrid fundamental function, 52
 - Bode Integral, 77
 - lower bounds, 70
 - Poisson Integral, 70–72
 - hybrid operator on L_2 , 85–93
 - frequency gain, 89
 - to plant uncertainty, 54, 131
- simultaneous stabilization, 36
- small-gain condition for robust stability, 106
- stability, *see* closed-loop stability
- stability robustness, *see* robust stability
- steady-state
 - disturbance rejection, 61–68
 - frequency response, 52, 85
 - ramp tracking, 80
- strong stabilization, 117, 119
- structured singular value, *see* μ
- time-domain lifting, 83
- type of an entire function, 25n, 151
- uncertainty
 - divisive, 110
 - multiplicative, 102
 - sensitivity, 54
- weighted length of an interval, 41, 70, 154
- weighting function, 102, 110
- Youla Parametrization, 57
- Z-transform, 15
- zero placement, *see* GSHP zero placement
- zero-pole parity preservation, 118
- zeros
 - and Poisson Integral, 70
 - interpolation constraints, 60
 - of a discretized plant, 117
 - of a GSHP, 31–38, 45, 60
 - of the fundamental sensitivity, 60
 - phase lag, 41, 70, 154
- ZOH, 24, 33
 - better than GSHP, 27, 33, 46, 67–68
 - disturbance rejection properties, 64, 68